Université Paris Cité

École doctorale Bio Sorbonne Paris Cité
ED nº 562 (Bio SPC)

Unité de Biologie Fonctionnelle et Adaptative
UMR 8251 / CNRS Université Paris Cité

The GLP-1 system in the olfactory bulb mediates the regulation of pre- and post-prandial glucose homeostasis in health and obesity

Par :
Mireia MONTANER MASSANA

THÈSE DE DOCTORAT

Discipline : physiologie et physiopathologie
Dirigée par Hirac Gurden

Présentée et soutenue publiquement le 23 septembre 2022

Devant un jury composé de :

Pr. **Virginie Rouiller-Fabre** *(Professeur des Universités, Université Paris Cité)* ..... Présidente
Dr. **Fabrizio Andreelli** *(PU-PH, Sorbonne Université, Hôpital Pitié Salpêtrière)* ..... Rapporteur
Pr. **Karyn Julliard** *(Professeur des Universités, Université Lyon 1)* ..... Rapporteuse
Dr. **Amandine Gautier-Stein** *(CR, INRA, Université Claude Bernard Lyon 1)* ..... Examinatrice
Dr. **Hirac Gurden** *(Directeur de Recherches, CNRS)* ..... Directeur de thèse

I que el més oposat de fer les coses bé no era fer-les malament

Era no fer-les, no fer-les mai.

Adapté de Pau Vallvé

Remerciements

Je remercie tous ceux qui ont contribué à la réalisation de cette thèse.

Dans un premier temps, je tiens à remercier les membres du jury qui me font l'honneur d'évaluer ce travail. Merci à l'examinatrice Amandine Gautier-Stein ainsi qu'à Virginie Rouiller Fabre d'avoir accepté de présider ce jury. Merci aux rapporteurs Fabrizio Andreelli et Karyn Julliard qui ont accepté d'évaluer ce manuscrit de thèse. Merci Karyn pour toutes les suggestions et écoute. Merci Fabrizio pour tes conseils et ta bienveillance.

Je remercie vivement mon directeur de thèse, Hirac Gurden, pour tout ce qu'il m'a apporté, aussi bien sur le plan scientifique que personnel. Hirac, merci pour ton encadrement, ta disponibilité et ton aide inestimable pendant ces années de recherche. Merci aussi pour tes conseils, tes précieuses orientations et ton soutien (plus que nécessaire) pendant la rédaction de ce manuscrit. Ce fut un réel plaisir de travailler avec toi.

Cette thèse n'aurai pas pu être possible sans l'aide de toute mon équipe, REGLYS, dont je remercie très chaleureusement tous les membres.

Christophe, merci de m'avoir accueilli dans ton équipe il y a 5 ans. Je ne pouvais rêver meilleur accueil ! Merci aussi de ton aide pour mener à bien mes travaux, ainsi que pour l'intérêt et l'attention que tu portes toujours à mes doutes et questions.

Je souhaite aussi remercier Stéphanie, merci beaucoup pour ton encadrement au cours de cette thèse, ton aide et tes conseils avisés.

Je souhaite témoigner toute mon affection à Claude, ça a été un vrai plaisir pour moi d'apprendre de tes connaissances et de ta sagesse. Merci aussi Céline pour m'avoir introduit dans le monde de l'enseignement et aidé à y voir plus clair quand j'en ai eu besoin.

Mention très spéciale à Jess, ma partenaire de travail. Travailler en binôme avec toi a été un véritable plaisir. Grâce à toi, j'ai pu vite devenir autonome sur le plan expérimental. Tu as toujours été présente et disponible pour faire avancer ce projet. Merci pour tous ces bons moments de partage que je garderai toujours avec moi.

Amy, Delphine et Ilyès, un grand merci pour votre aide avec les dernières manips ainsi que pour vos encouragements qui m'ont fait énormément de bien.

Mention spéciale à Haleh, pour le chemin parcouru ensemble et l'article en co-premières auteures. Je souhaite aussi remercier Claire Martin, pour sa disponibilité et gentillesse.

Un grand merci à Justine, ancienne co-thésarde et toujours amie, pour son soutien indéfectible. Je garde avec moi tous les moments partagés au labo, les nerfs passés lors des congrès, les rires en soirée et bien plus.

Je tiens également à témoigner ma reconnaissance à toute l'équipe de l'animalerie « Buffon » pour son aide, les conseils ainsi que le soin des souris au cours de ma thèse.

J'ai aussi une pensée pour toutes les personnes avec qui j'ai eu la chance de partager des expériences pendant ces années, au sein de l'unité BFA, de l'Université Paris Cité ou plus largement.

Je n'oublie pas mes proches « hors labo », qui m'ont accompagnée et fortement encouragée dans cette aventure. Un sincère merci à tous eux. Paula et Lucia, mes catalanes parisiennes, qui sont devenues des véritables amies; merci d'être de telles personnes sur qui je peux toujours compter. Simone, merci pour ton soutien dans les moments les plus difficiles. Aina, Congo et Maria, amies biologistes depuis des années et des années, dignes de confiance. Mimi, Anna et Clàudia, pour être toujours à mes côtés. Clara, pour la sérénité qu'elle m'apporte. Et Mar, ma source constante d'inspiration et future partenaire d'aventures britanniques !

Je voudrais terminer en remerciant tout particulièrement Victor, pour les jolis moments vécus ensemble à Paris. J'ai la tête remplie de bons souvenirs. Merci de m'avoir constamment encouragé dans cette aventure, de m'épauler dans les moments difficiles, mais surtout de m'avoir rendu la vie plus belle.

Enfin et surtout, de grands remerciements à toute ma famille pour son soutien et son aide précieuse, en particulier à Martí, à ma mère et à mon père. Vous êtes mon principal atout. Mama, papa, cette thèse vous est dédiée.

Résumé substantiel

Nouveaux rôles du système GLP-1 dans la régulation de la balance énergétique via le bulbe olfactif : impact sur l'obésité et le diabète de type 2

L'homéostasie énergétique est définie comme un état d'équilibre entre les apports alimentaires et les dépenses énergétiques de l'organisme. La stabilité du poids corporel et de la masse grasse reflète cet état d'équilibre. En effet, hormis certaines périodes de la vie durant lesquelles le poids corporel n'est pas stabilisé (croissance, gestation, allaitement ou vieillesse), les mécanismes de régulation du poids corporel à long terme sont particulièrement efficaces.

Dans ce contexte, un déséquilibre entre les apports et les dépenses énergétiques entraîne des pathologies majeures qui dégradent la qualité de vie des patients. L'obésité est une maladie chronique due à un surplus énergétique résultant d'un déséquilibre énergétique entre les calories consommées et dépensées, et elle est caractérisée par un excès de masse grasse et une modification du tissu adipeux. La mesure la plus courante du surpoids et de l'obésité est l'indice de masse corporelle (IMC) qui est calculé en divisant le poids en kilogrammes par la taille en mètres carrés (kg/m^2) de l'individu testé. Un IMC supérieur à 25 est considéré comme une surcharge pondérale, et supérieur à 30, comme une obésité. Une augmentation de l'IMC indique donc un risque de maladie chronique telles que les pathologies cardiovasculaires (incluant les accidents vasculaires cérébraux), les troubles musculo-squelettiques (arthrose), les troubles du sommeil (apnée), certains cancers et l'hypertension artérielle. Les déséquilibres énergétiques associés à l'obésité conduisent à des effets délétères multiples centrés sur un manque d'efficacité de la sécrétion d'insuline (résistance à l'insuline) et aboutissent à une comorbidité très répandue, le diabète de type 2 (DT2). En effet, la régulation de l'équilibre énergétique est mise à mal dans nos sociétés, comme l'attestent régulièrement les rapports de l'OMS, qui souligne la progression inexorable de la pandémie mondiale d'obésité et du DT2 qui y est associé, y compris chez les enfants et les adolescents. Cette pandémie devient, avec les complications qu'elle induit, l'un des problèmes majeurs de santé publique du 21ème siècle.

Chez les obèses diabétiques, il existe un problème majeur de la régulation de la quantité d'insuline secrétée par les cellules β pancréatiques ainsi que de l'action de cette hormone sur ses cibles par l'activation de son récepteur. En effet, l'insuline est la seule hormone capable de diminuer la glycémie après une prise alimentaire. Parmi les antidiabétiques commercialisés figurent les analogues du Glucagon Like Peptide-1 (GLP-1), une hormone incrétine produite par les cellules L intestinales, qui stimule la sécrétion d'insuline pendant les repas. Le GLP-1 stimule aussi la prolifération des cellules β et inhibe la sécrétion pancréatique de glucagon et la vidange gastrique. Cette hormone diminue également la prise alimentaire *via* un effet sur le système nerveux central. Cependant, son action sur les circuits cérébraux n'est pas connue en détails à ce

jour. Dans le cerveau, le récepteur du GLP-1 (GLP-1R) est exprimé par les cellules de plusieurs structures telles que le noyau du tractus solitaire, l'hypothalamus et le bulbe olfactif (BO). Le BO joue un rôle fondamental dans l'appréciation de la palatabilité et de la toxicité des aliments. Le traitement initial de l'information olfactive est transmis en parallèle et simultanément au cortex olfactif et au système limbique pour donner une identité à la stimulation sensorielle. Cette identification est étroitement liée à un label hédonique, c'est à dire au plaisir que l'odeur procure, et également aux émotions et à la mémoire. Des études récentes montrent la sensibilité des neurones du BO aux hormones métaboliques telles que la cholécystokinine, la leptine ainsi que le GLP-1. Des données *in vitro* obtenues par enregistrement de cellules sur tranches de BO ont montré que les principales cellules du BO (appelées cellules mitrales) sont stimulées à la fois par le GLP-1 et l'Exendin-4 (Ex4, agoniste du GLP-1R). De plus, certaines populations neuronales du BO contiennent du preproglucagon (PPG) précurseur du GLP-1, ce qui renforce l'idée qu'il existe une action centrale du GLP-1 au sein du BO. Il a été montré chez les patients obèses que la structure et les fonctions du BO sont altérées. Dans ce contexte, mon projet de thèse a consisté en l'étude du rôle du GLP-1 dans la balance énergétique par son action dans le BO.

Le premier problème à résoudre dans ma thèse était le développement d'un modèle animal obèse qui puisse récapituler la pathologie humaine. Dans ce but, nous avons choisi la souris C57BL6 mâle rendue obèse par régime hypercalorique (Western Diet, WD) comme modèle expérimental. Ces souris constituent un modèle de Diet-Induced Obesity ou DIO. Elles ont été très bien caractérisé au niveau métabolique par notre équipe et des laboratoires internationaux et mime plusieurs paramètres physiopathologiques de l'obésité observés en clinique, notamment la survenue d'un DT2. Ce modèle de souris obèse *in vivo* reproduisant les grandes lignes la pathologie humaine a été mise en place face à l'impossibilité de mener mes expériences *in vitro* où il serait impossible d'étudier des paramètres métaboliques *in vivo*, notamment sanguins. De plus, il m'était impossible d'utiliser des invertébrés qui ne possèdent pas les structures cérébrales et endocrines équivalentes aux mammifères pour le contrôle de la glycémie et de la prise alimentaire. Sur la base de ce modèle murin, j'ai mené deux approches méthodologiques qui ont fait l'objet de trois projets éthiques validés par un comité d'éthique (CEEA-040) et par le ministère de la recherche.

1. Nous avons d'abord développé une approche pharmacologique qui a visé à étudier le rôle physiologique du GLP-1R dans le BO (GLP-1R^{BO}). Pour cela, j'ai implanté des canules par stéréotaxie dans le BO de souris anesthésiées. J'ai ensuite injecté *in vivo* dans le BO des molécules ciblant le GLP-1R dont l'agoniste Exendine-4 (Ex4), l'antagoniste Exendine-9 (Ex9) et l'hormone GLP-1 elle-même, et j'ai réalisé ensuite des tests métaboliques (i.e. test de tolérance au glucose oral: OGTT) et des tests de comportement olfactif.

2. Puis, par une technique chemogénétique qui a visé à étudier le mécanisme d'action du GLP-1R^{BO} grâce à la technologie DREADD (Designer Receptors Exclusively Activated by Designer Drugs), j'ai pu activer (grâce à l'injection de Clozapine N-oxide, CNO) de façon séquentielle et *in vivo* les neurones GLP-1R+ du BO (par le récepteur hM3Dq). Pour obtenir ces souris GLP-1RBO-hM3Dq, j'ai utilisé le système de recombinaison Cre-LoxP (injection stéréotaxique de virus adéno-associés (AAV) Cre-dependants chez des souris GLP-1R Cre), et pour mieux cibler le mécanisme d'action du GLP-1R^{BO}, j'ai aussi implanté une canule dans noyau paraventriculaire de l'HT (PVN). J'ai ensuite réalisé des tests métaboliques ainsi que de l'immunohistochimie (IHC), du RNAscope et du traçage neuronal.

Sur la base de ces développements méthodologiques, j'ai ensuite étudié deux phases cruciales du comportement alimentaire dans le modèle de souris obèse comparée aux souris de même âge mais sous régime standard (Regular Diet, RD) : l'état préprandial de préparation à la prise alimentaire, puis la phase postprandiale, une fois que le repas est consommé et que la glycémie augmente.

Pendant l'état préprandial, j'ai d'abord montré que chez les souris RD les odeurs alimentaires déclenchent une phase céphalique de la sécrétion d'insuline (CPIR), qui est bloquée par Ex9. De même, les souris RD auxquelles on a injecté un shRNA inhibiteur dirigé contre l'ARNm codant pour le peptide PPG dans les neurones PPG (souris PPG-shRNA), ne présentent pas de CPIR induite par les odeurs. Ainsi, nous avons mis en évidence que les cellules PPG+ dans le BO sont potentiellement activées par les odeurs alimentaires et jouent un rôle central dans le CPIR. De plus, cette phase céphalique est perdue chez les souris obèses qui présentent également une mauvaise détection olfactive. De manière intéressante, le CPIR ainsi que les performances olfactives sont améliorés chez les souris obèses par une injection aiguë d'Ex4 dans le BO.

En ce qui concerne le comportement alimentaire, nos résultats ont montré une augmentation aiguë de la prise alimentaire chez les souris RD après inhibition chemogénétique des cellules exprimant le GLP-1R dans le BO. Nous avons également observé une diminution de la prise alimentaire chez les souris obèses après activation des cellules GLP-1R+ bulbaires médiée par les DREADD, ce qui suggère un rôle du système GLP-1 bulbaire dans le contrôle de la prise alimentaire.

Pendant l'état postprandial, nos données montrent que l'injection aiguë dans le BO de GLP-1 ou d'Ex4 améliore la tolérance au glucose et stimule la sécrétion d'insuline en réponse au glucose chez la souris obèse. A l'inverse, l'injection dans le BO d'Ex9 aggrave l'intolérance au glucose des souris obèses, sans modification de l'insulinémie. En présence d'Ex9 dans le BO, l'effet potentialisateur sur la sécrétion d'insuline permettant d'améliorer la tolérance au glucose

d’une injection intrapéritonéale d’Ex4 est atténué. Ainsi, l'effet incrétine connu d'Ex4 nécessite l'activation du GLP-1R dans le BO.

Nous nous sommes ensuite interrogés sur les mécanismes neuronaux de transmission des informations entre le BO et les organes périphériques tels que le pancréas, aboutissant à une stimulation de la sécrétion d’insuline. Comment sont transmis les effets du GLP-1 bulbaire au pancréas, qui aboutissent à la stimulation de la sécrétion d’insuline ? Quelle est la voie nerveuse impliquée ?

Nous avons testé deux hypothèses de travail dont l’origine est dans la connexion entre BO et HT: La première est que le GLP-1 dans le BO induirait une augmentation de l’activité du système nerveux parasympathique (SNP) en connectant le BO à l’HT puis au noyau d’origine du nerf vague (DMX), lequel stimule la sécrétion d’insuline. La seconde est qu’il entraînerait une diminution de l’activité du système nerveux sympathique (SNS), qui inhibe la sécrétion d’insuline, *via* l’HT, puis le noyau intermédiolatéral (IML), source du nerf splanchnique qui innerve la périphérie par une transmission noradrénergique.

Pour étudier le rôle du SNP, nous avons procédé à une vagotomie subdiaphragmatique. Chez les souris vagotomisées, l’amélioration de la tolérance au glucose et l’augmentation de la sécrétion d’insuline suite à l’injection d’Ex4 dans le BO persistait, suggérant que le SNP ne pouvait expliquer l’effet sur la sécrétion d’insuline. Nous nous sommes alors focalisés sur la deuxième hypothèse : une diminution de l’activité du SNS. Suite à l’injection d’Ex4 dans le BO, nous avons observé une diminution du contenu en noradrénaline (NA, principal neurotransmetteur du SNS) dans le pancréas, ce qui pourrait expliquer, en partie, l’augmentation de la sécrétion d’insuline. En parallèle, mimer l’activation du SNS, *via* un agoniste des récepteurs adrénergiques α2 du pancréas (le UK14304), contrecarre les effets d’Ex4 dans le BO sur la tolérance au glucose et la sécrétion d’insuline. Ces résultats montrent que l’activation du GLP-$1R^{BO}$ entraine une inhibition du SNS vers le pancréas. Les neurones qui contrôlent la sortie du SNS sont localisés dans le noyau paraventriculaire (PVN) de l’HT et expriment le récepteur $GABA_A$ ($GABA_AR$). Une injection locale de Bicuculline (antagoniste $GABA_AR$) bloque l’effet bénéfique de l’activation des neurones bulbaires GLP-1R+ sur l’homéostasie glucidique chez la souris obèse. Nos données suggèrent donc que le PVN relaye l’action du BO vers le pancréas conduisant ainsi à une augmentation de la libération d'insuline.

Nous avons développé un réseau de collaborations pour valider la voie neuronale (OB → PVN → SNS → pancréas). Des techniques d’IHC (Daniela Cota et Vincent Simon, Institut NeuroMagendie, Bordeaux), de biologie moléculaire (Stefan Trapp et Wanqing Jiang, University College of London, UCL), de traçage neuronal et de RNAscope (Marie Holt, UCL) ainsi que des mesures de GLP-1 *in vitro* (David Jarriault et Xavier Fioramonti, Laboratoire NutriNeuro, Bordeaux) sont venues complétées nos expertises métaboliques et comportementales. De plus, en collaboration avec Lukas Van Oudenhove et Anne Christin Meyer-Gerspach (Université de

Louvain), nous avons étudié la connectivité neuronale entre différentes régions d'intérêt chez des sujets humains traités à l'Ex9 et au glucose. Cette étude IRM a montré une plasticité dans la connectivité entre le système olfactif, le système limbique et les régions de la récompense et du plaisir (hédoniques) en réponse à des changements métaboliques aigus incluant l'effet des GLP-1R.

L'ensemble de ces données acquises dans le cadre de ma thèse montre que, dans un modèle préclinique d'obésité, l'activation de la voie du GLP-1 dans le bulbe olfactif entraîne une diminution de l'activité nerveuse sympathique et, consécutivement, une amélioration de l'homéostasie glucidique. De plus, mes données valident le rôle important du système olfactif dans la régulation de l'homéostasie glucidique et elles permettent de le définir comme une structure cible de l'action centrale du GLP-1 *in vivo*. Ces nouvelles données sont particulièrement intéressantes compte tenu du potentiel thérapeutique du GLP-1 dans le cadre de l'obésité et du diabète de type 2 et du manque de données sur ses mécanismes d'action cérébraux.

List of content

ABBREVIATIONS 5

RESUME 6

SUMMARY 8

SECTION I

INTRODUCTION 11

CHAPTER I

FROM ENERGY HOMEOSTASIS TO METABOLIC SYNDROME 13

1. Role of organs in the regulation of glycemia and food intake..... 15

1.1. The biological mechanisms of energy homeostasis 15

1.2. Systemic responses to changes in the nutritional status..... 15

1.2.1. Gastrointestinal tract 15

1.2.2. Liver 16

1.2.3. Adipose tissue 16

1.2.4. Pancreas 17

a. Insulin 17

Structure 17

Synthesis and release 18

Physiological roles of insulin in systemic tissues 18

Physiological roles of insulin in the brain 18

Signaling pathway 19

Cephalic phase of insulin secretion 20

Insulin-regulating factors 21

Glucagon 21

Incretins 22

1.3. Central and autonomic neuronal regulation 23

1.3.1. Hypothalamus 23

Historical role of the hypothalamus in the control of food intake 25

Anatomy of the hypothalamus 25

The arcuate nucleus 26

The paraventricular nucleus 27

1.3.2. Central receptors to gastrointestinal hormones 27

Cholecystokinin 28

Ghrelin 29

Peptide YY_{3-36} 29

GLP-1 and GIP 29

1.3.3. Adiposity-related signals and its role in the CNS 30

Leptin 30

1.3.4. Nutrients 31

Amino acids and protein 31

Glucose 32

Free fatty acids 32

1.3.5. Autonomic Nervous System: the outputs. 33

a. The parasympathetic nervous system 34

b. The sympathetic nervous system 34

c. Parasympathetic and sympathetic innervation of the endocrine pancreas 35

2. Metabolic diseases 37

2.1. Obesity 37
2.2. Type 2 diabetes 38
2.3. Antidiabetic treatments 40
2.3.1. Therapeutic strategy for T2D 40
2.3.2. GLP-1 analogues 41

CHAPTER II

THE GLUCAGON-LIKE PEPTIDE-1 43

1. The discovery of GLP-1 and its identification as a gastrointestinal hormone 43

2. Synthesis and release of GLP-1 45

2.1. Expression and cleavage of preproglucagon gene 45
2.2. GLP-1 secretion by intestinal cells 46
2.3. GLP-1 degradation 48
2.4. GLP-1 release by cerebral structures 49

3. Effects of Glucagon-like peptide-1 51

3.1. GLP-1R localization in the body 51
3.2. Effects on β-cell insulin secretion 52
3.3. Central GLP-1R 54
3.3.1. GLP-1R localization in the brain 54
3.3.2. GLP-1 effects on food intake 54

CHAPTER III

THE OLFACTORY SYSTEM 57

1. Anatomical organization and function of the olfactory system 58

1.1. Olfactory receptors 60
1.2. The olfactory bulb: the first central relay of olfactory information 61
1.3. Olfactory system pathways 65
1.4. Behavioral assessment of mouse olfaction 66
1.5. Perceptual links between smell and the metabolic state in humans 68

2. Interplay between the olfactory bulb and energy homeostasis 70

2.1. Receptors to metabolic signaling molecules in the OB 70
2.1.1. Orexigenic signals 72
2.1.2. Anorexigenic signals 72
2.1.3. The voltage gated Kv1.3 channel 75
2.2. Physiology : interactions between the olfactory system and the energy balance regulation system 76
2.2.1. OB – hypothalamus – mesocorticolimbic system 76
2.2.2. Crosstalk between the metabolic state and olfactory perception 77
2.3. Pathophysiology : interactions between the olfactory system and the energy balance regulation system in the context of obesity 78
2.3.1. Animal models of obesity 78
a. Monogenic models of inducing obesity in animals 78
b. Diet-Induced Obesity models 79
2.3.2. Major axes linking olfaction, energy balance and obesity 80
2.3.3. Human studies (1). Does the sense of smell impact metabolic health and obesity? 83
2.3.4. Human studies (2). Glucose-induced brain activity in healthy and obese subjects assessed by fMRI 84

SECTION II.

THESIS STATEMENT 87

SECTION III

MATERIALS AND METHODS 91

1. Mice studies ***93***

1.1. Animal care *93*
1.2. Mice models *93*
1.3. Metabolic phenotyping *94*
1.4. Surgical and stereotactic procedures *94*
1.5. Metabolic tests *97*
1.6. Behavioral studies *98*
1.7. Noradrenaline levels *99*
1.8. Fluorescein-Trp25-Exendin-4 imaging *100*
1.9. Luxendin-647 fluorescence in the brain after IP injection *100*
1.10. cFos immunohistochemistry *101*
1.11. RNAScope *102*
1.12. Real time quantitative PCR *102*

2. GLP-1 content on OB slices ***103***

3. Human studies ***104***

3.1. Subjects and treatments *104*
3.2. fMRI data preprocessing *104*
3.3. Region of interest (ROI) definition *104*
3.4. Functional connectivity analysis *104*

4. Statistical methods ***105***

SECTION IV

RESULTS 107

1. The GLP-1 system is present in the OB ***109***

2. Odor-induced cephalic phase of insulin secretion is reversed by Ex9 in the OB and offers an optimal olfactory foraging in RD mice ***112***

3. Up and down chemogenetic modulation of GLP-1R+ neurons in the OB oppositely regulates food intake and glucose homeostasis ***115***

4. Pharmacological modulation of GLP-1R in the OB regulates glucose homeostasis ***119***

5. The activation of GLP-1R in the OB leads to an inhibition of the SNS outflow to the pancreas ***123***

6. A GABAergic inhibitory relay to the PVN, driven by GLP-1R^{OB} neurons, decreases the sympathetic nerve activity leading to an increase of insulin release from the pancreas in WD mice ***125***

7. Human brain connectivity under glucose and exendin9 + glucose conditions ***127***

7.1. Connectivity of the network across both conditions (Ex9+Glucose and Glucose conditions) *127*
7.2. Differences in connectivity of the network between both conditions Ex9+Glucose versus Glucose condition) *128*

SECTION V

DISCUSSION 131

1. Function of GLP-1/GLP-1R system in the OB 133

2. Preprandial regulation of glucose homeostasis. The role of the bulbar GLP-1R in odor-evoked CPIR 134

3. Preprandial regulation of glucose homeostasis. Can PPG cells in the OB mediate odor-evoked CPIR ? 137

4. Food intake modulation by GLP-1R+ neurons in the OB 137

5. Postprandial regulation of glucose homeostasis. Can circulating GLP-1 reach the OB? 138

6. Postprandial regulation of glucose homeostasis by GLP-1^{OB} and the effect on insulin secretion. 139

7. How are the effects of bulbar GLP-1 transmitted to the pancreas, leading to the stimulation of insulin secretion? Which neuronal pathway could be involved? 140

7.1. Decrease in sympathetic nerve activity 140

7.2. Decrease in PVN neuronal activity 141

8. Human brain connectivity under glucose and exendin9 + glucose conditions 144

9. Methodological considerations 145

9.1. "up and down" GLP-1R modulation strategy 145

9.2. Why did we choose to focus our work on WD mice halfway through the project? 145

9.3. In which point is our work based on the natural history of T2D? 146

9.4. What is the rationale behind doubling GLP-1 by Ex4? 146

10. Perspectives 146

10.1. OB to PVN circuits 146

10.2. PVN activity 147

10.3. OB activity 148

10.4. Further properties of PPG cells 148

10.5. GLP-1 system in the context of obesity: clinical vs pre-clinical studies 149

10.6. GLP-1 in the OB as a potential therapeutic target 150

11. Conclusion 151

ANNEX 153

BIBLIOGRAPHY 166

LIST OF FIGURES 196

MEETINGS AND PUBLICATIONS 198

Abbreviations

α-MSH: Melanocyte stimulating hormone
AgRP: Agouti-related protein
AMPK: AMP-activated protein kinase
ANS: autonomic nervous system
AON: anterior olfactory nucleus
AP: area postrema
AR : adreno-receptor
ARC: arcuate nucleus
BBB: blood brain barrier
BFT: buried food test
CAF: cafeteria (diet)
CART: cocaine- and amphetamine-regulated transcript
CCK: cholecystokinin
CNS: central nervous system
CPIR: cephalic phase of insulin secretion.
CRH: corticotropin-releasing hormone
CVO: circumventricular organs
DMH: dorsomedial hypothalamic nucleus
DMNX: dorsal motor nucleus of the vagus
DRG: dorsal root ganglia
dSAC: deep short axon cells
DTA: Diphtheria toxin gene A
EPAC: exchange protein directly activated by cAMP
Ex4: exendin-4
Ex9: exendin-9
FISH: fluorescent in situ hybridization
GC: granule cells
GCL: granular cell layer
GI: gastrointestinal
GIP: gastric inhibitory polyeptide
GL: glomerular layer
GLP-1: glucagon-like peptide-1
GLP-1RA: glucagon-like receptor agonists
GSIS: glucose-stimulated insulin secretion
HFD: high-fat diet
HGP: hepatic glucose production
i.p. : intraperitoneal
i.c.v. : intracerebroventricular
i.v. : intravenous
IGF-1: insulin growth factor-1
IHC: immunohistochemistry
IML: intermediolateral nucleus
IPL: internal plexiform layer
IR: insulin receptor
LHA: lateral hypothalamic area
LOT: lateral olfactory tract
MAPK: mitogen-activated protein kinase
MC: mitral cells
MCL: mitral cell layer
MRI: magnetic resonance imaging
NA: noradrenaline
NPY: neuropeptide Y
NTS: nucleus of the solitary tract
OB: olfactory bulb
OFC: orbitofrontal cortex
OM: olfactory mucosa
ONL: olfactory nerve layer
OR: olfactory receptor
OSN: olfactory sensory neurons
PC1/3 : prohormone convertase 1/3
PC2 : prohormone convertase 2
PC: piriform cortex
PFA: paraformaldehyde
PROK2: prokineticin 2
PKA: protein kinase A
PNS: parasympathetic nervous system
POMC: proopiomelanocortin
PPG: preproglucagon
PPG^{NTS}: preproglucagon neurons within the NTS
PPG^{OB}: preproglucagon neurons within the OB
PVN: paraventricular nucleus
Ra: raphe pallidus
RD: regular diet
SNS: sympathetic nervous system
SPANs: spinally projecting autonomic neurons
SVZ: subventricular zone
T2D: type 2 diabetes
TC: tufted cells
TUB: olfactory tubercle
VIP: vasoactive intestinal peptide
WD: western diet

Résumé

Nouveaux rôles du système GLP-1 dans la régulation de la balance énergétique via le bulbe olfactif : impact sur l'obésité et le diabète de type 2

L'obésité est un défi mondial pour la santé et est associée à des complications métaboliques majeures telles que le diabète de type 2. La consommation excessive des calories ainsi qu'une dérégulation de la communication hormonale entre le pancréas et d'autres organes comme le cerveau, impliqués dans la régulation de la balance énergétique, font partie des causes de ces troubles métaboliques. Parmi les hormones essentielles au métabolisme énergétique, le Glucagon-like peptide 1 (GLP-1) est une incrétine qui stimule la sécrétion d'insuline lorsque la glycémie est élevée. Bien qu'au niveau du système nerveux central (SNC) le GLP-1 augmente la satiété, ses mécanismes d'action sont mal connus. Dans le cerveau, le récepteur du GLP-1 (GLP-1R) est présent dans une grande variété de régions telles que le noyau du tractus solitaire, l'hypothalamus et le bulbe olfactif (BO). Le BO joue un rôle fondamental dans l'appréciation de la palatabilité et de la toxicité des aliments et des études récentes montrent sa sensibilité aux hormones métaboliques. Des données *in vitro* ont montré que les principales cellules du BO (appelées cellules mitrales) sont stimulées à la fois par le GLP-1 et l'Exendin-4 (Ex4, agoniste du GLP-1R). De plus, certaines populations neuronales du BO contiennent du preproglucagon (PPG) précurseur du GLP-1, ce qui renforce l'idée qu'il existe une action centrale du GLP-1 au sein du BO. Il a été montré chez les patients obèses que la structure et les fonctions du BO sont altérées. Dans ce contexte, mon projet de thèse vise à étudier le rôle du GLP-1 dans la balance énergétique par son action dans le BO dans l'obésité.

Le déroulement de mes travaux de thèse a nécessité la mise en place d'un modèle de souris obèse par régime hypercalorique (Western Diet, WD). Ce modèle récapitule plusieurs paramètres observés en clinique, tels que le surpoids, l'insulino-résistance ou l'intolérance au glucose. En utilisant des approches pharmacologiques (injections dans le BO de GLP-1, d'Ex4 ou d'Exendin-9, Ex9, antagoniste du GLP-1R) et pharmaco-chemogénétiques (DREADDs activateurs et inhibiteurs), combinées à des tests métaboliques, à l'immunohistochimie et au traçage viral, entre autres techniques, nous avons pu démontrer que la voie GLP-1 dans le BO est un nouvel acteur dans la régulation de l'homéostasie glucidique dans les états pré- et post-prandiaux.

Pendant l'état préprandial, chez les souris sous régime standard (Regular Diet, RD), les odeurs alimentaires déclenchent une phase céphalique de la sécrétion d'insuline (CPIR), qui est bloquée par Ex9. De même, les souris RD injectées dans le BO avec un shRNA ciblant l'ARNm codant pour le peptide PPG (souris PPG-shRNA) ne présentent pas de CPIR induite par les

odeurs. Ainsi, les cellules PPG+ dans le BO sont potentiellement activées par les odeurs alimentaires et jouent un rôle dans le CPIR. Cette phase céphalique est perdue chez les souris WD qui présentent également une mauvaise détection olfactive. De manière intéressante, le CPIR ainsi que les performances olfactives, sont améliorés par une injection aiguë d'Ex4 dans le BO des souris WD.

En ce qui concerne le comportement alimentaire, nos résultats ont montré une augmentation aiguë de la prise alimentaire chez les souris RD après inhibition chemogénétique des cellules exprimant le GLP-1R dans le BO. Nous avons également observé une diminution de la prise alimentaire chez les souris WD après activation des cellules GLP-1R+ bulbaires médiée par les DREADD, ce qui suggère un rôle du système GLP-1 bulbaire dans le contrôle de la prise alimentaire.

Pendant l'état postprandial, l'activation chemogénétique des cellules exprimant le GLP-1R, ainsi que l'activation pharmacologique du GLP-1R dans le BO, améliorent fortement l'homéostasie glucidique en augmentant la sécrétion d'insuline chez les souris WD. Cette amélioration de l'homéostasie du glucose persiste chez les souris vagotomisées tandis que la stimulation du GLP-1R bulbaire diminue les niveaux de noradrénaline pancréatique, ce qui indique une diminution du tonus du système nerveux sympathique (SNS) sur le pancréas. Ces résultats suggèrent donc que ce n'est pas le système parasympathique mais plutôt le SNS qui est le médiateur des effets du BO sur le pancréas, entraînant une augmentation de la sécrétion d'insuline.

Les neurones qui contrôlent la sortie du SNS sont localisés dans le noyau paraventriculaire (PVN) de l'hypothalamus et expriment le récepteur $GABA_A$ ($GABA_AR$). Une injection locale de Bicuculline (antagoniste $GABA_AR$) bloque l'effet bénéfique de l'activation des neurones bulbaires GLP-1R+ sur l'homéostasie glucidique chez la souris WD. Nos données suggèrent donc que le PVN relaye l'action du BO vers le pancréas conduisant ainsi à une augmentation de la libération d'insuline.

L'ensemble des résultats de mes travaux de thèse renforce le rôle important du BO dans la régulation de l'homéostasie glucidique et permet de le définir comme une zone cible de l'action centrale du GLP-1 *in vivo*. Nos données révèlent pour la première fois que la voie du GLP-1 dans le BO est un nouvel acteur essentiel de la régulation de l'homéostasie glucidique dans les états pré- et post-prandiaux dans le contexte de l'obésité.

Mots clés : obésité, GLP-1, GLP-1R, bulbe olfactif, circuits neuronaux, phase céphalique de la sécrétion d'insuline, sécrétion postprandiale d'insuline, homéostasie glucidique, prise alimentaire.

Summary

The GLP-1 system in the olfactory bulb mediates the regulation of pre- and post-prandial glucose homeostasis in health and obesity

Obesity is a worldwide threat for health and is associated with major metabolic complications such as type 2 diabetes. Excessive calorie consumption as well as disrupted hormonal communication between the pancreas and other organs such as the brain, involved in the regulation of energy balance, are among the causes of these metabolic disorders. Among the hormones essential for energy metabolism regulation, Glucagon-like peptide 1 (GLP-1) is an incretin that stimulates insulin secretion when blood glucose levels are high. Although at the level of the central nervous system (CNS) GLP-1 increases satiety, its mechanisms of action are not well understood. In the brain, the GLP-1 receptor (GLP-1R) is present in a wide variety of regions such as the nucleus tractus solitarius, hypothalamus and olfactory bulb (OB). The OB plays a fundamental role in the appreciation of food palatability and toxicity and recent studies have shown its sensitivity to metabolic hormones. *In vitro* data have shown that the main cells of the OB (called mitral cells) are stimulated by both GLP-1 and Exendin-4 (Ex4, a GLP-1R agonist). In addition, some neuronal populations in the OB contain the GLP-1 precursor preproglucagon (PPG), which supports the idea that there is a central action of GLP-1 within the OB. It has been shown in obese patients that the structure and functions of the OB are altered. In this context, my thesis project aims to study the role of GLP-1 in energy balance through its action in the OB in obesity.

The achievement of the objective required the establishment of a diet-induced obesity (DIO) mice model, allowing us to work in the pathophysiological context of obesity with an experimental model that brings together several parameters observed in clinics, such as overweight, insulin resistance or glucose intolerance. Using pharmacological (OB injections of GLP-1, Ex4 or Exendin-9, Ex9, GLP-1R antagonist) and pharmaco-chemogenetic (activatory and inhibitory Designer Receptors Exclusively Activated by Designer Drugs, DREADD) approaches, combined with metabolic tests, immunohistochemistry and viral tracing, among other thechniques, we could demonstrate that the GLP-1 pathway in the OB is a new actor in the regulation of glucose homeostasis in both pre- and postprandial states.

During the preprandial state, in lean mice (Regular Diet, RD), food odors trigger a cephalic phase of insulin secretion (CPIR), which is blocked by Ex9. Consistently, RD mice injected with a shRNA targeting PPG mRNA (PPG-shRNA mice) lack odor-induced CPIR. Thus, endogenous PPG cells releasing GLP-1 in the OB are potentially activated by food odors and play a role, together with bulbar GLP-1Rs, in the CPIR. This cephalic phase is lost in DIO mice fed a

western diet (WD) which also present poor olfactory detection. Interestingly, CPIR as well as olfactory performances are improved by an acute injection of Ex4 in the OB in WD mice.

With regard to feeding behavior, our results have shown an acute increase in food intake in RD mice after chemogenetic inhibition of GLP-1R-expressing cells in the OB, as well as a decreased intake in WD mice after DREADD-mediated activation of bulbar GLP-1R+ cells, suggesting a role of bulbar GLP-1 system in the control of food intake.

During the postprandial state, chemogenetic activation of GLP-1R-expressing cells as well as pharmacological activation of GLP-1R in the OB strongly improve glucose homeostasis by increasing insulin secretion in WD mice. This improvement in glucose homeostasis persists in vagotomized mice whereas bulbar GLP-1R stimulation decreases pancreatic norepinephrine levels, indicating decreased sympathetic nervous system (SNS) outflow to the pancreas. Therefore, these results suggest that it is not the parasympathetic system but rather the SNS that mediates the output effects from the OB to the pancreas, leading to increased insulin secretion.

Neurons that control SNS output are located in the paraventricular nucleus (PVN) of the hypothalamus and express the $GABA_A$ receptor ($GABA_AR$). A local injection of Bicuculline ($GABA_AR$ antagonist) blocks the beneficial effect of OB GLP-1R-expressing cells activation on glucose homeostasis in WD mice. Our data therefore suggest that the PVN relays the OB action to the pancreas leading to an increase in insulin release.

Together, the results of my PhD reinforce the important role of the OB in the regulation of glucose homeostasis and allow to define it as a crucial zone of the central GLP-1 action *in vivo*. Our data unravel for the first time that the GLP-1 pathway in the OB is a new actor in glucose homeostasis regulation in both pre- and postprandial states in obesity.

Key words: obesity, GLP-1, GLP-1R, olfactory bulb, neuronal circuits, cephalic phase of insulin secretion, postprandial insulin secretion, glucose homeostasis, food intake.

SECTION I

Introduction

Chapter I

From energy homeostasis to metabolic syndrome

Energy homeostasis is defined as a state of equilibrium between food intake and the body's energy expenditure. The stability of body weight and body fat reflect this state of balance. In fact, apart from certain periods of life during which the body weight is not stabilized (growth, gestation, breastfeeding or old age), the mechanisms regulating body weight in the long term are particularly effective.

I became interested in energy metabolism during my first bachelor's year. At that time, I was also a high-level athlete. My passions for sport and the understanding of biology excited my interest in physiology and metabolism: how does the body adapt to our energy needs? How do the brain, the sensory systems, communicate with the peripheral organs in order to regulate the major physiological functions such as nutrition? As an athlete, I have personally experienced the hardness of maintaining the equilibrium of energy balance throughout the season, including bone health, coping with fatigue, recovering from injuries and avoid menstrual dysfunction. Maintaining energy homeostasis is primordial for health and well-being and deals with more aspects of our lives than one might think at first glance.

An imbalance between our energy intake and expenditure leads to health deregulations (Figure I.1). Undernutrition leads to deleterious effects on tissues with serious changes in body functions and/or body composition, metabolic deficiency, associated with a worsening of disease prognosis, a decrease in life quality, and especially in the elderly, an increased risk of dependency and caregiving. On the other side of the balance, an energy surplus can lead to obesity and associated metabolic diseases. Abnormal glucose and lipid levels in the blood as well as high blood pressure will be diagnosed as metabolic syndrome. In addition, metabolic syndrome refers to the presence of a set of metabolic and hemodynamic parameters that increase the risk of T2D, heart disease and stroke (Adreelli and Ziegler, 2015).

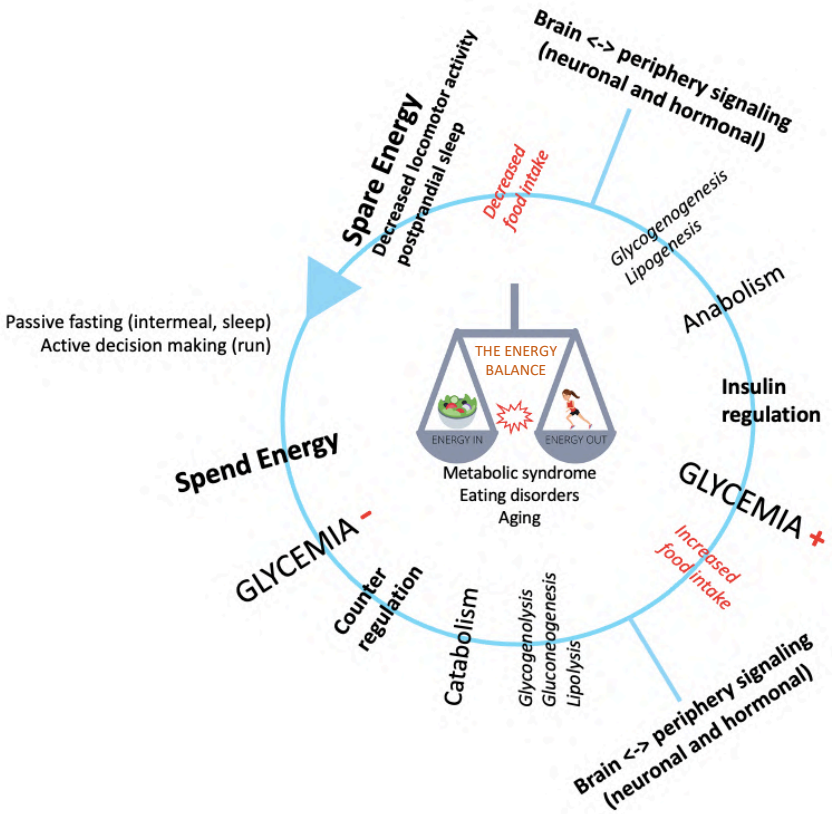

Figure I.1. The metabolic wheel, a dynamic equilibrium between energy intake and expenditure. Glycemia is tightly regulated thanks to fast and complex mechanisms on a daily basis: between meals and during night, glucose is consumed, glycemia (and insulinemia) slowly decrease activating counterregulatory mechanisms based on multiple hormonal regulation (catecholamines and cortisol followed by glucagon) of glycogenolysis, gluconeogenesis and lipolysis based on the feedback loops between the brain and the other organs. During a meal insulinemia rises and glycogen and triglycerides stocks are replenished by glycogenesis and lipogenesis mechanisms. Thus, catabolic and anabolic pathways are dynamically regulated by a constant brain to periphery crosstalk. Chronic hypercaloric intake combined with a sedentary lifestyle profoundly dysregulate these physiological mechanisms known as the energy balance, and lead to the pandemic of obesity and consequent T2D. Disturbed energy balance also occurs in eating disorders such as anorexia and bulimia and during physiological aging.

1. Role of organs in the regulation of glycemia and food intake

1.1. The biological mechanisms of energy homeostasis

Proposed for the first time by Kennedy in 1953, the biological mechanisms that this regulation system includes should be i) a processing center to control the state of reserves and ii) a crosstalk between energy reserves and this central operator. Most peripheral tissues are capable of sending a nervous or hormonal message to the brain, which is the operating center (Morton et al., 2014). To maintain energy balance, the brain must constantly collect and interpret hormonal, metabolic and nervous signals emitted by the peripheral tissues involved in the use and storage of energy (liver, muscle, fatty tissue).

Glucose homeostasis is highly dependent on a regulated dialogue between the brain and organs implicated in energy homeostasis such as the digestive tract, the liver, the adipose tissue, the pancreas… which runs on a basis of effective feedback loops that control food intake.

1.2. Systemic responses to changes in the nutritional status

In this subchapter, I will introduce metabolic changes following meal intake in peripheral tissues, as well as food anticipatory signals involved in the regulation of energy homeostasis. Central regulation of feeding will be described later.

1.2.1. Gastrointestinal tract

The gastrointestinal (GI) tract includes the mouth, the esophagus, the stomach, the small and large intestine, the rectum and the anus. It is continuously working in the background to maintain energy homeostasis, driving the digestion of nutrients and allowing all the systems to work properly, providing them proteins, carbohydrates, fats, vitamins, and minerals. Mechanical and chemical digestions are required for transforming food to energy. When we eat, our body converts food into energy. For that, mechanical (chewing and mixing), chemical (saliva or digestive juices like he bile) and enzymatic (e.g. amylases, proteases and lipases) digestions are essential. Some of these molecules could also participate in brain regulatory mechanisms (i.e. lipoprotein lipase, see review Cruciani-Guglielmacci and Magnan, 2017). Additionally, nutrients can also induce gut-brain signaling and thus have important implications in metabolic disorders (Van Oudenhove et al., 2011).

The stomach produces hormones that regulate food ingestion and digestion: gastrin and ghrelin. Gastrin increases gastric acid secretion and stimulates gastric epithelium proliferation, whereas ghrelin appears to be a strong stimulant of food intake and appetite. Its plasma concentration increases during long periods of fasting, has a peak in the period before meals and decreases after. A significant part of its increase before meals would be due to the anticipation of

the meal by the animal (Blum et al., 2009; Verhagen et al., 2011). In addition, when ghrelin is injected into the central nervous system, it has an action on the vagus nerve, the NTS and other hypothalamic nuclei (for review Suzuki et al., 2010) (c.f. *1.3. Central and autonomic neuronal regulation* for more details about the central role of ghrelin in food intake).

Other hormones secreted by the intestinal tract are for instance cholecystokinin (CCK), peptide YY (PYY), glucagon-like peptide-1 (GLP-1, c.f. *1.2.4. Pancreas -> Insulin-regulating factors -> Incretins* for its incretin role), gastric inhibitory polypeptide (GIP, c.f. the same *Incretins*), vasoactive intestinal polypeptide (VIP) along with others. The bacterial flora in the intestines also plays a crucial role in energy homeostasis. It can induce GI cells to secrete neurotransmitters of metabolic hormones that modulate brain function and behavior through a gut microbiota-to-brain signaling. The connection is bidirectional: the brain can in turn modify the microbiota composition and behavior *via* the ANS (Mayer et al., 2015).

Between meals, the non-liquefiable remnants are released from the stomach and reach the intestine to be eliminated. Everything is then put to rest, and the intestine can regenerate and repair its lining (epithelium). Continual cell renewal allows the epithelium to resist the continuous task of breaking down food, absorbing nutrients and eliminating the wastes.

1.2.2. Liver

The liver has long been seen as a mysterious organ. It was not until the 19th century, thanks to Claude Bernard's work, that its role began to be elucidated: he highlighted its ability to release glucose and, therefore, its role in the regulation of glycaemia. Nowadays, it is known that among systemic responses to an episode of acute energy deficiency (i.e. hypoglycaemia), the liver is playing a crucial role. It ensures glycogen storage, which is transformed into glucose (glycogenolysis) and released into the bloodstream to keep blood sugar levels constant when required (review Sharabi et al., 2015). Hence, during acute energy deficit, there is a rise of hepatic glucose production (HGP). This rise is not only due to glycogenolysis but also to hepatic gluconeogenesis, both partly mediated by increased plasma levels of glucagon and corticosterone (*via* the activation of the hypothalamus–pituitary–adrenal (HPA) axis). The increase in HGP results in a sufficient rise of blood glucose levels to normoglycaemia that turns off the hepatic response (review Lin et al., 2011).

1.2.3. Adipose tissue

The adipose tissue plays a key role in the regulation of energy homeostasis by acting as a caloric reservoir. It stores lipids under nutrient-surplus conditions, while releases energy to other tissues -through lipolysis- during deficit conditions (Birsoy et al., 2013). Storing and releasing lipids is just one role of this dynamic organ on energy homeostasis. The adipose tissue also secretes the adipocyte hormone leptin (Zhang, Y. et al. 1994) which reaches brain regions that

regulate energy balance through circulation. Leptin signal increases sensitivity to gut-derived satiety signals like CCK, which are released simultaneously with food ingestion and plays a crucial role on energy homeostasis (c.f. *1.3. Central and autonomic neuronal regulation* for more details).

1.2.4. Pancreas

The pancreas is a gland of the digestive system that produces pancreatic enzymes (exocrine part) and also hormones (endocrine part). The hormones produces by the endocrine pancreas regulate glucose homeostasis. These are insulin, which lowers blood sugar, and glucagon, which raises it. These hormones are produced and secreted according to the body's needs. Indeed, the precise control of glycaemia is directly dependent on the activity of the pancreas. Insulin is considered the main anabolic hormone of the body. Small variations in blood glucose levels observed throughout the day in healthy subjects are the result of a perfect balance between insulin sensitivity and insulin secretion (see the recent review Karpińska and Czauderna, 2022).

a. Insulin

Insulin is an anabolic peptide hormone secreted by β-cells of Langerhans islets in the pancreas. Its major role lies in the maintenance of carbohydrate homeostasis by regulating the balance between hepatic glucose production and its entry into the muscle and adipose tissue. It promotes lipid and protein metabolism as well as cell division and growth due to its mitogenic effects. The literature dealing with the insulin system is extremely large and not the main focus of my PhD. Therefore, I only provide a quick summary of elegant reviews that fully describe the insulin-dependent mechanisms (Rahman et al., 2021; Petersen and Shulman, 2018; Vecchio et al., 2018; Cahill, 1971).

Structure

Insulin is a 6 kDa hormone. It is a polypeptide containing two α and β chains linked together by two disulfide bridges. The α chain consists of 21 amino acids versus 30 for the β chain. This monomer of insulin is the active form of the protein. Insulin is, however, capable of dimerization. The combination of three dimers forms hexamers which are the major storage form of insulin within the secretory granules (Derewenda et al., 1989).

Synthesis and release

Insulin is initially synthesized as an immature polypeptide composed of a single chain of 110 amino acids: pre-pro-insulin. This pre-pro-insulin will be transformed into pro-insulin following a cleavage of a domain containing 24 amino acids in the within the rough endoplasmic reticulum (RER). Pro-insulin will then be transported from the RER to the Golgi apparatus where it will be transformed into insulin. This transformation is accompanied by the release of peptide-C. During the secretion of insulin, which occurs by exocytosis, peptide-C and insulin are co-secreted in an equimolar way (Wilcox, 2005). Insulin secretion is determined by the amount of glucose in the blood. Following a fasting, when blood glucose levels are low, the pancreas does not secrete insulin, or little amounts (physiological insulin levels at baseline). Conversely, after a meal, when blood sugar levels rise, the stimulation of insulin secretion is maximal (glucose-stimulated insulin secretion, GSIS).

Physiological roles of insulin in systemic tissues

In the skeletal muscle, insulin promotes glucose uptake as well as its conversion to glycogen. This tissue is the primary target of insulin, as it is the major site of glucose bioavailability *in vivo* (Kahn and Flier, 2000) and is known to be responsible for 70-80% of glucose uptake in response to insulin (Hegarty et al., 2003). In the liver, insulin stimulates glycogen synthesis by inhibiting gluconeogenesis and glycogenolysis, and prevents hepatic glucose release. Within adipose tissue, insulin stimulates glucose entry and conversion to triglycerides (TG) and inhibits lipolysis (Ahmadian et al., 2009). In addition to playing an important role in glucose metabolism, insulin is also involved in many cellular processes such as amino acid transport, protein synthesis and mitogenesis. The important role of insulin in the control of glucose metabolism explains the complexity of the regulatory systems in which this hormone is involved.

Physiological roles of insulin in the brain

In the brain, insulin acts as a neuropeptide involved in the phenomena of satiety, regulation of food intake, olfactory processing, memory and cognition (Gerozissis, 2004; Kim and Feldman, 2015; Woods et al., 1979). Insulin can be synthesized locally in the brain or be transported by blood flow (Gray et al., 2014) through the central nervous system (CNS) since it crosses the blood-brain barrier. Various studies in rodents have shown that a central injection of insulin reduces food intake and induces weight loss (Air et al., 2002).

Insulin receptors have been found in different brain structures including the olfactory bulb (OB) (Hill et al., 1986), hypothalamus, cerebral cortex, and hippocampus (Stockhorst et al., 2004; Ghasemi et al., 2013). They have been shown to be more numerous in neurons than in glial cells and be mainly located at the postsynaptic level (Unger et al., 1991). One study showed that a

deletion of insulin receptors in neurons promotes the development of obesity in female mice (Brüning et al., 2000).

Intranasal administration of insulin increases learning ability in both human and animal studies (Benedict et al., 2011; Thanarajah et al., 2019). It has also been shown that an injection of insulin directly into the hippocampus improves spatial memory (McNay et al., 2010). However, a disruption of the insulin signaling pathway makes neurons vulnerable to metabolic stress accelerating their dysfunction.

There is therefore accumulating evidence that insulin has a vast spectrum of functions in the brain controlling from food intake to several cognitive functions. Notably, metabolic and cognitive dysfunctions can be explained, in part, by impaired brain insulin actions (see Agrawal et al., 2021 for a review of insulin actions in the brain). We will further develop the impact of insulin on the OB in Chapter III (c.f. *2.1. Metabolic factors in the OB. Hormone-, peptide-, and energy-related receptors*).

Signaling pathway

Insulin has two important functions with different signaling pathways both emanating from the insulin receptor-IRS node:

- A metabolic function mediated by the phosphatidylinositol 3-kinase (PI3K, a lipid kinase)/AKT signaling pathway (Cantley LC., 2002). This one consists the general insulin signaling pathway (Figure I.2).
- A mitogenic function allowing proliferation as well as cell differentiation through the Raf/Ras/MEK/MAPK (mitogen activated protein kinase, also known as ERK) signaling pathway (Avruch J., 2007).

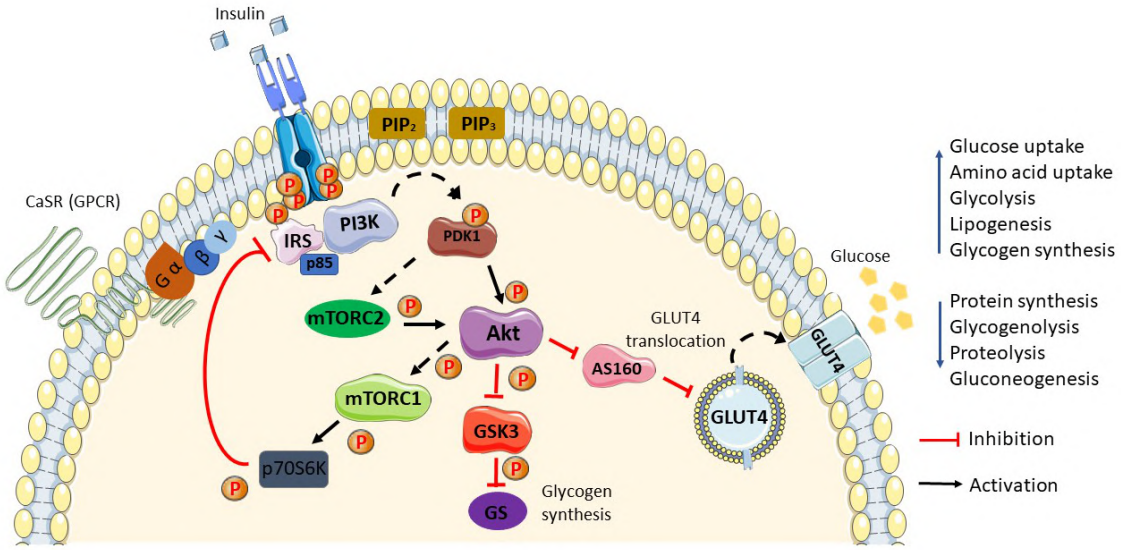

Figure I.2. Schematic illustration of the PI3K/AKT insulin signaling pathway. The phosphorylation of the receptor (tyrosine-kinase) recruits several downstream regulatory proteins. The insulin signal is transduced among the target proteins and enzymes until GLUT4 translocation to the plasma cell membrane.

Figure caption continued on next page

Phosphorylation activation (black arrow). Phosphorylation inhibition (red arrow). CaSR: calcium-sensing receptor; IRS: insulin receptor substrate; p85: phospho-PI3 kinase p85; PI3K: phosphoinositide 3-kinases; PIP2: phosphatidylinositol 4,5-bisphosphate; PIP3: phosphatidylinositol 3,4,5-bisphosphate; PDK1: phosphoinositide-dependent protein kinase-1; mTORC (1/2): mammalian/mechanistic target of rapamycin complex (1/2); Akt: protein kinase B; AS160: Akt substrate of 160 kDa; GLUT4: glucose transporter 4; GSK3: glycogen synthase kinase; GS: glycogen synthase; p70S6K: ribosomal protein S6 kinase β-1 (S6K1); P: phosphate. Image imported from *Encyclopedia.*

Cephalic phase of insulin secretion

Before the moment we start to eat, when we see food or we smell it, our body already starts sending signals and activates processes that precede digestion, called "cephalic phase responses". These anticipated responses allow the organism to prepare itself for the subsequent ingestion of food and its arrival in the gastrointestinal tract, and next for the postabsorptive arrival of nutrients in the blood stream. This unconscious anticipation moderates effectively the metabolic disturbances linked to the meal, for example by improving glucose tolerance.

It has been argued that these responses play an important role in regulating food intake and include physiological (salivary, gastric) –think about the sudden salivation felt by chefs preparing a vinaigrette– and endocrine responses such as pre-absorptive insulin release, also known as cephalic phase insulin response (CPIR). CPIR is a rapid and fleeting increase in blood insulin associated exclusively with sensory exposure to different food-stimuli that reliably predict the opportunity to eat but does not change glycemia. Hence, CPIR occurs prior to the increase in glycaemia observed following the intake of food and lasts for around 10 minutes. The amplitude of this cephalic response is shown to be strongly correlated with the palatability, or hedonic value, of food (Louis-Sylvestre and Le Magnen, 1980a). The authors of this work suggested that the quantity of food ingested could be affected by this pre-absorptive peak of insulin modulated by food palatability. Indeed, sensory systems seem to have an important role in food intake due to their involvement in the qualitative value of food – its aspect, its taste, its smell. It has been suggested that stimulation of sweet taste receptors on the tongue may act as a signal for evoking CPIR in rats (Berthoud et al., 1980). Olfaction also acts as a major indicator of the hedonic value of food, inducing preferences linked to pleasure (Le Magnen, 1999a).

After an analysis of the different onset times described in the literature, I think that the CPIR is best defined as all reflex responses, both secretory and motor, and is triggered in a conditioned, non-voluntary way by sensory stimuli usually associated with the context of the meal. CPIR occurs always prior to the first bite of food. As soon as there is food in the mouth, biochemical and neuronal activities rapidly change and we consider that the cephalic phase is over. Indeed, flavor, consistency, crunchiness... other type of information is available that you cannot get before, during the cephalic phase. Thus, the cephalic phase comprises the events

happening within the 10 minutes preceding a meal, e.g. when someone is queuing for its meal at the canteen. The peak of cephalic insulin, precisely, is reached 5±3 min after the presentation of the food stimulus (see thee review Lasschuijt et al, 2020).

Cephalic insulin secretion has been extensively studied and debated for many years. CPIR is recognized in animals [rats (Berthoud and Jeanrenaud, 1982; Berthoud et al., 1980), sheep (Herath et al., 1999) and dogs (Diamond and LeBlanc, 1988)], with a key role played by the vagus nerve (Woods and Bernstein, 1980). However, it is uncertain in humans. Despite a host of experimental data, human studies defined controversial results supporting (Parra-Covarrubias et al., 1971, Lorentzen et al., 1987; Teff, 2010, Wiedemann et al., 2020) or not (Teff et al., 1991; Teff et al., 1995) the presence of an early increase of insulin during the preprandial phase.

In rodents, the CPIR is dependent on vagal fibers that come from the brainstem and stimulate pancreatic β-cells, either directly by cholinergic pathway, or indirectly by prior stimulation of cephalic secretion of intestinal incretins such as GLP-1 (Louis-Sylvestre, 1978). A new study demonstrated that this vagal input mediating CPIR can be activated by the proinflammatory cytokine interleukin-1β (IL-1β) in healthy mice (Wiedemann et al., 2022). This molecule was previously shown to also stimulate postprandial insulin secretion, but its chronic excess is associated with insulin resistance and DT2 (Dinarello et al., 2010). Whether chronic inflammation also impairs CPIR in the context of obesity and T2D might be of relevance for further understanding of these chronic diseases.

Insulin-regulating factors

Insulin is secreted principally in response to a rise in blood glucose levels after eating. Nevertheless, other nutrients such as free fatty acids and amino acids can augment GSIS. Moreover, various hormones, such as melatonin, estrogen, growth hormone, leptin, glucagon and incretins also regulate insulin secretion.

Glucagon

Glucagon is a protein hormone produced and secreted by α-cells of Langerhans islets the pancreas, and consisting of 29 amino acids. As mentioned before, glucagon has antagonist effects on blood glucose to those of insulin (Figure I.3). In addition to its role rising blood glucose concentration, glucagon has also an intra-islet paracrine effect on insulin secretion from the islet β-cells, evoking a rise in insulin concentrations (Ahrén, 2015). This appears to provide a fine-tuned output in response to metabolic needs. In the 2010's, glucagon action on glycemia has drawn further attention with several studies reporting major effects on hepatic glucose regulation by this hormone (Ozcan et al., 2012; Wu et al., 2018).

Incretins

Glucose and other nutrients were shown to be more effective in stimulating insulin release when given orally than intravenously. This is due to what is called the "incretin effect", or the contribution of incretins to insulin secretion: the release of insulin by the pancreas is greater when the glucose stimulus is gastrointestinal, compared to when the stimulus is intravenous (i.v.). In fact, incretins are intestinal hormones released into the bloodstream in response to nutrient ingestion. They are involved in glucose homeostasis, regulating insulin and glucagon secretion in a glucose-dependent manner.

The suggestion that the gut produces factors following the ingestion of nutrients, that stimulate pancreatic release of hormones to modulate glycaemia, was proposed for the first time in the early 1900s (Starling, 1905; Moore, 1906). Few years later, the term "incrétine" was coined by the Belgian Jean La Barre, to name these gut hormones stimulating endocrine secretion from islet cells during the postprandial phase (La Barre, 1932). In 1967, Michael J. Perley and colleagues showed that in healthy subjects, oral glucose administration induces greater insulin secretion than i.v. administration (Perley et al., 1967). This result was confirmed by the work of Nauck et al. who, during isoglycemic clamps, showed that c-peptide levels of subjects whose glucose was administered orally was higher than that of subjects whose glucose was venously-administered (Nauck et al., 1986). 50 to 70% of the insulin secreted is due to the incretin effect. The development of molecular biology techniques made it possible to identify intestinal molecules that increase insulin secretion.

The first incretin that has been identified was the Glucose-dependent Insulinotropic Peptide (GIP) by Dupre et al. in 1973 (Dupre et al., 1973). In 1987, decisive works from the laboratories of Habener and Holst (Mojsov et al., 1987; Holst et al., 1987) added a second incretin, the Glucagon-like peptide 1 (GLP-1), providing evidence of its potent insulinotropic effect. Its structure was discovered during proglucagon (its precursor) investigations.

GIP is a 42 amino acid peptide hormone produced by K cells in the duodenum and jejunum. Its secretion is stimulated mainly by glucose. After a meal, GIP stimulates the release of insulin and glucagon by its action on GIP receptors (GIPR) in the pancreas (Christensen et al., 2011; Finan et al.,2016) (Figure I.3). The hormone has also an effect on food intake through the hypothalamus (Adriaenssens et al., 2019). Consistent with the latter, a recent study revealed the essential role of CNS GIPR signaling on systemic energy metabolism (Zhang et al. 2021), supporting metabolic effectiveness of GIP-based pharmacotherapies. Although GIP-R-expressing cells in the hypothalamus were shown to regulate food intake, the olfactory bulb is interestingly the rodent cerebral region with the largest GIP-R expression (The Human Protein Atlas). To date, there is no *in vitro* or *in vivo* studies about the action of this incretin in the OB so far.

GLP-1 is a 30 amino acid peptide hormone (GLP-1 7–36) cleaved from proglucagon in intestinal L cells, which are distributed through the distal small intestine and the colon. Levels of

GLP-1 increase drastically following glucose consumption, and to a minor amount following intake of other nutrients. In addition to enhancing GSIS, GLP-1 is nowadays known to exert numerous other effects, for instance inhibition of pancreatic glucagon secretion, gastric emptying and food intake or stimulating β-cell proliferation (Figure I.3) (c.f. *Chapter II* for more details about GLP-1).

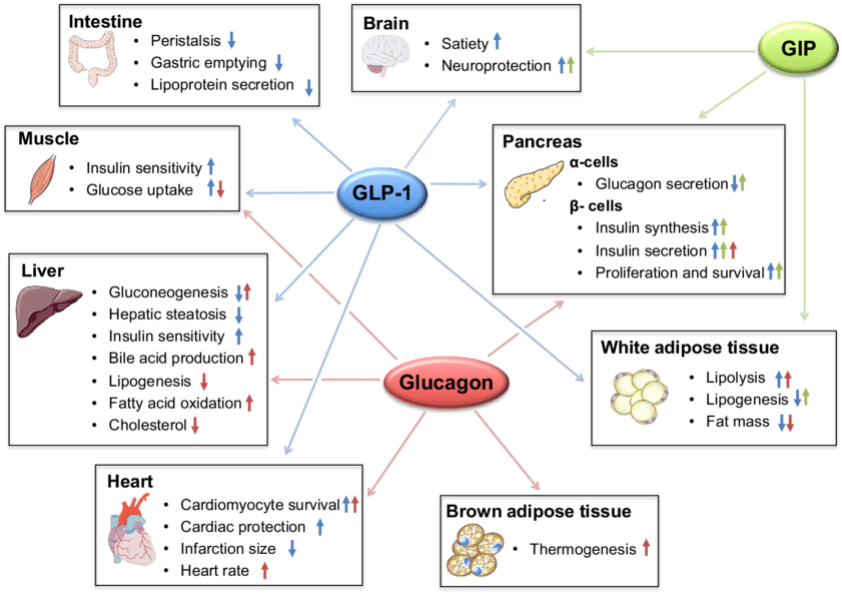

Figure I.3. Insulin-regulating factors. Effects of glucagon (red arrows), GIP (green arrows) and GLP-1 (blue arrows) on energy homeostasis in specific metabolic tissues. *From Brandt et al., 2018.*

1.3. Central and autonomic neuronal regulation

1.3.1. Hypothalamus

The hypothalamus and the brainstem are the main regions in the CNS for the regulation of energy balance. Nevertheless, these regions are not the only ones responsible of this balance. Both of them receive neural and hormonal inputs relaying information about the nutritional state of the body (energy availability and adiposity) (Murphy and Bloom, 2006) which are constantly integrated with higher brain centers (e.g. relaying reward with the limbic system). This integration allows a fine regulation of appetite and energy expenditure.

For the rest of this subchapter, I will give exclusive attention on the role of the hypothalamus in the control of energy homeostasis.

In Vertebrates, the hypothalamus is a CNS structure belonging to the diencephalon (Figure I.4A). It is located at the base of the brain, above the brainstem and below the thalamus, and is organized into a bilateral collection of nuclei divided symmetrically surrounding the 3rd ventricle (Baroncini et al., 2012). The release of hypothalamic neurohormones into the hypothalamus-

pituitary portal system or directly into the systemic circulation allows the hypothalamus to participate in the dialogue that exists between the nervous system and the endocrine system.

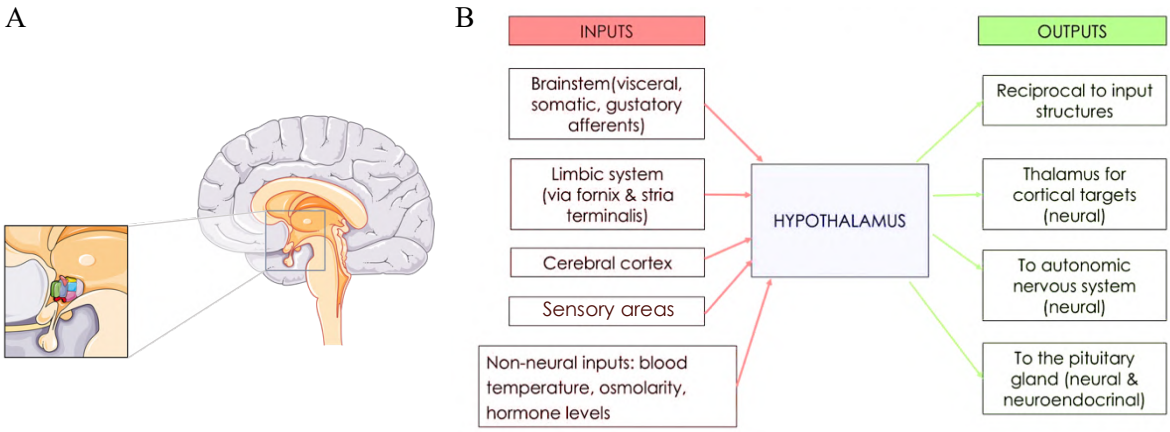

Figure I.4. Localization and connectivity of the hypothalamus. (A) Hypothalamus localization in the human brain. The hypothalamus is located at the base of the brain, above the pituitary gland with which it forms the hypothalamic-pituitary axis. It is composed of several nuclei (in color), is involved in the regulation of key physiological and behavioral processes such as the control of energy homeostasis. Image source: http://www.servier.fr. (B) Hypothalamic inputs and outputs. The brainstem, the limbic system, the cerebral cortex and sensory areas, as well as non-neural inputs such as hormone levels, send inputs to hypothalamic nuclei. As a result of hypothalamic signal integration, there is a reciprocal output to the input structures, as well as mainly to the thalamus or the autonomic nervous system. The neuro-endocrine cells of the pituitary gland also receive releasing signals from the hypothalamus, such as oxytocin or antidiuretic hormone (ADH).

The hypothalamus establishes afferent as well as efferent connections with many brain regions from the telencephalon to the myelencephalon such as the retina, olfactory areas, cerebral cortex, hippocampus, amygdala, circumventricular organs, or brainstem (Figure I.4B) (Lemaire et al., 2011). The organization of the hypothalamus as well as the connections it establishes with the rest of the brain give it a major role in the regulation of various physiological and behavioral processes such as thermoregulation, thirst, circadian rhythms, sexual differentiation, reproduction, respiration, lactation, cardiac rhythm, and energy homeostasis, the latter being the focus of this thesis.

Historical role of the hypothalamus in the control of food intake

The involvement of the hypothalamus, at least in part, in the control of energy homeostasis was speculated in the beginning of the XXth century (Keller et al.,1936). The concept evolved over time with studies demonstrating the involvement of the ventromedial and lateral hypothalamus in the development of hyperphagia and obesity in dogs, rats (Anand & Brobeck, 1951), cats and monkeys. These experiments gave rise to the schematic concepts of a "satiety center" for the ventromedial hypothalamus (whose lesion induces chronic hyperphagia leading ultimately to obesity) and a "hunger center" for the lateral area of the hypothalamus (whose lesion induces a decrease in food intake associated with weight loss).

Since then, the notions of functional satiety and hunger centers had evolved into a more complex hypothalamic organization in the form of groups of specialized neurons, the hypothalamic nuclei, expressing specific peptides and modulated by signals reflecting the energy status of the body (Schwartz et al., 2000; Williams et al., 2001).

It should be noted, however, that although the hypothalamus (along with the brainstem) is considered as the main structure involved in the maintenance of energy homeostasis, it is not the only brain area involved in this crucial regulation (Berthoud, 2006). Indeed, many studies have shown the existence of a complex brain network involving the parabrachial nucleus (Hajnal et al., 2009), area postrema (Beverly et al, 1990; Truong et al., 2002), nucleus accumbens and amygdala (Will et al., 2003), cerebral cortex and hippocampus (Davidson et al., 2009) as well as sensory structures such as the visual and the olfactory system (Chen et al., 2015, Riera et al., 2017, Faour et al., 2022).

Anatomy of the hypothalamus

Within the hypothalamus, a historical distinction was made between the so-called 1st order nucleus (arcuate nucleus, ARC), and the 2nd order nuclei (paraventricular, dorso and ventromedial nuclei, lateral hypothalamic areas) (Figure I.5). 1st order nucleus projects to the 2nd order nuclei and they act in concert to adapt food intake to the energy requirements of the body.

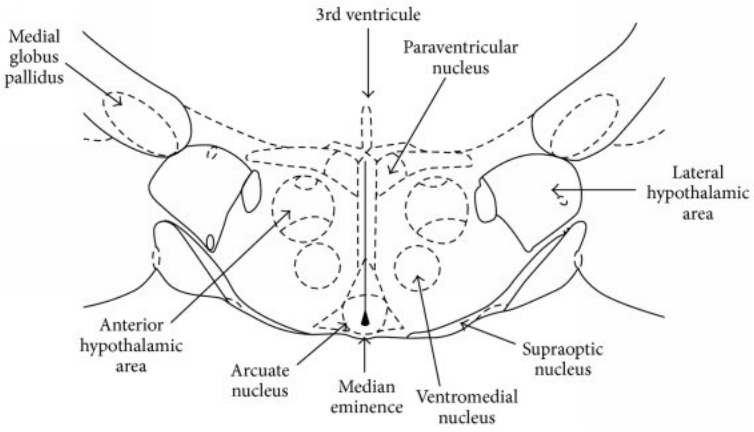

Figure I.5. Symmetric overview of the major hypothalamic nuclei.

Paraventricular nucleus, anterior hypothalamic area, lateral hypothalamic area, arcuate nucleus, ventromedial nucleus and supraoptic nucleus. *Image source: Bakos et al., 2016.*

From here on, a particular focus will be given to the arcuate and paraventricular nuclei for their role on the control of food intake and autonomic responses to periphery, respectively.

The arcuate nucleus

The arcuate nucleus extends rostro-caudally across the posterior half of the hypothalamus. It is located at the base of the 3rd ventricle and lies adjacent to the median eminence (Figure I.5), a circumventricular organ permeable to circulating peptides and proteins such as insulin and leptin. This anatomical location gives it particular accessibility to peripheral signals, making the arcuate nucleus the first hypothalamic relay between the peripheral organs and the CNS, thus integrating peripheral signals necessary to maintain energy homeostasis (Niswender et al., 2004). The arcuate nucleus hosts cell bodies of neurons that can be classified into two populations :

- A population of anorexigenic neurons located in the ventrolateral arcuate nucleus (Meister, 2007) and expressing POMC (Pro-opiomelanocortin), a protein precursor of two classes of peptides: melanocortins (such as α-MSH: Melanocyte Stimulating Hormone) and β-endorphins. Most POMC neurons in the arcuate nucleus also express CART (Cocaine and Amphetamine-Related Transcript) peptide. α-MSH and CART peptides exert an inhibitory action on food intake (Elias et al., 1998). POMC neurons are glutamatergic (Collin et al., 2003), third of them GABAergic (Hentges et al., 2004), or cholinergic (Meister et al., 2006).

- A population of orexigenic neurons co-expressing neuropeptide Y (NPY) and Agouti related Protein (AgRP) (Allen et al., 1983). Neuropeptides expressed by these cells stimulate food intake (Clark et al., 1984). These neurons have a GABAergic phenotype (Meister, 2007).

Neurons in the arcuate nucleus are located in a preferred site of expression of feeding-regulatory receptors for signals such as leptin (Schwartz et al., 1997) or insulin (Benoit et al., 2002). In response to these satiety signals, NPY neurons are hyperpolarized and experience a decrease in the rate of action potential firing (Cowley et al., 2003). The steady inhibitory tone that they exert on POMC neurons is then removed and POMC neurons are depolarized. This results finally in an inhibition of food intake. Hence, 1st order neurons of the arcuate nucleus are modulated by peripheral signals and constitute an essential relay between periphery and the CNS. These neurons project to the 2nd order neurons of the paraventricular nuclei and the lateral hypothalamic area (Williams et al., 2001).

The paraventricular nucleus

The paraventricular nucleus (PVN) is adjacent to the upper part of the 3rd ventricle in the anterior hypothalamus (Figure I.5). Within this structure, parvocellular and magnocellular neurons can be distinguished (Swanson and Sawchenko, 1983). Experiments involving lesions of the paraventricular nucleus have demonstrated its involvement in the regulation of energy balance (Sims and Lorden, 1986). The paraventricular nucleus constitutes an integrator center. In particular, it is the convergence site of projections from NPY/AgRP and POMC/α-MSH neurons of the arcuate nucleus (Elmquist et al., 1999). Orexin-expressing neurons from the lateral hypothalamic area (LHA) also project into the PVN.

PVN neurons express the melanocortin receptor MC4R, its agonist being α-MSH and, its antagonist, AgRP. They also express the NPY receptor Y1R allowing neuropeptide Y to stimulate food intake through this structure. The paraventricular nucleus is the site of synthesis of 2nd order anorectic neuropeptides such as Corticotropin Releasing Hormone (CRH) or Thyrotropin Releasing Hormone (TRH) (Schwartz et al., 2000). It also participates in the control of the autonomic innervation of peripheral organs such as the pancreas, liver, adipose tissue and adrenal glands (Kalsbeek and Buijs, 2002) (c.f. *2.3.2. Peripheral nervous system* for more details about the role of the PVN in the regulation of the sympathetic nerve).

1.3.2. Central receptors to gastrointestinal hormones

Many structures in the CNS have receptors for metabolic hormones synthesized in systemic tissues, and integrate qualitative and quantitative nutritional information from food as well as energy needs and reserve levels of the body (Figure I.6).

These hormones, which I have mentioned several of them before, induce the activation of central orexigenic or anorexigenic signaling and participate in the regulation of energy balance (Table I.1 - Luquet and Magnan, 2009).

Table I.1. List of central and peripheral signals involved in feeding behavior and energy balance. In plain character, central signals; in italic, circulating signals. *Adapted from Luquet and Magnan, 2009.*

Molecules that stimulate feeding and reduce energy expenditure	**Molecules that inhibit feeding and increase energy expenditure**
Neuropeptide Y (NPY)	α-melanocyte stimulating hormone (α-MSH)
Agouti-Related Protein (AgRP)	Cocaine and amphetamine-related transcript (CART)
Melanin-Concentrating Hormone (MCH)	Corticotropin-releasing hormone (CRH)
Norepinephrine	Thyrotropin-releasing hormone (TRH)
Orexin A and B	Neurotensin
Opioids	Serotonin
Endocannabinoids	Oxytocin
β-endorphin	*Leptin*
Ghrelin	*Insulin*
	Glucagon-like peptide-1
	Gastric inhibitory polypeptide (GIP)
	Peptide YY_{3-36} (PYY_{3-36})
	Oxyntomodulin
	Cholecystokinin (CCK)

Cholecystokinin

Cholecystokinin (CCK) is a peptide hormone secreted by I-cells of the upper small intestine in response to peptides, amino acids and fatty acids into the stomach or duodenum. CCK regulates intestinal motricity and stimulate pancreatic and gastric secretions in the periphery *via* the CCK-R1 receptor in the digestive tract (Moran, 2004). In the CNS, it acts preferentially *via* the CCK-R2 receptor, particularly in the lateral hypothalamic area, the dorsomedian nucleus, the paraventricular nucleus and the nucleus of the solitary tract (NTS). Various studies have shown that endogenous CCK acts as a short-term satiety factor regulating meal size (Konturek et al., 2003). In addition, both peripheral and central administration of CCK reduces meal size and duration (Figlewicz et al., 1986; Kissileff et al., 2003).

The effect of CCK has been shown to be mediated by vagal inputs since both sub-diaphragmatic vagotomy and vagal deafferentation abolishes CCK satiety action (Cummings and Overduin, 2007).

Ghrelin

To date, Ghrelin is the only peripheral orexigenic signal known. Its role in the regulation of energy balance is now well established in rodents (Tschöp et al., 2000). It is a 28 amino acid peptide mainly synthesized by the endocrine cells of the stomach epithelium as well as by the upper part of the intestine (Date et al., 2000). At the level of the hypothalamus, ghrelin has been detected in the neurons of the arcuate nucleus, as well as its receptor, GHS-R (growth hormone secretagogue receptor). In the arcuate nucleus, it activates orexigenic neurons, stimulates the production of NPY and AgRP, and inhibits anorexigenic neurons, opposing the action of leptin and thus inducing an increase in food intake and body weight (Cowley et al., 2003). Studies in animals have shown that i.c.v. administration of ghrelin induces an increase in hunger coupled with an increase in food intake and body fat as well as gastric acid secretions (Szentirmai et al., 2007; Tschöp et al., 2000).

In humans, plasma ghrelin levels increase during fasting (Ariyasu et al., 2001) and peak transiently during the preprandial phase, suggesting a role for the hormone in the initiation of food intake (Cummings et al., 2001).

Peptide YY_{3-36}

Peptide YY_{3-36} is the active anorectic form of peptide YY. This 36 amino acid peptide is synthesized by L-cells in the distal part of the intestine. Peripherally, PYY_{3-36} controls gastric motility and water and electrolytes absorption by the intestines. PYY_{3-36} production occurs during the postprandial phase, correlated to calories ingested (Adrian et al., 1985) and its plasma concentration is maintained high for several hours after meal termination. Peripheral administration of PYY_{3-36} inhibits food intake and decreases body weight (Batterham et al., 2007). Centrally, it stimulates α-MSH release and inhibits NPY production in the arcuate nucleus (Wynne et al., 2004).

GLP-1 and GIP

GIP and GLP-1 are the two primary incretin hormones secreted from the intestine during nutrients ingestion and thought to be strongly involved in the central control of appetite.

I decided to mention them in this subchapter as they are crucial in the list of gastrointestinal hormones controlling appetite, but I won't give further details since I have described GIP before (c.f. *1.2.4. Pancreas -> Insulin-regulating factors -> Incretins*) and I will dedicate a whole chapter to GLP-1, the main focus of this project (c.f. *Chapter II*).

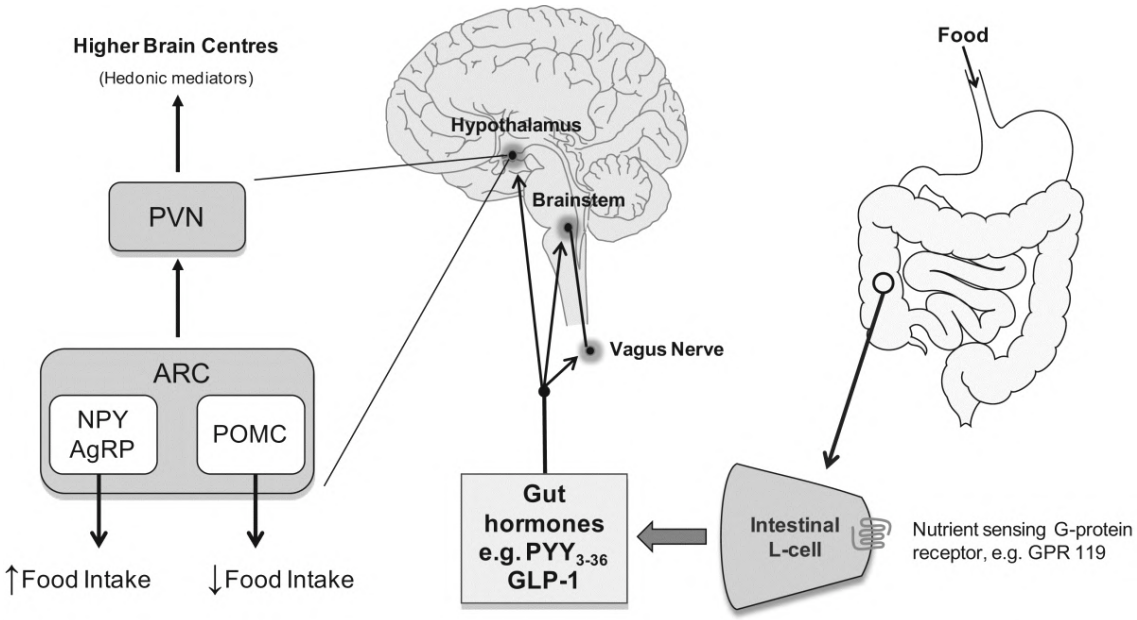

Figure I.6. Overview of the gut-brain axis and the regulation of food intake. Nutrients resulting from food digestion may activate G-protein coupled receptors on the luminal side of enetroendocrine cells in the intestines (e.g. L-cell). This stimulates the release of gut hormones which may influence food intake *via* vagus nerve afferences, the brainstem and the hypothalamus. Within the ARC, two neuronal populations are essential for the integration of peripheral signals controlling feeding: the orexigenic NPY/AgRP neurons and the anorexigenic POMC neurons. Extra connections between hypothalamic nuclei and higher brain centers allow the control of the hedonic value of food. ARC: arcuate nucleus; AgRP: agouti related peptide; GLP-1: glucagon-like peptide-1; NPY: neuropeptide Y; POMC: propiomelanocortin; PVN: paraventricular nucleus; PYY: peptide YY_{3-36}. *Image source: Field et al., 2010*.

1.3.3. Adiposity-related signals and its role in the CNS

Leptin

Leptin is a 16 kDa hormone mainly synthesized by the adipose tissue. It is produced by the mouse *obese* gene primarily in the adipose tissue and acts as a satiety factor by modulating the activity of specific hypothalamic nuclei. In effect, its discovery revolutionized the understanding of the central networks controlling energy balance (Zhang et al., 1994).

The leptin receptor can be presented in six isoforms resulting from alternative splicing of the db (or *Lepr*) gene. The long isoform ObRb ensures the physiological actions of leptin such as the maintenance of energy balance. This form is highly expressed in the hypothalamus. Mice lacking leptin (ob/ob) become morbidly obese due to metabolic disruption and hyperphagia. Diabetic db/db mice has a comparable phenotype to that of ob/ob mice.

In the CNS, the hypothalamus represents a major target for the anorectic action of leptin. Indeed, various studies have shown that intraperitoneal injections of leptin, which is produced in

proportion to body fat, induce the activation of hypothalamic nuclei neurons (Schwartz et al., 1996; Ahima, 2000). In the arcuate nucleus, leptin modulates the activity of orexigenic and anorexigenic neurons. Indeed, it inhibits the expression of orexigenic neuropeptides NPY and AgRP and activates the expression of anorexigenic neuropeptides POMC and CART. Leptin induces i) a depolarization of POMC/CART neurons (Hill et al., 2008) and ii) a decrease of GABAergic inhibitions exerted by orexigenic neurons on anorexigenic neurons (van den Top et al., 2004). In addition to its predominant role in the control of energy homeostasis, leptin has a neurotrophic action during the development of hypothalamic pathways for the control of food intake.

Various studies present the arcuate nucleus as the main center of action of leptin. However, a more global role for leptin in the brain has been proposed (Myers and Simerly, 2010), suggesting that the broad spectrum of functions regulated by leptin cannot be solely due to the activation of the ventromedial hypothalamus. More specifically, the control of energy homeostasis would result from the combined action of leptin on several extra-hypothalamic brain regions, such as the ventral tegmental area (VTA), the striatum -for the hedonic value of food intake (Hommel et al., 2006)- or the nucleus of the solitary tract for the sensation of satiety.

1.3.4. Nutrients

Amino acids and protein

The involvement of dietary proteins and circulating amino acid concentrations in the regulation of food intake was suggested as early as the 1970s (Mellinkoff et al., 1997). Dietary protein has a short-term satietogenic effect (Porrini et al., 1997). This decrease in food intake is due to increased portal vein glucose levels, mainly from intestinal gluconeogenesis (Mithieux et al., 2005), which has been shown to be crucial for early metabolic changes after gastric bypass (Troy et al., 2008).

The work of Monda et al. (1997) emphasize the role of the lateral hypothalamic area in the cerebral modifications of amino acid homeostasis. Indeed, the activity of lateral hypothalamic neurons is modified by the injection of L-threonine into the prepiriform cortex in rats fed a threonine-free diet. Additionally, leucine exerts its satiety effect by stimulating POMC neurons in the arcuate nucleus (Blouet et al., 2009). Furthermore, the administration of phenylalanine or tryptophan, precursors of monoamine neurotransmitters (e.g. catecholamines), induced food intake (Rogers and Blundell, 1994).

Glucose

In addition to its role as a primary energy substrate for brain function, it is now well established that glucose plays a role as a metabolic signal to regulate food intake (Mayer, 1996). Indeed, studies in humans and/or animals have shown that hypoglycemia is associated with increased hunger and food intake (Smith and Epstein, 1969; Thompson and Campbell, 1977). In the CNS, intracerebroventricular (i.c.v.) infusion of glucose induces a decrease in food intake and an increase in energy expenditure (Fujita et al., 2003; Le Feuvre et al., 1991). Conversely, induction of glucopenia in the lateral hypothalamus induces a decrease in energy expenditure in rats (Egawa et al., 1989).

Some neurons in the hypothalamus have an activity that is modulated by glucose concentration. They are called GR (Glucose Responsive) neurons, whose activity increases when glucose levels rise, and GS (Glucose Sensitive) neurons, whose activity is inhibited by high glucose concentrations. These neurons were first identified in the ventromedian nucleus (VMN) and the LHA (Anand et al., 1964; Oomura et al., 1969), however it is now known that the arcuate and paraventricular nuclei also have such neurons (Penicaud et al., 2002; Routh, 2010). The cellular and molecular mechanisms by which these neurons detect blood glucose variations would involve Glut-2 transporters (Leloup et al., 1998), glucokinase (Yang et al., 1999) and ATP-dependent potassium channels (Miki et al., 2001), common mechanisms also described for the pancreas. These type of neurons have also been found in other areas than the hypothalamus including the brainstem, the cortex, the hippocampus, the thalamus, the amygdala, or the olfactory bulb (reviewed in Steinbusch et al., 2015). I will further describe the sensitivity of bulbar mitral cells to glucose levels in Chapter III. This online detection of glucose content is essential for the survival of brain cells that depend tightly on continuous glucose supply. As a matter of fact, pronounced hypoglycemia can easily lead to fainting, i.e. loss of consciousness. For further information about the new advances on the study of glucose detection by hypothalamic neurons, see the review Fioramonti et al., 2017.

Free fatty acids

For a long time, the possibility that circulating fatty acids (FA) may have an action on the brain was ignored because they were thought to not cross the blood-brain barrier (BBB). However, a solid growth of data confirm that the source of cerebral lipids come from both local synthesis and plasma origin (Rapoport et al., 2001). Since the hypothalamus have different BBB structure and function compared to other parts of the brain (reviewed in Abbott et al., 2006), substances may reach it easily. Similar BBB-permeability properties have been found in the olfactory bulb (Ueno et al., 1991).

The so called “FA sensing”, or “lipid sensing”, and its implication in the control of food intake, HGP and insulin secretion is demonstrated by several studies. For instance, an i.c.v.

injection of triglycerides (as an emulsion) alters insulin secretion and HGP in rats (Clement et al., 2002, Cruciani-Guglielmacci et al. 2004). Also, i.c.v. administration of oleic acid induces a

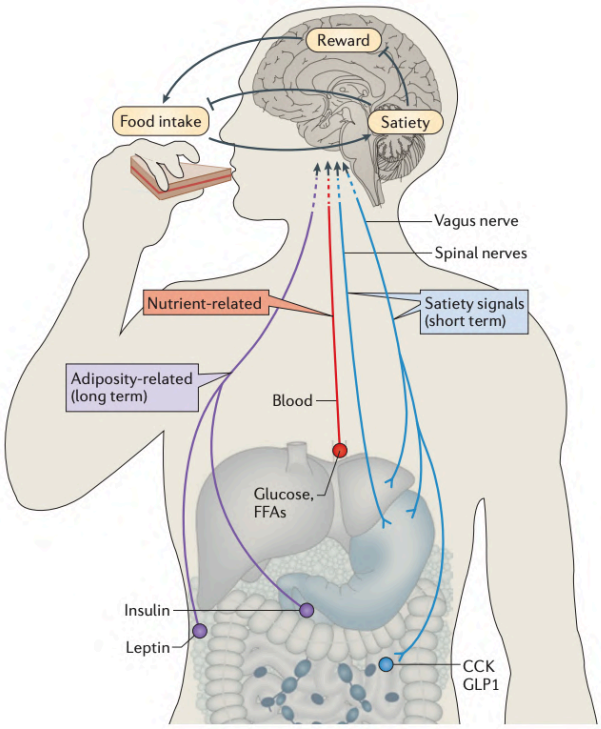

decrease in NPY expression levels in the hypothalamus associated with a decrease in food intake (Obici et al., 2002). In addition, studies have shown that a deregulation of FA sensing could lead to metabolic disease and thus be involved in the etiology of obesity and type 2 diabetes (Elmquist, 2003).

Figure I.7. Brain integration of peripheral signals for the regulation of energy homeostasis. The central nervous system integrates adiposity-related (leptin) as well as satiety signals (CCK, GLP-1) to regulate food intake and energy expenditure in order to maintain body fat stores stable over time. Positive energy balance inhibits food reward while increasing meal-induced satiety, thereby reducing food intake. Under energy deficiency, central responses are engaged on increasing food reward and reducing satiety signals, resulting in increased food consumption until deficient fat stores are replenished again. CCK, cholecystokinin; FFAs, free fatty acids; GLP1, glucagon-like peptide. *Figure from Morton et al., 2014.*

1.3.5. Autonomic Nervous System: the outputs.

In response to the central integration of all this nutritional information, the CNS sends adapted signals to the periphery *via* the autonomic nervous system (ANS) and the hypothalamo-hypophyseal complex. This results in an adapted response at both the behavioral level (i.e. eating or fasting) and the metabolic level [e.g. HGP, lipolysis, counter-regulatory response to hypoglycaemia (during energy-deficit periods) or energy storage (during energy-abundance periods)]. There is therefore a regulatory loop between the CNS and peripheral organs, allowing precise adaptation of energy intake to the body needs.

In this subchapter, I will address the ANS efferent outflow controlling energy homeostasis, with a special attention on autonomic pancreatic islet innervations.

The ANS [and its components, the enteric (ENS), the parasympathetic (PNS) and the sympathetic (SNS) nervous systems] control the internal physiological processes in association with the endocrine system. Its activity is independent of voluntary control and functions autonomously, adjusting the functions the organs to the needs of the organism. Nervous control of these processes allows for very rapid adaptation, while the endocrine system regulates them in the long term.

The balance between the secretion of pancreatic hormones (i.e. insulin and glucagon) and their action on target tissues is necessary to maintain normoglycaemia (around 5 mM). This balance is under the control of the ANS (PNS vs. SNS), which modulates pancreatic hormone secretion and certain metabolic functions of peripheral tissues (Morton et al., 2014). The tone of the ANS is controlled by CNS neurons, whose activity is, in turn, dependent on nutritional signals such as blood glucose (glucose-responsive neurons) or signaling peptides that are expressed by neurons in the CNS (e.g. GLP-1, CCK…). These neurons control, by modulating the activity of the sympathetic and parasympathetic branches of the ANS, the secretion of insulin and glucagon, as well as certain functions of insulin-sensitive tissues such as liver, muscle and adipose tissue.

a. The parasympathetic nervous system

The PNS controls involuntary functions and actions, slowing down body functions in order to save energy. The main neurotransmitter of this system is acetylcholine (ACh), which acts through muscarinic and nicotinic receptors present on peripheral target tissues (e.g. intestines, heart, pancreas, lungs).

The main component of the PNS is the vagus nerve that arise from preganglionic neurons in the dorsal motor nucleus of the vagus (DMNX). When innervating pancreatic islets, DMNX receives input from hypothalamic nuclei such as the PVN, LHA and VMN through the periaqueductal grey (PAG) and/or raphe pallidus (Ra) and noradrenergic cell group 5 (A5) (Figure I.8).

b. The sympathetic nervous system

The SNS has globally opposite effects as those of the PNS. Its functions allow, in a simplified way, to prepare the human body for action (i.e. to face a stress situation - "fight or flight" response). The main neurotransmitter of this system is noradrenaline (NA), which binds to adrenergic receptors on target tissues.

SNS motor neurons are located in the interomediolateral (IML) column of the spinal cord. They receive neuronal input from hypothalamic regions such as the PVN and the LHA among others, with a relay on NTS neurons (Buijs et al., 2001) (Figure I.8).

Intra-PVN regions such as parvocellular or mediocellular subdivisions contain neurons projecting to the spinal cord and the medulla. These neurons are called spinally-projecting sympathetic pre-autonomic neurons (SPANs), and play a crucial role on the regulation of SNS activity. In turn, SPANs are regulated by a GABAergic inhibitory input from the perinuclear region of the PVN, or peri-PVN region, *via* $GABA_A$ receptors (Herman et al., 2002). GABAergic neurons from the LHA also project to $GABA_AR$-expressing neurons (Wu et al., 2015). Thus, as for the PNS, the SNS activity is finely controlled by several higher brain regions such as the PVN, also involved in the regulation of energy balance.

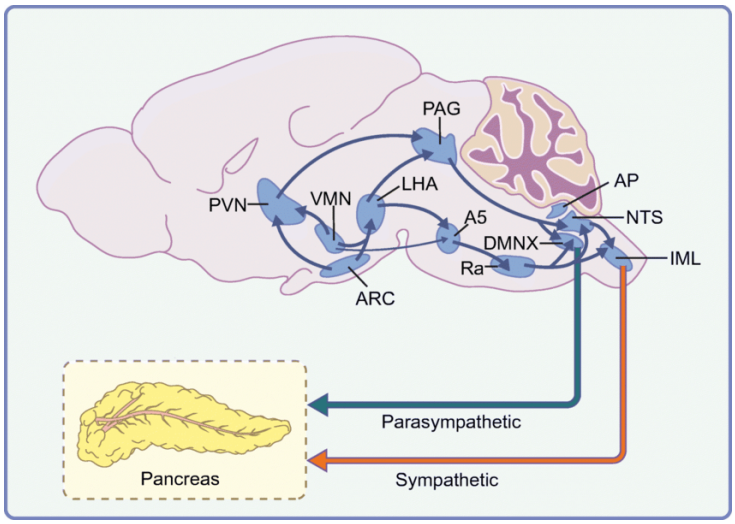

Figure I.8. Brain circuits involved in the outflow to the pancreatic islet. SNS and PNS efferent neurons receive neuronal input from several overlapping brain regions, including both hypothalamic and hindbrain nuclei. PVN: paraventricular nucleus, VMN: ventromedial nucleus, ARC: arcuate nucleus, LHA: lateral hypothalamic area, PAG: periaqueductal grey, A5: noradrenergic cell goup A5, Ra: raphe pallidus, DMNX: dorsal motor nucleus of the vagus, NTS: nucleus of the solitary tract, AP: area postrema, IML: intermediolateral column. *From Faber et al., 2020.*

c. <u>Parasympathetic and sympathetic innervation of the endocrine pancreas</u>

Despite Langerhans' early work suggesting a rich innervation of pancreatic islets in the 1860's, the idea that a brain-islet-insulin axis could exist was not really believed. The potential CNS influence was ignored for years, even if growing evidence consistent with a nervous control of the endocrine pancreas was emerging.

Early studies showed that local α-adrenergic stimulation inhibits insulin secretion in humans (Porte and Williams 1996), supporting that it is under sympathetic control. However, other studies supported that insulin secretion was stimulated by acetylcholine, indicating a PNS involvement (Campfield et al, 1984). Cholinergic activation of insulin secretion was, in turn, decreased by epinephrine (Campfield et al., 1986), suggesting an intricate neural regulation

involving both PNS and SNS control of β-cells. Nowadays, thanks to all this work, it is strongly supported that islets are richly supplied by sympathetic and vagal nerves and can modulate the secretion of all pancreatic hormones.

SNS activation inhibits both basal and GSIS, acting *via* the α_2-adrenergic (α_2-AR) receptor on pancreatic β-cells through release of noradrenaline, whereas PNS activation augments GSIS *via* β-cell muscarinic receptors (M3R) through the release and binding of acetylcholine (Ahrén, 2000) (Figure I.9). In terms of signaling, α_2-AR stimulation decreases insulin release by inhibiting β-cell adenylyl cyclase (less predominantly, β_2-AR receptors can increase insulin secretion through an activation of adenylyl cyclase in β-cells). M3R activation by acetylcholine or vagal stimulation causes insulin release by β-cell through IP_3/DAG signaling. In α-cells, both β_2 -AR and M3R activation increases glucagon secretion.

Even if it has been shown that human islets had less PNS and SNS innervation than what was reported in mice (Rodriguez-Diaz et al., 2011), it is now known that islets present a dense amount of PNS and SNS fibers, modulating islet hormone secretion in a similar way than in rodents (Chien et al., 2019).

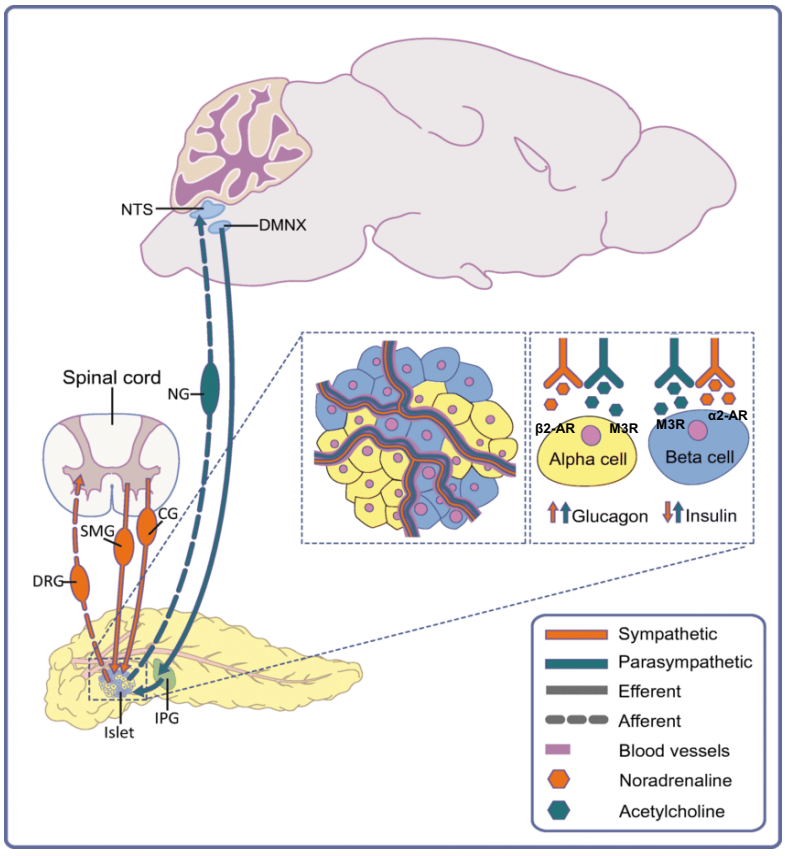

Figure I.9. Autonomic innervation of the endocrine pancreas. Islets receives afferent innervation (solid lines) from both SNS (orange) and PNS (green). Projections from the IML in the spinal cord present cell bodies of SNS efferences in the superior mesenteric ganglia (SMG) and the celiac ganglia (CG). Sympathetic fibers enter in the islet along blood vessels and release NA to α and β-cells, stimulating

Figure caption continued on next page

glucagon secretion (through binding to β-AR) and inhibiting insulin secretion (through activation of α2-AR) respectively (figure insert). Intrapancreatic ganglia (IPG) relays PNS efferences originating in the DMNX, which enter the islet to stimulate insulin and glucagon secretion from β and α-cells through a local release of Ach in M3R receptors. Sympathetic and parasympathetic afferent branches (dashed lines) are also present in an islet. The sympathetic ones present their cell bodies in the dorsal root ganglia (DRG) and project to the spinal cord, whereas parasympathetic ones have their cell bodies in the nodose ganglion (NG) and project to the NTS. *Modified from Faber et al., 2020.*

2. Metabolic diseases

2.1. Obesity

Obesity has been defined by the World Health Organization (WHO) as "an abnormal or excessive fat accumulation that presents a risk to health". The most common measurement for overweight and obesity is the body mass index (BMI), which is calculated by dividing the weight in kilograms by the height in meters squared (kg/m2) of the individual tested. An increase in BMI increases the risk of suffering certain chronic pathologies such as cardiovascular diseases (mainly heart disease and stroke), musculoskeletal disorders (osteoarthritis), sleep disorders (apnea), certain cancers and high blood pressure. A BMI over 25 is considered overweight, and over 30, obese. Among the deleterious effects of obesity, several energy imbalances lead to a lack of efficiency of insulin secretion as well as to an insulin resistance, leading to Type 2 diabetes.

Indeed, homeostatic defense of energy balance regulation is undermined in our societies, as regularly attested by the reports of the WHO, which highlights the inexorable progression of the global obesity pandemic. This pandemic is becoming, with the diseases and complications it induces, one of the major public health problems of the 21st century. According to the latest available estimates, 1.9 billion adults are overweight and 650 million are obese worldwide. Over 4 million people die from the consequences of being overweight each year worldwide (https://www.who.int/). In addition, 80% of people who have developed obesity have obesity-related diseases such as diabetes, hyperlipidemia, hypertension or cardiovascular problems (Simpson et al., 2009). Dramatically, obesity also affects very young children: 38,2 million children under 5 years of age were affected by overweight or obesity problems in 2019. The origins of these disorders are numerous and involve, among other things, a sedentary lifestyle, genetic predisposition and, in the first instance, a disruption of eating habits. The last World Obesity Atlas 2022 reports an unceasing increase in the prevalence of obesity worldwide (https://www.worldobesity.org/).

In France, an epidemiological survey (ObEpi) carried out every three years from 1997 to 2012, has shown that in 2012, one third of French adults were overweight, of which 15% were obese. In 2020, the “Ligue Contre l’Obésité” decided to re-launch the national epidemiological survey that had been on hold since 2012. The proportion of people with obesity had increased from 3.3 million in 1997 to 8.5 million in 2020. This means that in 2020, 17% of the French population was suffering from obesity. One in two people is thus overweight or obese (Figure I.10).

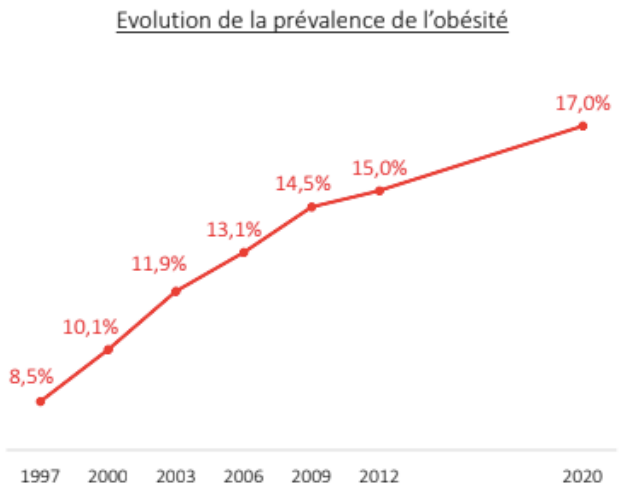

Figure I.10. Evolution of the prevalence of obesity in France. *Source: Obepi data.*

2.2. Type 2 diabetes

Diabetes is a chronic long-lasting health condition defined by an abnormal increase in basal blood glucose levels (hyperglycaemia). This leads, over the years, to serious complications affecting especially the nerves and blood vessels (see Annex, Soleimanzad, Montaner et al. 2021). By 2040, the International Diabetes Federation (http://www.diabetesatlas.org) predicts that one in ten adults will be affected by this disease. In recent decades, its prevalence has steadily increased, making it a major health problem. There are several types of diabetes including type I and type II diabetes (T2D). T2D, also known as "diabetes mellitus", is highly common, in fact, it accounts for more than 95% of patients with diabetes and even if until recently it was only seen in adults, it is now also occurring increasingly in children. The IDF Diabetes Atlas (10th edition) provides very frequent updates confirming a continued global rise in the prevalence of diabetes, and describing it as a main global challenge to individuals, families and society health and well-being (https://diabetesatlas.org/).

The study of this pathology is complex because of the multifactorial parameters that may come into play. Nowadays, the etiology of T2D is still poorly defined due to the numerous controversial arguments that exist about it. Despite this controversy, it is generally accepted that a combination of genetic and environmental factors such as physical inactivity or excess body weight, is involved in the development of this disease (Unger et al., 1995).

The onset of T2D is relatively slow and silent, and frequently diagnosed once complications have already arisen, as hyperglycemia remains asymptomatic for a long time. This hyperglycemia results from a decrease in the sensitivity of target tissues cells - in particular those of the liver, muscle and adipose tissue - to insulin (Defronzo et al., 2009). To meet the increased demand for insulin resulting from this insensitivity, the insulin-secreting cells of the pancreas produce more insulin until they run out. In addition, a potential decrease in β-pancreatic cell mass adds to its factors. Hence, insulin production becomes insufficient and glucose accumulates irreparably in the blood (Figure I.11).

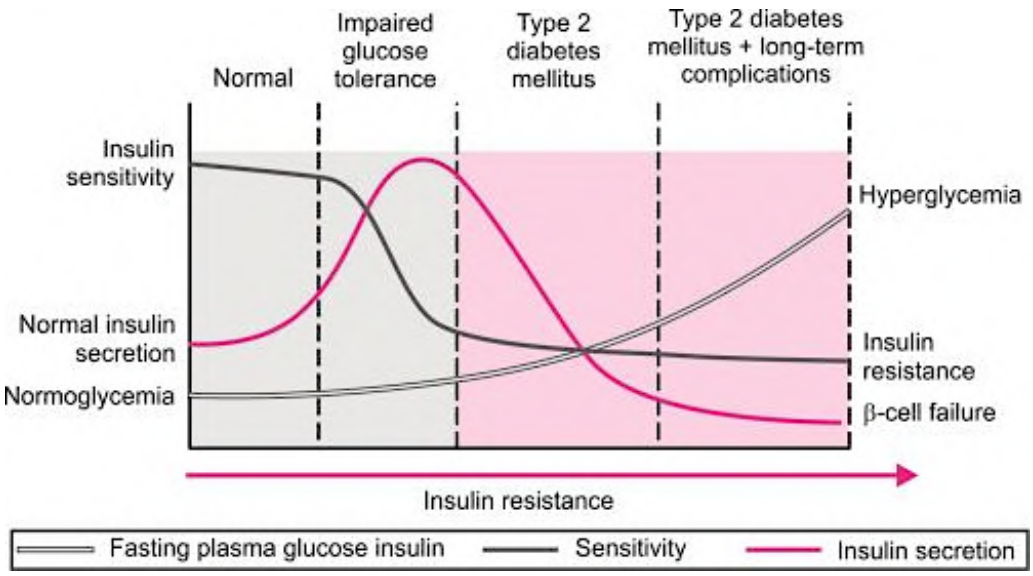

Figure I.11. Natural history of T2D. Insulin secretion deficit is characteristic in the natural history of type 2 diabetes, which worsens progressively over time. In this figure, grey and pink backgrounds represents before and after diabetes diagnosis. β-cell function and increasing plasma glucose are related. Insulin resistance appears before the onset of diabetes, which requires also loss of insulin secretion. Over time, most T2D patients lose the capacity to secrete insulin. *Figure from RSSDI Diabetes Update 2016.*

2.3. Antidiabetic treatments

2.3.1. Therapeutic strategy for T2D

In the case of an early-diabetic stage, diet and exercise may be enough to control glycaemia on T2D patients. However, when they are no longer effective, anti-diabetic drugs should be prescribed. Medication will either be taken orally or be injected. Among oral hypoglycemics commercialized, one can find Biguanides (metformin), Sulfonylureas, Alpha-glucosidase inhibitors, Thiazolidinediones (glitazones) and serine protease dipeptidyl peptidase IV (DPP-IV) inhibitors (gliptins), whereas injected antidiabetic drugs include glucagon-like peptide-1 receptor (GLP-1R) agonists and insulin.

The therapeutic strategy for T2D is based on drug escalation. The level of glycated hemoglobin (HbA1c) is defined as the amount of glucose attached to hemoglobin (physiological maximum of 5.6%) and is used for the diagnosis of T2D. An antidiabetic treatment normally starts with non-insulin monotherapy like metformin medication. If HbA1c target is not maintained over 3 months and the drug maximum dose is already achieved, a second agent might be added to the regimen. This second agent is normally a GLP-1 analog or basal insulin (Chaudhury et al., 2017). If HbA1c target is not at goal in 3 more months, a triple therapy may be required, proceeding to or intensifying insulinotherapy.

In parallel to the recognized antidiabetic medication, bariatric surgery has emerged as an effective treatment for morbid obesity but also for associated co-morbidities such as T2D. Some surgical techniques have the capacity to normalize in a few days glycemia independently of weight loss *via* an early post-surgical enhancement of insulin secretion. The underlying mechanisms are still poorly understood and motivate deeper research with the objective to find the best-suited operative technique (Amouyal and Andreelli, 2017). Recently, a study underlines novel miRNA-gene interactions within the islet after enterogastro-anastomosis (a surrogate of human Roux-en-Y gastric bypass) in ob/ob mice. This underlies a new potential mechanism that may finally explain the remission of T2D after bariatric surgery (Amouyal et al., 2020).

The "incretin effect" is altered in patients with T2D and contributes to impaired regulation of insulin and glucagon. The incretin effect can be enhanced in two ways: either by developping a GLP-1 that is not inactivated by DPP-IV (i.e., a GLP1 analog) or by inhibiting this enzyme that inactivates incretins (by means of DPP-IV inhibitors). I will only discuss the actual GLP-1 analogue therapy, which may restore the regulation of blood glucose to near optimal levels.

2.3.2. GLP-1 analogues

Targeting the incretin system has become an important therapeutic approach for treating T2D. Since circulating GLP-1 is rapidly inactivated by DPP-IV (Mentlein, Gallwitz and Schmidt, 1993) (further details in Chapter II; *c.f. 2.2. GLP-1 degradation*), several analog molecules have been designed to be resistant to this enzyme and intensify GLP-1 effectiveness for the treatment of T2D.

These GLP-1 biochemically modified analogs regulate blood glucose levels by stimulating insulin secretion and glucagon-dependent biosynthesis and by stopping glucagon secretion, thus delaying gastric emptying and increasing the feeling of satiety (Gupta, 2013). They are administered by subcutaneous injection and divided into 2 principal groups:

● Exendin-4 derivatives, originally isolated from the venom of the Gila monster (Heloderma suspectum) (Rowzee et al., 2011). *Exenatide* binds to the human GLP-1R with comparable affinity to that of human GLP-1 itself (53% homology). Amino acid modifications make the molecule more resistant to DPP-IV inactivation, prolonging its half-life. Depending on preparations, commercialized drugs can require from two injections per day (Byetta®) to once-weekly administration (Bydureon®). *Lixisenatide* has similar homology to that of exenatide but is resistant to degradation by DPP-IV. It has a 4 times more affinity to the GLP-1R than that of human GLP-1 (Scott, 2013). The drug is administered daily.

● Derivatives modified from the active fragment of the human GLP-1 (7–36) (Christensen et al., 2014). *Dulaglutide* analog portion has approximately 90% homology to native human GLP-1 (7-37). The drug is resistant to degradation by DPP-IV, and its large size slows absorption and reduces renal clearance. Hence, it is considered as long-acting, allowing for a single weekly subcutaneous administration. *Liraglutide* has 97% homology to human GLP-1 (Novo Nordisk. Victoza prescribing information). Its ability to binding circulating albumin strongly prolongs its half-life compared to human GLP-1. It allows once-daily injections. *Semaglutide* has similar homology to that of liraglutide and is linked to albumin thanks to its hydrophilic spacer and fatty acid side chain (Figure I.12). It allows once-daily dose.

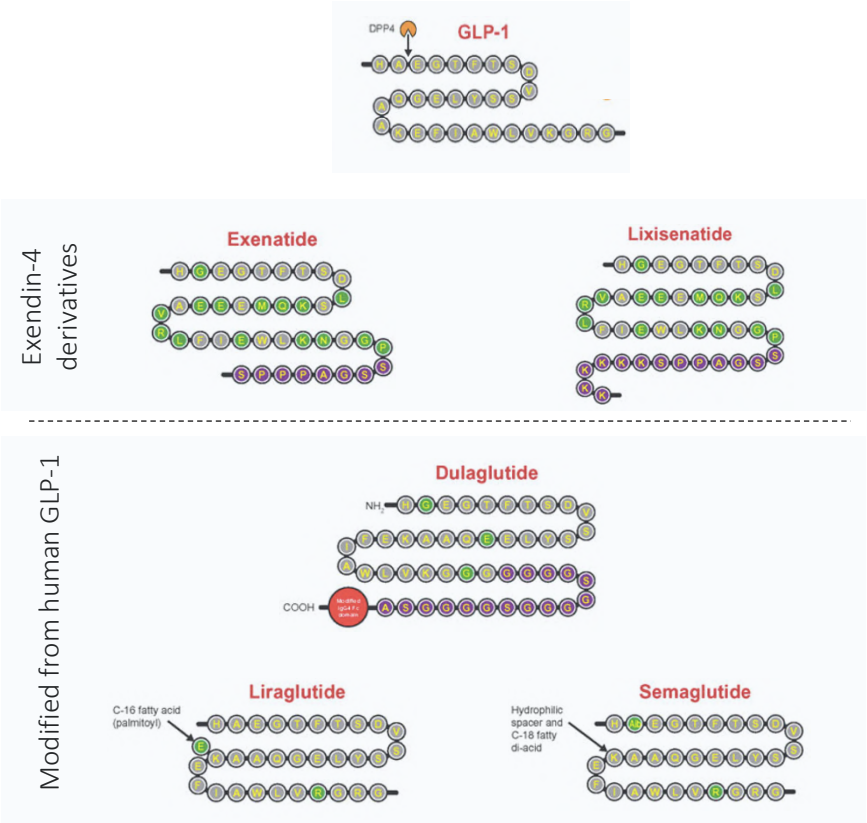

Figure I.12. **Chemical structure of GLP-1 and GLP-1R agonists (GLP-1RAs).** Exendin-4 derivatives (Exenatide and Lixisenatide) and agonists modified from the human GLP-1 (Dulaglutide, Liraglutide and Semaglutide). *Adapted from Gentilella et al., 2019.*

Pharmacological innovation in diabetes is a real challenge. Dual receptor agonists GIP/GLP-1 have recently been developed and represent an important therapeutic advance to improve the management of type 2 diabetes (T2D). The new family of GIP/GLP-1 receptor co-agonists present additive metabolic effects compared to those achieved with GLP-1 receptor agonists alone, particularly on blood glucose and excess weight (Phan and Andreelli, 2021). Newer dual analogues are assessed for its efficacy, safety and tolerability. Trizepatide, a novel one, is shown to strongly improve glycaemia and body weight control in T2D patients (Rosenstock et al., 2021).

Chapter II
The Glucagon-like peptide-1

The Glucagon-like peptide-1 is a hormone with multifaceted nature presenting a wide pharmacological potential. GLP-1 is involved in numerous metabolic functions such as GSIS, inhibition of food intake, decrease of gastric emptying, increase of diuresis and natriuresis, and modulation of β-cell proliferation in rodents. Very interestingly, GLP-1 presents also neuro- and cardio-protective properties, decreases inflammation and apoptosis, and is involved in learning, memory, reward, and palatability.

GLP-1 receptor agonists are a successful treatment for T2D. To date, clinical evaluation of pharmacotherapies based on GLP-1 is in progress for the treatment of obesity.

1. The discovery of GLP-1 and its identification as a gastrointestinal hormone

Following the discovery of the first gastrointestinal hormone, secretin, a substance secreted by duodenal epithelial cells that stimulated pancreatic juice (Starling, 1905; Moore et al., 1906), Best and Basting discovered insulin in 1921 (see review Creutzfeldt, 2005). In 1930, a crude secretin preparation was separated into two fractions: one that increased exocrine pancreatic secretion (secretin) and a second that lowered blood glucose concentrations (La Barre and Still, 1930). In 1932, assuming that this decrease in blood sugar was due to the ability of the second fraction of secretin to stimulate the release of pancreatic insulin, La Barre called it "incretin", as previously mentioned in Chapter I (c.f. *1.2.4. Pancreas -> Insulin-regulating factors -> Incretins*).

In 1948, Sutherland and De Duve wanted to localize the intestinal cells that induce insulin secretion (Sutherland and De Duve, 1948). They suggested that intestinal extracts might contain glucagon, since glucagon was thought to stimulate insulin secretion at that time – an idea that was rejected later. With the arrival of the radioimmunoassay for glucagon, it was confirmed that distal intestinal cells contained substances with immunoreactivity (i.e. glucagon-like immunoreactive material was secreted after oral glucose intake). However, contrary to glucagon, these cells

stimulated the release of insulin (Unger et al. 1966) and had different morphology, ultrastructure, and diverse secretory granules than the pancreatic islet α-cells (Grimelius et al. 1976). Therefore, they were called L-cells (Buffa et al., 1978).

Several studies demonstrate that these glucagon-like immunoreactive substances were also present in the pancreas, and were larger than glucagon. This suggested that glucagon and the glucagon-like substances might derive from a larger precursor molecule that is post-translationally processed to provide several fractions with different sizes and functions. This 18 KDa precursor molecule is now classified as proglucagon (Patzelt et al., 1979), a protein resulting from the cleavage of preproglucagon (PPG). PPG is encoded by the gcg gene, which is composed of 6 exons and whose transcript is cleaved in a differential manner depending on the tissue (c.f. *2.1. Expression and cleavage of preproglucagon gene*).

In the pancreas, proglucagon is cleaved producing two fractions, glucagon and another 10KDa protein named major proglucagon fragment (MPGF) (Figure II.1). In the intestines, a peptide designated glicentin comprising the glucagon sequence was described as the largest form of intestinal glucagon-immunoreactive material. Since glicentin was also present in the pancreas, it was thought to be part of proglucagon too (Moody et al., 1981). The cleavage of proglucagon was found to be tissue-specific therefore, the fractions found in the intestine might be different than the pancreatic ones. In 1982, a smaller intestinal fraction was discovered, oxyntomodulin (Bataille et al., 1982). This discovery leaded to believe that intestinal-specific processing of proglucagon resulted in glicentin and oxyntomodulin, whereas its pancreatic-processing formed glucagon and a fragments of glicentin, glicentin-related polypeptide (GRPP) as well as intervening peptide-1 (IP-1) (Figure II.1).

In the early 1980s, a different glucagon-related peptide encoded inside the preproglucagon cDNA was discovered (Heinrich and Habener, 1984). Two peptides were next identified in the human and hamster proglucagon sequence, named glucagon-like peptides 1 and 2 (GLP-1 and GLP-2) (Bell et al., 1983) (Figure II.1). A different profile of proglucagon-derived peptides (PGDPs) in the intestine and the pancreas was then recognized, with the production of GLP-1 and GLP-2 in the intestine and liberation of glucagon and MPGF in the pancreas.

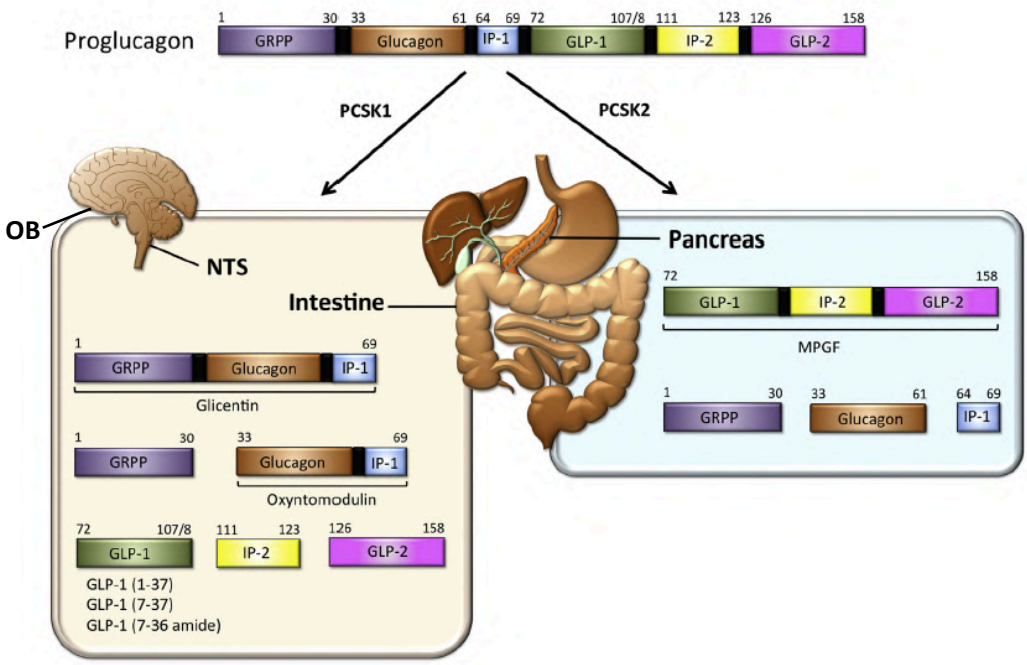

Figure II.1. Tissue-selective processing of proglucagon. In the intestine and brain cleavage of the proglucagon protein generates 5 peptides: glicentin, oxyntomodulin, glucagon-like peptide 1 and 2 (GLP-1, GLP-2) and intervening peptide-2 (IP-2). In the pancreas, the proteins produced are GRPP (Glicentin related polypeptide), glucagon, IP-1 (intervening peptide-1) and MPGF (major proglucagon fragment). PCSK1: prohormone convertase 1/3 (PC1/3); PCSK2: prohormone convertase 2 (PC2); NTS: nucleus of the solitary tract. *Adapted from: Müller et al., 2019.*

2. Synthesis and release of GLP-1

2.1. Expression and cleavage of preproglucagon gene

As mentioned before, one single gene called gcg encodes the preprotein preproglucagon in mammals. The same PPG-mRNAs are created in the pancreas and the gut, more precisely in the distal ileum and colon (Novak et al., 1987). PPG mRNA is also expressed in the NTS of the brainstem (Mojsov et al., 1986) and the OB (Merchenthaler et al. 1999). Ablation of PPG neurons in the NTS demonstrated that this population is the main source of GLP-1 in the brain (Holt et al., 2019).

Cleavage sites in the proglucagon protein along with tissue-specific prohormone convertase enzymes expression defines which smaller PGDPs peptides are formed (Figure II.1): glicentin (aa 1 to aa 69), GRPP (aa 1 to aa 30), glucagon (aa 33 to aa 61), oxyntomodulin (aa 33 to aa 69), MPGF (aa 72 to aa 158), glucagon-like peptide 1 (aa 72 to aa 107/8) and glucagon-like peptide 2 (aa 126 to 158). Prohormone convertase 1 (PC1, also known as PC1/3 or PCSK1) is expressed in PPG+ cells in the gut and the brain. PC1/3 has been demonstrated to be necessary and sufficient for the processing of proglucagon and liberation of GLP-1, GLP-2, glicentin,

oxyntomodulin and IP2 (Zhu et al., 2002). Prohormone convertase 2 (PC2, also known as PCSK2) is expressed in pancreatic cells. PC2 is necessary and sufficient for the cleavage of proglucagon to glucagon, GRPP, MPGF and IP-1 (Rouille et al., 1994).

Numerous PGDPs play an important role on systemic metabolism (and present well-defined pharmacological effects), including the modulation of food intake and satiety (GLP-1, glucagon, oxyntomodulin), gastric emptying (glucagon, GLP-1, GLP-2), gastrointestinal motility (glucagon, GLP-1, GLP-2), lipid metabolism (GLP-1, glucagon, GLP-2) and thermogenesis (glucagon). GLP-1 from intestinal L-cells and Glucagon secreted from pancreatic α-cells and have opposite effects on blood glucose. Thus, expression and cleavage of proglucagon as well as ensuring PGDPs secretion requires precise and controlled cell-specific processing.

After the cleavage of *gcg*, GLP-1 is initially an immature peptide of 37 amino acids (GLP-1 (1-37)), with lower insulinotropic efficacy (Holst et al., 1987). It is then cleaved into an active form of 30 amino acids, GLP-1 (7-37). The latter is partially truncated at position 37, composed of a glycine (glycine-extended GLP-1, Figure II.1), to give the peptide 7-36. An amide group, is added to the arginine residue at position 36 to form GLP-1 (7-36) NH2 by peptidylglycine α-amidine monooxygenase (GLP-1 (7-36 amide)) (Hansen et al., 2000). This maturation increases the half-life of the peptide and accounts for the majority of circulating GLP-1 (Mojsov et al., 1990). In healthy humans and rats, these two forms (7-36 amide) and (7-37) are biologically active (Gallwitz et al., 1990) and equipotent in their ability to induce insulin and c-peptide secretion (Orskov et al., 1993).

2.2. GLP-1 secretion by intestinal cells

Oral, but not intravenous, glucose administration stimulates GLP-1 secretion in humans. Thus, GLP-1 secretion is clearly meal related (Ye et al., 2014). During fasting, plasma concentrations are low (5-10 pmol/L) and correlate with plasma insulin levels. Hence, in response to a meal, they can increase up to 40 pmol/L (Orskov et al., 1996). These values are however certain for total GLP-1 (including metabolites generated after DPP-IV degradation, c.f. *2.3. GLP-1 degradation*), but plasmatic concentrations of biologically active GLP-1 are much lower, from less than 2 pmol/L at fasting to a 5-10 pmol/L peak following meal ingestion (Kuhre et al., 2015). Since GLP-1 levels are detectable during fasting, it is likely that GLP-1 is tonically secreted into the systemic circulation in basal conditions (Toft-Nielson et al., 1996). One article has shown evidence for a cephalic phase of GLP-1 in rats during the pre-prandial state (Vahl et al., 2010).

The amount of GLP-1 secreted is meal-size and meal-composition dependent. In healthy humans, a 520 kcal-meal (orally) induced a bigger increase of total and active GLP-1 than a 260 kcal-meal (Vilsboll et al., 2003). Carbohydrates are not solely the nutrients increasing circulating

GLP-1; dietary lipids (Reimann and Gribble, 2002) and proteins also induce a rise of GLP-1 in post-prandial through specific L-cell receptors (Husted et al., 2017). In fact, L-cells are sensible to glucose, fructose, galactose as well as non-metabolizable monosaccharides, long-chain fatty acids, proteins and specific amino acids.

In healthy humans, the ingestion of carbohydrates or proteins stimulates a rapid increase in circulating GLP-1 (peak between 30 and 60 minutes following a meal) while lipid ingestion elicits a later and more prolonged increase (>120 minutes) (Herrmann et al., 1995). Although the 30-60 window-time established for carbohydrate-induced GLP-1 secretion, an early GLP-1 increase is thought to occur within the first 10-15 minutes after stimulation by glucose (early phase of GLP-1 secretion).

In enteroendocrine L-cells, glucose increase GLP-1 secretion in a dose-dependent way through a closure of K_{ATP} channels and subsequent cell depolarization (Gribble et al., 2003). This membrane depolarization induced by glucose, triggers the opening of voltage-dependent Ca^{2+} channels, and thus an influx of Ca^{2+} enters the cell. The Ca^{2+} concentration within the cell is thus increased enough to trigger the exocytosis of GLP-1 vesicles and its secretion into the bloodstream (Tolhurst et al., 2009).

The distribution of L-cells varies between species (Holst, 2007). In humans, they are mainly distal (ileum, proximal colon), whereas in mice, they are more proximal and distributed in the jejunum and ileum. Although species variation, the lowest density is always found in the proximal small intestine and increases distally along the gut (Eissele et al., 1992; Drucker et al., 2006). The apical L-cell surface faces the lumen of the bowel and thus has directly contact with nutrients. Consistently, in healthy humans, plasmatic GLP-1 levels quickly increase following direct administration of carbohydrates or lipids into the ileum (Layer et al., 1995). However, after a real meal, GLP-1 secretion is initiated during the first minutes of duodenal and jejunal absorption of nutrients, whereas, as said, L-cells are mainly found in a more distal part of the intestine. It is thus unlikely that early GLP-1 secretion phase can be mediated by direct stimulation of nutrient content in the distal lumen. This suggests that there is a nervous relay from the proximal part of the intestine to the distal part to stimulate GLP-1 secretion during the intake of food (Eissele et al., 1992) (Figure II.2). Nevertheless, the ability of L-cells to directly secrete GLP-1 in response to nutrients once they are in the ileum is still considered as the first mechanism of intestinal GLP-1 secretion.

The distal position of L-cells, in contact with nutrients, justifies the prolonged high level of GLP-1 during meals. Since surgical repositioning of the distal part of the intestine after sleeve gastrectomy exposes distal L-cells sooner to the arriving nutrients (Larraufie et al., 2019), this might be an explanation for the characteristically increased levels of GLP-1 after gastric bypass. The increase in GLP-1 levels leads to an improving metabolic state in obese individuals which

might also be explained by a boost in gastric GLP-1 (increased density of gastric GLP-1-positive cells) after bariatric surgery (Ribeiro-Parenti et al., 2021).

Controversy exists around glucose-induced GLP-1 secretion in T2D. A study suggested that GLP-1 response to oral glucose is reduced in pre- or diabetic patients (Faerch et al., 2015) whereas others revealed no difference in T2D-patients glucose-induced GLP-1 compared to non-diabetic controls (Calanna et al., 2013).

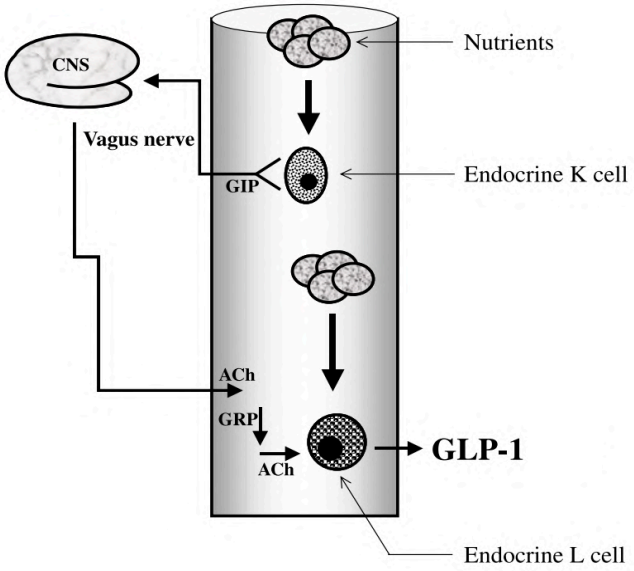

Figure II.2. Direct (late) and indirect (early) nutrient-induction intestinal GLP-1 secretion. The plausible hypothesis described for GLP-1 secretion would be that nutrients detected in the proximal part of the intestine trigger the secretion of GIP from K cells, which would then activate the vagus nerve. The nervous information would be then transmitted to the brain. In turn, the brain would modulate a nervous message to the distal cells of the intestine *via* vagus nerve efferences. The vagal transmission is mediated by Ach and gastric-releasing peptide (GRP) neurotransmitters release. This gut-brain neural loop would end inducing the early secretion of GLP-1. The second peak of GLP-1 would come later, once nutrients had reached the distal gut through direct contact with L cells. *Adapted from Brubaker and Anini, 2003.*

2.3. GLP-1 degradation

In rats, active GLP-1 (7-37) is rapidly secreted and its plasma secretion reaches 25 to 50 pM. It is immediately degraded in the bloodstream after 2 minutes into GLP-1 (9-37) and (9-36), with 20 minutes the half-life for these last two peptides. These peptides are eliminated mainly by renal clearance (Deacon et al., 1995). In humans, GLP-1 secretion is thought to occur in rapid oscillations and in two phases: the first 10-15 minutes after stimulation by glucose and the second at 30-60 minutes. Less than 25% of GLP-1 secreted into the mesenteric vessels would reach the portal vein and liver in an intact form as it is already degraded in the capillaries of the distal gut.

Thus, only 25% of active GLP-1 reaches the liver and around 10-15% would reach the systemic circulation and organs (Holst et al., 2007) (Figure II.6). This finding draws attention to the powerful role of the active GLP-1 degrading enzyme, dipeptidyl peptidase IV (DPP-IV).

DPP-IV is a ubiquitous glycoprotein, composed of two 120 kDa subunits. DPP-IV is a serine protease, known to be a marker of T lymphocytes. It is found on the brush border of intestinal and renal cells, on endothelial cells and, in plasma as a free form (Hansen et al., 1999). DPP-IV cleaves polypeptides containing an alanine residue in the antepenultimate position in the NH_2 part of the peptide. Thus, active forms of GLP-1 (intestinal GLP-1(7-37) and (7-36)), are rapidly metabolized to two inactive forms, GLP-1(9-37) or GLP-1(9-36) producing also a dipeptide residue of histidine-alanine (His-Ala).

Only the N-terminal portion would be required for the substrate to be effective in increasing cAMP (c.f. *3.1. The GLP-1 receptor and its signaling*). Degradation of GLP-1 by its N-terminal part therefore generates inactive metabolites. Indeed, the metabolites GLP-1(9-37) and GLP-1(9-36)NH_2 are reported to have no effect on insulin and glucagon secretion (Zander et al., 2006). However, a study showed that the metabolite (9-36) would also be able to decrease glycemia by a mechanism independent of insulin in pigs (Deacon et al., 2002). In healthy humans, GLP-1 (9-36amide) has no effect on insulin secretion nor glucose clearance (Vahl et al., 2003). Actually, this GLP-1 inactive form acts as a feeble GLP-1R antagonist, by opposing the effects of active GLP-1 in vitro (Knudsen and Pridal, 1996).

2.4. GLP-1 release by cerebral structures

Within the primate and rodent CNS, preroglucagon mRNA is transcribed and translated in the caudal nucleus of the solitary tract, the caudal medullary reticular formation and the olfactory bulb (Merchenthaler et al., 1999). Within the OB in rodents, it has been described that GLP-1 is produced and plays a role locally (Thiebaud et al., 2016, 2019). Additionally, GLP-1-immunopositive neurons are expressed in the human brain (Zheng et al., 2015).

PPG^{NTS} neurons are thought to project its axons, containing GLP-1 vesicles, to several brain regions such as the hypothalamus. However, they do not project to the OB (Llewellyn-Smith et al., 2015) (Figure II.3). Thus, bulbar GLP-1 is considered to act locally as a part of a unique microcircuit controlled by bulbar PPGs (Thiebaud et al., 2019).

Protein levels of active GLP-1 were detected in numerous brain regions using an MSD kit (Holt et al., 2019). Concentrations (normalized to total protein) are 2,5 pg/mg in the brainstem, 3,75 pg/mg in the hypothalamus, 17,5 pg/mg in the spinal cord, 0,6 pg/mg in the blood and less than 0,25 pg/mg in the cerebellum and OB.

L-cell-secreted GLP-1 acts as a hormone and binds to peripheral receptors, firstly to receptors within the gut, in order to rapidly trigger its incretin effect and act on vagal afferences (Berthoud et al., 2021) to update the brain of the digestive meal status. In turn, this would involve satiation or satiety pathways. It is unlikely that gut-derived GLP-1 reaches the CNS through circulation. However, systemic administration of GLP-1RAs, do access GLP-1Rs in the brain that are located in structures presenting leaky BBB (Orskov et al., 1996) (Figure II.3). This is due to their capacity to resist DPP-IV degradation.

For a long time the idea that the peripheral and central GLP-1 systems work together in a unique gut-brain satiation circuit, mediated by the vagus nerve, was considered well-known. However, recently, it has been discovered that PPG^{NTS} neurons do not receive vagal inputs from GLP-1R-expressing neurons (Brierley et al., 2021). Thus, the idea that the central GLP-1 system suppresses eating independently from the peripheral GLP-1 system has emerged. A recent review discussed the existing data about the physiology of GLP-1 and supported the existence of two separate (gut-derived and brain-produced) GLP-1 systems (Trapp and Brierley, 2022).

GLP-1 may be thus redesigned as both a hormone and a neurotransmitter (or neuromodulator), depending on its origin (Figure II.3). This would provide a more realistic understanding of the central action mechanisms of PPG-derived GLP-1, as well as improved pharmacological opportunities for GLP-1-based obesity treatments.

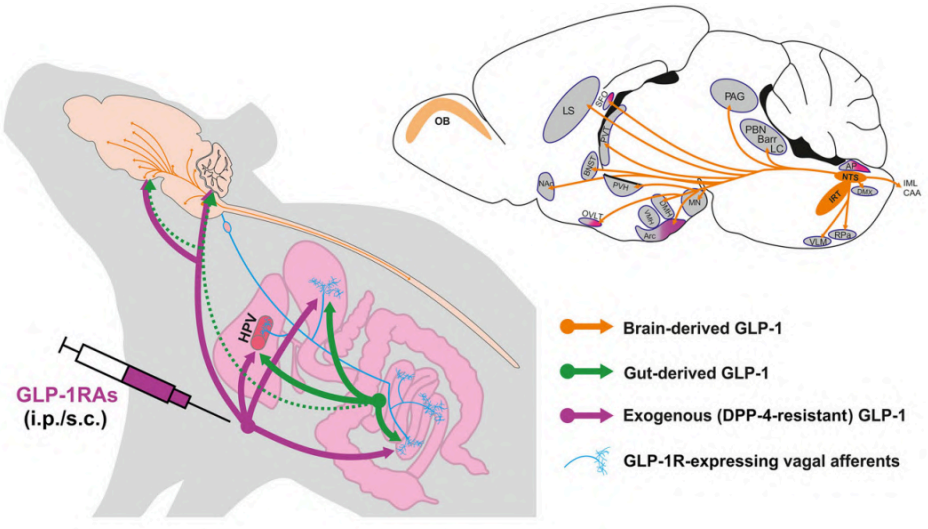

Figure II.3. Brain-derived, gut-derived and exogenous GLP-1 action pathways. PPG cells (orange) are located in the OB and the NTS, from where projections (orange arrows) reach several brain and spinal cord structures. Gut-derived GLP-1 (green) is released into the circulation and acts in the gastrointestinal system (green arrows), and maybe, reach brain structures with highly permeable capillaries (circumventricular organs, CVOs) (dotted green arrows). Intraperitoneal (i.p.) or subcutaneous (s.c.) administration of GLP-1RAs acts in the gastrointestinal system and also reaches, in a minority manner, the CNS, acting within the CVOs. GLP-1 and GLP-1RAs can act on vagal afferents projecting to the brain (blue) controlling satiety. AP: area postrema; Arc: arcuate nucleus; Barr: Barrington's nucleus; BNST: bed nucleus of the stria

Figure caption continued on next page

terminalis; CAA: central autonomic area; DMH: dorsomedial hypothalamus; DMV: dorsal motor nucleus; DPP-4: dipeptidyl peptidase IV; HPV: hepatic portal vein; IML: intermediolateral nucleus; IRT: intermediate reticular nucleus; LC: locus coeruleus; LS: lateral septum; MN: mammillary nucleus; NAc: nucleus accumbens; NTS: nucleus tractus solitarii; OB: olfactory bulb; OVLT: organum vasculosum of the lamina terminalis; PAG: periaqueductal grey; PBN: parabrachial nucleus; PVH: paraventricular nucleus of the hypothalamus; PVT: paraventricular thalamus; RPa: raphe pallidus; SFO: subfornical organ; VLM: ventrolateral medulla; VMH: ventromedial hypothalamus. *Figure from Trapp and Brierley, 2022.*

3. Effects of Glucagon-like peptide-1

3.1. GLP-1R localization in the body

The GLP-1 receptor is a seven transmembrane domain Class B receptor coupled to a G protein (Frimurer and Bywater, 1999; Mayo et al., 2003). It was cloned by Bernard Thorens from pancreatic islets in 1992 (Thorens, 1992). The murine structure of the GLP-1R is 90% identical with the amino acid structure of the human receptor, which was also cloned subsequently. Thorens also confirmed that exendin-4, the 53% homologous Heloderma suspectum lizard peptide, is an agonist and synthetic exendin-4 (9-39) an antagonist of the receptor (Thorens et al., 1993) without any agonistic properties. Note that exendin-4 (4.3 kDa) has higher molecular weight than GLP-1 (3.1 KDa) and exendin-4 (9-39) (3.4 KDa). In fact, exendin-4 (9-39) is generated from a 8-animo acid N-terminal truncation of the exendin-4 agonist.

In situ mRNA hybridization or binding studies using radiolabeled GLP-1 (I^{125}GLP-1) localized the receptor in several tissues including pancreas (Thorens, 1992), heart and stomach (Bullock et al., 1996), lung (Lankat-Buttgereit et al., 1994), brain (Alvarez et al., 1996) (c.f. *3.2. Central GLP-1R localization and central effects*) and, afferent fibers of the vagus nerve of the gastrointestinal tract (Nakagawa et al., 2004). Although there is no expression of the receptor in the liver and muscle, it is found in human visceral white adipose tissue (Vendrell et al., 2011).

Nowadays, fluorescent probes compatible with super-resolution microscopy are used to target endogenous GLP-1R distribution and dynamics in tissues such as the pancreas and the brain. In 2020, Ast and colleagues presented LUXendin645, a far-red fluorescent GLP-1R antagonistic peptide label based on exendin-4 (9–39) that intensely labels GLP-1R (Ast et al., 2020). The study of GLP-1R expression patterns with new fluorescent probes will provide an updated view of GLP-1R organization and new pharmacological insights for the treatment of metabolic diseases.

Despite the several many effects of GLP-1, including modulation of β-cell proliferation and apoptosis, glucagon secretion, cardiac performance, heart rate, blood pressure or steatosis (Figure II.4), I will only provide a detailed explanation about its insulinotropic effect on β-cells

as well as its central role within the CNS (see the following reviews for further details about other GLP-1 roles: Holt et al., 2007, Müller et al., 2019).

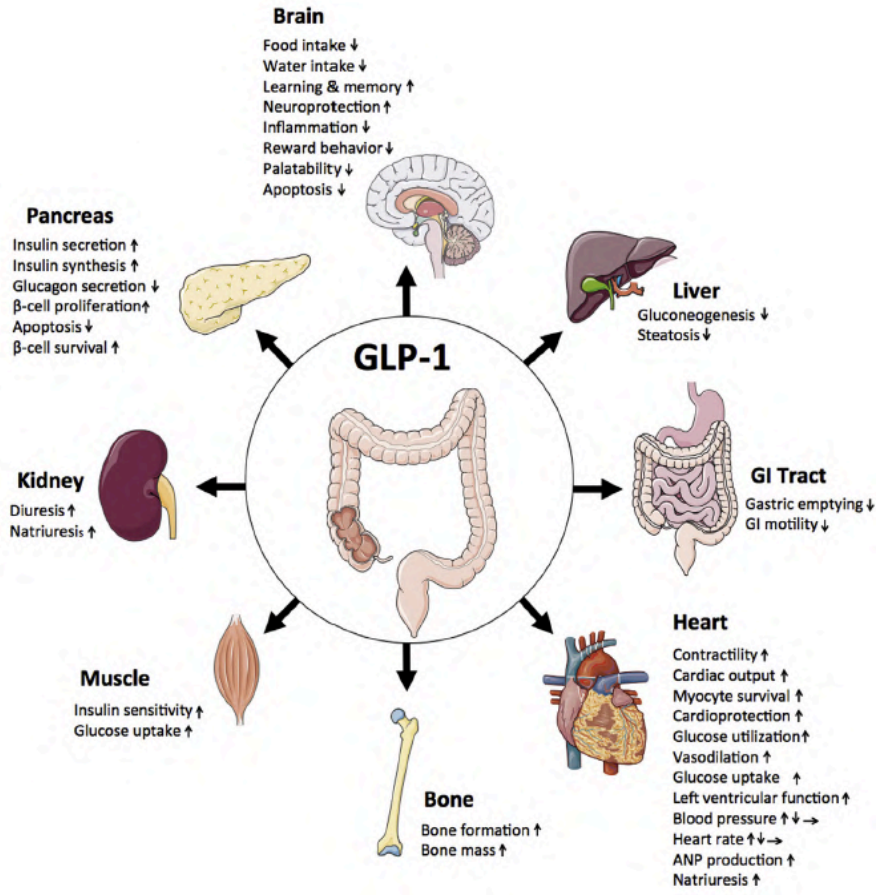

Figure II.4. Illustration of the metabolic effects of GLP-1. The schematic include direct and indirect GLP-1 effects. *Image source: Müller et al., 2019.*

3.2. Effects on β-cell insulin secretion

It is known that GLP-1 acts directly on the β-cell of the pancreas by binding to its receptor to activate adenyl cyclase (Drucker et al., 1987) *via* a stimulatory G protein, triggering a downstream signaling cascade that increases the glucose sensitivity of the β-cell. The rise in cAMP leads to activation of PKA (Protein Kinase A) and Epac (exchange protein directly activated by cAMP). PKA activation stimulates the closure of ATP-sensitive K+ (K_{ATP}) channels, leading to depolarization of the cell membrane and opening of L-type VDC channels, which, in turn, lead to Ca^{2+} influx. The entry of Ca^{2+} is responsible for exocytosis of insulin granules and insulin secretion to circulation. Concomitantly, PKA blocks Kv (voltage-dependent) channels to prevent membrane repolarization and enhancing more the Ca^{2+} influx extending the time in which VDC channels remain opened (Müller et al., 2019) (Figure II.5). Epac proteins has an important

role on the insulinotropic effect of GLP-1 since around 50% of insulin release induced by GLP-1 is mediated via the cAMP-dependent activation of the Epac2 protein. They stimulate the release of Ca^{2+} from the endoplasmic reticulin (ER), and thus, increase the Ca^{2+} intracellular pool. When glucose concentrations are higher, a calcium-induced calcium release (CICR) is triggered (i.e. ryanodine Ca^{2+} channels (RYR) in the ER are opened by Epac2), which, at the same time, depends on the continuous Ca^{2+} influx from VDC channels (Figure II.5). This process confirms the delicate regulation of the insulinotropic GLP-1 effect, being clearly dependent on glucose concentrations. In fact, in isolated pancreas of the rat, GLP-1 is not able to stimulate insulin release at low glucose concentrations (<2.8 mM), but enhances insulin secretion when glucose is higher than >6.6 mM (Drucker et al., 1987). Consistently, the risk of hypoglycemia of GLP-1-based therapy for T2D is very low (Nauck et al., 2002).

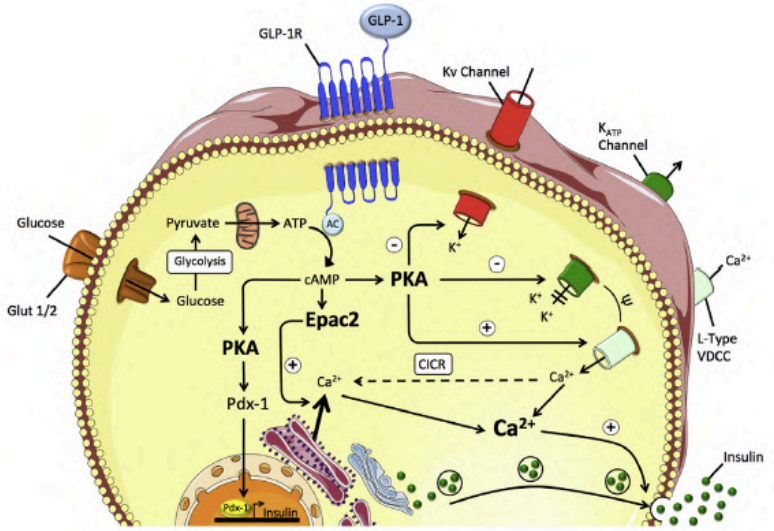

Figure II.5. GLP-1 mediated insulin secretion in the β-cell. Binding of GLP-1 to its receptor on the pancreatic β-cell activates adenylate cyclase (AC), which induces a molecular cascade whose main events are the closure of KATP channels, activation of Ca2+ channels, closure of Kv (voltage-dependent) channels *via* PKA activation; and release of Ca2+ from the endoplasmic reticulin (ER) via Epac2. Together with the effect of GLP-1, and in an inseparable manner, glucose is transported inside the β-cell (across Glut1/2) and metabolized to enable insulin secretion. GLP-1 is also thought to activate transcription of the gene coding for insulin *via* a PKA-mediated increase of Pdx-1 expression in the nucleus. AC: adenylate cyclase; PKA: protein kinase A; Epac2: exchange protein activated by cAMP; CICR: calcium-induced calcium release; GLUT1/2: glucose transporter 1/2; Pdx-1: pancreatic and duodenal homeobox 1. Image from Müller et al., 2019

3.3. Central GLP-1R

3.3.1. GLP-1R localization in the brain

In 1996, a study demonstrated the presence of GLP-1R in the rat brain by *in situ* hybridization, specifically localized in certain nuclei of the hypothalamus such as the supraoptic, paraventricular, ventromedian and arcuate nuclei (Shughrue et al., 1996; Navarro et al., 1996). The presence of GLP-1R in other brain regions such as the thalamus, the olfactory cortex and the choroid plexus was also established in the same year (Alvarez et al., 1996).

In 2018, by *in situ* hybridization with a novel antibody, GLP-1R+ cells in mice were observed in numerous regions of the telencephalon (amygdala, septum, preoptic area, nucleus accumbens, OB), diencephalon (ARC, PVN, DMH, LHA, supraoptic nucleus) and areas of the mesencephalon. Within the medulla, GLP-1R was identified in the AP, NTS and lateral reticular nucleus (Jensen et al., 2018).

Using GLP-1R binding assays, GLP-1R immunocytochemistry and injection of fluorescent-labeled GLP-1 analogue exendin-4, GLP-1Rs were found in the mouse OB, within the soma of the principal cells of the bulb, the mitral cells (c.f. *Chapter III*), distributed in an orderly row within the mitral cell layer (Thiebaud et al., 2016).

Interestingly, GLP-1R is also present in astrocytes and plays a role in the maintenance of mitochondrial integrity as well as in fatty acid oxidation on mice (Timper et al., 2020).

In humans and non-human primates, GLP-1R has been identified in the cerebral cortex, hypothalamus, hippocampus, thalamus, CVOs, substantia nigra, cerebellum and brainstem (see the review Rowlands et al., 2018).

Among the numerous extrapancreatic effects of GLP-1R analogs, one of the most frequently described is their ability to centrally reduce food intake and body weight. In this manuscript, I will thus only provide further details about central regulation of feeding circuits by GLP-1.

3.3.2. GLP-1 effects on food intake

Food intake suppression by GLP-1R agonists has been established in mice, rats, pigs, non-human primates and humans (reviewed by Müller et al., 2019). This effect has been demonstrated to be centrally mediated in both healthy individuals and T2D patients. It can thus be considered that central GLP-1 activity is required for optimal energy balance (Barrera et al., 2011).

The decrease in body weight mediated by GLP-1 analogs is due to its potent role in reducing food intake (Finan et al., 2013). When injected systemically, different signaling pathways transmitting the GLP-1 signal to the brain seem to be necessary depending on the

peptide (whether it is native GLP-1 or a synthetic GLP-1 analog) and the administration route (whether s.c., i.p. or i.v.) (Baumgartner et al., 2010). Nevertheless, collectively, the signals may be mediated by vagal afferents in mice, rats and humans. Also, different brain areas seem to be involved in mediating the anorexigenic effects of GLP-1. Leaky-BBB areas as the median eminence are preferred entering sites for long-acting GLP-1 analogs. Nevertheless, it is uncertain whether native GLP-1 from the gut (with a half-life < 2 minutes), at physiological doses, inhibits food intake with the same power as more resistant GLP-1RAs at pharmacological doses.

Central delivery of GLP-1 promoting acute anorectic effect was described for the first time in 1996 (Turton et al., 1996; Tang-Christensen et al., 1996). In rodents, the inhibition of food intake triggered by i.c.v-injected GLP-1R agonists is blocked by exendin (9-39) (Larsen et al., 1997) and lacking in GLP-1R KO mice (Baggio et al., 2004). The same food intake inhibition is accompanied by increased cFos activity in the NTS, AP, PVN, ARC, amygdala and lateral parabrachial nucleus, aligning with the CNS GLP-1R expression list mentioned above.

GLP-1R induces acute modulation of AMPK (AMP-activated protein kinase) in the hypothalamus (Secher et al.,2014), attenuating the release of NPY and AgRP, as well as increasing POMC neuropeptides. GLP-1R activation within the hindbrain stimulates PKA and MAPK (Mitogen-activated protein kinase). This results in inhibition of AMPK in the NTS (Hayes et al., 2011). Ablation of PPG neurons in the NTS by diphtheria toxin had no effect on chow food intake or glucose homeostasis (Holt et al., 2019), leading to think that PPG^{NTS} neurons are involved in other specific feeding roles such as the control of larger, and more caloric, meals.

Several studies have suggested that the GLP-1RA liraglutide modulates energy balance by acting *via* the CNS, specifically the hypothalamus (Beiroa et al., 2014), and that tanycytic transport of i.p. injected liraglutide is crucial for its anti-obesity actions (Imbernon et al., 2022). However, Burmeister and colleagues suggested that the hypothalamic GLP-1R was “sufficient but not individually necessary” for the regulation of energy balance and glucose homeostasis, since the anorectic and glucose tolerance effects of systemically administered exendin-4 and liraglutide were preserved in hypothalamic GLP-1R KO mice (Burmeister et al., 2017). Thus the exact location of central GLP-1R and downstream recruited circuits that are involved in glucose and energy homeostasis remain unclear.

At present, the role of GLP-1 produced locally in the OB in food intake or glucose metabolism is unknown and only data showing changes in the excitability of mitral cells after GLP-1 addition *in vitro* (Thiebaud et al., 2016, 2019) were published so far.

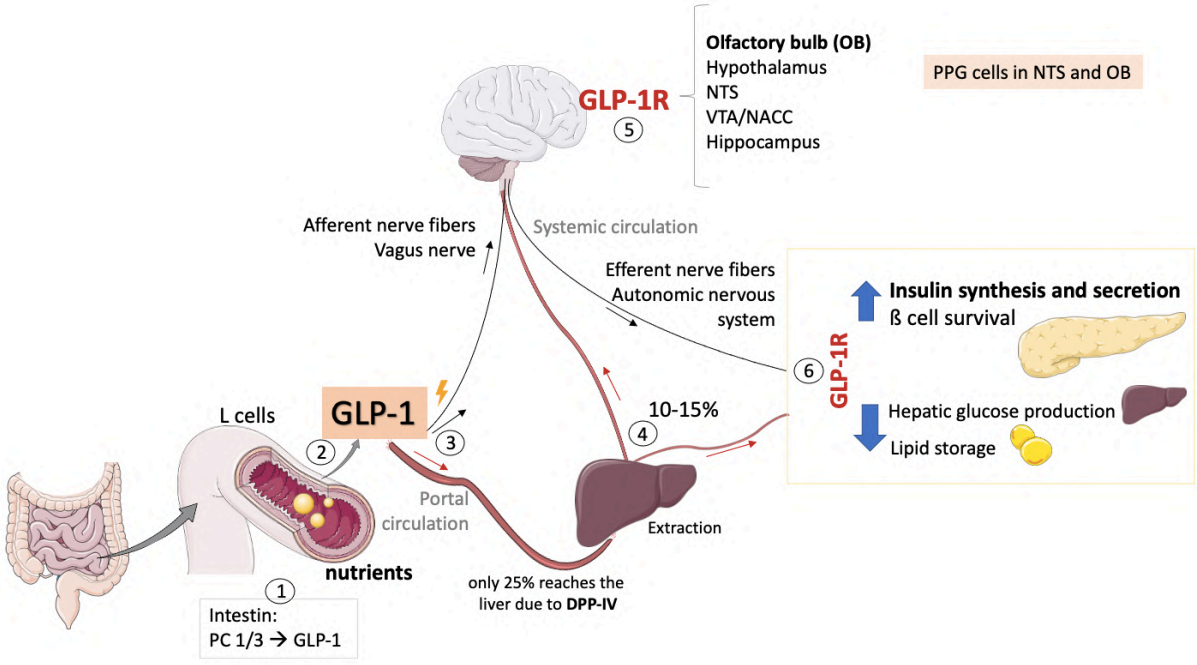

Figure II.6. Nutrient-induced stimulation of L-cell GLP-1 secretion and main GLP-1 biological activities. The schematic illustration includes intestinal synthesis (1) and secretion (2) of GLP-1, binding to activate vagal afferent neurons, or capillary take up (3), DPP-IV degradation and hepatic clearance of GLP-1, systemic circulation of GLP-1 (4), central GLP-1R and PPG-positive regions (5), ANS efferent projections and peripheral GLP-1 roles in glucose homeostasis (6). For further explanations, see subchapters.

Chapter III
The olfactory system

For hygienic and spiritual goals, humans are culturally embedded in olfactory environments, laundry liquids for clothes, perfumes on skin, essential oils in the house, incense burning for divinities, food cooking… Unconscious yet very much present in everyday life. Indeed, food odors play a crucial role in the appreciation of food quality, providing essential information about its composition.

There is a huge difference between humans and other mammals in the process of food consumption. For humans living in Western countries, food is available *ad libitum*, cheap concerning the junk food, and cooking is a highly sensory and cognitive process that enriches the chemical world of every human being. In wild mammals, the olfactory system is focused on survival behavior, especially for the detection of food and the appreciation of its quality.

The detection and perception of chemical signals from the environment requires the combination of three systems that are very important in the mammals relationship to food. Even if this relationship is very complex and involves all the sensory modalities, it is the chemical senses that are particularly solicited for the search, detection and appreciation of ingested food. They include three complementary systems: the gustatory system, the trigeminal system and the olfactory system (ortho- and retronasal). The flavor of food is defined by the integration of these three modalities.

Among all sensory modalities, olfaction, one of the oldest senses in terms of evolution, plays a very important role in the survival of many animal species. It allows to probe the external chemical environment for adapted behavioral response. Odors offer the possibility to identify and locate food, to take flight in case of detection of a predator or an aggressive congener, to execute a courtship when a partner emits the adequate signals, or to orientate over long distances.

In mammals, the olfactory system makes possible the perception of environmental odors, challenging the detection and the perception of thousands of unknown and exogenous molecules. Rodents have a strong olfactory-feeding crosstalk since they are nocturnal animals and rely on their smell for food foraging. However, not only in rodents but also in all mammals including

humans, olfaction is crucial for appreciating the quality of food (think about how we use our sense of smell to tell if food is in good condition, or to experience the flavor of a good wine).

1. Anatomical organization and function of the olfactory system

The olfactory system is composed of a peripheral part, the olfactory mucosa (OM) -a sensory organ for the detection of odorant molecules which is located at the back of the nasal cavities- and a part located within the CNS, which comprises the cerebral structures dedicated to the processing and the encoding of olfactory information, including its first relay, the main olfactory bulb (OB) (Figure III.1).

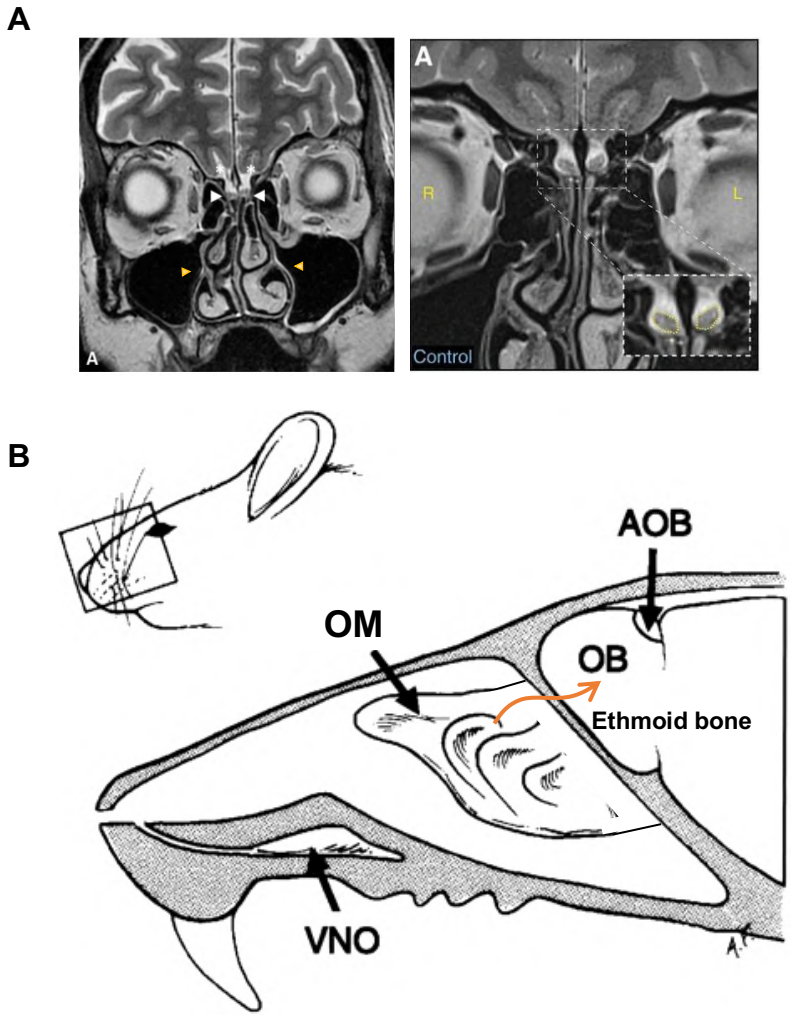

Figure III.1. Structures of the olfactory system. (A) Frontal MRI view of human olfactory bulbs (white arrowheads) and nasal cavity (yellow arrowheads) on coronal T2-weighted imaging (left). Zoom of the coronal view of the olfactory bulbs (right) located between the eyes. *Adapted from Braun et al. (2019).* (B) Schematic of a sagittal section of a mouse nasal cavity. The olfactory mucosa (OM) and the vomeronasal organ (VNO) are part of the peripheral olfactory system. The first stage of the central olfactory system consists of the main olfactory bulb (OB) and the accessory olfactory bulb (AOB) which receives the pheromonal information from the VNO. The peripheral olfactory system is separated from the central one by the ethmoid bone. *Adapted from Liman and Corey, 1996.*

Prior to reaching higher ascending pathways, it all starts when airborne odorants enter the nasal cavity after smelling. These molecules are solubilized in the mucus by adsorption on odorant binding proteins (OBP) and are concentrated within the OM in the nose. Detection of odors is possible thanks to the expression of olfactory receptors (OR) in olfactory sensory neurons (OSN), also named olfactory receptor neurons, inserted in the OM in the nose. Neurogenesis of OSN exists in the OM of mammals and persists into adult life: in the mouse the complete turnover of OSN is estimated to be around 6 weeks. Any molecule (or set of molecules), carried by breathing, detected by the olfactory receptors can be defined as an odor. Most of these molecules, found naturally in the environment, are small (<300 Da), light, volatile and hydrophobic (e.g. Vanillin, 152g/mol). However, many "odors" that we perceive on everyday life, in particular food odors, are artificially produced by food industry. The strategy is either to mimic natural odorants such as vanillin or to synthesize molecules *de novo* such as Ethylvanillin (Figure III.2). Pure natural molecules are rare. Rather, odors are mixtures of different odor molecules produced, for example, during cooking or baking (e.g. peanut butter cookies). These mixtures are also named food aromas. The characteristics -how they influence olfactory perception and the cognitive processing they undergo- are detailed in the review of (Thomas-Danguin et al., 2014).

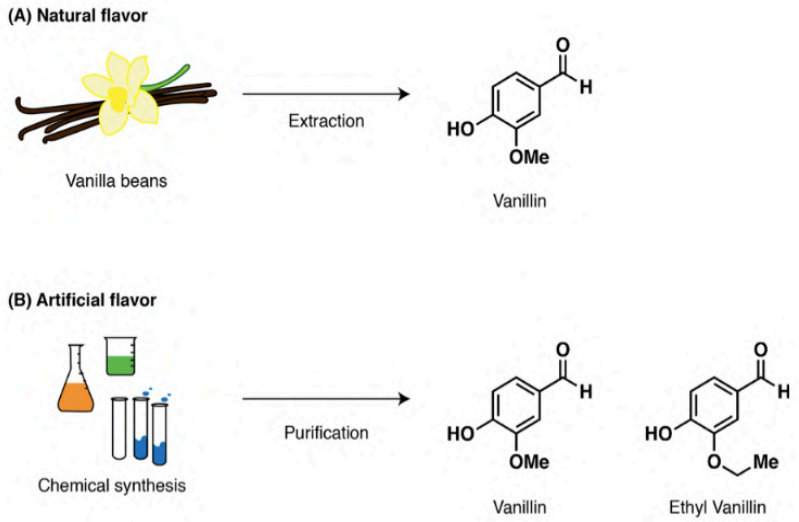

Figure III.2. Vanilla flavoring molecules from natural or artificial sources. (A) Vanillin extraction from vanilla beans is challenging and costly. (B) Chemical synthesis of artificial vanillin and ethylvanillin, another vanilla flavoring molecule not found in nature and only made by humans. It is a cheaper alternative to vanilla, strongly used by food industry.

An immense variability, even infinite, of odorant molecules exist which could be detected by the OR and coded in the OB of the mammals olfactory system. Main functional chemical

groups detected by OR include aldehydes, ketones, alcohols, benzene cycles along with others. The detection system is so sensitive that molecules differing by only one atom, or even molecules with the same formula but enantiomers can be distinguished: pairs of stereoisomers such as (+)carvone, smelling of anise, and (-)carvone, smelling of mint, can be discriminated. However, some enantiomers such as the two limonenes [(-)limonene and (+)limonene], remain indistinguishable in rodents when sampled without association but become distinct after learning (Linster et al., 2001).

Since the mouse has been the experimental animal model chosen for my PhD project, I will rely on the abundant literature on the rodent olfactory system to describe the anatomical architecture and functions of the OB, not only as a sensory system but including its role on energy balance regulation. A section will be dedicated to human olfaction at the end of this subchapter (c.f. *1.5. Perceptual links between smell and the metabolic state in humans*).

1.1. Olfactory receptors

The understanding of the functional organization of the olfactory system was made possible by the work of Buck and Axel (1991), who received the Nobel Prize in Medicine and Physiology in 2004 for their discovery of the family of genes coding for olfactory membrane receptors. In rodents, there are about a thousand genes, which represents 2% of the active genome. This is an extremely large number for a single family of receptors, but it is still quite small compared to the almost unlimited variability of odorant molecules.

Bioinformatic analyses comparing the entire genomes of various species have revealed large interspecific variations in the number of OR genes, potentially reflecting adaptation to specific environments (Niimura, 2012): dolphins that have adapted to aquatic life have very few OR genes (14) (Hayden et al., 2010) while humans have about 396 (Niimura and Nei, 2003; Matsui et al., 2010) and mice and rats 1130 and 1207, respectively. The largest current repertoire of OR genes is the African elephant, with nearly 1948 genes (Niimura et al., 2014). Surprisingly, among all these genes, each OSN expresses only one coding gene that itself produces a single type of OR (Chess et al., 1994; Firestein, 2001; Mombaerts, 2004). OR are composed of seven transmembrane domains and are coupled to G proteins. Once a functional OR gene is expressed, the OR itself exerts a negative feedback control by blocking the activation of expression of other OR genes (for more details, see the review Nishizumi and Sakano, 2015). Thus, despite the millions of OSNs present in the OM, each cell recognizes only a limited number of chemical molecules. However, the efficiency of the olfactory system is redoubtable.

Even if OSN express only one type of receptor, they are nevertheless able to recognize several odorant molecules by detecting a particular feature of the odorant (carbon chain length, aromatic cycles, spatial configuration, chemical groups…). If a molecule has several features, then it will be able to activate several OSN subtypes. Importantly, the odorant-receptor interaction

is made with a variable affinity; some receptors will present high affinity and others low affinity, but all of them will be considered in the coding processing. The repertoire of OSN activated per odorant molecule is specific even though an OSN may participate in the detection of several odorant molecules, what lays the building of the combinatorial detection. Each odor activates a unique set of OSN, not only according to its chemical composition but also according to its concentration in the inspired air. Because each OSN can be part of a combinatorial set for many odorants, this system allows for the detection of a very large number of odorants (Malnic et al., 1999).

1.2. The olfactory bulb: the first central relay of olfactory information

The OB is the most anterior structure of the brain in rodents. It is also the first structure to encode odors: after receiving signals from the OR that have been activated by an odorant molecule within the OM (Figure III.3A), these signals are encoded in the OB to give rise to a specific spatiotemporal representation of the odor perceived in the periphery. Neurons in the OB will thus establish spatial odor maps (chemotopic organization of olfactory glomeruli) (Figure III.3B) and multiple temporal strategies including changes in oscillatory patterns by the interplay of mitral and granule cells (for an elegant review on OB oscillations and olfactory memory, see Martin and Ravel, 2014). This initial processing of olfactory information is then transmitted in parallel and simultaneously to the olfactory cortex (mainly the piriform cortex) and the limbic system to give an identity to the sensory stimulation. Identification is tightly linked to olfactory hedonics, emotions and memories.

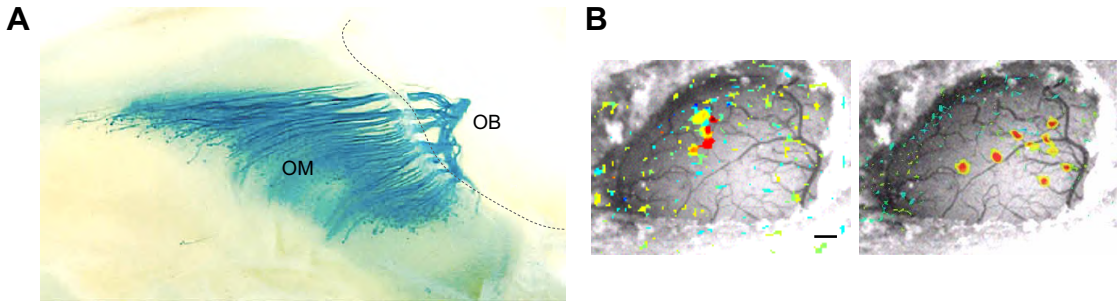

Figure III.3. (A) View of the olfactory mucosa and the medial aspect of the OB in mice. Olfactory sensory neurons expressing one subtype of OR (P2) are stained in blue (X-Gal staining on P2-IRES-tau-lacZ mice) and project their axons to a single glomerulus within the OB (convergent point in the image, at right). *Image from Mombaerts et al., 1996*. Scale bar = 200 µm. **(B) Olfactory maps at the dorsal surface of the OB in rats** in response to 2% phenol (left) or 2% acetophenone (right) recorded by optical imaging. Each dot corresponds to the activation of a single glomerulus *in vivo*. Scale bar = 200 µm. (Buonviso and Gurden, 2013 in "Odorat et goût: de la neurobiologie des sens chimiques aux applications").

The OB consists of two symmetrical hemibulbs with six concentric layers of which only four have cell bodies. Hereinafter I describe the structural organization from the most superficial to the most internal layer and their different cell types (Shepherd, 2004; Tavakoli et al. 2018).

The Olfactory Nerve Layer (ONL)

The ONL is the most external layer. It consists of the distal endings of the OSN axons projecting to the OB. These axons are surrounded by olfactory ensheathing cells, and then enter the glomerular layer to form synapses with different cell types within the olfactory glomeruli (Pinching and Powell, 1971).

The Glomerular Layer (GL)

The GL contains the functional modules of the OB, the olfactory glomeruli. Glomeruli are spherical structures about 100 micrometers in diameter where synapses are formed between thousands of OSNs axons and few dozens of mitral and tufted cells (M/TC) dendrites (it is a neuropil area). Although M/TC both project their axons to the olfactory cortex, the position of their cell bodies, their connections and the way they encode odors differ (Figure III.4).

Each glomerulus is bounded by a glial capsule composed of astrocytes (Daumas-Meyer et al., 2018) with several types of interneurons, the juxtaglomerular cells (JC), interspersed among them:

- Periglomerular cells (PGC) which are GABAergic and dopaminergic inhibitory interneurons that allow local inhibition of the incoming signal allowing normalization that could explain the invariance with respect to odor concentrations.
- External tufted cells (ETC) which are excitatory cells whose cell bodies are in the EPL but which send their primary dendrites inside the glomeruli where they receive monosynaptic input from the axon of the OSN and form excitatory synapses with the projections of the other cell types in the glomeruli.
- Superficial short axon cells (SAC) are mainly glutamatergic cells surrounding the glomeruli. Their dendrites emit extensions and receive afferents from the ETC, but more importantly they project to several glomeruli, activating PGC and potentially allowing lateral interglomerular inhibition (Kiyokage et al., 2010).

The External Plexiform Layer (EPL)

The EPL contains the cell bodies of tufted cells, which project their main dendrite to a single glomerulus, and whose axons carry the output signal to the olfactory cortex faster than mitral cells. The EPL also contains the apical and secondary dendrites (lateral dendrites) of the M/TC and the secondary dendrites of the granule cells from the deepest layer of the OB.

The Mitral Cell Layer (MCL)

The MCL is a thin single-cell layer composed of the cell bodies of mitral cells (MC), which are the main output neurons of the OB (together with tufted cells, TC). The MC have the characteristic pyramidal shape of the main cells of a cortical structure. Each MC projects a single apical dendrite within a glomerulus and 20 to 25 MC converge into a single glomerulus. The MC also project secondary dendrites, which terminate in the EPL, interacting dendrodendritically with granule cells. The axon of a MC crosses the deep layers of the OB, is embedded into the lateral olfactory tract (LOT) and establishes divergent synaptic connections with other neurons in several structures of the olfactory cortex (Sosulski et al., 2011) (Figure III.4).

The Internal Plexiform Layer (IPL)

The IPL is extremely thin and contains little amount of cell bodies (dSAC, see next paragraph). Mainly the dendrites of granular cells projecting towards the outer layers pass through the IPL, as well as the axons of MC and TC which conversely go towards deeper layers of the OB.

The Granular Cell Layer (GCL)

The GCL is extremely dense and contains cell bodies of GABAergic granule cells (GC). GC do not have axons, but instead develop a very dense dendritic arborization that allows them to establish important synaptic connectivity with the secondary dendrites of the MC within the EPL. The GCL also contains cell bodies of deep short axon cells (dSAC), which have axons that reach the MCL and EPL but do not project outside the OB (Price & Powell, 1970; Nagayama et al. 2014). Morphologically, dSAC, containing the PPG positive cell population, have an intermediate diameter between GC (6-8µm) and MC (15-30µm) and their cell bodies are found in the GCL and IPL in rats (Eyre et al. 2008).

Finally, in the innermost zone of the OB there is a subependimal zone. It constitutes the terminal part of the rostral migratory flow, which carries new formed cells from the SubVentricular Zone (SVZ) (Luskin, 1993). In adult rodents, these SVZ primary progenitors migrate to the OB where they differentiate into multiple types of interneurons (PGC and GC).

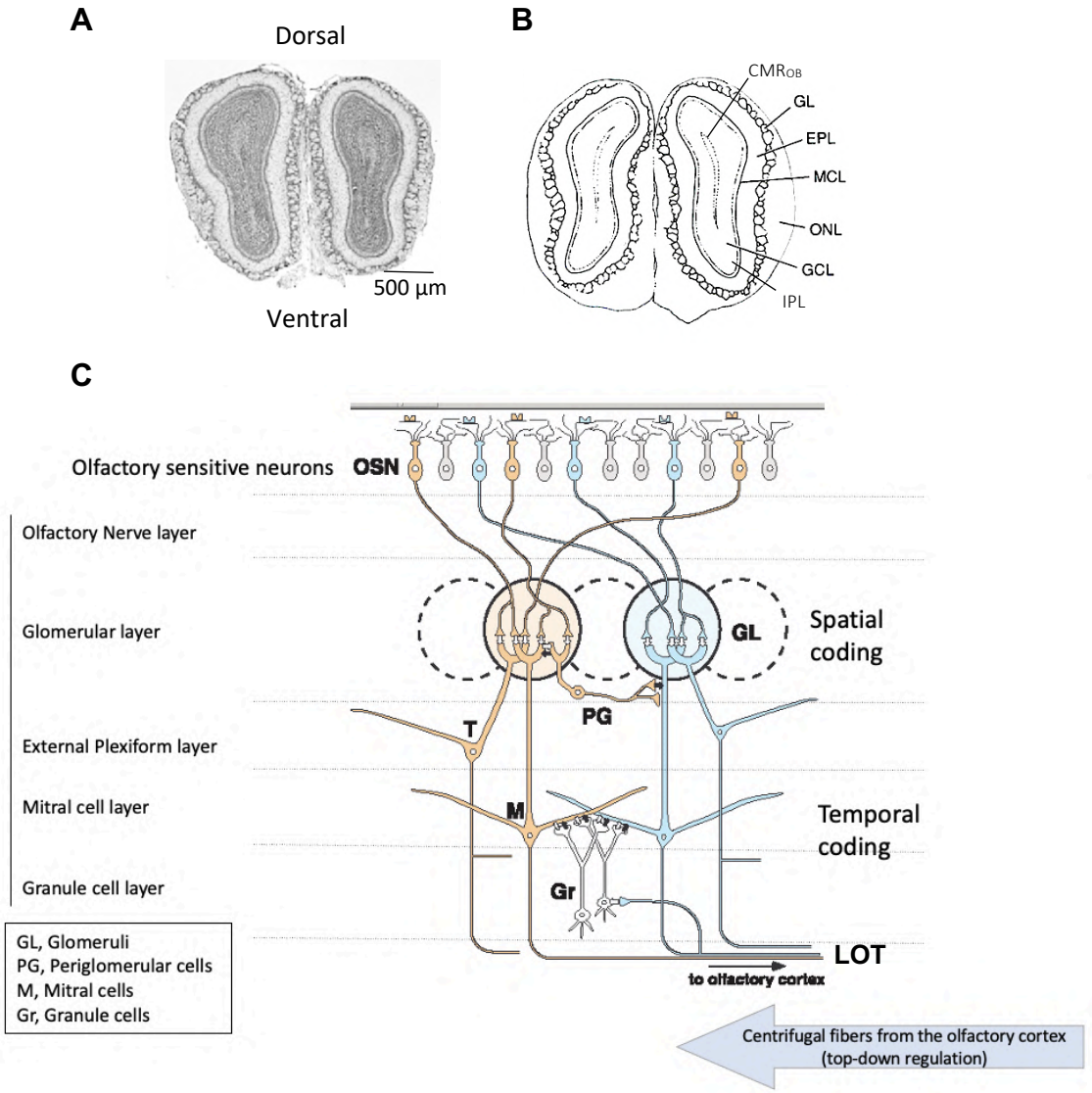

Figure III.4. Synaptic organization within the OB. (A) Cresyl violet staining of the different cell layers of the OB on a coronal section of the rat OB. (B) Representative OB section showing the different OB layers. CMR_{OB}: bulbar part of the rostral migration stream; GL: glomerular layer; EPL: external plexiform layer; MCL: mitral cell layer; ONL: olfactory nerve layer; GCL: granular cell layer; IPL: internal plexiform layer. *Adapted from Mombaerts et al., 1999*. C) Schematic illustration of the neuronal network in the OB. OSNs project their axons into the GL, where they form synapses with mitral cells in the OB within a glomerulus. Three types of neurons surround the glomeruli in the GL: PGs (periglomerular cells), ETCs (outer plume cells, not shown), and SAC (short axon cells, not shown). Mitral cells (M) and tufted cells (T) form synapses within the glomeruli, but the cell bodies of M are located in the MCL, whereas those of Ts are located in the EPL. The dendrites of the M/TC extend into the EPL and MCL, where they form dendrodendritic synapses with the granule cells (GC). The densely packed GCL contains mainly the cell bodies of the GC. M projections reach the olfactory cortex through the LOT (bottom-up regulation). Centrifugal inputs from the limbic system also project inside the OB (blue arrow, top-down regulation). *Adapted from Mori et al., 1999.*

1.3. Olfactory system pathways

Anatomical connections within the olfactory system were studied since the 1970's and the initial work of Pinching and Powel (1971). Odorant molecules are detected by the OSNs which send their afferents to the corresponding glomeruli at the level of the OB. At the exit of the glomeruli, the projections of the M/TC are diffusely distributed *via* the lateral olfactory tract (LOT) to a set of structures forming the "primary olfactory cortex" (Figure III.5A). This cortex includes the anterior olfactory nucleus (AON), the piriform cortex (PC) - the structure that receives the greatest number of OB inputs from M/TC (Figure III.5B)-, the hypothalamus, the olfactory tubercle, the lateral entorhinal cortex and the anterior and post-lateral cortical nucleus of the amygdala (Price, 1985). These structures are all part of the limbic system.

Then, the olfactory information is transmitted to higher brain structures (Figure III.5A, 5C). The posterior piriform cortex projects into the insula, the orbitofrontal cortex (highest projections), the hypothamalus (Price et al. 1991), the amygdala. Multisensory integration is performed in the piriform cortex, amydala, insula and orbitofrontal cortex (OFC). Flavor is built in the insula which integrates olfactory, taste and trigeminal information from food consumption. The entorhinal cortex, which receives inputs from the AON, projects to the hippocampus and is implicated in spatial navigation based on olfactory cues. The olfactory tubercle projects into the nucleus accumbens thus into hedonic, motivational circuits. The OB therefore represents a direct and powerful source of sensory input to the limbic system dealing with emotions, memory and feelings. The "Madeleine de Proust" phenomenon, a sudden vivid recall of precise events due to odors and taste centered on food consumption, is due limbic activity since odors are powerful cues that trigger episodic memories and strongly activate the limbic system (see the review of Saive et al., 2014). The Madeleine memory includes joy, pleasure, nostalgia… thus it is widespread in the limbic system.

Except for the OT, the modulation is bidirectional for the other regions of the primary olfactory cortex. They project back to the OB through centrifugal fibers that return to the GL and GCL *via* the LOT (Matsutani and Yamamoto, 2008; Padmanabhan et al., 2019). These loops are crucial for optimal olfactory processing and memory (Figure III.5). Indeed, the difficulty of odor discrimination of very close molecules is compensated by learning: the accumulation of trials triggers top (olfactory cortex) - down (olfactory bulb) mechanisms that will refine odorant representation in the OB space.

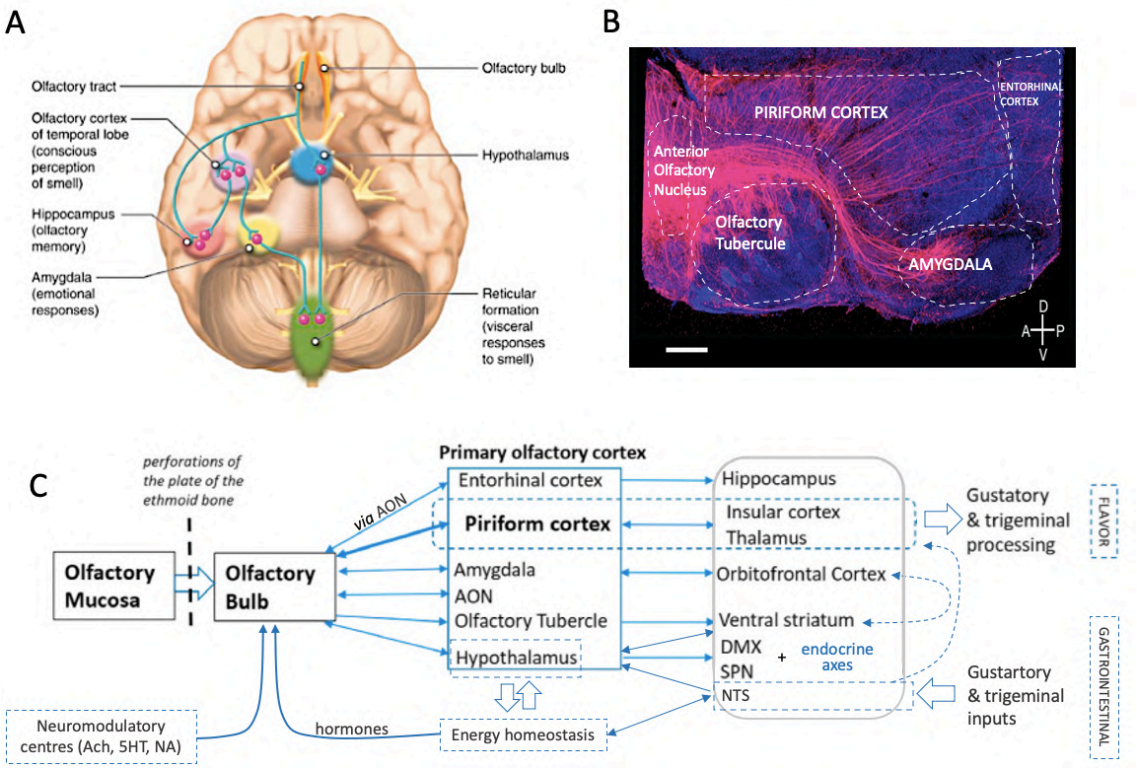

Figure III.5. The pathways of olfactory information processing. A) Human brain from a ventral angle. The OB and other brain structures involved in olfactory processing are colored. B) M/TCs exhibit distinct patterns of projections to numerous areas of the mouse olfactory cortex. Scale bar = 700 µm. *Modified from Sosulski et al., 2011.* C) The major ascending neural pathways of the olfactory system and other neural/metabolic signaling involved (details in the text). AON: Anterior Olfactory Nucleus; DMX: dorsal motor nucleus of the vagus nerve; SPN: sympathetic preganglionic neurons; NTS: nucleus of the solitary tract; Ach: Acetylcholine; 5HT: serotonin; NA: noradrenaline. *A) and C) are modified from Faour et al., 2022.*

1.4. Behavioral assessment of mouse olfaction

Olfactory information is essential for a wide-range of mice behaviors (e.g. navigation, sexual behaviors, predator avoidance and foraging) (Doty, 1986; Schellinck et al., 1993; Kavaliers et al., 2005). In lab research, several behavioral tests developed for mice depend on olfactory cues, including learning and memory tests, or social choice tests. Thus, in this subchapter I present two procedures that offer a rapid assessment of the perception capacities and integration of olfactory information in mice: the buried food test (BFT) and the olfactory habituation/dishabituation test. These tests rely on the spontaneous behavior of rodents and are not guided by an appetite reinforcement or an aversive experience (i.e. by an odor valence). They usually present more heterogeneous data than conditional tasks.

The buried food test

This test was first described in the early 1970s (Alberts and Galef, 1971). Since then, it has been used to check for the ability to smell volatile odors, measuring the time spent for an overnight-fasted animal to find a tiny piece of familiar palatable food (e.g. cookies, chocolate) buried underneath the bedding of the cage. The latency is measured and indicates whether mice have normal olfaction or olfactory deficiency. Food-deprived mice presenting optimal olfaction usually find the hidden palatable piece of food within 1 (Jamain et al., 2008) or few minutes. If mice spend a significant larger time, or they fail to locate the food, poor olfactory detection is assumed.

Olfactory habituation/dishabituation test

This second test was first described in the early 1980s (Gregg and Thiessen, 1981). It is commonly used to assess whether a mouse can detect and discriminate different (and same) odors (Wersinger et al., 2007), including both non-social and social odors. It can also be used to test the ability to distinguish different concentrations of the same odor. The test consists of sequential presentations of diverse odors. Olfactory habituation is defined by a progressive reduction of olfactory exploration (sniffing) for a repetitive exposure with the same odor. Olfactory dishabituation is described as a restoration of the sniffing when a novel odor is presented. The indicator of normal olfactory performance is a significant habituation-dishabituation, i.e. a reduced sniffing time during the habituation and a quick restoration of sniffing when a novel odor is presented.

Other olfactory tests are principally focused on feeding behavior and reflect the strong link between olfaction and the metabolic state. A Pavlovian learning paradigm is required for this learning, to settle an association between a potent stimulus and a previously neutral stimulus. The learning can be either appetitive (e.g. go/no-go task) or aversive (COA or conditioned olfactory aversive test).

COA is acquired by aversive learning. A food odor (the neutral stimulus) can be strongly aversive in case of an associated digestive pain (the potent stimulus). This case is studied in laboratories using a COA task, associating an odor with the injection of lithium chloride, which causes the gastrointestinal discomfort (Aimé et al. 2007). The group of Karyn Julliard in Lyon Neuroscience Research Center has published several articles based on COA where rats learn to avoid an odor of isoamyl acetate mixed with their drinking water because it has been previously associated with lithium injection. This association strongly activates the olfactory and the limbic systems and is encoded in long-term memory (e.g. in the amygdala or the insula) helping animals to survive in nature since a food poisoning experience is strongly retained in memory. A similar issue happens in humans (in both adults and adolescents): memories are more powerful when an

experience is accompanied by unpleasant odors (Cohen et al., 2019), including food odors, which consequently appear to be strong influences on sensory-specific appetite (Boesveldt and de Graaf, 2017), food preferences, meal sizes (Ferriday and Brunstrom, 2008) and calorie intake.

1.5. Perceptual links between smell and the metabolic state in humans

Appetite is driven by large structural networks in the brain including nutritional state, environmental cues, mood, and reward pathways that are balanced in brain networks. Food preference, selection, and consumption are determined by multiple sensory inputs including sight, sound, smell, taste and touch (hand somatosensory activation, tongue trigeminal activation). Thus, environmental cues detected by external senses strongly influence feeding together with internal chemical senses (think about food poisoning) and are associated with a large range of valence (from appetitive to aversive) of food depending on the history of the subject. Among them food odors strongly modulate appetite (Zoon et al., 2016; Proserpio et al., 2019) and can signal qualitative information about food, including the calorie (energy) density and specific macronutrient content (that other senses can't identify). For example, subjects can use odors to distinguish fat content in a dish (Boesveldt and Lundstrom, 2014). Odor-taste-nutrient associations are developed through repeated learning during food consumption, the most repetitive activity in Homo sapiens (Stevenson and Boakes, 2004; Boesveldt and de Graaf, 2017; Morquecho-Campos et al., 2019).

Olfactory experience starts very early in life, at the third trimester of pregnancy when the olfactory system is mature, and the new-born already expresses and builds basic olfactory preferences and memory (Schaal et al., 2020). In fact, olfactory memory is the oldest in a human's life. In addition, olfactory memory is the basis of the autobiographical odor memory during childhood and is a strong label of olfactory and food preferences (Willander and Larson, 2006; Saive et al., 2014). Indeed, empirically, we know that in western countries, food odors are powerful markers during childhood. Family meetings are organized around food consumption and every year each kid lives a hyper-hedonic and sensory event, the birthday party, an association of high fat high sucrose food intake with familial and social interactions granted by many gifts. In other parts of the world, food is enriched by aromas from spices or other odoriferous and tasty condiments and plants. These olfactory and taste preferences linked to food are nicely reviewed by Ventura and Worobey (2013).

Liking and wanting are the 2 main rewarding qualities for food consumption described in the literature. Liking is the pleasure triggered after food ingestion. Wanting is the desire or motivation to consume the food item. Both are strong for palatable food (Morales and Berridge,

2020). As a result of the two first ones, judgment and choice are built and lead to decision making. In the context of our study, we will not detail hedonic dopamine-dependent circuits, but clearly Ventral Tegmental Area neurons, releasing dopamine onto the nucleus accumbens, amygdala and medial prefrontal cortex neurons, express the same receptors than hypothalamic and bulbar cells to anorexigenic and orexigenic hormones (Abizaid et al., 2006; Figlewicz et al., 2003).

There are three known odor-related and food-specific mechanisms to suppress appetite: Olfactory sensory-specific satiety (OSS), *alliesthesia* and conditioned satiety. OSS is a perceptual link between smell and the metabolic state, characterized by a specific decrease in the odor pleasantness of a food eaten to satiety (Rolls et al., 1981) or smelled without ingestion for as long as it would be in the mouth during a meal. *Alliesthesia* is described as the modulation of the rewarding value of a stimulus according to the internal state. In fact, studies presenting food-related stimuli to participants have shown that the same stimulus can be perceived as either pleasant during a state of hunger (positive *alliesthesia*) or unpleasant during a state of satiety (negative *alliesthesia*) (Cabanac & Fantino, 1977). Thus, OSS and *alliesthesia* are difficult to separate because olfactory food cues are very often rewarding and trigger *alliesthesia*. The third perceptual link between smell and the metabolic state is conditioned satiety, first described by Le Magnen in 1955 (Le Magnen, 1955). It can be acquired by classical conditioning (aversive learning, odor valence) as already mentioned above for COA.

It is certain that food odors (mainly unconsciously but also consciously) are attractive sensory cues and motivate feeding behavior. However, contrary to general belief, there is no evidence that a food odor itself would trigger further food intake in quantity in healthy people: rather, it is more likely that food odors serve as a proxy of food quality influencing complex hedonic parameters such as liking and choices/preferences (Morquecho-Campos et al., 2020; Yeomans, 2006). This means that there is no linear relationship between olfactory cues (olfactory identity and concentrations) and food intake (rather feeding patterns) in lean organisms (Boesveldt and de Graaf, 2017), but what about obese organisms? It was shown that olfaction is impaired in obese organisms and could participate in triggering it (Faour et al., 2022). However, losing olfaction in itself would not trigger hyperphagia and sensory specific satiety does exist in obese people (controversial results exist: see Reichelt et al. 2014 vs. Myers, 2017). Another brain function should be considered: it was shown that obese humans present a stronger attentional bias toward foods when they were primed with a non-attentively perceived high- energy dense food odor. Thus, specific attentional biases toward foods with olfactory priming exist in obesity (Mas et al., 2019) and attention to the sensory surrounding of the meal should be further studied. These authors also think that cognitive vulnerability in obese may change the processing of food-related stimuli and only while food cues are non-attentively perceived. This concept is also supported by

the fact that i) the middle frontal gyrus involved in attention, executive functions and motor functions, present connectivity changes in MRI studies of obese subjects compared to lean ones (García-García 2015) and ii) high reward value odors such as chocolate are further detected by obese subjects (Stafford and Whittle, 2015) and activate reward-related structures (Han et al., 2021).

2. Interplay between the olfactory bulb and energy homeostasis

Strongly present in every day of humans life, a food odor can be described as a complex set of odorant molecules that have acquired a specific valence by association and learning during recurrent food intakes (imagine when you pass every day in front of a bakery and the scent of a baking croissant is flooding out and filling the street). Because of their volatility, food odorant molecules can take the orthonasal pathway to access directly the nasal cavity during the preprandial phase (smelling the croissant from a distance before buying one), but also the retronasal pathway (Negoias et al., 2008) when they are in the oral cavity during food consumption (eating the croissant releases additional odorants in the mouth). The olfactory system is thus constantly stimulated, not only while eating but also during the early phases prior to meals. Indeed, the odor-food association is intensely hedonic (relishing the croissant flavor) and its complexity is established over time, during development.

The nutritional status of an individual influences his or her ability to detect food odors. In general, fasting facilitates the detection of them (the croissant smells stronger and better when you did not had breakfast before leaving home), whereas satiety, with respect to a particular food, reduces the ability to detect the odor specifically associated with that food (O'Doherty et al., 2000; Mulligan et al., 2002). The peptides of energy metabolism and hormones are likely to be among the signals responsible for the cellular mechanisms underlying hunger and satiety and present numerous receptors in different parts of the olfactory system such as the OM and the OB.

Even if, as I mentioned before, it is accepted that smell plays a crucial role on controlling appetite and satiety in humans (Yeomans, 2006; Proserpio et al., 2019; Aimé et al., 2012; Faour et al., 2022). understanding the crosstalk between olfaction and energy balance regulation under physiological states is still at an initial stage.

2.1. Receptors to metabolic signaling molecules in the OB

Metabolic hormones and peptides governing the mechanisms of satiety and hunger are usually classified as either orexigenic or anorexigenic factors. In the 1980s, receptors for metabolic hormones and peptides were suggested to be expressed in olfactory-related brain areas. The consistent growing data brought since then have demonstrated that the OB, and also the OM,

are real targets for these metabolic factors. Additionally, a recent study has shown that a complex between metabolic factors (e.g. CCK, leptin) and neuromodulators (e.g. acetylcholine, serotonin) could fine-tune olfactory networks (Huang et al., 2021).

The olfactory system and energy homeostasis regulation system share several common molecular pathways: there is evidence that the olfactory bulb is not just a sensory tissue but also a metabolic sensor (Palouzier-Paulignan et al., 2012). Additionally, like the hypothalamus, the OB presents a more permeable blood-brain barrier (Ueno et al., 1991) and its blood capillaries are highly dense. Indeed, most of the hormones and neuropeptides produced by peripheral organs and brain centers of energy homeostasis regulation seem to be able to bind to their receptors expressed in the OB (Figure III.1). The OM and piriform cortex also present several receptors for metabolic signals. In turn, a number of these hormones and neuropeptides are also produced by olfactory structures.

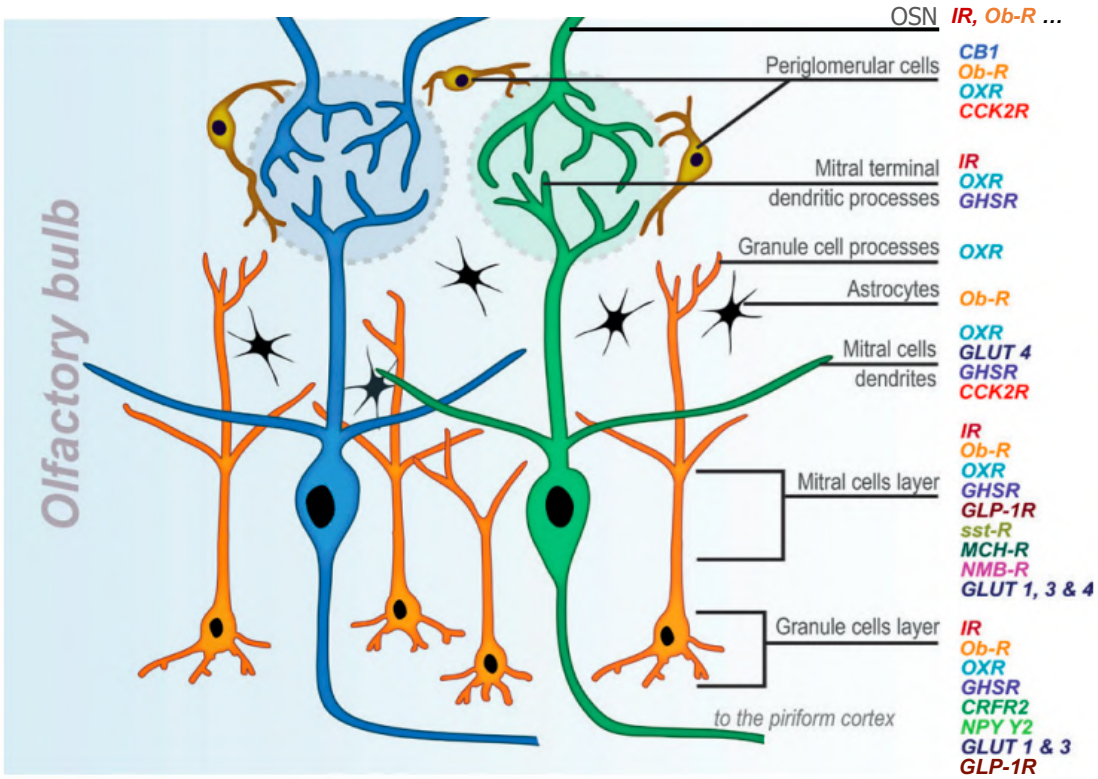

Figure III.6. Representation of the different receptors found in the olfactory bulb in the context of energy balance regulation. Distribution of receptors in the different cells coexisting within the olfactory bulb. OSN: olfactory sensory neuron, IR: insulin receptor kinase, Ob-R: leptin receptor, OXR: orexin receptor, GLUT: glucose transporter, CB1: cannabinoid receptor 1, SUS: sustentacular cells, NPY Y1: neuropeptide Y receptor Y1, AdipoR: adiponectin receptor, CCK2R: cholecystokinin receptor 2, GHSR: ghrelin receptor, GLP-1R: glucagon-like protein receptor-1, sst-R: somatostatin receptor, MCH-R: melanin-concentrating hormone receptor, NMB-R: neuromedin B receptor, CRFR2: corticotropin-releasing factor receptor-2. *Adapted from Palouzier-Paulignan et al., 2012 adding a datum from Thiebaud et al., 2016.*

2.1.1. Orexigenic signals

Ghrelin

The ghrelin receptor GHSR-1a is present in the GL, MCL and GCL of the OB (Tong et al., 2011). In the same paper, the authors show the importance of ghrelin for the regulation of conditioned olfactory aversion in rodents and for the modulation of smell in both rodents and humans.

NPY

NPY is a neuropeptide that is present in the OB as well as in the OM. In the OB, NPY is localized sparsely on the cell bodies of the GL (Jia and Hegg, 2010) as well as its receptor NPY Y2 (Figure III.6). NPY fibers that project to the OB are thought to originate from the locus coeruleus (Bouna et al., 1994) or more likely from the hypothalamus.

KO deletion of one of the NPY receptors, NPY Y1 present in the OM, leads to a moderate but specific deficit in olfactory functions (Doyle et al., 2008). In effect, NPY enhances OM responses to odorant in hungry rats (Negroni et al., 2012).

Endocannabinoids

The endocannabinoid receptor CB1, involved in the regulation of appetite and palatable food intake, is present in large numbers of centrifugal fibers in the OB and regulates its activity Endocannabinoid synthesis enzymes are also present in GL neurons (Soria-Gómez et al., 2014). These authors showed that activation of CB1 receptors decreases the hyperphagia that follows a 24-hour fasting in lean mice and triggers a decreased olfactory sensitivity. They also demonstrate that CB1 receptor modulates OB activity *in vitro*.

Orexins

Orexin receptors are highly expressed by M/TC (Caillol et al., 2003) and seem to have an effect on the OB spontaneous activity and odor responsiveness in rats (Apelbaum et al., 2005). Gascuel et al. reported orexin projections from the hypothalamus in the OB and demonstrated that orexin could play a role in olfactory perception depending on the energy balance in mice (Gascuel et al., 2012).

2.1.2. Anorexigenic signals

Insulin

In the OB, insulin is transported across the blood-brain barrier via saturable transport. It is noteworthy that it is transported to the OB much faster than to any other brain region and that the OB is the brain region with the highest concentration of insulin, where its receptors are extremely densely distributed (Banks et al., 1999). Lacroix et al. (2008) indicate the existence of

a local source of insulin within the OM: the presence of transcription factors coding for insulin (Pdx1) as well as convertases involved in the maturation of insulin precursors in the OM suggests the existence of a local transcription, which would also be possible in the OB. The density of insulin receptors (IR) cannot be doubted: immunolocalization has allowed the visualization of a high density of IR in the OB as well as in the olfactory cortex and the limbic system, such as the AON, the PC, the olfactory tubercle, or the entorhinal cortex (Unger et al., 1989). More precisely, in the OB, IRs are expressed in synapse-rich dendritic areas, such as the EPL, and to a lesser extent in the GL layer (Lacroix et al., 2008; Marks et al., 2009), GCL and MCL. In sum, the highest binding affinity of insulin to its IR, the highest density of IR and the highest IR-kinase activity in the brain are observable at the level of the OB, confirming that IR signaling is active from the earliest stages of odor detection and olfactory information transduction *(*for the insulin function within the OB, c.f. *2.3. Crosstalk between the metabolic state and olfactory perception).*

GLP-1 and GIP

As already mentioned before, the OB cells express GLP-1R (Figure III.7) (Thiebaud et al., 2016) and GIPR (Seino et al., 2010). These two primary incretins can also be found in the olfactory system. While GLP-1 is detected in the OB, GIP is strongly localized in the AON and the accessory olfactory bulb (Nyberg et al., 2007). The presence of PPG cells in the OB may be the principal source of GLP-1 found in this structure (Holt et al., 2019). However, physiopathological roles of bulbar PPG cells, and how they are stimulated *in vivo*, are still unknown and are the focus of my PhD research.

Leptin

Leptin has always been thought to be produced in small amounts in both the OM (Morash et al., 1999; Baly et al., 2007) and the OB. Ob-Rs (both isoforms) are quite widely observed in olfactory areas, such as in LOT (Elmquist et al., 1998) or in all the OB layers (Caillol et al., 2003; Prud'homme et al., 2009). The expression of Ob-Rs (Baly et al., 2007) as well as IR (Lacroix et al., 2008) increase after 48h of fasting. In 2006, Getchell et al. showed that ob/ob mice, deficient in leptin, have better olfactory performances to find their food than wild mice, suggesting that leptin would have the role of reducing the olfactory performance in mice (Getchell et al., 2006). In these mice, the oscillatory activity in the OB as well as the behavioral patterns in a go/no go task are deeply modified, with the release of inhibitory brake exerted by leptin (Chelminski et al., 2017). A recent work has shown that leptin reduces odor discrimination by a decreased neural activity in M/TC due to a modulation of potassium channels in these cells (Sun et al., 2019).

CCK

CCK is one of the most abundant neuropeptides in the brain. After crossing the blood-brain barrier, it is detected in the brainstem, hypothalamus, but also in the OB, AON, olfactory tubercle and PC (Gutièrrez-Mecinas et al., 2005). In the OB, CCK is detected in all neuronal layers except the ONL. CCK-positive TC cells, which receive direct input from OSN, modulate olfactory processing by driving inhibitory activities within the OB (i.e. by synaptic transmission to GC and glomerular interneurons) (Sun et al., 2020).

CCK receptors are distributed throughout the olfactory cortex, and CCK2R is notably present in the AON and PC (Honda et al., 1993). In the OB, CCK2R is specifically present in the IPL, and in MC and juxtaglomerular cells (Ma et al., 2013).

Prokineticin 2

Prokineticin 2 (PROK2) is a hypothalamic neuropeptide involved in feeding behavior with an anorectic function. Its receptors (PROKR) are found in the OB and a recent work from our lab led by Stephanie Migrenne-Li -in which I collaborated- showed that an injection of human recombinant PROK2 (rPROK2) in the OB decreases food intake and impacts olfactory behavior (Mortreux et al., 2019).

Vasoactive-intestinal-peptide

Vasoactive-intestinal-peptide-expressing (VIP) interneurons project to MC and present an important role in odor processing and olfactory behaviors. More precisely, the inactivation of VIP interneurons increases the firing of MC cells and impairs olfactory detection and odor discrimination (Wang et al., 2022).

Glucose

In addition to peptidergic signaling, the OB presents glucose-sensing markers such as insulin-dependent glucose transporters (GLUT) (Figure III.6) and sodium glucose co-transporter type 1 (SGLT1) involved in different metabolic functions. OB neurons respond to glucose (Tucker et al., 2010, Aimé et al., 2014) and are influenced by steady or dynamic feeding states since GLUT4 -but not SGLT1- expression is regulated in a metabolic-dependent way (Al Koborssy et al., 2014). These data further support the idea that the OB is a metabolic sensor (see review by Julliard et al., 2017). However it has to be noted that before our study no data was available on how the OB impacts the physiopathology of energy homeostasis; the study from Riera et al. (Riera et al., 2017, in obese mice) and the newest work from Debra A. Fadool (Kolling et al., 2022, in lean mice) are the first studies performing glucose tolerance tests under global changes of olfactory neurons and mitral cell activity respectively.

Insulin-like growth factor 1

The Insulin-like growth factor 1 (IGF1), a polypeptide hormone with a similar structure as insulin, is detected in the OB. By activating MAPK and PI3K signaling pathways, it helps promoting tissue growth and maturation. It was shown that this hormone is crucial for neurogenesis regulation in the OB as well as for olfactory memory during social learning. IGF1 is mainly synthesized in the liver but local brain production exists. IGF1 mediates its effects by binding to its receptor -IGF1 receptor (IGF1R)- a receptor tyrosine kinase expressed widely in the brain (Hurtado-Chong et al., 2009; Liu et al., 2017).

2.1.3. The voltage gated Kv1.3 channel

The Kv1.3 channel is predominantly expressed on MC where it is known to mediate a great fraction of the outward current detected in these neurons, which also express the insulin receptor (IR) (Figure III.7). Kv1.3 channel appears to be downregulated by insulin, *via* the phosphorylation of numerous tyrosine residues in the channel, decreasing its current magnitude (Fadool & Levitan, 1998; Fadool et al., 2000). It is likely that IR kinase (Fadool et al., 2000; Fadool et al., 2011), glucose (Tucker et al., 2013) and GLP-1 signaling converge at the level of the Kv1.3. In fact, GLP-1 through its receptor increases the excitability of mitral cells *via* the inhibition of Kv1.3 (Thiebaud et al., 2016). (for further details, c.f. *2.3. Pathophysiology : interactions between the olfactory system and the energy balance regulation system in the context of obesity).*

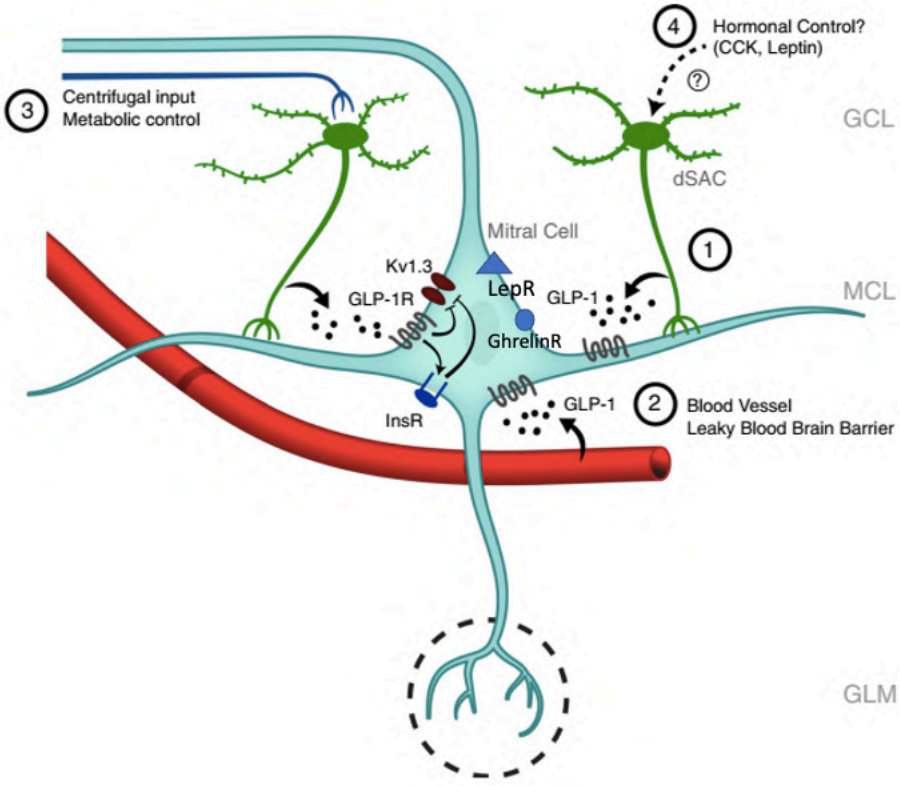

Figure III.7. Different hypothesis for the roles of GLP-1 in the OB. (1) GLP-1 could be released by dSAC to MC for local transmission or combined neurotransmission/neuromodulation of MC activity. (2) MC could sense gut-derived GLP-1 reaching the OB *via* circulation, and informing about the nutritional state. (3) centrifugal or (4) hormonal input could control dSAC-release of GLP-1 to MC. Despite the way GLP-1 is inducted or its release is regulated (through 1, 2, 3 or 4), the voltage-gated Kv1.3 channel (green) is in all cases a downstream target. MC also express other metabolic receptors such as those for ghrelin or leptin. *Modified from Thiebaud et al. 2016.*

2.2. Physiology : interactions between the olfactory system and the energy balance regulation system

2.2.1. OB – hypothalamus – mesocorticolimbic system

From an anatomical point of view the OB and the hypothalamus -the heart of the energy homeostasis regulation, containing, in turn, pre-autonomic neurons controlling the ANS (Luquet et al., 2010)- share common neuroanatomical pathways and are reciprocally connected (Figure III.5). Electrical stimulation of the OB induces an electrophysiological response in the lateral hypothalamus and the PVN (Guevara-Aguilar et al., 1988; Price et al., 1991). Additionally, many of the structures to which the OB projects, such as the AON, the olfactory tubercle and the PC, also project to the lateral hypothalamus (Barone et al., 1981; Price et al., 1991; Astic et al., 1993). Direct projections from the OB to the ARC also exist (Russo et al., 2018). In the opposite direction, afferents from various hypothalamic nuclei project to the olfactory system (De Olmos et al., 1978; Shipley and Adamek, 1984). In particular, the OB is the direct target of orexinergic fibers originating from the lateral hypothalamus (Peyron et al., 1998; Nambu et al., 1999). In addition, some neurons from the PVN project to the olfactory tubercle (Newman and Winans, 1980).

Recent studies support that the sense of smell can influence brain areas regulating energy homeostasis such as the hypothalamus. Chen et al. determined that in fasted mice, simple food presentation (without eating it) immediately inhibited AgRP neurons and activated POMC ones, the same effect than circulating nutrients of hormones do on them during the postprandial state (Chen et al., 2015). This suggests that the ARC has immediate input from sensory cues associated with food.

In regards to food palatability and hedonic content, olfactory cues dominate over the rest of sensory cues (e.g. auditory, visual or haptic cues). Food palatability is mediated through the mesocorticolimbic pathways. The olfactory tubercle (Figure III.5), together with other regions such as the nucleus accumbens, is involved within these dopaminergic pathways (Midroit et al., 2021).

In summary, neural circuits linking the olfactory system, the hypothalamus and the mesocorticolimbic system consolidate a strong network that regulates energy metabolism and food behavior.

2.2.2. Crosstalk between the metabolic state and olfactory perception

Cabanac's early work in humans showed that the hedonic value of a food changes according to the nutritional state (i.e. *alliesthesia)* (Cabanac and Duclaux, 1973). Indeed, the hedonic value of a food odor is greater on a hungry state/empty stomach than at satiety (Jiang et al., 2008). More recent results confirm that nutritional signals modulate olfactory behavior and perception. For example, Prud'Homme and colleagues showed that the exploration time of a food odor was increased in rats fasted for 48 hours (Prud'Homme et al., 2009). In addition, rats fasted for 22 hours detected and avoided an aversive odor (acquired by aversive learning with lithium, (c.f. *1.4. Behavioral assessment of mouse olfaction ->Olfactory habituation/dishabituation test*) at lower concentrations than fed rats, suggesting that the threshold for detection of an aversive associated odor to a food is lowered by fasting (Aimé et al., 2007). A recent study (Wu et al., 2020), described in the awake fasted mice, showed an increase in the single mitral cell activity as well as in oscillatory patterns in the OB, further confirming the early elegant work of Pager et al. in 1972. Thus, olfactory capacities of the animals are modulated according to their nutritional state.

As mentioned before, in humans, sensory stimuli, perceived before the intake of food, are largely involved in the central regulation of food intake. These stimuli are indeed preparing the organism to receive food during the minutes before consuming it (e.g. during the highly sensory and enriching process of cooking) (for review see Mattes, 1997). Exposition to food odors can be the triggering factor for initiating cephalic phase responses (Ferriday and Brunstrom, 2011) such as the cephalic phase of insulin release. A reminder that the preprandial cephalic phase of insulin is a quick, low-amplitude peak in insulin secretion that is triggered by the sight, smell, and taste of food before the nutrients are ingested. Insulin levels vary depending on the time cycle between meals, which would give it both opposing effects -orexigenic and anorexigenic action-: insulin is released during the cephalic phase (Le Magnen, 2001) serving as an orexigenic signal, inducing mild hypoglycaemia and promoting the regulation of postprandial blood glucose (Louis-Sylvestre and Le Magnen, 1980b) through the vagus nerve. In fact, the administration of insulin (i.p.) in fasting rats increases their sense of hunger and their food consumption (Le Magnen & Julien, 1999; Powley & Berthoud, 1985). After meals, in the postprandial phase, there is the typical longer peak corresponding to the anorectic effect of insulin, similar to the action of leptin (Woods and D'Alessio, 2008). Indeed, insulin has been shown to lower the response of olfactory neurons to an odorant signal *in vitro* (Savigner et al., 2009) and, in fasted rats, intracerebroventricular injection of insulin (dose equivalent to that found in the satiated state) triggers a decrease of

olfactory detection to the level of satiated rats (Aimé et al., 2007). These studies support an opposite role of insulin in the OB network on olfactory processing in pre- and postprandial states.

2.3. Pathophysiology : interactions between the olfactory system and the energy balance regulation system in the context of obesity

What about the impact of obesity on olfactory ability and performances? Surprisingly, it is difficult to find a clear answer since a lot of clinical studies have technical limits such as lack of power, gender balance or age differences (Islam et al., 2015). In this context, it is necessary to have an extensive number of obese animal models, which are much more informative than human studies and provide specific experimental evidence of the interactions between olfaction and energy balance in the context of obesity.

2.3.1. Animal models of obesity

In the literature there are two rodent models of obesity, one of genetic origin (ob/ob in mice, fa/fa in rats), the other of dietary origin (diet induced obesity or DIO). In the context of this thesis, it is therefore interesting to compare the way olfaction is impacted in these two different models, one focused on the involvement of leptin (single-gene models of leptin-dependent rodents), the other reproducing a globally disturbed energy metabolism, whose causes are multifactorial, and generally closer to what is observed in humans. During my PhD, I myself have used extensively the DIO model (obesity induced by a western diet in my case).

a. Monogenic models of inducing obesity in animals

Ob/ob mice

A spontaneous mutation is the cause of the noticeable obese phenotype of ob/ob mice. The product of the mutated gene, leptin, was identified by Zhang et al. in 1994, and subsequently, the study of genetic origins of obesity emerged. Phenotypically, the absence of leptin leads to rapid development of obesity characterized by hyperphagia, reduced energy expenditure and hypothermia, as well as other side effects including, insulin resistance associated with hyperglycemia and hyperinsulinemia, hypothyroidism, growth hormone deficiency and hypercorticosteronemia. Obesity in ob/ob mice is one of the few forms of obesity that can be rescued by exogenous administration of leptin. Rare cases of human obesity present leptin deficiency (O'Rahilly, 2009).

db/db mice

Although they are able to secrete leptin, db/db mice do not have a functional Ob-R receptor. Its phenotype is similar to that of ob/ob mice: they are hyperphagic, have a reduced energy expenditure leading to marked and early obesity, are hypothermic and also have a deficiency in growth hormone. However, some of them have even more marked hyperglycemia than ob/ob mice. These mice are insulin resistant and develop a partial phenotype of T2D, which has led to their frequent use in the study of obesity, T2D and metabolic syndrome. This leptin receptor mutation is extremely rare in humans, as with ob/ob.

Zucker, ZDF and Koletsky rats

Similar to db/db mice, several leptin-resistant rat models have a mutation in the Ob-R receptor gene. Obese Zucker (fa/fa or "fatty") and Koletsky rats carry mutated forms of the extracellular domain of the leptin receptor. They develop a similar phenotype of hyperphagia and reduced energy expenditure, leading to morbid obesity. These rats have reduced glucose tolerance, growth deficiency (potentially related to the activity of the gonadotropic axis GH/IGF-1), hypothyroidism and reduced fertility. In contrast, the fa/fa mutation in Zucker rats is associated with a transport defect of the leptin receptor: the hormone is well produced but retained in the intracellular compartment). Zucker rats cells express the receptor on their surface, but their number is very low and reduces leptin detection and signal transduction. In contrast, Koletsky rats have a mutation that abolishes the expression of leptin receptor mRNA (Friedman, 1998). Koletsky rats show high blood pressure and a more severe insulin resistance phenotype compared to Zucker rats.

Finally, ZDF (Zucker Diabetic Fatty) rats are derived from a strain of Zucker rats with early deregulation of glucose metabolism. ZDF rats rapidly develop diabetes when fed a high-fat diet, and part of their propensity to develop early diabetes is thought to be related to altered expression of the glucose transporter in skeletal muscle (Zierath et al., 1998).

These are the main monogenic models of obesity in rodents. Note that there is no rodent model of obesity based on genetic manipulation of insulin receptors.

b. Diet-Induced Obesity models

Compared to genetically modified models, DIO models reflect the majority of obesity cases observed in humans (i.e. of non-genetic origin, but induced by diet) and constitute a privileged target for various therapeutic trials. They are also models of obesity that are not purely dependent on the leptin system but of multifactorial origin. Different strains of mice respond differently to the proposed fatty diets.

At present, there is a range of commercial obesogenic diets that efficiently make rodents obese: high-fat (HFD), western (WD) or cafeteria (CAF) diets (for review, Bastías-Pérez et al., 2020). However, which of them better reflects the pathology of obesity remains unclear. The WD, based on the human western diet (which contains high amounts of processed food, high fat dairy products and red meat), seems to be a robust inducer of metabolic disruption, but CAF and HFD are also potent mirrors to evaluate closely human obesity. A HFD can be calorically equal to a WD, but the latter, in addition of being high in fat, also present a high percentage of sucrose, and cholesterol. In CAF, the palatability is improved since it is composed of mainly sugar and butter, as well as a variety of highly palatable food such as peanut butter and condensed milk.

Regarding HFD, different kind of diets can be chosen (e.g. 45% or 60% kcal from fat) accordingly to the objective of the DIO study (Speakman, 2019) triggering intravariation within a solely diet. Even more variability is added if we consider the different companies that commercialize it (e.g. SAFE high-fat diets are different from the ones that Research Diets offers). Different percentages of fat, sugar or other nutrients can be found, which is a priori an advantage while choosing the diet that better fits on each study, but may in the long run lead to problems when comparing studies since a lack of homogeneity will exist.

C57BL6/J mice, which I used during my PhD, are highly prized for DIO studies since they develop a phenotype similar to the human metabolic syndrome (obesity, hyperinsulinemia, insulin resistance) when fed on a HFD diet (Collins et al., 2004), WD or CAF diet (Table III.1). In rats, the Sprague Dawley or Long Evans strains are frequently used for this type of study.

Table III.1. Fasting glucose and insulin levels of lean and DIO mice *vs.* healthy and prediabetic humans. *Data from Bruce et al., 2021.*

	Lean mice	**DIO mice**	**Healthy humans**	**Prediabetic humans**
Fasting glucose (mM)	8 ± 0,2	10,2 ± 0,2	5,3 ± 0,1	6,3 ± 0,1
Fasting insulin (pM)	330 ± 33	608 ± 72	24,9 ± 2,4	29,1 ± 6,6

2.3.2. Major axes linking olfaction, energy balance and obesity

We have seen that rodent models represent an experimental tool of choice given the large diversity available for the study of obesity and T2D. These models have provided great findings that deserve to be cited here. Thus, in this subchapter, I will summarize the major references from the literature linking, in the form of a triangle, olfaction, food intake and obesity, not only in animal research but also in clinics (Figure III.8).

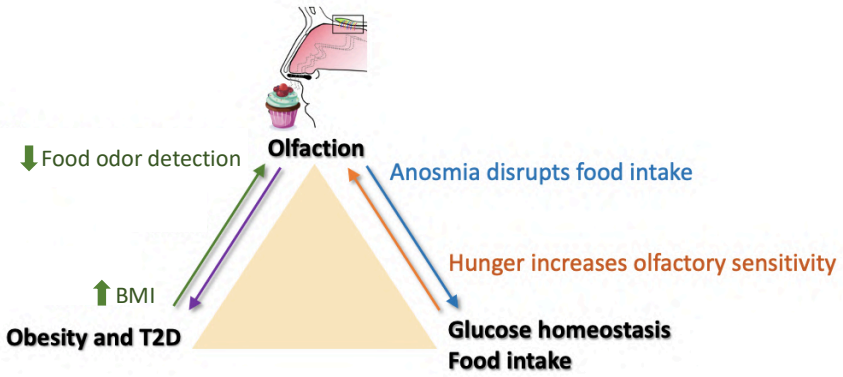

Figure III.8. Schematic representation of the interactions between the olfactory system, glucose homeostasis and food intake, and obesity and T2D. The axes are described in the text below.

The base of the triangle is established by the well-known link between an energy imbalance and metabolic diseases such as obesity and T2D. Data in rodents and humans indicate that increased food intake is strongly implicated in obesity. In this research field, several rodent models of obesity are used, in particular ob/ob and diet induced-obesity (DIO) ones (c.f. *2.3.1 animal models of obesity*).

The green axis corresponds to how obesity impacts olfactory plasticity. In this axis, Deborah Fadool's team studied olfactory plasticity in the OM in a DIO model, showing that a high fat diet can cause long-lasting loss of OSN and reduce olfactory discrimination in mice (Thiebaud et al., 2014). The purple axis shows a correlation between olfactory impairment and obesity in humans. It also suggests that olfactory disorders could participate to the origins of obesity. A recent clinical study has shown that olfactory dysfunction mediated adiposity in obese T2D patients with cognitive impairment. Interestingly, a GLP-1RA treatment improved the cognitive and olfactory function lost in obese T2D patients (Zhang et al., 2019).

The blue axis is characterized by the influence of olfaction on food intake and is historically based on the data of Jacques Le Magnen. In fact, he was the first to highlight the involvement of the olfactory system in food intake (for review, Le Magnen, 2001). He demonstrated that the appearance of new olfactory stimuli inhibited the satiety signal and leaded the animal to consume more than its physiological needs (Le Magnen, 1999 b,c). Additionally, this blue axis also comprises the more recently work of Soria-Gómez et al. (2014) showing that the acute injection of a CB1 receptor agonist in the OB reduces hyperphagia in mice. An actual sensible topic that can be reflected in this axis is the olfactory loss and distortion on appetite that COVID-19 patients suffered during the pandemic. I had been involved in the translation of an olfactory training protocol developed by Hirac Gurden for Anosmie.org association. The protocol is intended for people suffering anosmia and has been downloaded more than 150K times across Europe and the United Kingdom. This last piece of work had a particularly positive impact during

the pandemic, helping sufferers to regain a sense of smell and thus improving the recovery of COVID-19 patients with severe anosmia.

In turn, the orange axis describes the influence of metabolic mechanisms on olfactory activity and is historically based on data from Pager et al. (1972) showing the modification by nutritional status of electrophysiological activity recorded in the OB in unanesthetized rats.

An evident impact of obesity can be seen in the olfactory system of numerous rodent models. Disruptions can happen in the level of the OM, and subsequently impact OB circuits, but also can directly affect OB neurons. 5-6 months of dietary fat consumption induces OSN loss and damage of related circuitry, and this impairment is not rescued by voluntary exercise in mice (Chelette et al., 2021). Middle-aged DIO mice after 8 months under HFD, but not after 3 months, presented decreased olfactory sensitivity. However, odor-evoked cerebral blood flow was reduced in DIO mice at both ages (Soleimanzad et al., 2021, c.f. *Annex*), indicating abnormal brain function from rather early in obese mice life. In addition, impairment of bulbar GLUT transporters function in obese fa/fa rats is shown to affect olfactory sensitivity (Aimé et al., 2014). OB neurogenesis, PC neuronal activation and PC volume do not present any changes after 8 months of HFD mice (Lietzau et al., 2020). However, OB neurogenesis is reduced in T2D Goto-Kakizaki rats (Lietzau et al., 2018), which is attenuated by chronic treatment with the dipeptidyl peptidase-IV inhibitor (DPP-IVi) linagliptin. Moreover, chronic GLP-1R agonist Ex4 treatment reduced T2D-induced neuronal changes in the PC in Goto-Kakizaki rats (Lietzau et al., 2016).

Changes in the levels of hormones and nutrients can also explain olfactory impairment. OB cells are sensitive to insulin and glucose, two parameters that are found to be disadjusted in obesity. The laboratory of Debra A. Fadool widely studied a mechanism by which an obesogenic diet can potentially disrupt insulin modulation by M/TCs. They examined the role of Kv1.3, a voltage-dependent insulin-regulated potassium channel mainly expressed in M/TCs (Fadool et al., 2000). They demonstrate that the removal of Kv1.3 on mice ($Kv1.3^{-/-}$), very similar to its pharmacological inhibition by margatoxin, presented increased insulin sensitivity and energy expenditure as well as DIO resistance (Tucker et al., 2012). Olfactory capacities of $Kv1.3^{-/-}$ mice are also improved. They were called “super-smeller”. Taken all together, Fadool’s data indicate that the increase of MC activity brings metabolic benefits in the context of murine obesity. Interestingly, a polymorphism in the human gene coding for Kv1.3 has been related to glucose intolerance, bad insulin sensitivity and olfactory dysfunction in homozygous males (Tschritter et al., 2006).

2.3.3. Human studies (1). Does the sense of smell impact metabolic health and obesity?

Human perception of the odor environment is highly variable and is due to within and in between individual differences. It depends on the quality and quantity of odors, the functional olfactory receptors and the perceptual activities such as hedonic valence, emotions and memory. Dysosmia includes olfactory disorders such as hyposmia and anosmia for quantitative decrease in olfactory sensitivity but also parosmia, cacosmia and phantosmia for qualitative disturbances. The level of sexual and metabolic hormones and aging are also strong internal determinants of olfactory sensitivity. Thus age (hyposmia after 65 years, i.e. the gradual decrease of sense of smell due to aging process, Joussain et al., 2016) and gender (women perform better than men in olfactory tests, Sorokowski et al., 2019) are important factors in modulating sensory processing.

Dysosmia was characterized both in psychological and neurodegenerative diseases. They were also observed in metabolic syndrome. Odors are tightly linked to food preferences and consumption not only in healthy but also in obese subjects (Proserpio et al., 2019) and can drive craving for palatable foods (Larsen et al., 2012). Obese people are more susceptible to external food cues (visual and olfactory) than those of normal weight (Belfort- DeAguiar and Seo, 2018). Although obese people present impaired sensory/olfactory sensitivity, their exacerbated wanting and liking of palatable food compensates, by motivational processes, their performance in response to food odors associated to palatable food, such as chocolate (Stafford and Whittle, 2015; Han et al., 2021). Note here how strong is the hedonic value of food in the context of obesity. Indeed, calorie-restricted diets, which do not leave a place for hedonic hunger, might constitute a challenging treatment that, together with severe obesity-related olfactory problems such as anosmia, may lead to other major public health concerns like depression. The link between obesity and depression is however shown to present bidirectional causality (Luppino et al., 2010).

It is unlikely that a cause-effect relationship does exist between olfaction and obesity, nevertheless, since humans respond primarily to sensory qualities of food, olfaction can potentially accentuate the disease in the context of an energy imbalance. Indeed, a difference in olfactory sensitivity in obese individuals compared to normal-weighted ones has been shown to modify food choices and calorie intake (Drewnowski et al., 1995, 1997). In 2017, Riera et al., described a connection between the OM and peripheral metabolic organs, suggesting that the olfactory system would impact metabolic health and obesity (Riera et al., 2017).

The prevalence of obesity among children and adolescence aged from 5 to 19 years old is dramatically rising over the years (c.f. *Chapter I, 2. Metabolic diseases*), and with that, obesity-related olfactory disruptions also in the youngest emerge. A study has shown that children from 10 to 16 years old presented lowered odor detection thresholds compared to a control healthy group (Obrebowski et al., 2000). In fact, elevated BMI is associated with an increased threshold

of olfactory detection (Figure III.8, purple axis). Olfactory dysfunction is correlated with a reduction of the OB volume and leads to a disturbed olfactory performance (Gudziol et al., 2009). Additionally, increasing BMI, body fat percentage and levels of plasma leptin is associated with reduced OB volume (Poessel et al. 2020a).

Olfactory dysfunction has been reported (Weinstock et al., 1993) and reviewed (Zaghloul et al., 2018) in T2D subjects since 1960's (Jørgensen and Buch, 1961). Olfactory dysfunction can be predicted by the shape of the OB (Yan et al., 2022), which is reduced in obesity (Poessel et al., 2020a). Patients on early stages of T2D present simplest olfactory impairment (Naka et al., 2010) whereas the more complications patients accumulate, the worse their olfactory capacity becomes, until reaching the point of suffering from severe hyposmia (Brady et al., 2013; Catamo et al., 2021). Indeed, insulin resistance is the major parameter implicated in the significant correlation between increased BMI and decreased food odor sensitivity (Poessel et al., 2020b).

Interestingly, treating diabetic obese subjects with a GLP-1R agonist for 3 months has been shown, by functional magnetic resonance imaging (fMRI) task, to reverse its poor olfactory function (Zhang et al., 2019).

Food preferences after bariatric surgery (BS) are shown to be modified (Coluzzi et al., 2016) and can be added to the profound changes seen post-surgery in the peripheral level, such as the improved levels of GLP-1, which, in turn, seem to play a role on the process of weight loss after BS (Moffett et al., 2021). This changing in food preferences suggests a modification at the level of sensory perception, including the sense of smell. In fact, a study in 2015 has shown that within the whole group of morbidly obese and hyposmic patients, half of them presented better olfactory function six month after BS (Holinski et al., 2015). Some cases of aversion to specific foods are also seen after BS in patients who experienced profound weight lost post-surgery (Tichansky et al., 2006).

2.3.4. Human studies (2). Glucose-induced brain activity in healthy and obese subjects assessed by fMRI

In human brain imaging, two types of functional mapping can be performed to question the fate of brain activity in response to changes in acute (glucose absorption) and chronic energy state (obesity and T2D) and also in response to odor stimulation, three themes of major interest in the context of my thesis (Figure III.8.).

With the Blood Oxygenation Level Dependent (BOLD) fMRI, it is possible to follow changes in the brain oxygenation and hemodynamics in response to different kind of stimulations (pharmacology, glucose, odor stimulation). This kind of analysis has shown decreased prefrontal executive control connectivity (OFC) in response to liquid glucose and fructose intake but heightened homeostatic and hedonic (hypothalamus) responses in obese adolescents (Jastreboff et al., 2016). More recently, heightened reward and flavor processing areas activity in response

to chocolate versus cucumber odors were shown (Han et al., 2021), further explaining higher chocolate odor sensitivity in obese subjects (Stafford and Whittle, 2015).

The second type of MRI imaging relies on the endogenous synchronized patterns of activity of resting-state networks (RSN). RSN are detected by a spontaneous covariation of BOLD signals between different brain areas and are transiently activated or deactivated at the second timescale, mainly in the anteroposterior axis (precuneus, posterior cingulate cortex, medial prefrontal cortex, temporoparietal junctions and hippocampus). These networks disengage as soon as a specific attentional demand occurs. RSN are intensely studied in different pathologies and were shown to be strongly affected in Alzheimer Disease (Puttaert et al. 2020).

Using RSN analysis in lean subjects, increased functional connectivity after the ingestion of sugars (both glucose and fructose) could be detected in appetite and reward-related structures, meaning the insula, anterior cingulate, striatum, and posterior cingulate cortex (Page et al., 2013). These results were not fully confirmed by (van Opstal et al., 2020) who showed that glucose ingestion leads to decreased activity and connectivity in brain areas and networks linked to energy seeking and satiation in normal weight adult males. More recently, differential effects of glucose administration on central appetite signaling in young and old healthy adults were detected in RSNs (Peters et al., 2020), especially higher connectivity of insula was detected in response to glucose administration in old subjects compared to young ones.

Without surprise, multiple brain areas are affected in the obese brain detected both in BOLD-fMRI and RSN recordings. In odor-evoked fMRI recordings, a decreased activity in the left hippocampus and right insula was revealed in the brain of DT2-obese patients. Patients also presented dysfunctional olfaction. This impaired pattern was reversed by GLP-1 analog treatment (Zhang et al., 2019).

In obese adolescents, the strength of the functional connectivity between left OFC and right putamen (RSN analysis) was positively correlated with fasting insulin levels (Kullmann et al., 2012). In addition, a decreased middle frontal gyrus connectivity involved in attention, executive functions and motor functions (García-García et al., 2015) and a decreased reward system connectivity including the ventral striatum (Marqués-Iturria et al., 2015) were recorded. The impact of antidiabetic treatments in these RSN circuits was not tested. In this thesis, in collaboration with the University of Leuven, we addressed the question of brain connectivity changes including the primary olfactory cortex in response to glucose alone or to systemic exendin-9 in addition to glucose.

SECTION II

Thesis statement

Thesis statement

We have seen in the first Chapter of the introduction that obesity is a global health scourge and the leading risk factor for T2D. Excessive calorie consumption as well as disrupted hormonal communication between the pancreas and other organs such as the brain, involved in the regulation of energy balance, are among the causes of these metabolic disorders. Marketed anti-diabetic drugs include analogues of GLP-1, an incretin hormone produced by intestinal L-cells, which stimulates insulin secretion during meals. As explained in Chapter II, GLP-1 also decreases food intake via an effect on the CNS, potentially by acting as a neuropeptide. However, its mechanism of action on brain circuits is not well known.

Within the CNS, the GLP-1 receptor is expressed in the hypothalamus and NTS, but also by some cells of the olfactory bulb (mitral and granule cells). In fact, as seen in chapter III, there is considerable evidence that the olfactory system and the homeostatic control of energy balance share common neuroanatomical and neurochemical pathways, which may represent the basis for functional interactions between these two systems. The olfactory system is essential for odor-related sensory interactions with food, and allows the estimation of food quality, hedonics, and energy content even before ingestion. Impaired olfaction can dramatically affect eating behavior and be a causal and/or aggravating factor in obesity. Moreover, olfactory sensitivity in patients with T2D is greatly improved by treatment with a GLP-1R agonist, and that the OB contains cells (PPG neurons) capable of synthetizing GLP-1 locally. GLP-1R are expressed by several types of neurons within the olfactory bulb. Electrophysiological recordings in OB slices have suggested the existence of a specific circuit driven by the GLP-1 system within the OB. Together, these studies from the literature strongly suggest that the central action of GLP-1 could be mediated by the OB. However, no study has demonstrated a role of GLP-1R in the OB on glucose homeostasis nor food intake yet.

As a general hypothesis of this work, we have proposed that the GLP-1/GLP-1R system in the OB constitutes a new metabolic pathway controlling energy balance in the context of obesity and T2D.

Our first objective was to assess whether the GLP-1R signaling pathway in the OB plays a role on the control of glucose homeostasis in both physiology and obesity conditions. It is well-known that the main regulating factor of glucose homeostasis is insulin, therefore, in this work, insulin secretion was assessed in pre- (CPIR) and postprandial states in response to changes in GLP-1R activity in the OB. Since feeding behavior is another important index of energy homeostasis, the impact of the bulbar GLP-1 system in food intake was also tested.

Because the central GLP-1 system can be considered as a different entity from the peripheral GLP-1 system, it is suggested to act as a neuropeptide within the CNS. Thus, the second objective of my thesis was to know whether PPG cells can release GLP-1 within the OB. In addition, the role of PPG cells was assessed during pre- and postpandial states.

The olfactory system and the energy homeostasis regulation system share common neuroanatomical pathways and are connected. Thus, our third goal was to focus on the study of the plausible GLP-1-driven neuronal network and decipher molecular actors that can link the bulb with peripheral organs such as the pancreas through the ANS, mainly in the context of obesity.

SECTION III

Materials and Methods

Materials and Methods

The achievement of my objectives has required the use of a DIO model in mice, allowing us to mimic the pathophysiological context of obesity. A multidisciplinary approach has been used combining metabolic phenotyping, pharmacological and chemogenetic techniques, behavioral analysis. In addition, collaborations with several laboratories focused on FISH, IHC, quantification of GLP-1 release *in vitro* and human MRI. These materials and methods are presented as a form of an article and will be followed by the results obtained by these techniques. Results will also be presented in the form of an article.

1. Mice studies

1.1. Animal care

All animal studies were performed with approval of the Buffon Ethics Committee (CEEA40), under agreement no. B751317, conforming with the French Ministry of Research legislation. All mice were housed individually in cages in a room maintained at 22 ± 1°C with lights on from 07:00 hours to 19:00 hours (12-h/12-h light-dark (L/D) schedule). All the animals of this study were accustomed to daily manipulation.

1.2. Mice models

1.2.1. Diet-induced obesity model

6 week-old C57BL/6J male mice were purchased (Janvier Labs, Le Genest Saint Isle, France) and fed *ad libitum* with a mixed high-fat/high-sucrose diet (HF230 diet 5317 Kcal/kg, Safe, Augy, France) and regular chow (Complete maintenance diet A04, 2791 kCal/kg, Safe, Augy, France) diet throughout the whole study. Age-matched controls were fed with regular chow diet *ad libitum*.

1.2.2. Genetic model

For selective Cre-dependent viral targeting, we used GLP-1RCre:GcAMP3 mice (C57BL/6 background), constructed and kindly provided by Frank Reimann (Institute of Metabolic Science, Cambridge). From 6 week-old, they were fed as DIO and age-matched controls.

All the experiments run on both models were done after 6 to 10 months of high-fat/high-sucrose diet (WD mice), thus at the age of 7.5 to 11.5 month year old for both groups.

1.3. Metabolic phenotyping

Body weight was measured all along the study, once per week between 09:00 hours and 10:00 hours. Body mass composition (amount of lean and fat mass) was assessed using an Echo Medical Systems EchoMRI 100 (EchoMRI, Houston, TX, USA) at week 16. RD mice >40g were excluded from all the procedures assessed on this work.

1.4. Surgical and stereotactic procedures

1.4.1. Implantation of a guide cannula in the OB and drug administration

After 3 months under WD (13 weeks of age), mice received an intraperitoneal injection (i.p.; 10 mg/kg) of Buprécare® (Buprenorphine 0.3 mg) diluted 1/100 in NaCl 0.9%. Mice were anesthetized with isoflurane (Isoflurin 1000 mg/ml, Axience, France) and positioned in a stereotaxic frame (Phymep – Model 940 Small Animals). A double stainless steel guide cannula (26 gauge in diameter, Phymep, France) was implanted into the OB through stereotactic procedures (AP: +4.8 mm from bregma, ML: ±1 mm and DV: -1.7 mm from brain surface) after exposing and properly scrubbing the skull of the animal. To fix the guide cannula onto the skull, plastic screws and dental cement (Super-Bond Universal Kit, Sun Medical and Unifast Trad) were used. A dummy was placed in the guide cannula to assure its patency. Finally, a reversible cap was screwed in the guide cannula to protect its tip. Mice received an i.p. injection (10 mg/kg) of Ketofen® (Ketoprofen 100 mg) diluted 1/100 in NaCl 0.9%. Caged mice were placed on a heated pad until they recovered from anesthesia. Mice were single-housed 1 week before surgery and metabolic and behavioral tests started after a recovery period of 3 weeks. Mice were submitted to habituations 1 or 2 weeks before the tests. On the test day, acute injections of the GLP-1R agonist Exendin-4 (Ex4; 0,5µg/µl; Sigma-Aldrich), Fluorescein-Trp25-Exendin-4 (FLEX; 0,5µg/µl; Eurogentec), the GLP-1R antagonist Exendin-9 (Ex9; 12,5µg/µl or 25 µg/µl Sigma-Aldrich), the GLP-1 itself (0,5µg/µl; Sigma-Aldrich) or NaCl 0,9%, for 4 minutes (0,125µl/min), bilaterally, were performed 12 minutes before the beginning of the metabolic test, or 13 minutes before the behavior tests, in awake behaving mice. The injection of Ex9 at 25 µg/µl in the OB was combined

with an i.p. injection of Ex4 (3µg/kg) or NaCl 0,9%; and only in one cohort of Ex4 OB-injected WD mice, UK14304 tartrate (Bio-Techne; 1µg/kg), an α2-AR agonist was administered i.p. The respective tests on which mice were submitted will be described below.

Animals that did not undergo an entire OB perfusion due to methodological issues (i.e. injection catheter not well-placed within the OB cannula) were excluded from the analysis.

1.4.2. Vagotomy and drug administration

At 26 weeks of age and 6 months under WD, 6 cannulated WD mice and 6 cannulated RD mice were submitted to a bilateral sub-diaphragmatic vagotomy. Before surgery and during 3 days post-surgery, mice were fed with jelly food (DietGel Boost Clear H_2O) to avoid solid food in the passageway of the digestive system. Mice received an i.p. injection (10 mg/kg) of Buprécare® (Buprenorphine 0.3 mg; diluted 1/100 in NaCl 0.9%) and were anaesthetized with isoflurane during surgery. Their body temperature was maintained at 37°C all along the surgery. Vagus nerve branches (right and left) were cautiously isolated along the esophagus using a binocular loupe and sectioned in vagotomized mice or left integral in sham ones. This procedure has been done by our collaborator Ewout Foppen old member of BFA unit (team COFFEE, University of Paris).

Mice recovered for at least 3 weeks post-surgery before running metabolic tests. After recovery, mice were submitted to habituations. The day of the metabolic test, Ex4 (0,5µg/µl) or NaCl 0,9% injections in the OB were performed 12 minutes before the test started.

At a later time after the metabolic test, each mouse received an i.p. injection of FluoroGold (0.8 mg/0.4 ml saline; Sigma-Aldrich). One week after the injection, all animals were transcardially perfused with PBS 1X (pH 7,4) followed by ice-cold 4% paraformaldehyde (PFA; pH 7.4). The brains were removed and post-fixed in 4% PFA overnight, and cryoprotected in 30% sucrose until the tissue sank. After cryoprotection, the brainstem was separated and cut on a cryostat (Leica, 1800) into 18µm coronal sections, which were mounted on microscope slides (SuperFrost Ultra Plus™ GOLD), for later imaging using fluorescence microscopy. Each brainstem section was examined for FluoroGold label in the DMNX. The presence of fluorescent label in the DMNX was accepted as a marker of incomplete vagotomy. Only animals with complete or no vagotomy (for shams) were included in the study.

1.4.3. Viral injections in the OB, cannulation in the PVN and drug administration

At 13 weeks of age and 3 months under WD, 11 GLP-1RCre:GcAMP3 RD and 16 GLP-1RCre:GcAMP3 WD mice were anesthetized with isoflurane as described above and placed on a stereotaxic frame. Bilateral injections of AAV vectors encoding for stimulatory (AAV8-hSyn-

DIO-hM3Dq-mCherry) or inhibitory (AAV8-hSyn-dF-HA-KORD-IRES-mCitrine) Designer Receptors Exclusively Activated by Designer Drugs (DREADDs) were then performed in the OB (AP: +4.8 mm from bregma, ML: ±1 mm and DV: -1.7 mm from brain surface) at a rate of 0.125 µl/min for 4 minutes, on GLP-1RCre:GcAMP3 RD and WD groups. Groups were called GLP-1R^{OB} KORD RD and GLP-1R^{OB} hM3Dq WD respectively.

During the same surgery session, after the viral injections, 10 WD mice from the total of 16 were cannulated into the PVN. A double stainless steel guide cannula (26 gauge in diameter, Phymep, France) was implanted into the PVN through stereotactic procedures (AP: -0.9 mm from bregma, ML: ±0,3 mm and DV: -4.8 mm from dura mater) as described above. To fix the guide cannula onto the skull, dental cement (Super-Bond Universal Kit, Sun Medical and Unifast Trad) was used. The incision of the mice not submitted to PVN cannulation was sutured with Coated VICRYL suture (Ethicon). Mice were placed in cages on a heated padl until they recovered from anesthesia. Mice were single-housed 1 week before surgery and metabolic tests started after a recovery period of 3 weeks. Mice were submitted to habituations 1 or 2 weeks before the tests.

On the test day, clozapine N-oxide (CNO; Sigma-Aldrich) was administered intraperitoneally at 3 mg/kg in GLP-1R^{OB} hM3Dq mice. PVN-cannulated GLP-1R^{OB} hM3Dq mice were submitted to acute injections of Bicucculine Methiodide (0,25µg/µl) or NaCl 0,9% in the PVN (bilaterally, for 2 minutes at a rate of 0,05µl/min) just before CNO 3mg/kg or NaCl 0,9% i.p. administration. 15 minutes after CNO administration, metabolic tests were run for all groups.

1.4.4. Viral delivery of shRNA in the OB

Selective gene silencing was performed in order to target the loss-of-function of PPG cells in the OB. Hence, an AAV expressing a shRNA targeting preproglucagon (AAV8-hSyn1-shRNA(mGcg)-EGFP) was injected in the OB of 10 RD mice. A control group of 10 RD mice were injected with a scrambled-shRNA (AAV8-hSyn1-shRNA(Non-Silencing)-EGFP). Mice were anesthetized with isoflurane as described above and placed on a stereotaxic frame. Bilateral injections were performed at a rate of 0.125 µl/min for 4 minutes (AP: +4.8 mm from bregma, ML: ±1 mm and DV: -1.7 mm from brain surface). The incision was sutured with Coated VICRYL suture (Ethicon) and mice were placed on a heated panel until they recovered from anesthesia. 3 weeks after surgery, mice were submitted to behavioral tests as described later.

This procedure has been done by our collaborator Wanqing Jiang from Stefan Trapp's laboratory (UCL). PPG knock down on RD mice will be soon validated by qPCR in the same laboratory.

1.5. Metabolic tests

1.5.1. Glucose tolerance test

Oral glucose tolerance tests (OGTT) were performed right after pharmacological injections or chemogenetic modulations. Three experimental groups were concerned by this metabolic test: i) GLP-1, Ex4 or Ex9 were perfused in the OB, in both WD and RD cannulated mice (combined with either Ex4 or UK14304 i.p. when required), as described above. ii) Vagotomized WD mice underwent the OGTT after a perfusion of Ex4 in the OB. iii) Chemogenetic activation of GLP-1R^{OB} neurons was performed in GLP-1R^{OB} hM3Dq WD mice. When required, Bicuculline Methiodide was also perfused in the PVN prior to CNO administration.

Mice were fasted for 5 hours at the beginning of the test, and a glucose solution (1g/kg) was administrated by oral gavage. Blood was collected from the tail vein for glucose monitoring (Glucofix Tech, Menarini Diagnostics) and blood sampling. Blood cells were removed from plasma by centrifugation in order to assay plasma insulin (ng/mL) and C-peptide (ng/mL) with a wide-range Ultra Sensitive Mouse Insulin ELISA Kit (catalog no. 90080; Crystal Chem, Inc.) and Mouse C-Peptide ELISA Kit (catalog no. 90050; Crystal Chem, Inc.), respectively. I.p. glucose tolerance tests (IPGTT) were performed the same way, starting with an i.p. administration of glucose at 1g/kg instead of the gavage. For all glucose tolerance tests, each mouse has been its own control.

Since the metabolic state of mice is already changing due to central (OB or PVN) perfusions and before glucose delivery, areas under the curve (AUC) were measured from baseline (before central perfusions) to the end of glucose tolerance tests, at time = 120 minutes (t120).

1.5.2. Insulin tolerance test

Insulin tolerance tests (ITT, 0.75 U/kg) were performed after 5 hours of fasting in cannulated mice. Pharmacological injections of GLP-1, Ex4 or Ex9 were performed in the OB. Mice were given an i.p. injection of insulin (0.75 UI/kg of body weight; Novo Nordisk), and glycemia (mg/dL) was monitored following the same protocol as was used for GTT. For all insulin tolerance tests, each mouse has been its own control.

Since the mice metabolic state is already changing due to OB perfusions before insulin delivery, AUCs were measured from baseline (before central perfusions, t-12) until t30 following insulin delivery (t0). Starting from t-12 leaded to positive AUC values. Because main changes

on blood glucose concentrations happened within t-12 and t30, we target this 42-minute time frame to assess insulin sensitivity.

1.5.3. Fasting refeeding

Non-cumulative food intake was measured following an overnight fasting (5 pm - 9 pm) in single-housed GLP-1R^{OB}KORD RD mice and GLP-1R^{OB} hM3Dq WD mice. At 9 pm, Salvirorin B (10mg/kg; SALB; Sigma-Aldrich) and CNO (3 mg/kg) were administered i.p. in GLP-1R^{OB} KORD RD mice and GLP-1R^{OB} hM3Dq WD mice respectively. Mice given a pre-weighed amount of food with free access to water following drug administration. Food was then weighed 1, 2, 4, 8 and 24 h after refeeding. Each mouse has been its own control for this test.

1.6. Behavioral studies

1.6.1. Odor-induced cephalic phase of insulin secretion

Peanut butter (PB) aroma drops (0 kcal) were diluted at 0,4% in NaCl 0,9%. The same PB drops were used to make PB cookies (15g flour, 10g of sugar, 15ml water, 12 PB drops - dough microwaved per 1 minutes).

7 single-caged cannulated WD and 6 RD mice, as well as 20 PPG-shRNA RD mice, underwent ten consecutive days of habituation prior to the test day. Cannulated mice were fasted for 5 hours every day in an isolated room. saying this is confusing, let's keep it for ourselves. In the morning, mice were placed into the experimental cage equipped with a tea ball hung in its lid. The cage didn't contain food but *ad libitum* access to water. The habituation (days 1 to 10) started in the afternoon when 20µl of PB dilution were dispensed on a 1x1cm filter paper. The PB-odorized filter paper was placed into the tea ball and mice were allowed to smell it during 8 minutes. After that period of time, one PB cookie per mice was placed in a visible random location of the cage. Total food consumption was checked before putting mice back onto its home cages, re-supplied with food and water *ad libitum*. On the test day (day 11, afternoon), blood was collected from the tail vein of mice fasted for 5 hours in its experimental cage (glycaemia measurement and blood sampling at time=0 min (t0)). Pharmacological injections of Ex4 or Ex9, in WD and RD cannulated mice respectively, were performed in the OB as mentioned before. PPG-shRNA RD mice skipped this step. A PB-odorized filter paper was placed into the tea ball and mice were allowed to smell the PB odor during 8 minutes. After that period of time, no cookie was given but blood was collected a second time from the tail vein of mice (glycaemia measurement and blood sampling at t13 min). Mice were put back onto its home cages re-supplied with food and water *ad libitum*. Blood cells were removed from plasma by centrifugation in order to assay plasma insulin with a wide-range Ultra Sensitive Mouse Insulin ELISA Kit (catalog no. 90080; Crystal Chem, Inc.).

Prior to these tests, in order to assess whether pre-prandial insulinemia profiles potentially change after food odor stimulation, a first assay with neither pharmacological nor gene knock-down manipulations was done on 4 RD and 4 WD mice. For that, on the test day (day 11, afternoon), blood was collected at t0 (prior to odor presentation) and at t5, t10, t15, t20 post-odor.

1.6.2. Olfactory foraging: Buried food test

Single-caged cannulated WD and RD mice underwent two consecutive days (day 1 and day 2) of odorized-food familiarization in order to prevent neophobia during the test. A tiny piece of chocolate (1g) was placed in the home cage, in a visible location, before the night shift and left overnight. The next morning, total food consumption was checked. The day before the test day (day 3), mice were submitted to an overnight fasting. The test was performed on day 4 in the morning. Ex4 in 6 WD mice and Ex9 in 6 RD mice were infused in the OB 13 minutes prior to the behavior test, as mentioned above. RD mice also received an i.p. injection of insulin at 0,25 UI before the test starts. The test cage contained 5 cm of fresh mouse bedding and was equipped with a video camera. 5-minute acclimatization to the new exploratory environment was considered before OB perfusions. A piece of chocolate was buried 2 cm beneath the surface of the bedding in a random corner of the cage. Latency time (sec) was defined as the amount of time between the introduction of the mouse in the cage and retrieval of the little chocolate after foraging. Each mouse had to find the cookie to be included in statistics. Latency was manually counted using Kinovea video tool.

1.7. Noradrenaline levels

1.7.1. Drug administration and tissue sampling

Ex4 was injected in the OB of cannulated RD and WD mice, deprived of food for 5 hours. Mice were killed by decapitation and their brains were quickly removed and dissected on ice to separate the OB and the hypothalamus. Pancreas, gut, liver and epididymal adipose tissue were also dissected. Tissues were immediately deep frozen in liquid nitrogen, and stored at -80°C until used. Each frozen tissue were weighed and dissolved in 200µL of lysing tissue solution (40 mg EDTA; $HClO_4$ 1mL of MilliQ water qs 100 mL) and then bead grinded for 2 minutes. The homogenates were centrifuged at 3000 rev/min for 30 min at 4°C, the supernatants were collected and centrifuged again at 16000 rev/min for 2 minutes. 20µL of the last supernatant was used for the HPLC-ED analysis.

1.7.2. High-performance Liquid Chromatography with Electrochemical Detection (HPL-EC)

NA measures were performed in a HPLC instrument (Shimadzu, LC20AD pump) equipped with a SiL20AC autosampler coupled with an electrochemical detector Waters 2465. NA separation was performed using an Ultrasphere column (Beckman, 150x4.6mm C18 5µM) equipped with two Phenomenex C18 filters in a security guard system. The mobile phase contained 150mM octane sulfonic acid, 8.2 mM ammonium acetate, 15% v/v methanol (pH=3.8, adjusted with glacial acetic acid) and was filtered (0.8mL/min, degassed before use) through a 0.2µM membrane filter. Elutes were detected at 700 mV (versus the reference electrode). The column and the detection cell were housed within the Faraday cage of the electrochemical detector (25.5°C). Samples were placed in the autosampler and kept at 4°C until the injection (20µl). Reference elution profiles were given by standard solutions of NA (50 ng/ml; Sigma-Aldrich) prepared in HCl 0.1N and stored at -20°C until use. Only pancreatic NA levels will be discussed in this thesis.

1.8. Fluorescein-Trp25-Exendin-4 imaging

Fluorescein-Trp25-Exendin-4 was injected into the OB of cannulated RD and WD mice. After drug administration, an OGTT was performed as described before, until 90 minutes post-injection. At that moment, mice were transcardially perfused with PBS 1X followed by 4°C PFA 4% for 5 minutes. Brains were collected, post-fixed in 4°C PFA 4% overnight and cryoprotected in sucrose 30% for 2-3 days. Brains were then snap-frozen in isopentane and the OB was cut into 18 µm-thick sections afterwards, using a cryostat (Leica Biosystems). Brain slices were collected on microscope slides (SuperFrost Ultra Plus™ GOLD), mounted with mounting media (Fluoromount-G™ with DAPI) and stored at -20°C until imaging. Image acquisition was performed with a confocal microscope (Zeiss LSM980 Airyscan2).

1.9. Luxendin-647 fluorescence in the brain after IP injection

Microscopic images of the olfactory bulb of luxendin-647 i.p. injected mice were provided by our collaborator Wanqing Jiang from Stefan Trapp's laboratory (UCL) and have been used for detailed analysis of luxendin distribution within the OB. For luxendin-related methods, see Ast et al., 2020.

1.10. cFos immunohistochemistry

1.10.1. Tissue collection

Ex4 was injected into the OB of 5 cannulated RC and 5 WD mice cannulated mice. Control mice (n=5 RC and 5 WD) were submitted to NaCl 0,9% injections in the OB. After drug administration, an OGTT was performed as described before, until 90 minutes post-injection. At that moment, mice were transcardially perfused with ice-cold PBS 1X followed by RT PFA 4% for 5 minutes. Brains were collected, post-fixed in PFA 4% at room temperature for 24h, under mild agitation. The following day, brains were transferred into PBS 1X on ice, under heavy agitation for 24h. Brains were then cryoprotected in a 30% sucrose solution in PBS 1X for 2-3 days, at 4ºC. Brains were then snap-frozen in isopentane and the PVN was cut into 30 µm-thick sections afterwards, using a cryostat.

1.10.2. cFos staining in the PVN

The day 1, PVN slices were washed 3x5 min in PBS 0.01M @ RT – 4 mL/well (12-well plate) and then incubated 30 min in [PBS 0.01M + 0.3% Triton + 50 mM Glycine + 2% NDS] – 475 µL/well (24-well plate). Subsequently, PVN slices were incubated in guinea-pig anti-cFos (Synaptic Systems, 1:1000) diluted in [PBS 0.01M + 0.3% Triton + 10 mM Glycine + 0.1% H2O2]. O/N @ RT – 475 µL/well (24-well plate). The day 2, slices were washed 3x5 min in PBS 0.01M @ RT – 4 mL/well (12-well plate) and incubated in donkey anti-guinea pig-AF647 (Jackson ImmunoResearch, 1:500) diluted in [PBS 0.01M + 0.3% Triton]. 2 h @ RT – 475 µL/well (24-well plate). Next, 3 more washes of 5 min in PBS 0.01M @ RT – 4 mL/well (12-well plate) were performed and then PVN slices were incubated in DAPI, diluted 1:20000 in PBS 0.01 M. 5 min @ RT – 475 µL/well (24-well plate). One more wash 3x 5min in Tris-HCl 50mM (pH=7.5) @ RT – 4 mL/well (12-well plate) was done before mounting the slices on gelatin coated slides (adding Prolong Gold antifade mounting medium, Invitrogen). This procedure has been done by our collaborator Vincent Simon from Daniela Cota's laboratory (University of Bordeaux).

Imaging data capture and analysis

OB sections processed for cFos in situ hybridization were imaged with a confocal microscope. Image adjustments (brightness and contrast) as well as the generation of image montages were all performed using the open-source software ImageJ. The overlay of the atlas onto the brain slices was performed using an ImageJ plugin. cFos quantification was performed within two subregions named "PVN" and "PVN descending division=PVNd". One NaCl-injected mice was removed from the analysis due to an unfound PVNd.

1.11. RNAScope

1.11.1. Tissue collection

GLP-1R^{OB} hM3Dq-mCherry GCaMP3 mice (previously injected with viruses expressing hM3Dq-mCherry under the control of the GLP-1R promoter) were transcardially perfused with PBS 1X followed by 4°C PFA 4% for 5 minutes. Brains were collected on ice, post-fixed in 4°C PFA 4% overnight and cryoprotected in sucrose 30% for 2-3 days.

1.11.2. *in situ* hybridization of Glp1r mRNA

Sections from OB of mice were processed for in situ hybridization of Glp1r mRNA using the same previously optimized protocol for RNAscope assay (Brierley et al., 2021). 10µm-sections were cut on a cryostat (Leica Biosystems) and collected on Superfrost Plus slides, then air-dried at room temperature for 1h. OB slides were subsequently dipped in molecular biology grade ethanol and further allowed air-dry overnight at room temperature. RNAscope in situ hybridization was performed on these sections using the RNAscope Multiplex Fluorescent Kit v.2 (Advanced Cell Diagnostics) following the manufacturer's directions, with a variation to the pretreatment procedure (20-min protease IV incubation at room temperature) that aids in the conservation of the fluorescent reporter signal while also keeping optimal signal from the target mRNAs. Probes for *glp1r* (Advanced Cell Diagnostics) and appropriate positive (Ubc, Advanced Cell Diagnostics) and negative (DapB, Advanced Cell Diagnostics) controls were hybridized and at the end of the procedure slides were directly cover slipped using Prolong Antifade medium. This procedure has been done by our collaborator Marie Holt from Stefan Trapp's laboratory (UCL).

1.11.3. Imaging data capture

OB sections processed for RNAscope in situ hybridization were imaged with a Leica TCS SP8 confocal microscope at x20. Image adjustments (brightness and contrast) as well as the generation of image montages were all performed using the open-source software Fiji.

1.12. Real time quantitative PCR

All animals were sacrificed by cervical dislocation. The brain was harvested and the olfactory bulb and hypothalamus were dissected and immediately deep frozen in liquid nitrogen and stored at -80ºC. Total RNA was isolated using RNeasy Lipid Tissue mini kit (Qiagen). Real-time quantitative polymerase chain reaction (PCR) was carried out in a LightCycler 480 detection system (Roche) using the LightCycler FastStart DNA Master plus SYBR Green I kit (Roche).

The primers were derived from mouse sequences. We targeted the GLP-1R (cggcgtcaactttcttatcttca R GLP1 mouse NK_S / gggcgtgttcgtccatca R GLP1 mouse NK_AS), InsR (Insulin R_m_S tctttcttcaggaagctacatctg/ Insulin R_m_AS tgtccaaggcataaaaagaatagtt), PC1/3 (PCSK1_m_S tggagttgcatataattccaaagtt/PCSK1_m_AS agcctcaatggcatcagttac), PC2 (PCSK2_m_S ctctgtgcagaaccctgaaa/PCSK2_m_AS tgactgtgatgacagcttgga), DPP-IV (DPP4_m_S cggtatcatttagtaaagaggcaaa/DPP4_m_AS gtagagtgtagaggggcagacc), GIPR mRNA (GIPR_m_S tgggtccctacactggagac/ GIPR_m_AS tgtaattggctcccacacaa) normalized against the mean of two reference house-keeping genes (TBP_m_S ggggagctgtgatgtgaagt/TBP_m_AS ccaggaaataattctggctca; rpL19_m_S gggcaggcatatgggcata/rpL19_m_AS ggcggtcaatcttcttggatt).

2. GLP-1 content on OB slices

10 RD mice and 10 WD mice were transcardially perfused with ice-cold NMDG saline buffer. The brain was harvested and the olfactory bulb dissected and immediately sectioned in 12 slices of 150µm using a vibratom. Slices were then transferred to NMDG at 34°C for ~12 min and divided into different wells (~1 bulb per well). Slices were then incubated for 10 minutes at 34°C (monitoring of bubbling, keeping slices in motion using a pipette) in wells containing 600µL of aCSF at 34°C (including 1mM or 5mM glucose) under fine bubble carbogen perfusion (1Hz). Addition of protease inhibitors (DPP-IV at 24µL/600µL) and Aprotinin (9µL/600µL) was performed before the transfection of slices into the wells. Slices were then transferred to wells filled with 600 µL of ACSF (+100mM KCl) with DPP-IV inhibitors (24µL/600µL) and Aprotinin (9µL/600µL) and incubated for 20 min at 34°C (monitoring of bubbling, keeping slices in motion using a pipette). The 1st incubation wells (ACSF + inhibitors) were aspirated (bottom of the well (~500µL)) with a pipette. Supernatant samples were named “t0” and stored at -80 until dosage. Next, the 2nd incubation wells (ACSF + inhibitors + KCl) were aspirated. Supernatant samples were named “t20” and stored at -80 until dosage. OB slices were recollected apart. GLP-1 content in the supernatant of t0 and t20 samples was assessed using a Glucagon-Like Peptide-1 (GLP-1) Total ELISA KIT (96-Well Plate Cat. # EZGLP1T-36K, EZGLP1T-36BK, Millipore). This procedure has been done by our collaborator David Jarriault from Xavier Fioramonti’s laboratory (NutriNeuro, Bordeaux) and Victor Gault (GLP-1 dosage, Ulster University).

3. Human studies

3.1. Subjects and treatments

The data from Meyer-Gerspach et al. (2018) were reanalyzed by our collaborator, Professor Lukas Van Oudenhove (Translational Research Center for Gastrointestinal Disorders, Catholic University of Leuven, Belgium) from scratch for the purpose of our study. Briefly, 12 healthy male volunteers (mean age of 24.8 years) and mean BMI of 22.9 kg/m2 were imaged. Participants were fasted overnight for at least 10 hours before each treatment. Recordings of MRI images to assess resting-state last for 5 minutes right after the administration of intravenous-ex9-39 (600 pmol/kg/min) + an intragastric (ig polyvinyl feeding tube was inserted into the stomach) glucose (75g glucose dissolved in 300mL tap water) load. These images were compared to the intragastric glucose condition alone.

3.2. fMRI data preprocessing

First, raw Data Information Object Definition (DICOM) data were converted to Neuroimaging Informatics Technology Initiative (NIfTI) format and organized according to Brain Imaging Data Structure (BIDS) convention (Gorgolewski et al., 2016) using the in-house custom bash shell script KUL_dcm2bids.sh. Quality control and preprocessing were performed using the state-of-the-art pipelines MRIQC (Esteban et al., 2017) and fMRIprep (Esteban et al., 2019, fMRIPrep: a robust preprocessing pipeline for functional MRI), respectively.

3.3. Region of interest (ROI) definition

For the primary olfactory cortex, which constitutes the principal region of interest, we included 4 subregions based on a recent parcellation (Zhou et al., 2019): the anterior olfactory nucleus (AON), the olfactory tubercle (TUB), and the frontal (anterior) and temporal (posterior) piriform cortex (PrF and PrT, respectively). The following additional regions of interest in the network were taken from the Johns Hopkins University atlas (Faria et al., 2012).

3.4. Functional connectivity analysis

3.4.1. First level analysis

ROI-to-ROI connectivity matrices were calculated for each subject and each session, consisting of Fisher r-to-z transformed bivariate correlation coefficients between each pair of ROI BOLD timeseries (https://web.conn-toolbox.org/fmri-methods/connectivity-measures/roi-to-roi and Nieto-Castanon, 2020).

3.4.2. Second-level analysis

At the second (i.e. group) level, ROI-based inference was made using parametric multivariate statistics, as described in https://web.conn-toolbox.org/fmri-methods/cluster-level-inferences#h.p_XkNU7W1TOYW5. Briefly, this results in a ROI-level p-value indicating whether the given ROI is characterized by significant functional connectivity to other ROIs in the network, combined with connection-level p-values to identify significant connections from this ROI to other ROIs in the network. CONN's default threshold settings were adopted (False Discovery Rate (FDR)-corrected $p < 0.05$ at the ROI level, uncorrected $p <$ at the connection level for illustrative purposes.

This analysis was performed both across conditions (connectivity of the network) and contrasting both conditions (difference in connectivity of the network between conditions).

4. Statistical methods

Data in representative are given as means ± standard error of the mean (SEM). Statistical analysis was performed using Student's t test (to compare the means of specifically two groups) or ANOVA (to analyze the difference between the means of more than two groups) after normality was assessed by a Shapiro-Wilk test. One-way ANOVA or two-way ANOVA tests were selected when data was collected about one or two independent variables, respectively. ANOVA tests were followed by two-by-two comparisons using Bonferroni's post hoc test (GraphPad Software, La Jolla, CA, USA). Differences were considered significant at $p < 0.05$.

SECTION IV

Results

Results

1. The GLP-1 system is present in the OB

Central GLP-1 is produced by preproglucagon (PPG) neurons in the brain (Trapp and Brierley, 2022). Thiebaud et al. (2016) confirmed a large population of PPG-neurons in the granular cell layer of the OB using transgenic mice expressing the YFP under the control of the glucagon promoter (PPG-YFP mice, Reimann et al. 2008). We reproduced the same imaging on PPG-YFP mice and our results support and confirm the identification of PPG cells demonstrated in 2016 (Figure IV.1A).

Extracellular brain glucose concentrations ($[Gluc]_{ECF}$) could reach 5mM during peripheral hyperglycaemia (Silver & Erecinska, 1994). More precisely, in the OB, Al Koborssy et al. showed that $[Gluc]_{ECF}$ in both satiated and fasted rats is around 1 mM (Al Koborssy et al., 2014). To provide further insights into bulbar GLP-1 production, we are working on measuring the GLP-1 content in OB slices from RD and WD mice bathed with a bath solution containing either 1mM or 5mM glucose before and after neuronal stimulation by potassium chloride (KCl) addition (Figure IV.1B left). At the moment, we only can provide preliminary results for RD mice OB slices under 5mM-glucose condition. Interestingly, our first data suggested an encouraging increase total GLP-1 content (tendency), from 28,3 to 47,3 nmol/mg total protein (Figure IV.1B right).

We next aimed to assess the location of GLP-1R in the OB. Thus, GLP-1R-expressing OB cells were targeted using a fluorescently labeled Exendin-4 (Fluorescein-Trp25-exendin-4; FLEX). FLEX was present in the mitral cell layer and granular cell layer (Figure IV.1C) of RC and WD mice, as reported previously using fluorescent Ex4-647 in RD mice (Thiebaud et al. 2016). A nicely aligned number of cells in the MCL could be visualized as well as scattered stained cells within the GCL.

We also assessed *glp1r* expression in mitral cells using RNAscope fluorescence *in situ* hybridization on GLP-$1R^{OB}$ hM3Dq-GCaMP3 mice, expressing mCherry fluorescence on GLP-

1R-expressing cells (Figure IV.1D). Several mCherry-expressing neurons were found to be mitral cells, and colocalization with *glp1r* RNAscope was confirmed for each mCherry-labelled mitral cell (Figure IV.1D, representative magnifications in Section 1 and 2). These results identify GLP-1R RNA on mitral cells *in vivo*. This was consistent to the RT-PCR quantification that confirmed mRNA expression levels of GLP-1R in the OB, in both RC and WD mice (0.40 and 0.47 mRNA a.u., respectively). Moreover, the OB expressed mRNA levels coding for the pro-convertase PC1/3 ($a.u._{RD}$=0.41±0.03; $a.u._{WD}$=0.61±0.05) and the enzyme DPP-IV ($a.u._{RD}$=0.84±0.06; $a.u._{WD}$=1,26±0.05), which, interestingly, were both significantly increased in WD mice compared to RD mice ($P_{PC1/3}$=0.0099; P_{DPP-IV}=0.0005; Figure IV.1E). The presence of PC2, GIPR and InsR, was also assessed. While PC2 was significantly more expressed in the OB of WD mice compared to RD mice ($a.u._{RD}$=0.33±0.04; $a.u._{WD}$=0,63±0.07; P=0.0033, Figure IV.1E), GIPR ($a.u._{RD}$=5,79±0.9; $a.u._{WD}$=7,9±0.5) and InsR ($a.u._{RD}$=8±1.5; $a.u._{WD}$=11,7±2.6) mRNA levels remained unchanged (P=0,0681 and P=0.2196; Figure IV.1F).

Furthermore, i.p. injected Luxendin 645, a fluorescent GLP-1R antagonist based on Ex9 (Ast et al. 2020) stained several GLP-1R-expressing brain structures such as the hypothalamus or the area postrema, but did not label bulbar GLP-1R in the OB (Figure IV.1G). This led to the hypothesis that circulating GLP-1 might have restricted access in this region, and thus, it is reasonable to think that PPG cells in the OB should be the main source of bulbar GLP-1.

Overall, these findings support the fact that several OB cells are sensitive to GLP-1 *in vivo* through the expression of GLP-1R.

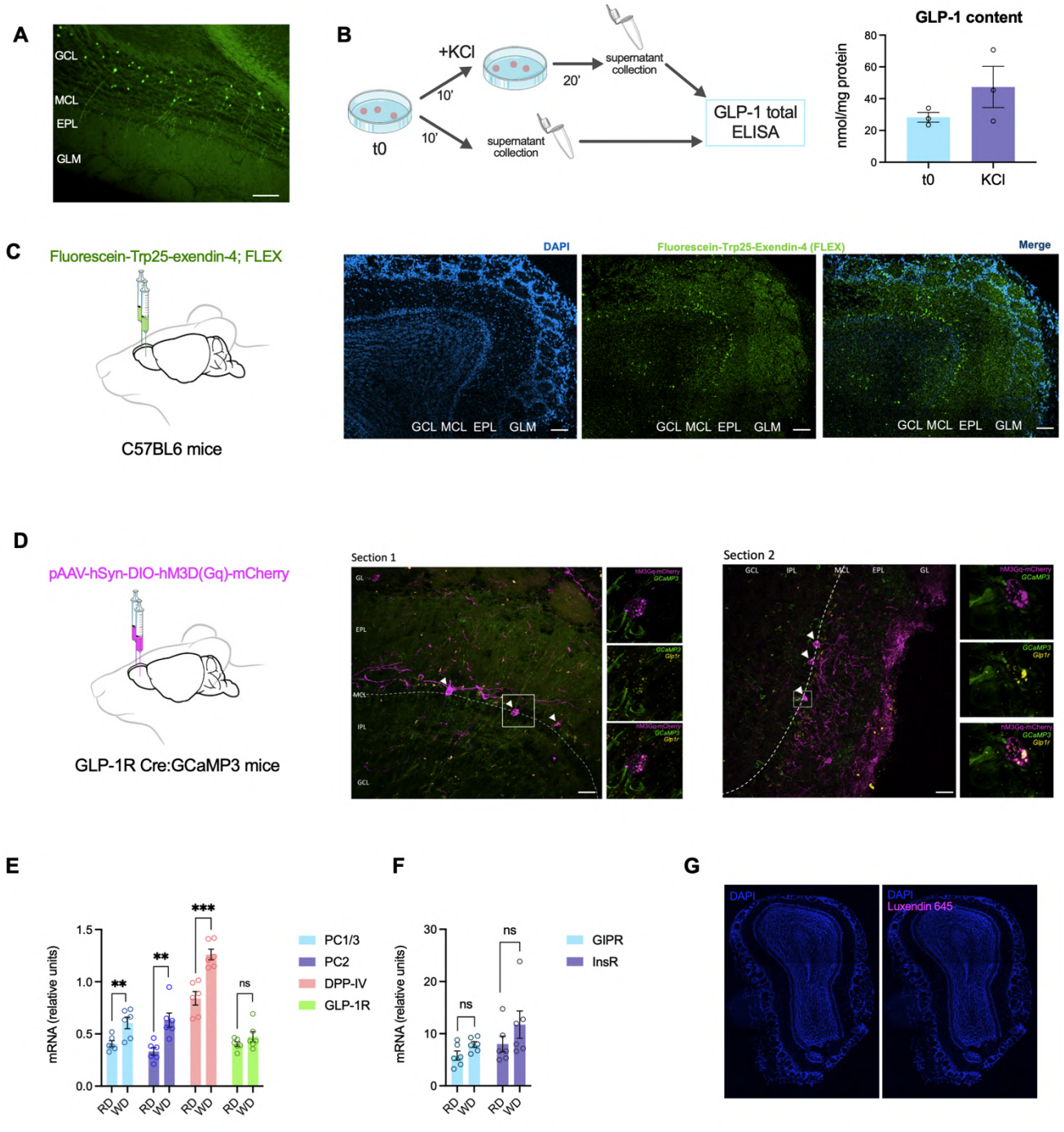

Figure IV.1. The GLP-1 system is present in the OB.

(A) Representative photomicrograph of a PPG-YFP mouse OB showing YFP labelling of PPG cells in the GCL. GCL: granular cell layer; MCL: mitral cell layer; EPL: external plexiform layer; GLM: glomerular cell layer. Scale bar = 100µm.

(B) Schematic illustration of the strategy targeting GLP-1 production in the OB (left) and quantification of GLP-1 content before (t0) and after neuronal stimulation (KCl) *in vitro* (right). (n=3 RD/group).

(C) Strategy to deliver fluorescent Ex4 in the OB of OB-cannulated C57BL6 mice and photomicrograph of representative OB sections from a fluorescent Ex4-injected mouse. Scale bar = 100µm. Fluorescence of Ex4 is stained in green, DAPI in blue.

Figure caption continued on next page

(D) Strategy to deliver AAV8-hSyn-DIO-hM3Dq-mCherry in the OB of GLP-1R Cre:GCaMP3 mice (left) and representative image of RNAscope for *glp-1r* in hM3Dq-injected GLP-1R Cre:GCaMP3 mice (right). Scale bar = 50 µm. Fluorescence of m-cherry is stained in magenta, GCaMP3 in green and *glp-1r* in yellow.
(E, F) RT-PCR of PC1/3, PC2, DPP-IV, GLP-1R (E) as well as GIPR and InsR (F) in the OB of 50-week-old RD and WD mice.
(G) Photomicrograph of representative OB sections from RD mice injected with luxendin 645 i.p. Fluorescence of luxendin 645 is stained in magenta, DAPI in blue.
Data are given as mean ± SEM. *p <0.05; **p < 0.01; ***p < 0.001; ns, not significant.

2. Odor-induced cephalic phase of insulin secretion is reversed by Ex9 in the OB and offers an optimal olfactory foraging in RD mice

The pre-prandial cephalic phase of insulin secretion occurs during the first ten minutes of a meal and before glucose levels rise. This early anticipatory response, that prepares the organism for an efficient use of the subsequent glucose ingestion, has been well documented on animals but its presence in humans has become controversial (Veedfald et al. 2016). In order to gain deeper insight into this issue, we explored the existence of a cephalic phase of insulin secretion in RD and WD mice after being exposed to 10 days of habituation to the odor of peanut butter (PB), a palatable and rewarding food commonly used in chemical senses studies (Chelminski et al., 2017; Qiu et al. 2021). This odor was used to aromatize a home-made cookie. Learning odor to food association (PB odor to PB cookie) was remarkable on mice during the first training days since they performed faster on each trial. No neophobia-induced stress was noticed on the test day, where blood was collected. A cephalic increase of insulin secretion was present in RD mice 20 min after odor presentation (+129%, P=0.0450), whereas in the WD group, insulin secretion was decreased from t5 following PB-odor exposure (-75%, P=0.0495). Hence, odor-induced cephalic phase of insulin secretion was present in RD mice, whereas lost in WD mice (Figure IV. 2B).

In view of these results, we wanted to assess whether the GLP-1 system in the OB plays a key role in the odor-induced cephalic phase insulin response. Hence, in cannulated RD mice, which did present an early insulin release (Figure IV.2B), we injected Ex9 in the OB (Figure IV.2A, 2C). Given that WD mice lost its cephalic insulin phase (Figure IV.2B), bulbar injection of Ex4 was performed instead on this group (Figure IV.2A, 2D). Interestingly, an acute injection of Ex9 in the OB of RD mice blocked the early increase in blood insulin induced by PB-odor exposition (t0 Ex9 vs. t13 Ex9, -25%, Figure IV.2C). Glucose levels were increased after Ex9 delivery in the OB and odor exposure in RD mice (t13 Ex9 vs. t13 NaCl, P_{AUC}<0.0001; t13 Ex9 vs. t0 Ex9, P_{AUC}<0.0053; Figure IV.2C, insert AUC). Inversely, the injection of Ex4 in the OB

seems to be a potential way for restoring the loss of odor-evoked CPIR (t13 Ex4 vs. t13 NaCl, P<0.0213, Figure IV.2D). Glycaemia did not change during the test (Figure IV.2D, insert AUC).

To assess whether PPG-neurons in the OB, supposed to be the source of local GLP-1, play a role in the odor-evoked anticipatory insulin response, we performed the same odor-induced CPIR on RD mice injected with a shRNA targeting PPG mRNA in PPG neurons to knock down GLP-1 production in the bulb (Figure IV.2E). Concomitant to Ex9 results (Figure IV.2C), PPG-shRNA mice presented absence of odor-induced cephalic phase of insulin secretion while scrambled-shRNA mice showed an early increase of insulinemia following odor exposure (P=0.0198). Besides, insulinemia on scrambled-shRNA mice (controls) was significantly higher after odor presentation (t13 scrambled-shRNA vs. t13 PPG-shRNA, P=0.0158, Figure IV.2F). Glucose levels were increased in PPG-shRNA group compared to controls at t0 (t0 vs. t0, NaCl P=0.0273; Figure IV.2F). Glycaemia was also increased in PPG-shRNA group after odor presentation (t0 vs. t13, P=0.0354). Together, these results suggest that odor-induced cephalic phase of insulin secretion is controlled by PPG-released GLP-1 in the OB *via* GLP-1R signaling.

We next assessed the possible relationship between food odor detection and GLP-1R signaling in the OB. To this end, we performed a buried food test (BFT) on overnight fasted mice (Figure IV.2G). BFT is a standard behavioral approach which depends on rodent's natural tendency to use olfactory cues for foraging (Wang et al. 2021; Mortreux et al., 2019). Prior to the BFT, cannulated WD and RD mice underwent Ex4 and Ex9 injections in the OB, respectively.

WD mice presented weak ability to find the buried piece of smelly chocolate (94.50±24.12 sec), which reflected a significant decrease of olfactory sensitivity, caused by the obesogenic diet, as reported previously (Soleimanzad et al., 2020). Interestingly, the injection of Ex4 into the OB of obese mice corrected their loss of olfactory sensitivity compared to the NaCl-injected WD group (P=0.0263, Figure IV.2H). NaCl-injected RD mice, instead, presented normal olfaction and optimal foraging time (18.84±3.047 sec). The injection of Ex9 in the OB of RD mice significantly increased (P=0.0041) the latency to uncover the hidden piece of smelly chocolate compared to controls (Figure IV.2I). To assess whether an early insulin release could play a role in olfactory foraging during BFT, we injected insulin in RD mice after an OB injection of Ex9, or NaCl (Figure IV.2I). The dose was checked as not being hypoglycemic prior to the test (Figure IV.2J). Insulin reversed the deleterious effect of Ex9 on olfactory foraging, restoring the food discovery time to the level of NaCl-injected RD mice (P=0.0057, Figure IV.2I). This result suggest a role of preprandial insulin during BFT. Together, these findings confirm that bulbar GLP-1R is involved in the control of olfactory foraging.

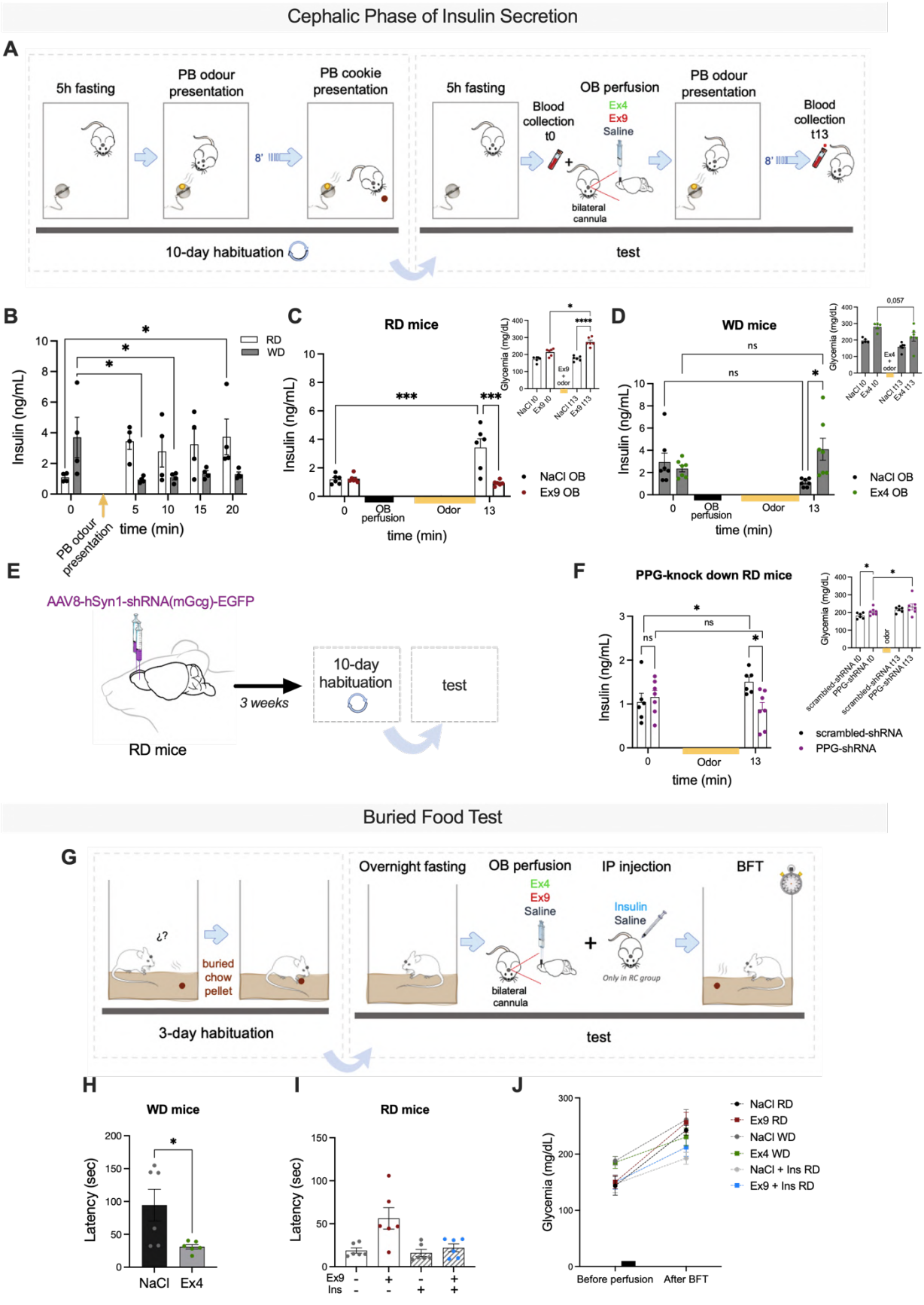

Figure IV.2. Odor-induced cephalic phase of insulin secretion is reversed by Ex9 and allows an optimal olfactory foraging in RC mice.

Figure caption continued on next page

(A) Schematic illustration of the 11-day protocol performed to assess odor-induced cephalic phase of insulin secretion in RD and WD mice. Round yellow: PB odor inside a tea ball. Round grey: PB cookie. t=time.
(B) Plasma insulin levels in RD and WD mice before (t0) and after (t5, t10, t15, t20) PB odor presentation (2-way ANOVA, n=4/diet group).
(C, D) Plasma insulin and glucose levels before (t0) and after (t13) OB perfusion of Ex9 (C) or Ex4 (D) combined with 8-minute PB odor presentation, in RD and WD mice respectively (2-way ANOVA, n=6-7/group).
(E) Schematic illustration of viral delivery in the OB and subsequent 11-day protocol performed to assess odor-induced cephalic phase of insulin secretion in PPG-shRNA RD mice.
(F) Plasma insulin and glucose levels before (t0) and after (t13) 8-minute PB odor presentation, in PPG-shRNA and scrambled-shRNA RD mice (2-way ANOVA, n=10/genotype group).
(G) Schematic illustration of the BFT combined with pharmacological injections in the OB of RD and WD mice.
(H) Latency of WD mice during BFT after Ex4 injection in the OB (unpaired Student's t test, n=6/group).
(I) Latency of RD mice during BFT after Ex9 injection in the OB combined with i.p. injected insulin (2-way ANOVA, n=6/group).
(J) Glucose levels before and after BFT in all RD and WD mice groups (n=6/group).
Data are given as mean ± SEM. *p <0.05; **p < 0.01; ***p < 0.001; ns, not significant.

3. Up and down chemogenetic modulation of GLP-1R+ neurons in the OB oppositely regulates food intake and glucose homeostasis

Obesity is a complex disease partly defined as abnormal amount of body fat due to an excessive consumption of high amounts of energy, particularly fat and sugars. WD mice (Figure IV.3A) developed in a few months several signs of obesity as overweight and fat accumulation. Since week 9, body weight in GLP-1RCre:GCaMP3 WD mice was significantly increased (P=0.0417) compared to GLP-1RCre:GCaMP3 RD mice, which maintained their body weight fairly stable over time (Figure IV.3A). 16 weeks under obesogenic diet (1 week before surgery and viral injections) caused significant body weight gain in GLP-1RCre:GCaMP3 WD mice (+78%, P=0.0016) compared with age-matched GLP-1RCre:GCaMP3 RD mice (Figure IV.3A). Overweight in WD mice was accompanied by a significant increase in fat mass (+298%, P<0.0001) to the detriment of lean mass (−39%, P<0.0001) compared to RD mice (Figure IV.3B).

It has been reported that central administration of GLP-1 potently reduces food intake in rats and mice (Turton et al., 1996; Jessen et al., 2012). Hence, we next investigated the possible role of GLP-1R^{OB} neurons on feeding. Since GLP-1RCre:GCaMP3 RD mice did not present excessive weight gain nor fat accumulation, we assumed that they had an optimal food intake. In

order to challenge their healthy profile, we assessed viral-vector delivery of KORD (κ-opioid) DREADD in the OB of GLP-1RCre:GCaMP3 RD mice (Figure IV.3C), for the purpose of chemogenetically downregulate GLP-1R^{OB} neurons (GLP-1R^{OB} KORD RD). GLP-1RCre:GCaMP3 WD mice, instead, displayed overweight and increased fat mass, factors that can be explained by consuming energy in surplus. Thus, in order to reduce its intake and validate if GLP-1R^{OB} neurons suppress feeding in the context of obesity, we up-regulated GLP-1R^{OB} neurons on GLP-1R^{OB} hM3Dq WD mice, previously generated by viral-vector delivery of hM3Dq DREADD in the OB of GLP-1RCre:GCaMP3 mice.

Fasting-refeeding test on GLP-1R^{OB} KORD RD mice and GLP-1R^{OB} hM3Dq WD mice were performed. GLP-1R^{OB} neurons inhibition on KORD RD mice increased food intake of RD at 0-1h (P=0.0163) and 6-8h (P=0.0205) post-injection of the KORD-activator Salvinorin B (SALB, Figure IV.3D). Furthermore, the activation of GLP-1R^{OB} neurons on hM3Dq WD mice by clozapine N-oxide (CNO i.p.), fed with both HF230 and A04, reduced food intake of both diets during the first hour following the i.p. injection (CNO vs. NaCl, P_{HF230}=0.0117 and P_{A04}=0.0497, Figure IV.3E). CNO-injected control WD mice (GLP-1R^{OB} mCherry RD) did not present any changes in food intake during the test (Figure IV.3F). Therefore, GLP-1 signaling in OB neurons could be implicated in food intake regulation after an overnight fasting.

Since GLP-1 was shown to be a key determinant of energy balance, we next investigated the possible role of GLP-1R^{OB} neurons in glucose homeostasis during the post-prandial state through an OGTT. We kept performing the up and down modulation of GLP-1R^{OB} neurons in GLP-1R^{OB} hM3Dq WD mice and GLP-1R^{OB} KORD RD mice, respectively.

GLP-1R^{OB}KORD RD mice were injected with SALB or NaCl prior to the OGTT (Figure IV.3G). NaCl-injected GLP-1R^{OB}KORD RD mice (NaCl-KORD, control condition) presented an optimal response to glucose (Figure IV.3G) and a fine-tuned glucose-induced insulin secretion (t0 vs. t15, P=0.0027, Figure IV.3H). The inhibition of GLP-1R^{OB} neurons by SALB in RD mice did not have any significant impact on glycaemia (Figure IV.3G), and insulinemia remained significantly increased (t0 vs. t15, P=0.0162, Figure IV.3H), compared to the control condition on the same GLP-1R^{OB}KORD RD mice.

GLP-1R^{OB} hM3Dq WD mice were beforehand i.p. injected with CNO or NaCl (Figure IV.3I). NaCl-injected GLP-1R^{OB} hM3Dq WD mice (NaCl-hM3Dq) were glucose intolerant compared to GLP-1R^{OB}KORD RD mice (AUC_{WD} vs. AUC_{RD}). Specific activation of GLP-1R^{OB} neurons by CNO in WD mice leaded to a drastic improvement of glucose tolerance (CNO vs. NaCl, P<0.0001, Figure IV.3I). The dose of CNO injected was confirmed as not affecting glycaemia in control WD mice transduced with the control virus (AAV8-hSyn-DIO-mCherry) (Figure IV.3I).

Insulin secretion in CNO-injected GLP-1R^{OB} hM3Dq WD mice was strongly increased at t15 minutes compared to the injection of NaCl on the same GLP-1R^{OB} hM3Dq WD mice (P=0.0003, Figure IV.3J). WD mice injected with the mCherry control virus did not present any changes on insulinemia during the OGTT. These results show that upregulating the levels of GLP-1R activity in the OB by chemogenetic approaches leads to an improved glucose homeostasis in the context of obesity.

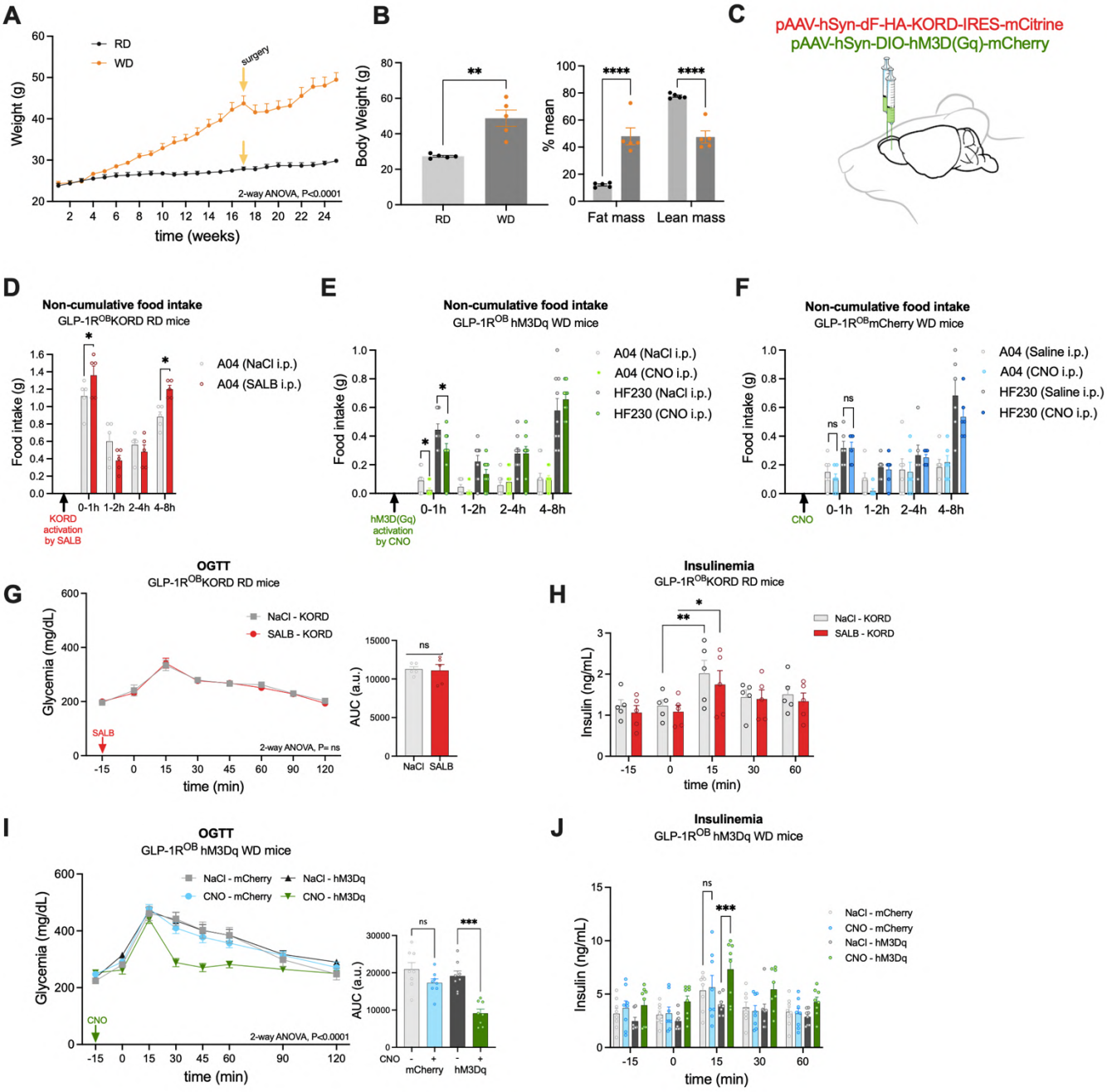

Figure IV.3. Up and down chemogenetic modulation of GLP-1R+ neurons in the OB regulates food intake and glucose homeostasis.

(A) 25-week weight gain of GLP-1RCre:GCaMP3 WD and RD mice (n=5/diet group).

Figure caption continued on next page

(B) Body weight, fat mass and lean mass of GLP-1RCre:GCaMP3 RD and WD mice at 16 weeks under WD diet (n=5/diet group). Body composition (fat and lean mass) was expressed as a percentage of body weight.

(C) Schematic illustration of viral delivery in the OB of GLP-1RCre:GCaMP3 RD and WD mice.

(D-E) Fasting refeeding in GLP-1R^{OB} KORD RD mice (D) GLP-1R^{OB} hM3Dq WD mice (E) after i.p. injection of SALB or CNO, respectively. Black arrows indicate the injection time. (paired Student's t tests, n=5-9/diet group).

(F) Fasting refeeding in OB mCherry-injected WD mice after i.p. injection of CNO. Black arrows indicate the injection time (n=6).

(G) Left: OGTT test preceded with an i.p. injection of SALB in GLP-1R^{OB} KORD 24 week-old (two-way ANOVA, n=5). The red arrow indicates the SALB injection before the glucose challenge (t0). Right: area under the curve (AUC) of the metabolic test (paired Student's t test).

(H) Plasma insulin levels of GLP-1R^{OB} KORD RD mice after SALB i.p. injection (two-way ANOVA, n=5).

(I) Left: OGTT test preceded with an i.p. injection of CNO in GLP-1R^{OB} hM3Dq WD mice and GLP-1R^{OB} mCherry WD mice at 20 weeks under WD (24-week old, two-way ANOVA, n=8/genotype group). The green arrow indicates the CNO injection before the glucose challenge (t0). Right: AUC of the metabolic test (paired Student's t test).

(J) Plasma insulin levels of GLP-1R^{OB} hM3Dq WD mice after CNO i.p. injection (two-way ANOVA, n=8/genotype group).

Each mouse has been its own control. Data are given as mean ± SEM. *p <0.05; **p < 0.01; ***p < 0.001; ns, not significant.

4. Pharmacological modulation of GLP-1R in the OB regulates glucose homeostasis

Body weight was significantly increased in cannulated WD mice since week 7 under WD, whereas RD mice presented a stable body weight over time (Figure IV.4A). In accordance with what we defined for GLP-1RCre:GCaMP3 mice (Figure IV.3B), 16 weeks under obesogenic diet caused significant body weight gain in WD mice (+52%) compared with age-matched RD mice (Figure IV.4B). Weight gain in WD mice resulted in an increase in fat mass (+207%, P=<0.0001) and a decrease in lean body mass (−29%, P<0.0001) compared to RD mice (Figure IV.4B).

We next evaluated the effect of bulbar GLP-1R modulation on glucose homeostasis. With this aim, we performed OGTT tests in cannulated WD and RD mice after pharmacologic injections of GLP-1 or drugs targeting the GLP-1R in the OB (Ex4 and Ex9, Figure IV.4C). Each of the three compounds were tested for both WD and RD mice.

WD mice presented an impaired glucose tolerance under the control condition (NaCl OB) whereas RD mice showed optimal glucose levels during OGTT tests (Figures IV.4D, 4E, 4F). We observed a strong improvement in glucose tolerance over time in WD mice after GLP-1 injection in the OB (GLP-1 vs. NaCl, P_{OGTT}<0,0001), while glycaemia was decreased at t15 in RD mice (GLP-1 vs. NaCl, P_{OGTT}=0.0379, Figure IV.4D). Since total whole glucose excursion, given by the area under the curve (AUC), is also considered to finely represent glucose tolerance, we assessed this value in RD and WD mice. AUC was decreased in both RD and WD mice after GLP-1 injection in the OB compared to RD and WD control conditions (P_{AUC}=0,0013 and P_{AUC}<0,0001 respectively, Figure IV.4D, insert AUC). Ex4 injection in the OB triggers the same beneficial effects on glucose tolerance compared to GLP-1 in WD mice (P_{OGTT}<0,0001), whereas no changes on glycaemia were shown in RD mice (Figure IV.4E). Inversely, Ex9 in the OB worsened glucose intolerance in WD mice (P_{OGTT}<0,0001, P_{AUC}=0,0034) while no significant changes were seen on RD mice (Figure IV.4F). Since under Ex9 there is no GLP-1 increase (triggered endogenously or exogenously), the Ex9 result, in accordance to the increase of glycaemia seen on RD mice under bulbar Ex9-delivery during the pre-prandial phase (Figure IV.2C, insert AUC) clearly indicate that there is a tonic release of GLP-1 in the OB.

Impaired glucose homeostasis is associated to a wide number of downstream effects, including a loss of insulin sensitivity, which is enhanced by GLP-1 *via* multiple ways, among them, *via* central GLP-1R signaling (Cabou et al., 2011). This loss of insulin sensitivity is associated to excessive insulin levels circulating in the blood, in proportion to the level of glucose. Hence, we measured insulin secretion levels during OGTT. WD mice presented hyperinsulinemia from t-12 (RD vs. WD, Figures IV.4G, 4H, 4I, P<0.05) and a lack of glucose-induced insulin response under the control condition (WD_{t0} vs. WD_{t15}, P>0.9999). Age-matched RD mice presented normal glucose-induced insulin secretion on the same condition (P<0.05). Pancreatic insulin secretion was intensely increased in WD mice after GLP-1 injection in the OB at t0 and

t15 of the OGTT, whereas no changes were seen in RD mice (GLP-1 vs. NaCl, Figure IV.4G). The injection of Ex4 in the OB had comparable effects to that of GLP-1 on insulin secretion, which was strongly increased during the whole OGTT test (Figure IV.4H) and at t15 during an IPGTT test in WD mice (data not shown). Ex9 did not impact insulinemia during OGTT in both RD and WD mice (Figure IV.4I).

We next assessed insulin sensitivity by ITT tests on cannulated WD and RD mice after GLP-1, Ex4 or Ex9 injections in the OB. Our WD mice developed insulin resistance, as already described before on dietary C57BL6 models of obesity (Collins et al., 2004).
which was significantly improved by an acute injection of GLP-1 in the OB (P=0.0012, Figure IV.4J). RD mice presented good insulin sensitivity, and no changes were observed after GLP-1 injection in the OB (Figure IV.4J). Globally Ex4 triggered similar beneficial effects on insulin resistance compared to GLP-1 in WD mice (Ex4 vs. NaCl, P=0.0149, Figure IV.4K). No changes were observed in RD mice either (Figure IV.4K). The injection of Ex9 in the OB worsened insulin resistance in WD mice (P=0.0127, Figure IV.4L), whereas RD mice did not present any significant change on AUC, compared to the control condition.

An important question in the literature is to determine whether central GLP-1R has a significant impact in mediating the effects of GLP-1 released in periphery during the prandial phase on glucose homeostasis. To determine whether GLP-1R in the OB is involved in the improved effects on glucose homeostasis due to systemic activation of GLP-1R, we injected Ex9 or NaCl in the OB of obese mice, followed by an i.p. injection of Ex4 or NaCl (Figure IV.4M). We immediately started an OGTT afterwards. Whereas glucose intolerance was worsened by Ex9 in the OB alone (and NaCl i.p.), systemic Ex4 (under OB-injected NaCl) drastically improved glucose tolerance in obese mice (NaCl OB - Ex4 i.p. vs. NaCl OB - NaCl i.p.; P_{OGTT}<0,0001, P_{AUC}=0,0143; Figure IV.4N). While Ex9 OB and Ex4 i.p. were administered together, the ameliorating effect of systemic Ex4 was lost (NaCl OB - Ex4 i.p. vs. Ex9 OB - Ex4 i.p., Figure 4N, P_{OGTT}<0,0001, P_{AUC}=0,0182). Equivalent results were obtained on insulinemia, measured all along the OGTT, since the potentiating effect of systemic Ex4 on insulin secretion was attenuated by the injection of Ex9 in the OB (P=0.0267, Figure IV.4O). These results suggest that GLP-1R in the OB is required for an optimal control of glucose balance.

Taken together, these findings indicate that the GLP-1R signaling pathway in the OB plays a crucial role in the control of glucose homeostasis during the post-absorptive phase, mainly in the context of obesity.

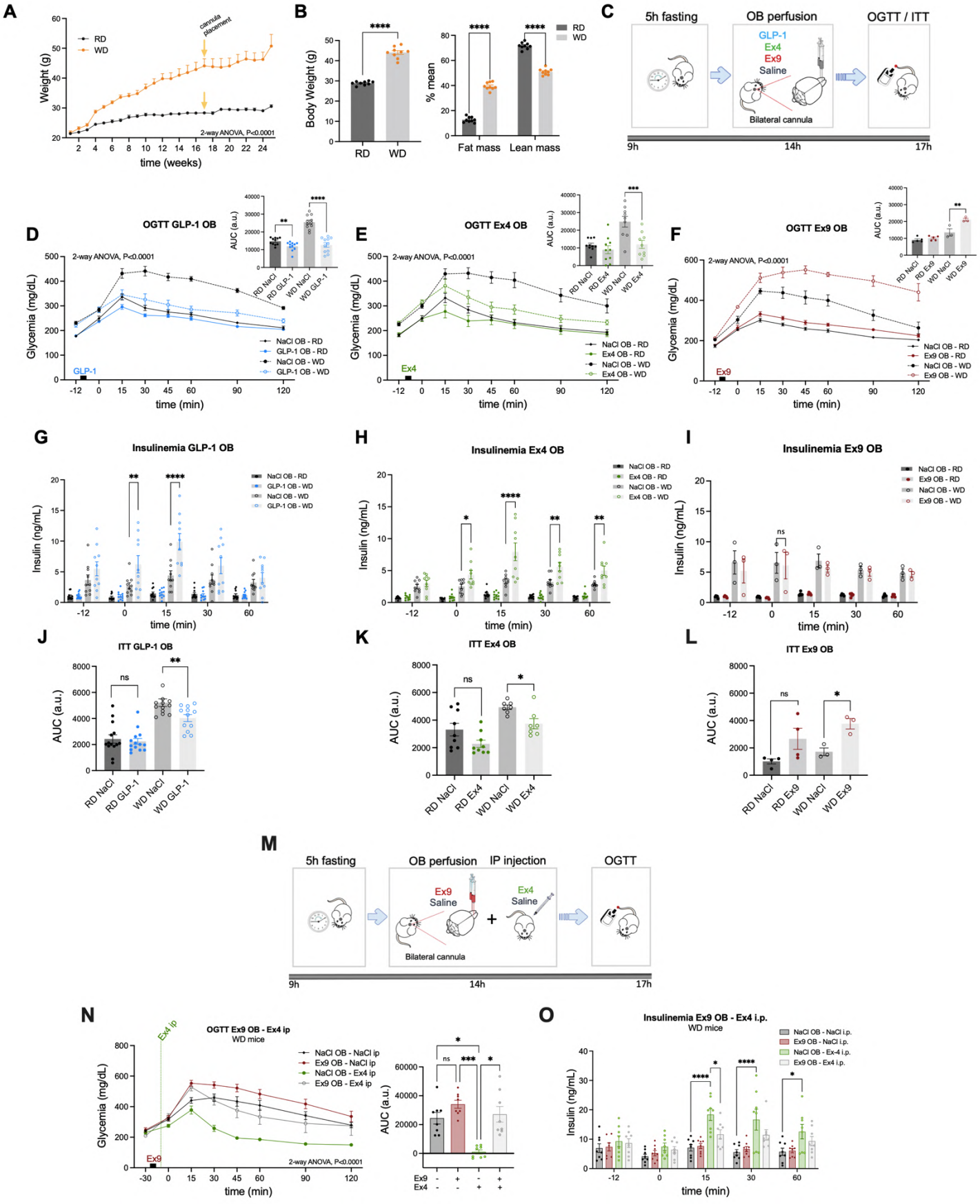

Figure IV.4. Pharmacological modulation of GLP-1R in the OB regulates glucose homeostasis.

Figure caption continued on next page

(A) 25-week weight gain of WD and RD mice (n=9/diet group).
(B) Body weight, fat mass and lean mass of OB-cannulated WD and OB-cannulated RD mice at 16 weeks. Body composition (fat and lean mass) was expressed as a percentage of body weight (n=9/diet group).
(C) Schematic illustration of bilateral OB-injections of GLP-1 (0,5µg/µl), Ex4 (0,5µg/µl) and Ex9 (12,5µg/µl) followed by an OGTT or ITT in OB-cannulated WD and OB-cannulated RD mice.
(D -F) OGTT tests combined with a previous OB injection of GLP-1 (D) Ex4 (E) and Ex9 (F) in OB-cannulated WD and OB-cannulated RD after 20 weeks under WD (two-way ANOVA, n=3-10/drug group). Black squares on X axis indicate drug delivery before the glucose challenge (t0). Right, above: AUC of the metabolic test (paired Student's t test).
(G-I) Plasma insulin levels of OB-cannulated WD and OB-cannulated RD during the respective GLP-1 OB-injected (E) Ex4 OB-injected (H) and Ex9 OB-injected (K) OGTT tests (two-way ANOVA, n=3-10/drug group).
(J-L) AUC of ITT tests combined with a previous OB injection of GLP-1 (D) Ex4 (G) and Ex9 (J) of OB-cannulated WD and OB-cannulated RD after 24 weeks under WD (two-way ANOVA, n=3-9/drug group).
(M) Schematic illustration of the Ex9 OB - Ex4 i.p. pharmacologic strategy followed by an OGTT in OB-cannulated WD and OB-cannulated RD mice.
(N) OGTT test preceded with an OB injection of Ex9 (25 µg/µl) and an i.p. injection of Ex4 (3µg/kg) in OB-cannulated WD after 20 weeks of WD (two-way ANOVA, n=8). The black square and the green line indicate Ex9 and Ex4 delivery, respectively, before the glucose challenge (t0). Right: AUC of the metabolic test (one-way ANOVA).
(O) Plasma insulin levels of OB-cannulated WD during the OGTT test preceded with OB-injected Ex9 and i.p. injected Ex9 (two-way ANOVA, n=8).
Data are given as mean ± SEM. *p <0.05; **p < 0.01; ***p < 0.001; ns, not significant.

5. The activation of GLP-1R in the OB leads to an inhibition of the SNS outflow to the pancreas

To define how the effect of activating the GLP-1R in the OB is transmitted to the pancreas, resulting in the stimulation of insulin secretion, we then focused our work on the study of the neural circuit involved in this mechanism. It has been repetitively described that pancreatic control is under the control of ANS projections, with a inhibitory role of noradrenergic sympathetic nervous system (SNS) as opposed to a stimulating effect of cholinergic parasympathetic nervous system (PNS) (Campfield and Blocker, 1979; Campfield et al., 1984). Total vagotomy was confirmed using fluorogold-tracer injections. Vagotomized mice presented no staining of the DMNX while the sham group express labeling within the DMNX (Figure IV.5A). We started performing OGTT tests on vagotomized RD and WD mice after an Ex4 injection in the OB. The effect of Ex4 on glycaemia after removing the vagus nerve persisted in RD (P_{AUC}=0.0065, Figure IV.5B) and WD mice (P_{AUC}=0.0009, Figure IV.5C), meaning that PNS is not sufficient for explaining the effects on pancreatic insulin secretion due to bulbar GLP-1R activation. We thus assumed that they might mainly be under sympathetic control. We observed that GLP-1R^{OB} stimulation by Ex4 decreased pancreatic noradrenaline levels in both RD and WD group (P=0.0426 and P=0.0411 respectively, Figure IV.5D). Hence, Ex4 in the OB could decrease the sympathetic tone in the pancreas.

It has been reported that stimulation of pancreatic α_2-adrenoceptor (α_2-AR) of β-cells inhibited insulin secretion in mice (Peterhoff et al. 2003) and in humans (Porte and Williams, 1966). Since our hypothesis was that GLP-1R activation in OB leads to decreased noradrenaline in the pancreas hence to decreased activation of α_2-AR, we decided to potentially counteract that inhibition by triggering a pharmacological activation of these receptors. We assessed glucose tolerance and insulin secretion in obese mice over an OGTT after an i.p. administration of UK14304 (or NaCl), an α_2-AR agonist, while Ex4 (or NaCl) was previously injected locally in the OB (Figure IV.5E). Ex4 injection in the OB combined with NaCl i.p. strongly improved glucose tolerance (P<0.0001, Figure IV.5F) as described before (Figure IV.4E). In parallel, insulin secretion was increased in obese mice during the test (Figure IV.5G), accordingly to our previous results from the OGTT run after Ex4 injected in the OB (Figure IV.4H). The activation of α_2-ARs by i.p. injected UK14304, mimicking an increased sympathetic tone, counteracted the enhancing effects of Ex4 in the OB on insulin secretion at t15, t30 and t60 of the OGTT (P_{t15}=0.0157, P_{t30}=0.0009 and P_{t60}=0.0259, Figure IV.5F). The dose of UK14304 injected in combination with NaCl perfusion in the OB on the same WD mice did not have any blocking effect on insulin secretion nor on glucose tolerance (Figure IV.5E and 5F). Overall, these results showed that the activation of GLP-1R in the OB could trigger an inhibition of the SNS in the pancreatic β-cell by the mean of a reduction in noradrenaline contents resulting in a decreased α_2-AR activity.

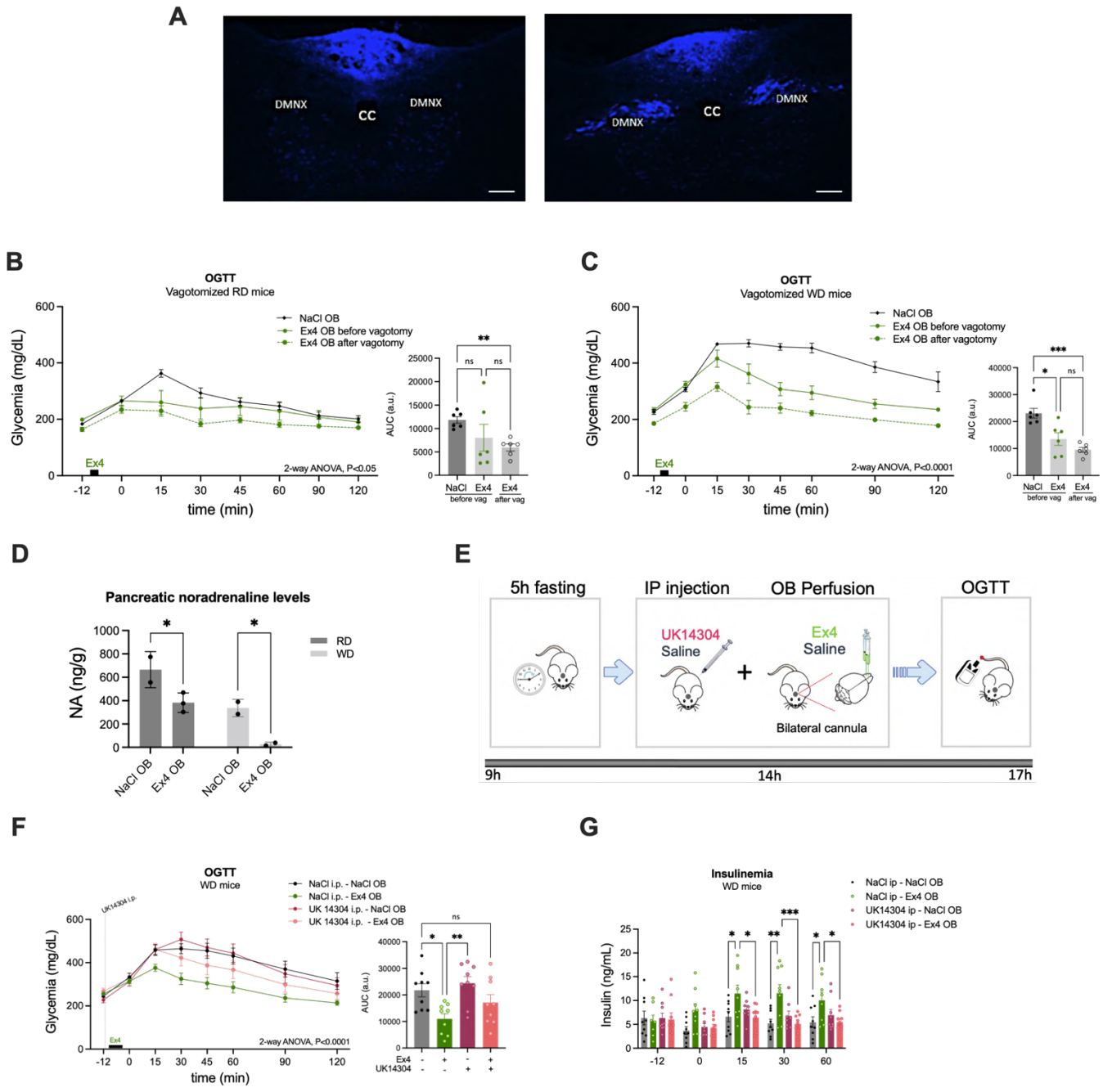

Figure IV.5. The activation of GLP-1R in the OB leads to an inhibition of the SNS outflow to the pancreas

(A) Representative photomicrographs of fluorogold staining in the DMNX. Absence of fluorescence in vagomotized mice (left image) or fluorescence labeling in sham mice (right mice). Images taken in a fluorescence microscope (4x, 8,5s, scale bar = 40 µm). cc: corpus callosum.

(B, C) Left: OGTT tests preceded by a bulbar injection of Ex4 in OB-cannulated RD (B) and OB-cannulated WD mice (C) before and after vagotomy (two-way ANOVA, n=6/diet group). Black squares on X axis indicate Ex4 delivery before the glucose challenge (t0). Right: AUC of the metabolic test (one-way ANOVA).

(D) Pancreatic NA levels of RD and WD mice after Ex4 injection in the OB (n=3/group).

Figure caption continued on next page

(E) Schematic illustration of bilateral Ex4 injections and i.p. administration of UK14304 followed by an OGTT in OB-cannulated WD and OB-cannulated RD mice.
(F) OGTT test preceded with an i.p. injection of UK14304 and an OB injection of Ex4 in OB-cannulated WD after 20 weeks of WD (two-way ANOVA, n=9). The black square and the green line indicate Ex9 and Ex4 delivery, respectively, before the glucose challenge (t0). Right, above: AUC of the metabolic test (one-way ANOVA).
(G) Plasma insulin levels of OB-cannulated WD during the OGTT test preceded with OB-injected Ex4 and i.p. injected UK14304 (two-way ANOVA, n=9).
Data are given as mean ± SEM. *p <0.05; **p < 0.01; ***p < 0.001; ns, not significant.

6. A GABAergic inhibitory relay to the PVN, driven by GLP-1R^{OB} neurons, decreases the sympathetic nerve activity leading to an increase of insulin release from the pancreas in WD mice

Since PVN is the control center of the SNS (Nunn et al., 2011), we next investigated its potential role on the neural pathway involved in the mechanism of action of GLP-1 in the OB. Pre-sympathetic neurons (SPANs) in the PVN, which express $GABA_A$ receptors, are inhibited by a GABAergic input resulting in a reduced SNS activity (Ding et al., 2015). Decreasing the GABAergic tone or inhibiting the $GABA_A$ receptors increases PVN and SNS activity (Kalsbeek et al., 2008).

To ascertain if the decreased sympathetic tone could be explained by the activation of GLP-1R^{OB} neurons, through a GABAergic relay in the PVN, we performed OGTT tests on PVN-cannulated GLP-1R^{OB}hM3Dq WD mice. These mice were generated by OB viral-delivery combined with a cannula placement in the PVN 3 weeks before the tests (Figure IV.6A). An acute injection of Bicuculline, a $GABA_A$ receptor antagonist, was delivered in the PVN of GLP-1R^{OB}hM3Dq WD mice, which also received an i.p. injection of CNO prior to the OGTT to induce GLP-1R^{OB} neurons activation. Control conditions were run under NaCl injections on the same mice (Figure IV.6B). GLP-1R^{OB}hM3Dq WD mice presented glucose intolerance under the control condition (NaCl PVN - NaCl i.p.) (AUC=19112 ± 1095 a.u., Figure IV.6C). Hyperinsulinemia was already remarkable from t-15. Chemogenetic activation of GLP-1R^{OB} neurons combined with NaCl in the PVN strongly improved glucose tolerance (NaCl PVN - NaCl i.p. vs. NaCl PVN - CNO i.p., P<0.0001, Figure IV.6C) and increased insulin secretion at t15 (NaCl PVN - NaCl i.p. vs. NaCl PVN - CNO i.p., P<0.0001, Figure IV.6D) in GLP-1R^{OB}hM3Dq WD mice. When Bicuculline was injected in the PVN combined with NaCl i.p., no changes on glycaemia nor insulinemia were shown compared to the control condition on the same mice. Interestingly, the enhancing response of hM3Dq activation in GLP-1R^{OB} neurons, under the effects of Bicuculline in the PVN, on glucose tolerance and insulin secretion was lost (NaCl PVN

- CNO i.p. vs. Bic PVN - CNO i.p., P_{OGTT}<0.0001 and P_{AUC}=0.001, Figure IV.6C) (NaCl PVN - CNO i.p. vs. Bic PVN - CNO i.p., P=0.0001, Figure IV.6D). We therefore think that the enhancing effect on insulin secretion observed in WD mice, either using a pharmacological approach (Figures IV.4G, 4H) or by chemogenetics, to activate bulbar GLP-1R-expressing cells (Figure IV.1C, 1D), is controlled by a GABAergic inhibitory relay in the PVN via $GABA_A$ receptors which finally decreases the sympathetic nerve activity (Figure IV.5).

cFos quantification of the PVN and PVNd (Figure IV.6E) activity after local injections of exendin-4 or NaCl in the OB of WD mice did not shown any differences between the two conditions. The total cFos signal within the total PVN was very strong in both cases (exendin-4 vs. NaCl) (Figure IV.6F, 6G). Further studies will be thus required to accurately assess cFos within the PVN, targeting exclusively pre-autonomic neurons (c.f. *Discussion, 10.2 PVN activity).*

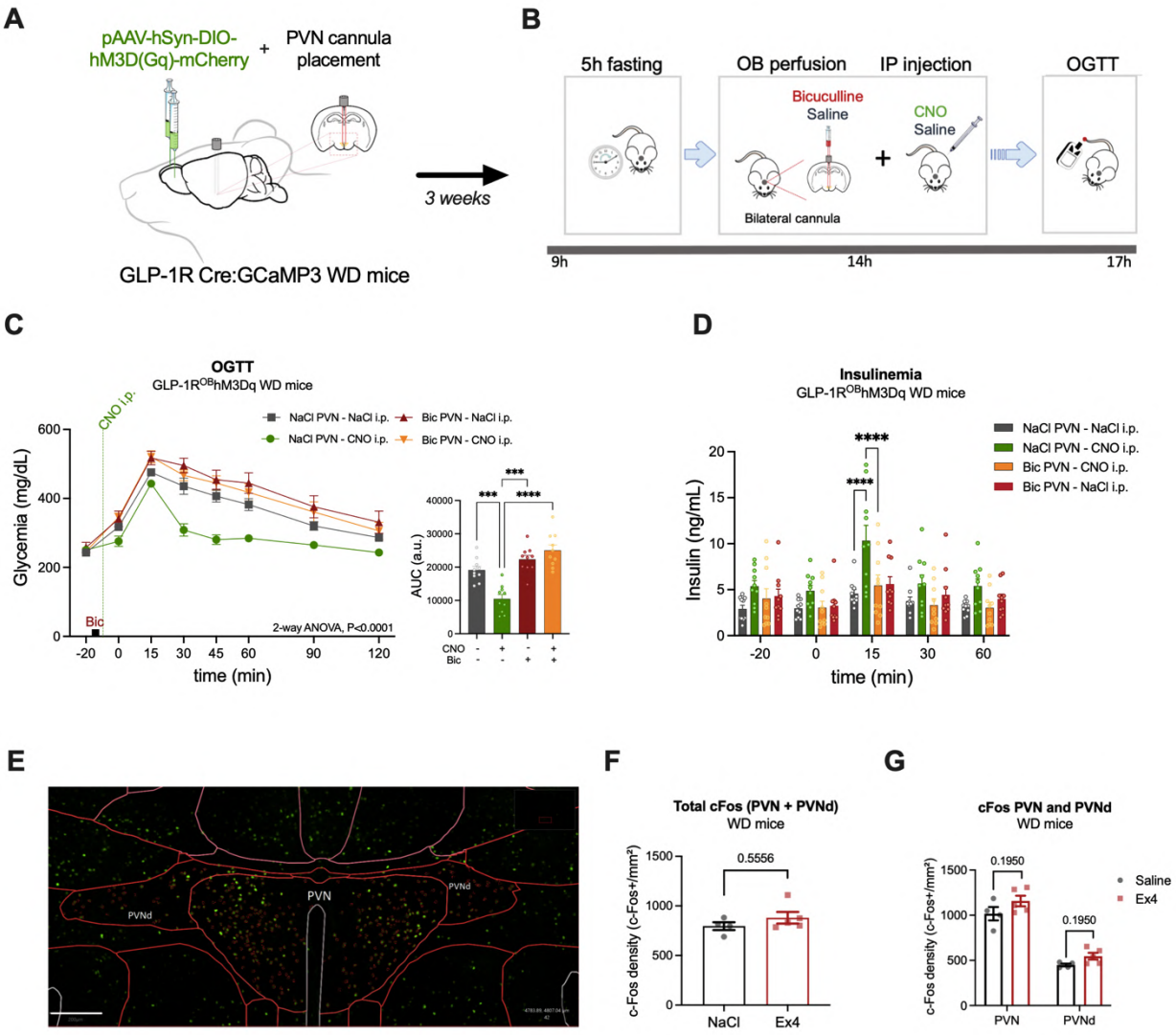

Figure IV.6. A GABAergic inhibitory relay to the PVN, driven by GLP-1R^{OB} neurons, decreases the sympathetic nerve activity leading to an increase of insulin release from the pancreas in WD mice.

Figure caption continued on next page

(A, B) Schematic illustration of viral delivery in the OB and bilateral cannula placement in the PVN of GLP-1RCre:GCaMP3 WD mice followed by the metabolic tests. Scale bar: 200 µm.
(C) Left: OGTT test preceded with an i.p. injection of CNO in GLP-1R^{OB} hM3Dq WD PVN-cannulated mice at 20 weeks under WD (24-week old, two-way ANOVA, n=6/genotype group). The black square and the green line indicate Bicuculline and CNO delivery, respectively, before the glucose challenge (t0). Right: AUC of the metabolic test (one-way ANOVA).
(D) Plasma insulin levels of GLP-1R^{OB}hM3Dq WD PVN-cannulated mice after SALB i.p. injection (two-way ANOVA, n=10).
(E) Representative photomicrographs of cFos immunoreactivity and automated cell counting using ImageJ in the PVN and the PVNd.
(F, G) Total (F) or individual (G) cFos density (cFos+/mm^2) of the PVN and PVNd.
Data are given as mean ± SEM. *p <0.05; **p < 0.01; ***p < 0.001; ns, not significant.
All studies were performed in male mice between 24 and 36 weeks of age.

7. Human brain connectivity under glucose and exendin9 + glucose conditions

7.1. Connectivity of the network across both conditions (Ex9+Glucose and Glucose conditions)

Resting-state MRI images were analyzed for all connectivity patterns possible right after the administration of (intravenous-ex9-39+intragastric (i.g.) glucose) load or the (i.g. glucose) condition alone. All regions of interest (ROIs) were significantly connected to other ROIs in the network, no single or orphan regions were detected (Figure IV.7A). In each structure, different subregions showed high connectivity (red lines within the insula, the OFC and the parahippocampal region). Within the primary olfactory cortex, the frontal piriform cortex (PrF) and olfactory tubercule (TUB) are connected. Anatomofunctional pathways centered on the OFC revealed high connectivity pattern to the ventral striatum, the parahippocampal region, the insula and the PC. While the hypothalamus shows connectivity with the OFC and the ventral striatum, it does not show interactions with the primary olfactory cortex.

Figure 7B zooms on the connectivity of the four ROI in the primary olfactory cortex. The tubercule is mainly connected with the parahippocampal region. The temporal piriform cortex and the AON are connected to the ventral striatum. The analysis also led to the detection of interactions between the frontal piriform cortex (PrF) and respectively the right insula (Ins-R) and the lateral right OFC (Figure IV.7B).

7.2. Differences in connectivity of the network between both conditions Ex9+Glucose versus Glucose condition)

No significant ROIs nor connections were found at the default thresholds specified in Material and Methods to run for multiple comparisons in all regions between the two conditions. 12 subjects is very likely to be a short number to run such a stringent and complex analysis (c.f. *Discussion, 8. Human data*). However, when exploring the results at an uncorrected threshold of $p<0.05$ at both the ROI and connections levels, a number of significant ROIs and connections were found, including the primary olfactory cortex (Figure IV.7C, red line = glucose > glucose + exendin; blue line = glucose < glucose + exendin).

Decreased connectivity between the PrF and the pallidum on one side, and temporal PC (PrT) and the left parahippocampal gyrus (PHG-L) on the other were observed. In contrast, PrF showed higher connectivity to the left globus pallidus (GP-L) and Pr T to the left parahippocampal gyrus. Since no change in hypothalamic connectivity with any of the analyzed ROIs was detected in the MRI analysis, it appears that this structure is completely disengaged from the resting-state network by the Ex9 injection.

Ex9 injection resulted in the decrease in contralateral OFC regions connectivity, between the left lateral fronto-orbital gyrus (OFC-lateral-L) and the right gyrus rectus (OFC-rect-R), and the left / right gyrus rectus. In contrast, left gyrus rectus is further connected to left globus pallidus. In addition, decreased connectivity is present between the left hippocampus and left parahippocampal gyrus.

Taken together, our MRI study showed a plasticity in the limbic to basal ganglia connectivity in response to acute metabolic changes. In addition, connectivity within and throughout the OFC and the primary olfactory cortex is modified in the Ex9+glucose condition versus glucose load alone. In particular, antagonizing GLP-1 receptors changed the pattern of connectivity of the piriform cortex. Most importantly, the primary olfactory cortex to hypothalamus connectivity is not detected in either condition thus is not influenced by the Ex9 peripheral injection over glucose load. NB: these results should, however, be interpreted with maximal caution since no multiple testing correction was applied, and should therefore be regarded as hypothesis-generating, requiring confirmation in follow-up studies, ideally with a larger sample size.

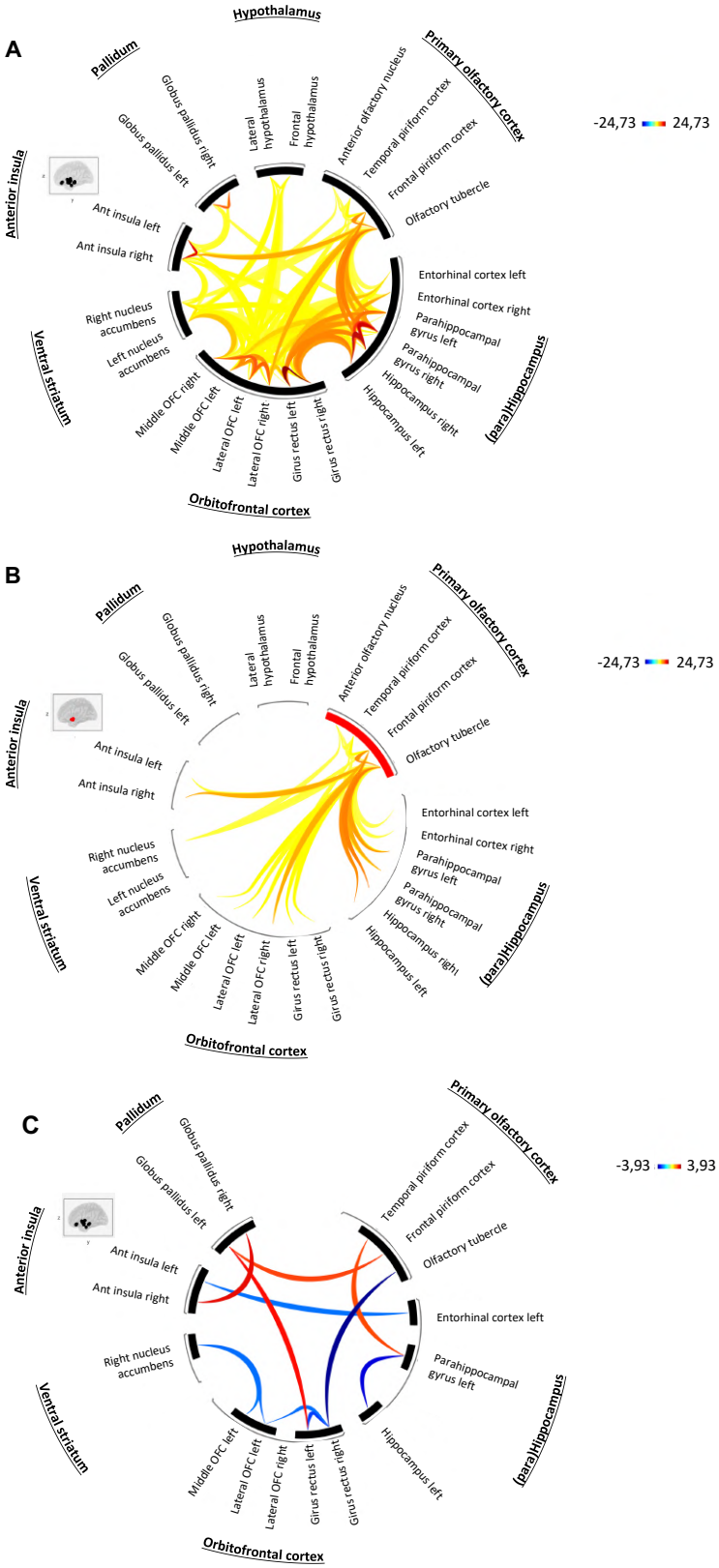

Figure IV.7. Human brain connectivity under glucose and exendin9+glucose conditions.

(A) Connectivity schematics of the brain networks across both conditions in healthy subjects (Ex9+Glucose and Glucose conditions).

(B) Zooms on the connectivity of the four ROI in the primary olfactory cortex in healthy subjects.

Figure caption continued on next page

(C) Connectivity explored at an uncorrected threshold of $p<0.05$ at both the ROI and connections levels in healthy subjects.

Middle OFC right: middle fronto-orbital gyrus right; Middle OFC left: middle fronto-orbital gyrus left; lateral OFC left: lateral fronto-orbital gyrus left; latetal OFC right: lateral fronto-orbital gyrus right.

SECTION V

Discussion

Discussion

In this section we will discuss the contribution of our results in the understanding of the modulation of energy balance by central GLP-1 circuits, and we will define a functional model illustrating the mechanisms and implications of bulbar GLP-1 on the regulation of energy balance and feeding behavior, in physiological and pathological conditions. Finally, I will examine some methodological aspects associated with our experimental protocols and propose various perspectives for future work.

1. Function of GLP-1/GLP-1R system in the OB

Glucagon-like peptide 1 originates within two separate locations in the mammalian body: intestinal L cells and central PPG neurons, from the NTS (major brain source), the OB, the PC, and the lumbar-sacral spinal cord. The study of Thiebaud et al. in 2016 was the first to show neuromodulation of MC by GLP-1 in the OB. However, before our work, no role in energy homeostasis regulation has been described for bulbar GLP-1. In Thiebaud's study, PPG neurons were identified using PPG-YFP transgenic mice in the granular cell layer (Thiebaud et al., 2016), and they were speculated to be responsible for releasing GLP-1 within the OB since they express the precursor of GLP-1 (Thiebaud et al., 2019). We reproduced the same YFP staining marker and our results support and confirm the identification of PPG cells demonstrated in 2016 (Figure IV.1A). However, are PPG neurons in the OB really responsible for local processing of GLP-1 in health and obesity? The question is not yet answered but data in favor of this possibility are:

i) Diphtheria toxin gene A (DTA) ablation of PPG neurons in the NTS confirmed that this cell population is the main source of GLP-1 in the brain, since active GLP-1 levels were dramatically reduced in several PPG^{NTS}-projecting brain regions after the ablation (Holt et al., 2019). Interestingly, $GLP\text{-}1^{OB}$ content was not affected by DTA ablation. This result gives particular importance to the local role of PPG^{OB} cells as the source of the remaining-intact GLP-1 content within this structure after PPG^{NTS} ablation, and is consistent with our preliminary data suggesting the existence of GLP-1 producing cells in the OB.

ii) Here we provide a very first proof for the existence of GLP-1-releasing cells in the OB since our encouraging preliminary data suggest an increase of total GLP-1 content after KCl stimulation on OB slices from RD mice (Figure IV.1 B). A previous study has reported lower amounts of GLP-1 in the OB in mice (Holt et al., 2019). However, experimental conditions were different than ours since the latter dosage was assessed for only active (i.e. still not inactivated by DPP-IV) GLP-1 levels, in *ad libitum*-fed mice and under basal conditions.

iii) Our results from RT-PCR show that the OB presents the enzymatic machinery required for the local processing of the GLP-1: Not only mRNAs coding for the GLP-1R are expressed, but also those for the pro-convertase PC1/3 and the enzyme DPP-IV. The GLP-1 system within the OB can thus be considered independent from the NTS. Interestingly, both PC1/3 and DPP-IV mRNAs are more expressed in WD mice compared to RD mice (Figure IV.1E), which lead us to think that bulbar GLP-1 release could occur in response to KCl in WD mice, stronger than the one seen in RD mice (Figure IV.1B) (also see *10.4. Further properties of PPG cells*).

In the brain, the GLP-1R is widely expressed in different regions including the OB, in both the mRNA-expression level (in rats, Merchenthaler et al., 1999) and the protein-expression level (in mice, Thiebaud et al., 2006). On the one hand, and in line with the first study, we demonstrate the presence of GLP-1R mRNA by RT-PCR in the OB of RD and WD mice. On the other hand, consistent with Thiebaud et al., we demonstrate the presence of the GLP-1R in the MCL and GCL by the use of a probe (fluorescent exendin-4) stimulating the receptor activation. The fact that the GLP-1R is mainly localized in MC, the first order neurons within the OB and the only ones projecting to higher brain regions, anatomically supports the GLP-1R-driven network connecting bulbar GLP-1R-positive cells with pancreatic β-cells (the network will be further discussed later).

2. Preprandial regulation of glucose homeostasis. The role of the bulbar GLP-1R in odor-evoked CPIR

As we have seen in the introduction, the literature suggests that there is a strong and bilateral link between the olfactory system and the endocrine system in relation to energy balance, and highlights the importance of olfaction in feeding behavior (Palouzier-Paulignan et al., 2012; Faour et al., 2022). During the preprandial phase, food odors can trigger hormonal responses anticipating the upcoming meal (i.e. avoiding exaggeration in prandial blood glucose), such as the cephalic phase of insulin secretion. A CPIR induced by gustatory/oral sensory signals (Berthoud et al., 1980) or sham-feeding (Berthoud and Jeanrenaud, 1982) has been recognized in rats. In the latter, sham-feeding (mimicking normal ingestion of food but without digesting neither

absorbing it) was assessed by inserting a tube into the esophagus or the stomach, that leaks out anything that is swallowed. However, if we consider that as soon as food is in the mouth, the phase is not cephalic anymore, a more restrictive protocol only including techniques that use non-ingestive stimuli is required. To our knowledge, food-related olfactory signals have never been assessed during the CPIR in rodents before our work. Here we demonstrate for the first time a (palatable) food odor-evoked CPIR in RD mice. Additionally, we have shown that the injection of Ex9 in the OB completely blocks CPIR in RD mice, suggesting that bulbar GLP-1R is involved in the cephalic phase of insulin secretion. The GLP-1 system in the OB is also likely to be activated by food odors.

To go a step further, we wanted to include a second study factor, obesity, and whether the disease disrupts cephalic insulin responses induced by palatable food odors. Interestingly, odor-evoked CPIR is lost in WD mice. This is consistent with a new work showing that CPIR is impaired in visually stimulated DIO mice (2-week-HFD) (Wiedemann et al., 2022). Also, the injection of Ex4 in the OB seems to be a potential tool for restoring the loss of odor-evoked CPIR (Figure IV.2D), again emphasizing the importance of the GLP-1 pathway in the OB as a mediator of this cephalic effect.

In regard to olfactory capacities, there is evidence that obesity triggers olfactory disruption. Fadool's team demonstrated in 2014 that a HFD triggers a reduction of olfactory discrimination in mice (Thiebaud et al., 2014), which is consistent with our findings demonstrating a poor olfactory detection in WD mice during a buried food-seeking test (Figure IV.H) and as also shown in my co-first author article (Soleimanzad, Montaner et al., 2021).

Concerning olfactory capacities and contrary to WD mice, RD mice present optimal foraging time, reflecting normal olfactory performances (Figure IV.2I). The time they spend seeking a palatable piece of food after an overnight fasting is consistent with previous work showing optimal olfaction during a BFT: less than a minute of latency (Jamain et al., 2008; Mortreux et al., 2019). In fact, presenting food odors in fasted rats results in a strong awakening effect (Gervais and Pager, 1979, 1982) and increased exploration time (Prud'Homme et al., 2009). Remarkably, bulbar Ex9 increases the foraging time in RD mice, mimicking the olfactory impairment shown in WD mice. Moreover, an i.p. injected -and non-hypoglycaemic- insulin dose reverses this deleterious effect of Ex9 on olfactory foraging in RD mice (Figure IV.2I). This last result suggests that insulin, within the preprandial state, can amplify olfactory sensitivity. Thus, the cephalic secretion of insulin by the pancreas may, in return to the olfactory system, facilitate foraging activity, by acting potentially within the OB (Figure V.1). Another study has shown that i.c.v. injected insulin in fasted rats, causes a decrease of olfactory detection to the level of satiated rats (Aimé et al., 2007). This last study may at first sight look opposite to our results, but it should be noted that the administration route is different, and that the high dose of insulin used was equivalent to that found in a postprandial state (satiation following a meal), whereas our low dose

corresponds to that found on preprandial levels, in which insulin is known to act as an orexigenic signal.

Within the timing of this thesis, we were not able to determine the precise bulbar GLP-1R-mediated network triggering odor-evoked CPIR. However, there is evidence that CPIR is neuronally mediated by the vagus nerve through Ach release on pancreatic β cells (Louis-Sylvestre, 1978). Thus, it is likely that the vagus nerve induces the odor-evoked cephalic insulin response shown in our work. However, to date, it is impossible to exclude that a decrease of the sympathetic tone would explain the CPIR. Indeed, a study in humans demonstrates that the CPIR is dependent on both cholinergic and noncholinergic mechanisms (Ahrén and Holst, 2001). Further studies will thus be needed to accurately determine the exact neuronal network sustaining the GLP-1R^{OB}-mediated odor-evoked CPIR, including viral tracing or surgical/pharmacological approaches such as vagotomy or muscarinic receptor blockade.

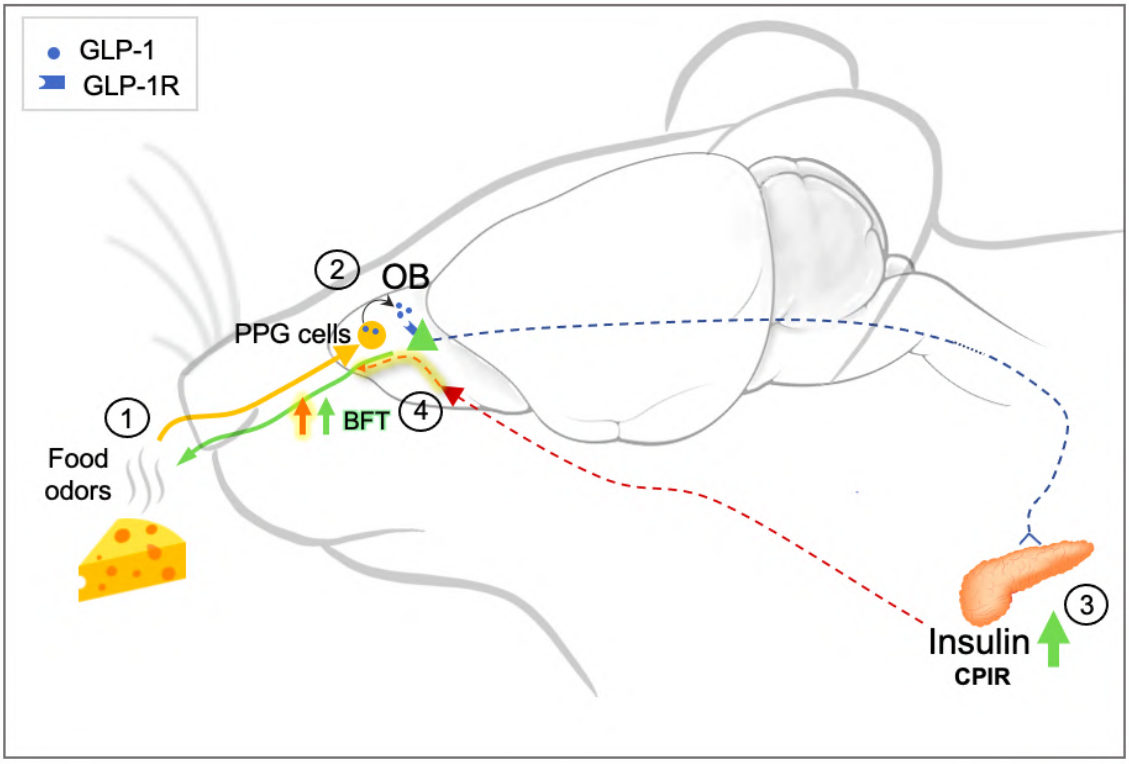

Figure V.1. Schematic illustration of the hypothetical circuits involving odor-evoked CPIR in foraging activity. (1) PPG cells (yellow circle) may release GLP-1 within the OB (2) (onto GLP-1R-expressing MC, green triangle) in response to palatable food odors, which, subsequently, induces CPIR (3). In turn, insulin released during the cephalic phase may reach the OB (red dotted arrow) and reinforce OB activity (4), potentially emphasizing foraging (green arrow) during the preprandial phase (orange dotted arrow).

3. Preprandial regulation of glucose homeostasis. Can PPG cells in the OB mediate odor-evoked CPIR ?

As previously seen, the injection of Ex9 in the OB completely blocks CPIR in RD mice. This result strongly suggests a role of GLP-1-releasing cells in the OB during CPIR. In a condition where there is no ingestion of food, no GLP-1 can be secreted from the gut. The main source of GLP-1 in the bulb can thus only be local. I have used gene silencing methods in the laboratory of our collaborator Stefan Trapp at UCL in order to knock down PPG cells, and so GLP-1 production, in the OB of RD mice. The results indicate that the silencing of PPG neurons hampers odor-evoked CPIR: to our knowledge, this is the first demonstration of the importance of GLP-1 produced in the OB for premeal episodes of insulin release in healthy RD mice.

Different specific roles for PPG cells in the NTS have been described, such as a modulation of heart rate (Holt et al., 2020), a control of stress-induced hypophagia and a limitation of extraordinary large intakes of food (Holt et al., 2019), but none of them has been shown as being involved in cephalic phase responses. Along with the Ex9 result, we suggest here that presynaptic PPG neurons in the OB can be stimulated by palatable food odors and, in response, release GLP-1 and mediate odor-evoked CPIR in a postsynaptic GLP-1R-signaling manner. Together, these roles of PPG-derived GLP-1 in the OB are consistent with the idea that its local release in specific regions determines its final neuropeptidergic function (Trapp and Brierley, 2022).

In the present study, we prove an involvement of the bulbar GLP-1 system in the cephalic phase of insulin secretion induced by food odor stimuli. In the last decades, other premeal anticipatory responses have been deeply studied such as CCK or glucagon responses. In one article, a cephalic phase of GLP-1 has also been described as being meal-anticipatory in meal-fed rats. However, this early response has been shown to be completely independent and at odds with preprandial changes in insulin since the early increase starts more than one hour before the scheduled meal (Vahl et al., 2010). It is thus unlikely that this cephalic GLP-1 could interfere with our bulbar GLP-1-mediated effect on odor-evoked CPIR.

4. Food intake modulation by GLP-1R+ neurons in the OB

Centrally administered GLP-1 suppresses food intake (Müller et al., 2019). Classic homeostatic control regions are located in the hypothalamus, such as the ARC or the PVN, structures that express the GLP-1R. This leads to think that the hypothalamus could individually control the effects of GLP-1RA on feeding and weight loss, but Burmeister et al. discarded this idea, since hypothalamic GLP-1R KO mice fed on a high-fat diet exhibited normal food intake, and present no anorectic effects of systemic administered GLP-1RA (Burmeister et al., 2017).

In the brain, PPG^{NTS} neurons are the main source of central GLP-1, but not necessary for the control of daily food intake. They play, in contrast, a role during large intakes of food (Holt

et al., 2019), what can be interesting in the context of obesity since obese people tend to eat larger -and more palatable- meals. Nonetheless, PPG^{NTS} neurons are not required for the anorectic effects of liraglutide and semaglutide (Brierley et al., 2021). Interestingly, our work demonstrates that chemogenetic activation of GLP-1R-positive cells in the OB in WD mice reduces acute food intake after an overnight fasting, while chemogenetic inhibition of GLP-1R-positive cells in RD mice increases it (Figure IV.3D, 3E). Thus, this last piece of work is perfectly complementary to the data published before, and adds a new scope for revealing the precise mechanism of central GLP-1 in suppressing eating.

5. Postprandial regulation of glucose homeostasis. Can circulating GLP-1 reach the OB?

Once the ingestion of food has begun, the process of digestion starts to break down carbohydrates. Glucose reaches the intestinal lumen and is sensed by L cells, which start secreting GLP-1 to the bloodstream. Circulating GLP-1 levels thus increase in a glucose-dependent manner and, maybe, reach brain structures with highly permeable capillaries such as the OB. This is thought to be unlikely given the quick inactivation of GLP-1 by DPP-IV (Trapp and Brierley, 2022).

Radiolabeled GLP-1, administered in periphery at pharmacological doses, was detected in leaky BBB regions such as CVOs (Orskov et al., 1996). However, postprandial increase in endogenous active GLP-1 was only detected in the hepatic portal vein but not in the systemic circulation in rats (Punjabi et al., 2014). Even if this is evidence suggesting that only pharmacological (and DPP-IV resistant) but not physiologically released (and DPP-IV sensible) doses of GLP-1 reach the CNS, we wanted to reconsider this assessment and exclude the remote possibility that peripheral GLP-1 could be found in the OB. In collaboration with Stefan Trapp, we i.p. injected a DPP-IV-resistant GLP-1R antagonist, luxendin 645, in mice. Luxendin 645 labeled several brain structures such as the AP and the NTS, two regions known as densely expressing GLP-1R, but did not label any GLP-1R-expressing cells in the OB (Figure IV.1G), meaning that even at pharmacological doses, the bulb remains unreachable. This result also reinforces the PPG cell as the main source of GLP-1 in the OB. In fact, throughout an IPGTT, thus bypassing the gastrointestinal secretion of GLP-1, acute activation of bulbar GLP-1R improves glucose tolerance and insulin secretion in obese mice (data not shown). Even if no gut-derived GLP-1 is present in this situation, we can still see the improvement of the metabolic profile in obesity. Additionally, local injections of exendin-9 in the OB of obese mice worsen glucose tolerance and insulin sensitivity, during OGTT and ITT respectively (Figure IV.4F, 4L). This is consistent with the results obtained during preprandial odor-induced CPIR: when exendin-9 is injected in lean mice, glycaemia levels are increased (before vs. after odor presentation) (Figure IV.2C, AUC insert). Since the effects of this GLP-1R antagonist depends on relative

concentration of the ligand GLP-1 within the OB, and i.p. injected luxendin 645 does not reach the bulb (so circulating GLP-1 has even fewer chance to get into it), it is very probable that an on-going (tonic) PPG cell-release of GLP-1 locally in the OB exists, not only in the preprandial phase but also on postprandial.

Whether PPG neurons could be sensitive to glucose following a meal and thus bulbar GLP-1 levels be modulated in a nutritional state-dependent manner is unknown (c.f. *10.4. Further properties of PPG cells*). The present study demonstrates a role of PPG-derived GLP-1 on glucose homeostasis directly in the preprandial phase and indirectly in the postprandial state.

6. Postprandial regulation of glucose homeostasis by GLP-1OB and the effect on insulin secretion.

One of the main complications of obesity is insulin resistance which favors the emergence of T2D and cardiovascular diseases. Numerous studies have been conducted to understand the link between obesity and insulin resistance, and assessed the role of the incretin system in T2D, mainly focusing on pancreatic β cells (Holst, 2007) and less on the CNS. The role of hypothalamic GLP-1R on glucose homeostasis has been shown to be individually unnecessary (Burmeister et al., 2016) and thus other CNS sites are required for the control of energy balance via GLP-1R signaling. Interestingly, arcuate NPY/AgRP and POMC neurons are known to be modulated by sensory systems (Chen et al., 2015) suggesting a role for the olfactory system. Our present study shows for the first time a role of GLP-1R in the OB on glucose homeostasis. Pharmacological activation of bulbar GLP-1R increases glucose-induced insulin secretion and insulin sensitivity in obese mice, thus improving drastically its glucose homeostasis. This is consistent with our chemogenetic approach, in which GLP-1R-positive cells in the OB are activated. Both approaches converge in a strong increase of insulin secretion at t15 of the OGTT and decreased AUC. This higher insulin secretory responses are coherent with the incretin role of GLP-1 and restore the reduced incretin effect seen in T2D. The latest work from Debra A. Fadool's lab (Kolling et al., 2022) shows that CRISPR gene-editing of Kv1.3, targeting the loss of these inhibitory channels in M/TC, enhances its excitability and improves metabolic health (including OGTT). Conversely, chemogenetic decrease of M/TC excitability in the OB worsens odor discrimination ability and lead to an obesogenic profile. In the present study, we have shown that pharmacological blockade of GLP-1R by Ex9 in the OB worsens glucose homeostasis (Figure IV.4F). Overall, it is thus likely that GLP-1 signaling in the OB, which increases mitral cell excitability through inhibition of Kv1.3 channels (Thiebaud et al., 2016), is a molecular mediator of the metabolic improvements shown in periphery, especially the increased insulin secretion. Reinforcing this idea, the potentiating effect on insulin secretion of systemic activation of GLP-1Rs by Ex4 is surprisingly attenuated by the blockade of GLP-1R in the OB (Figure IV.4O). Thus, the well-known effect of

the GLP-1RA Ex4 requires activation of GLP-1R in the OB. These results allow us to establish a strong link between the olfactory system and glucose homeostasis in the context of obesity.

7. How are the effects of bulbar GLP-1 transmitted to the pancreas, leading to the stimulation of insulin secretion? Which neuronal pathway could be involved?

7.1. Decrease in sympathetic nerve activity

Since the ANS modulates pancreatic hormone secretion through the PNS and the SNS in an opposite (PNS up and SNS down) manner (Campfield and Blocker, 1979), and we have shown that the PNS was not sufficient for explaining the effects on insulin release after bulbar GLP-1R activation (vagotomy data, Figure IV.5B, 5C), we hypothesize a relay exerted mainly by the sympathetic nervous system (SNS). The simulation of SNS activation via a pancreatic α_2 adrenergic receptor agonist (UK14304), counteracts the effects of Ex4 in the OB on glucose tolerance and insulin secretion (Figure IV5F, 5G). This reinforces the idea that bulbar GLP-1R activation results in SNS inhibition to the pancreas and is consistent with previous work showing that SNS activation inhibits insulin secretion via the α_2-AR through a release of noradrenaline (Ahrén, 2000).

A connection between the olfactory system and the periphery through the SNS has already been proposed in 2017 by Riera et al. In that study, they suggested that a reduction in the olfactory input stimulates SNS activity (DTA-ablated OSN, Riera et al., 2017), resulting in an increase of circulating noradrenaline (the main neurotransmitter of the SNS) and improved metabolic health (reduction of fat mass and insulin resistance). Conversely, in the present work, we show that the content of noradrenaline decreases after bulbar GLP-1R activation, suggesting a reduction of the SNS tone leading to a similar improving result on metabolic health (improved insulin secretion and insulin resistance). Is SNS activity then increased (Riera et al.) or decreased (our work)? This discrepancy can be explained by i) our mice were in a fasted state, rather corresponding to an increased olfactory sensitivity than the opposite, ii) even if in the context of obesity mice present an impaired olfactory function (thus leading to a potential reduction of the olfactory input as shown in Riera's work), the activation of GLP-1R improves olfactory performances in WD mice, restoring its capacities to the level of RD mice. It is thus likely that our mice present an optimal olfactory input after activating (either pharmacologically or chemogenetically) GLP-1 signaling in the OB and, in turn, an effect mediated via a decreased SNS activity is prioritized.

Large zinc lesions of the OM have repetitively shown that killing OSN results in mice with depressive phenotype (Liu et al., 2020; Ahn et al., 2018). The same neuroanatomical areas are dysfunctional in depressive vs anosmic organisms (Price and Drevets, 2012) and depression

is usually accompanied by changes in food motivated behavior, which could result in weight loss. Thus, Riera's conclusion can't be fully accepted since no test was performed to assess motivation, attention and hedonics in these DTA-OSN mice which are resistant to obesity. On the contrary, Fadool's lab has shown in several articles that upregulated activity of MC by impaired Kv1.3 such as "super smeller mice" is responsible for obesity resistance. We are convinced that disconnecting/lesioning the olfactory system from its limbic connections, including hippocampus, amygdala and hypothalamus, have such severe effects on rodent behavior that it must be used cautiously as a model to assess the link between olfaction and energy homeostasis.

7.2. Decrease in PVN neuronal activity

In the present study, we determined that the sympathetic activity inhibition mediated by bulbar GLP-1R activation is mediated by a decrease in the neuronal activities of the PVN, the control center of the SNS. The PVN harbors pancreas-dedicated pre-autonomic neurons that control pancreatic SNS activity (i.e. responsible for insulin release). These pre-autonomic neurons in the PVN (SPANs) can be controlled by inhibitory inputs. Using local administration of a $GABA_A$ receptor antagonist (bicuculline) in the PVN we demonstrated that the SNS inhibition, and thus, the increased insulin secretion after chemogenetic activation of GLP-1R-expressing cells, was controlled by a GABAergic inhibition of SPANs. Indeed, when Bicuculline was injected in the PVN combined with NaCl i.p., no changes on glycaemia nor insulinemia were shown compared to the control condition in GLP-$1R^{OB}$hM3Dq mice (Figure IV.6C). This is consistent with previous studies providing evidence for a hypothalamic control of the sympathetic pre-autonomic neurons in the PVN (Kalsbeek et al., 2004) by using the same $GABA_A$ receptor antagonist (Kalsbeek et al., 2008). In addition, the same team has shown a rise in blood glucose levels (i.e. hyperglycaemia) induced by i.c.v. administration of bicuculline in rats (Kalsbeek et al., 2006). However, they suggested that the hyperglycaemic state had hepatic origins, without mentioning any pancreatic involvement. This goes in the same direction as an early study in which it has been shown, by an euglycemic clamp, that the bicuculline-induced hyperglycaemia was due to increased HGP (Lang, 1995). Nevertheless, all these studies were, to a greater or lesser extent, focused on circadian control of metabolic parameters. Since our study is not based on daily rhythms of plasma glucose levels but an acute incretin-mediated effect within a precise time (after meal ingestion), it is thus plausible that in our study SNS-mediated pancreatic insulin release is solicited in a specific postabsorptive situation. Conformingly to our data, evidence exists for an increased GSIS related to a decreased sympathetic tone in HFD rats (Cruciani-Guglielmacci et al., 2005).

The next question is: where does the GABAergic input controlling pre-autonomic neurons activity in the PVN comes from? In our chemogenetic model, using anterograde viral

tracing techniques, we observed no MC projections to the PVN, supporting the idea of a polysynaptic connection between the GLP-1R-positive MC and SPANs within the hypothalamic nuclei. This is anatomically consistent with the early work of Price et al. in 1991, in which they showed no olfactory projections from the PC to the PVN but only to the lateral hypothalamic area (Price et al., 1991). Indeed, viral-labeled projections were shown in the piriform cortex suggesting a potential relay within the primary olfactory cortex (data not shown). A previous study has shown that GABAergic neurons within the LHA project to the PVN, triggering an increase of feeding in mice. In the study, the application of bicuculline confirmed the nature of $GABA_A$ receptor-mediated currents by electrophysiological recordings in brain slices (Wu et al., 2015). These results support the existence of the plausible network OB → PC → LHA → PVN. Additionally, it is also known that GABAergic neurons controlling SPANs activity can be located in the peri-PVN region (Herman et al., 2002) or the suprachiasmatic nucleus (SCN) (Kalsbeek A., et al., 2008). However, to our knowledge, no study has demonstrated which location -whether LHA, peri-PVN, SCN or another- is the main controller of pancreas-dedicated pre-autonomic neurons triggering GSIS modulation in the context of obesity. We are currently running retrograde tracing by injecting the neuronal tracer Fluorogold in the PVN of WD mice to further analyze the source of the GABAergic projections to the PVN in the context of obesity. This procedure is being done by our collaborator Marie Holt from Stefan Trapp's laboratory (UCL). Since the exploration of the network OB→PC→"GABAergic region" also requires further clarifications, additional analysis will be a prerequisite to entirely determine the neuronal network connecting GLP-1R-positive MC within the OB to $GABA_A$-expressing SPANs in the PVN in a postprandial condition (c.f. *10.1. OB to PVN circuits*). Whether the GLP-1 system in the preprandial phase is based on the same mechanism as the one considered for the postprandial condition is an open question and will require further investigation.

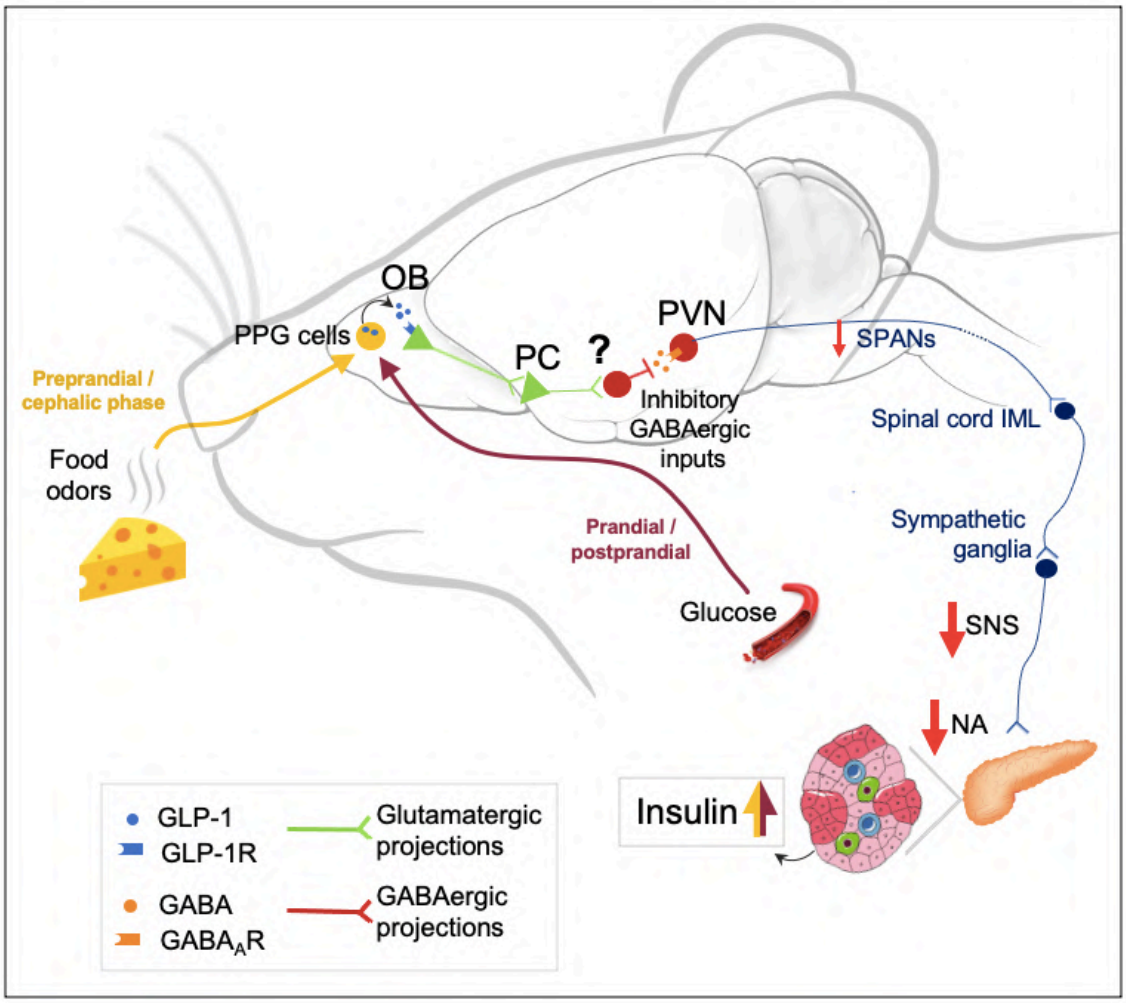

Figure V.2. Olfactory bulb-to-β cell circuit modulates insulin secretion: graphical abstract. In the preprandial state, PPG cells (yellow circle) may release GLP-1 to GLP-1R-expressing MC (green triangle) in response to palatable food odors, which, subsequently, induces CPIR. In the postprandial state, when blood glucose levels are high (dark red arrow), GLP-1 released within the OB by PPG cells might modulate GSIS through the following neuronal circuit: OB → PC → "GABAergic region" → PVN → SNS. Whether PPG cells are sensible to glucose, as well as the "GABAergic region" is still unknown. For further details, see text. PPG: preproglucagon; OB: olfactory bulb; PC: cortex piriform; PVN: paraventricular nucleus; SPANs: spinally projecting autonomic neurons; IML: intermediolateral nucleus; SNS: sympathetic nervous system; NA: noradrenaline.

8. Human brain connectivity under glucose and exendin9 + glucose conditions

In the MRI study run by our collaborators Anne Christin Meyer-Gerspach and analyzed by Pr. Lucas Van Oudenhove (Meyer-Gerspach et al., 2018), major brain systems were shown to be connected in the resting state: as expected, hedonic (ventral striatum, insula, orbitofrontal cortex), limbic (hypothalamus, hippocampus, amygdala, insula, orbitofrontal cortex) and olfactory (piriform cortex, olfactory tubercle, anterior olfactory nucleus) areas have dynamic bilateral relationships (Figure IV.7B, 7C). First, we would like to underlie the fact that a multiple statistical comparison did not reveal significant changes in the "glucose" compared to "glucose+Ex9" connectivity patterns. Thus, we decided to be very cautious in our description.

Taken the rough connectome by a voxel-to-voxel comparison, it was disappointing to observe that PC was not connected to the hypothalamus in neither glucose nor glucose+Ex9 condition. In fact, none of the primary olfactory cortex structures were found to be connected to the hypothalamus. Thus, logically, Ex9 cannot be a regulating factor of this PC-hypothalamus interaction in the 12 healthy and young subjects. In fact, Ex9 seems to remove the hypothalamus from the resting state network activity, a result which might be interesting to consider in the context of incretin treatments. However, of crucial importance, there is a main issue with the hypothalamus in MRI since individual nuclei are too small to be individualized by the image processing, thus, published data concern the entire structure and false negative results could happen.

Ex9+glucose condition triggers increased temporal PC to the left parahippocampal region connectivity which, in turn, is inhibited in its link with the left hippocampus. Interestingly, the reduced left hippocampus activity was shown by Zhang et al., 2019 to be a significant correlate in response to odors (BOLD-fMRI, no resting state analysis) in obese subjects with diabetes compared to healthy controls, and is restored by GLP-1R agonists. This is in line with a recent study that shows the much stronger activation of the hippocampus by odors compared to other senses (Zhou et al., 2021). As compared to the RSN literature in obese patients, we could also observe in our RSN analysis the implication of frontal (García-García et al., 2015) and ventral striatum (Marqués-Iturria et al., 2015) connectivity in Ex9-induced changes. As a conclusion on this preliminary fMRI study, we propose that these analyses could be considered as a very first encouraging step to further explore the functional connectome of the primary olfactory cortex in humans under different nutritional/pharmacological states.

9. Methodological considerations

9.1. "up and down" GLP-1R modulation strategy

RD mice presented a healthy metabolic profile, whereas WD mice were obese and suffered from several metabolic disturbances such as fat accumulation or insulin resistance. Since the GLP-1 system is present in the OB, we found it coherent to use GLP-1 pharmacology on WD mice for our behavioral olfactory tests, to see whether we could improve its olfactory performances. Under the same reasoning, as RD mice present optimal metabolic function, we decided that it was more realistic to treat them with exendin-9, in order to challenge their metabolic/olfactory system in the opposite direction: through a worsening.

Next, for the metabolic tests under chemogenetic regulation of bulbar GLP-1R-expressing cells, we continued with the same reasoning. We used an inhibitory DREADD (KORD) in RD mice, and an excitatory DREADD (hM3Gq) in WD mice for assessing food intake and glucose tolerance.

However, as you could have noticed, for the metabolic tests under pharmacological regulation of GLP-1R, we injected either exendin-4 or exendin-9 in WD or RD mice. At that point, what was the purpose of testing exendin-4 in RD mice since, as said, they already present an optimal metabolic profile? And why Ex9 in WD mice? The study of the GLP-1 system in the OB in the context of obesity is an open field. On the one hand, one explanation for RD mice is the null effect on glucose tolerance after both activation of the inhibitory KORD receptor on bulbar GLP-1R positive cells and inhibition of the bulbar GLP-1R by exendin-9. We thus considered the option to try GLP-1R activation by exendin-4 so as not to miss any important information. On the other hand, because evaluating glucose tolerance under exendin-9 was a potential tool to assess whether GLP-1 could be tonically released within the OB, we considered the possibility to inject the antagonist in WD mice, even if they already presented massive glucose intolerance. Instead, we could have directly assessed the localization of GLP-1 peptide within the OB by immunocytochemical approaches, but commercially-available antibodies are not specific enough and can yield unfair results. We thus avoided this issue by taking advantage of exendin-9 properties.

9.2. Why did we choose to focus our work on WD mice halfway through the project?

We started our work by working in parallel through an "up and down" strategy with RD and WD mice. We found interesting and really promising results on both groups such as for the odor-evoked CPIR task or the chemogenetic evaluation of food intake. However, since our main objective was to assess whether the bulbar GLP-1/GLP-1R system constituted a new metabolic pathway controlling energy balance in the context of obesity and T2D, we prioritize the WD

group as it seemed more relevant for our work in certain given experiments. Also, there was a question of time. Doubling the experiments by having an RD and a WD group requires much more effort, and in the framework of my thesis, we could not address everything. Further studies in RD mice can be envisaged to achieve a more complete and detailed vision of the work.

9.3. In which point is our work based on the natural history of T2D?

Since the modulation of insulin secretion by the bulbar GLP-1/GLP-1R system was our main target in all the metabolic or olfactory behavioral tests, we needed to work precisely within the time window of pre-diabetes, when β-cells are still capable to produce insulin secretion. Our mice presented hyperglycaemia and insulin resistance. If we had worked on diabetic mice, suffering from β-cell dysfunction (Furman, 2015), insulin secretion would have been completely impaired and we could not have seen the strong improving effects mediated by GLP-1R signaling in the OB. In the context of insulin resistance in which our project is based, insulin could still be secreted but insulin insensitivity is manifested in other target tissues.

9.4. What is the rationale behind doubling GLP-1 by Ex4?

In our work we assessed OGTTs under pharmacological injections of both GLP-1 and Ex4, and we obtained the same enhancing effect on insulin secretion. Why did we decide then to continue working with Ex4 while having already an effect with GLP-1 injections? Since our RT-PCR results show the presence of DPP-IV within the OB, we wanted to know if a prolonged GLP-1R activation by Ex4 compared to the one that GLP-1 is physiologically capable to have an effect on metabolic tests. Moreover, the choice to privilege Ex4 over GLP-1 on our pharmacological experiments has been made taking into consideration our olfactory behavioral tests, in which we must necessarily boost the GLP-1 system. Since the time period between drug administration and the behavioral test is longer than the one set for the metabolic tests, we wanted to make sure to not fall into the inhibitory effect of DDP-IV and obtain biased results.

10. Perspectives

10.1. OB to PVN circuits

To date, direct connectivity between the OB and the PVN has never been described. Thus, we could not anatomically consider a monosynaptic pathway between these two structures. Thanks to our OGTT results performed under bicuculline injections in the PVN, we know that a GABAergic inhibitory input to the PVN, driven by GLP-1R^{OB} neurons, decreases the sympathetic

nerve activity leading to an increase of insulin release from the pancreas in WD mice. However, the localization of this GABAergic region controlling the PVN is not known yet, and therefore its connection with GLP-1R^{OB} neurons is unknown either. One of our main perspectives is thus seeking to characterize more precisely this gap within the neuronal network described. We have two hypothetical circuits:

- The OB projects to the PC, which sends glutamatergic inputs to the LHA (Price et al., 1991). In turn, GABAergic neurons within the LHA could project monosynaptic to $GABA_A$ receptor-expressing PVN neurons, modulating the SNS tone.
- The OB projects to the PC, which sends glutamatergic inputs to the peri-PVN. In turn, GABAergic neurons in the peri-PVN could project to the PVN modulating pre-sympathetic autonomic neurons.

The very first step will be to validate the GABAergic source, whether it is the LHA or some structure within the peri-PVN region. To test it, retrograde viral tracing from the PVN using Fluorogold will be performed very soon.

Next, once the GABAergic source will be localized, we will focus on developing the neuronal circuit connecting the OB with this GABAergic region controlling the PVN activity by the use of both antero- and retrograde viral tracers. In turn, when the potential GABAergic region will be identified, we will perform immunostaining of the GABAergic markers GAD65/67 to confirm the inhibitory source projecting to the PVN.

10.2. PVN activity

cFos quantification of the PVN activity after local injections of exendin-4 or NaCl in the OB of RD and WD mice has been done by Vincent Simon in Daniela Cota's lab in Bordeaux. Only WD mice have been analyzed for the moment since we thought they were more relevant. Unfortunately we could not see any differences on them since the total cFos signal within the PVN was very strong in both cases (exendin-4 vs. NaCl). Because cFos immunohistochemistry (IHC) is not specific enough for labeling only pre-autonomic neurons, we could have missed any difference of SPAN neurons activity between the two conditions tested. Therefore, we are now redirecting the experiments through a new labeling by the use of $GABA_A$-receptor antibodies using fluorescent *in situ* hybridization (FISH), concomitant to IHC of cFos. This double staining approach will hopefully help us identify SPANs and see more accurately cFos changes between exendin-4 and NaCl-treated mice on this targeted subpopulation of neurons. The use of $GABA_A$ receptors as a marker of SPAN neurons would also be in line with our PVN-bicuculline injections that revealed a blockade of the effect of chemogenetic activation of GLP-1R^{OB} neurons on insulinemia.

It will be interesting to assess the staining in RD mice in order to see whether DIO can induce changes on neuronal activity within the PVN, and, consequently, explain why we see the a more enhanced effect of bulbar GLP-1R activation on glucose homeostasis in WD mice. We can hypothesize that pre-autonomic neurons in RD mice injected with exendin-4 in the OB will be more activated than those of Ex4-treated WD mice since less GABAergic input will be entering the PVN.

10.3. OB activity

cFos quantification of MC activity within the OB after local injections of exendin-4 or NaCl in RD and WD mice is in progress. Dan Brierley from Stefan Trapp's laboratory (UCL) has developed an accurate pipeline in *Cell Profiler* program which automatically counts cFos+ nuclei within the MCL. The quantification is planned. The results obtained will help us to confirm the exendin-4-induced activation of MC, cells appearing to strongly express both *glp1r* mRNA (RNAscope data) and GLP-1R protein (fluorescent exendin-4 data).

10.4. Further properties of PPG cells

In the OB, Al Koborssy et al., (2014) showed that extracellular brain glucose concentrations of steady state (satiated or fasted) rats is around 1 mM *in vivo*. Even though blood glucose was significantly different between hungry and satiated rats, extracellular brain glucose concentrations in the OB were the same between these two feeding states. Our preliminary data concerning the total GLP-1 content in OB slices after KCl stimulation let us hope for interesting results: a potential local GLP-1 production within the OB under high glucose concentrations (mimicking a postprandial state). To confirm this early data, we are running more experiments in order to increase the number of mice and assess the comparison of 2 states of glucose concentrations *in vitro* (low/preprandial: 1mM vs high/postprandial: 5mM). This is an experiment we are working on at the moment in collaboration with David Jarriault and Xavier Fioramonti (NutriNeuro, Bordeaux) and Victor Gault (Ulster University).

We have seen that, in the preprandial phase, PPG^{OB} cells were required for the existence of an odor-evoked CPIR. In the postprandial state, however, even if we have almost described the network connecting the OB to the pancreas, we still have little evidence about whether we could direct the network from the PPGs, leading to the regulation of insulin secretion. Previous studies in mice and rats have shown that GLP-1-producing neurons are consistently activated by stimuli from actual or anticipated threats to the energy homeostasis of the organism (Maniscalco et al. 2013; Rinaman, 1999). However, whether PPG neurons could be sensible to glucose following a meal is unknown. Since MC are known to be glucose sensors (Tucker et al., 2010, 2013), it is

thus possible that PPG cells also present the capacity to modulate their firing frequency according to fluctuations in glucose concentration. For now, however, we can only say that they could be modulated by food odor stimuli in a premeal situation. An ultimate approach for assessing this issue would be to continuously measure bulbar GLP-1 concentrations through microdialysis in behaving mice. This could be done while modulating glucose levels within the perfusate, which would be pumped through the probe implanted in the OB, in order to see whether glucose concentration changes within the extracellular fluid modulate GLP-1 production *in vivo*. It is important to note however, that since GLP-1 levels in the OB are very low, we could run the risk of not seeing any difference by using this technique.

Assessing the role of PPG cells through an OGTT is another perspective. We plan to run the metabolic test in the mice injected with the shRNA targeting PPG mRNA in bulbar PPG neurons, in order to more precisely study the role of PPG cells in energy balance, in health and obesity. If PPG cells are glucose sensitive and the main source of GLP-1 in the OB, we could hypothesize that PPG-shRNA RD mice would exhibit an impaired glucose tolerance (or worsened glucose intolerance in the case of WD mice) due to its lack of OB-derived GLP-1 in the postprandial state.

cFos quantification of PPG cells after palatable-food odor presentation on both RD and WD mice is another envisaged study that will provide crucial information about whether PPG cells within the OB are sensitive to food odors and promote odor-evoked CPIR.

10.5. GLP-1 system in the context of obesity: clinical vs pre-clinical studies

Controversy exists as to whether T2D patients present lower or normal post-prandial gut-derived GLP-1 levels. In 2010, Nauck et al. summarized the literature on this topic and their analysis did not support the common idea that T2D patients presented a deficient nutrient-related GLP-1 secretion by L cells (Nauck et al., 2010). Thus, gut-derived GLP-1 levels might not change in the context of obesity or T2D. However, to our knowledge, how T2D impacts GLP-1 production in the human brain is still poorly understood. This issue also remains unknown in preclinics since no studies have assessed the role of GLP-1 producing cells in the context of obesity before my PhD work. Against this background and focusing on our DIO model, we have some interesting questions to adress: could the GLP-1 system in the OB of WD mice be impaired? Is the role of PPG cells disrupted in the context of obesity? WD mice present less or more capacity to release GLP-1 within the OB?

We cannot answer these questions with precision yet, but we already have some proofs that some anatomical differences exist between RD and WD mice: i) fluorescent exendin-4 GLP-1R-labeling seem to show a higher amount of GLP-1R in WD mice compared to the RD group and ii) PC1/3 and DPP-IV mRNA are significantly more expressed in WD mice. This increase of

both the synthesis and degradation enzymes is consistent with the more enhanced effect of bulbar GLP-1 on glucose homeostasis in WD mice.

10.6. GLP-1 in the OB as a potential therapeutic target

Our experiments with GLP-1R pharmacological and pharmaco-chemogenetical treatments bring important reconsideration of the OB role in food regulation in mice. In our hands, OB-Ex9 impairs olfaction and GLP-1R^{OB} KORD RD increases food intake in lean mice mimicking an obese profile. On the opposite, OB-Ex4 improves olfaction and GLP-1R^{OB} hM3Dq WD decreases food intake and both improve glucose homeostasis in obese mice, mimicking the lean phenotype. OB- GLP1/GLP-1R is thus a very efficient pathway to shift on/off glucose homeostasis in lean and obese mice. This is true when carefully considering the basal nutritional condition of the mouse as well as the predictive reward value of the odor which are crucial factors for the influence of OB on food perception and regulation. Our view complements recent works on local VIP (Wang et al., 2022) and CCK (Sun et al., 2020) interneurons in the OB which were implicated in olfactory discrimination and oscillations and the fine tuning of the OB circuit but only in the only context of lean mice. Thus, our work highlights the potential of the GLP-1 system in the OB as a new medical target for the treatment of obesity and T2D.

In a therapeutic and non-invasive way (i.e. via intranasal delivery), the bulbar GLP-1 system modulation could help control metabolic imbalance. Some authors have shown that intranasal administration of insulin induces an increase in olfactory discrimination ability (Marks et al., 2009) and enter the cerebrospinal fluid affecting directly central feeding regulatory areas in the hypothalamus (Kern et al., 1999; Born et al., 2002). Leptin has also been tested intranasally showing a reduction of appetite thus promoting weight loss in DIO rats (Schulz et al., 2012) and attenuate obesity-related sleep disordered breathing in mice (Berger et al., 2019). Moreover, a nasal ghrelin vaccine has been demonstrated to be an obesity-attenuating strategy by decreasing fat accumulation and increasing energy expenditure in mice (Azegami et al., 2017). In clinics, a new GLP-1 compound developed for nasal delivery was suggested to be a potential treatment for T2D (Ueno et al., 2014). Interestingly, intranasal delivery of GLP-1 can rapidly be absorbed from the OM and transmitted to the OB.

Furthermore, since GIPR is strongly expressed within the OB (Figure IV.1F) (Seino et al., 2010), we can speculate that the use of dual GIP-GLP-1 receptor agonists could lead to a reinforcement of the role seen for the bulbar GLP-1 system alone.

Hence, the identification of the OB as an actor of CNS GLP-1R-mediated regulation of energy balance and feeding behavior may benefit the development of more effective therapies for T2D and obesity involving easy-self administration compared with intravenous or subcutaneous injections of GLP-1RAs.

11. Conclusion

During my thesis, I was interested for the first time in the role of the GLP-1R in the OB on energy balance regulation in metabolic health and obesity. Recent series of data are in favor of intestinal peptides such as CCK, VIP and GLP-1 as fulfilling the functional role of neuropeptides within the CNS (Thiebaud et al., 2016; Sun et al., 2020; Wang et al., 2022; Trapp and Brierley, 2022). Their receptors are expressed within the OB and control bulbar circuits. However, none of these major findings have shown an implication of these molecules on energy balance. My PhD work bridges the gap with unanswered issues concerning central GLP-1 effects in health or obesity. It provides new insights in the role of the GLP-1 system within the OB by adding a pathophysiological implication in the context of obesity, and revealing for the first time an important role of PPG neurons in the OB on odor-evoked CPIR. Taken together, our work highlights the GLP-1 system in the OB as a new potential therapeutic target for controlling glucose homeostasis.

Annex

Effects of obesity and aging on cerebral blood flow in the olfactory bulb

Obesity has a harmful impact on brain function, leading to further brain strokes and neurodegenerative diseases in people suffering from this disorder (Suk et al., 2003). To date, it has been shown in humans that diabetes, cardiovascular disease as well as hypertension exert complex deleterious effects on cerebral microvasculature that are cumulative on obesity-related dysfunction. These diseases might also accelerate the normal decay of the cerebral blood flow (CBF) in subjects as they age. Surprisingly, how obesity alters CBF at rest or during sensory stimulation is poorly understood. In order to provide further insights into this issue, we explored relative changes in CBF circulation at rest and in response to odor stimulation in the olfactory bulb of adult and middle-aged obese mice.

For this work, I collaborated with a PhD student in Physics, Haleh Soleimanzad, with whom I co-first authored an article in Obesity. Haleh, under the supervision of Frédéric Pain, our collaborator who is assistant professor in physics at Université de Paris-Saclay, and Hirac Gurden, developed a new optical imaging technique in the laboratory. Multiple Exposure Speckle Imaging (MESI) allows the recording of changes in endogenous optical indexes under illumination with a series of wavelengths. Calculations from these indexes make possible the computing of CBF changes in a sensory area (such as OB) in response to sensory stimulation (such as odor stimulation). This vascular signal arises from cerebral arterioles and capillaries.

Our work showed that obese mice present vascular dysfunction in the OB in both resting and sensory-evoked CBF regulation, compared to its age-matched controls. These findings also document a specific deleterious effect of aging in control mice as well as in obese mice, on brain hemodynamics. Additionally, adult obese mice already present metabolic disruption reflected with fasted hyperglycemia and glucose intolerance. Interestingly, similarly to other labs, we did not find significant changes in the architecture of the vascular network, discarding an anatomical basis for cerebrovascular dysfunction in obese animals. Metabolic imbalances are strongly aggravated in middle-aged mice, which present a shift from insulin sensitivity to insulin resistance (IR) and impaired olfactory foraging in the BFT. We thus suggest that the onset of insulin resistance could play a major role both in the decrease of olfactory sensitivity and the modulation of cerebrovascular function.

Original Article
OBESITY BIOLOGY AND INTEGRATED PHYSIOLOGY

Obesity

Obesity in Midlife Hampers Resting and Sensory-Evoked Cerebral Blood Flow in Mice

Haleh Soleimanzad[1]#, Mireia Montaner[1]*, Gaëtan Ternier[2], Mathilde Lemitre[3], Jean-Sébastien Silvestre[3], Nadim Kassis[1], Paolo Giacobini[2], Christophe Magnan[1], Frédéric Pain[4], and Hirac Gurden [1]*

Objective: This study aimed to investigate the effects of a high-fat diet (HFD) and aging on resting and activity-dependent cerebral blood flow (CBF).

Methods: To run a comparison between obese and age-matched control animals, 6-week-old mice were fed either with regular chow or an HFD for 3 months or 8 months. Glucose tolerance and insulin sensitivity were assessed for metabolic phenotyping. Resting and odor-evoked CBF at the microvascular scale in the olfactory bulb (OB) was investigated by multiexposure speckle imaging. Immunolabeling-enabled imaging of solvent-cleared organs was used to analyze vascular density. The ejection fraction was studied by using cardioechography. Olfactory sensitivity was tested by using a buried-food test.

Results: Glucose intolerance and compromised odor-evoked CBF were observed in obese mice in the younger group. Prolonged HFD feeding triggered insulin resistance and stronger impairment in activity-dependent CBF. Aging had a specific negative impact on resting CBF. There was no decrease in vascular density in the OB of obese mice, although cardiac function was impaired at both ages. In addition, decreased olfactory sensitivity was observed only in the older, middle-aged obese mice.

Conclusions: OB microvasculature in obese mice showed a specific functional feature characterized by impaired sensory-evoked CBF and a specific deleterious effect of aging on resting CBF.

Obesity (2021) **29**, 150-158.

Study Importance

What is already known?

- Obesity is a metabolic condition with higher risk for ischemic stroke.
- Aging affects brain hemodynamics in lean animals.

What does this study add?

- Obesity impairs odor-evoked cerebral blood flow (CBF).
- Aging specifically blunts resting CBF in lean and obese mice.
- Microvascular density does not decrease in the olfactory bulb of obese mice.

Introduction

The pandemic of obesity is a worldwide health threat; according to the World Health Organization (1), in 2016, more than 1.9 billion adults had overweight, and of these, more than 650 million had obesity. Obesity is a metabolic disease primarily defined as a condition in which excessive fat accumulation in the body adversely affects health (2). It is associated with comorbidities such as type 2 diabetes or cardiovascular disease and it also has a detrimental effect on brain activity (3-4). Because of a lack of energy storage, the brain needs a continuous supply of energy. The necessity of this ongoing energy feeding implies a tight and reliable regulation of cerebral blood flow (CBF) both at rest and during the activated states of cerebral networks (5). Obesity is a metabolic condition causing a higher risk of ischemic stroke in clinics (6) and a higher risk of toxicity along the human blood–brain barrier (7). In addition, rodent models of obesity have repetitively been shown to have worse outcomes after experimental stroke (8-10). Aging has been shown to be an important factor in exacerbating the deleterious effects of obesity on brain function (11-12) and it could be responsible for further disturbing brain hemodynamics of organisms with obesity as they age (13-15). However, the fate of CBF regulation at rest and in response to physiological neuronal activation over the course of high-fat diet (HFD) feeding (i.e., aging superimposed on obesity) remains unexplored.

[1] Université de Paris, Unit of Functional and Adaptive Biology (BFA), UMR 8251 CNRS, Paris, France. Correspondence: Hirac Gurden (hirac.gurden@u-paris.fr) [2] Université de. Lille, INSERM, CHU Lille, U1172 - LilNCog - Lille Neuroscience & Cognition, Lille, France [3] Université de Paris, Paris Cardiovascular Research Center (PARCC), INSERM, Paris, France [4] Université Paris-Saclay, Institut d'Optique Graduate School, CNRS, Laboratoire Charles Fabry, Palaiseau, France.

See Commentary, pg. 17.

*Haleh Soleimanzad and Mireia Montaner contributed equally to this study and should be considered co–first authors.

#Present address: Institut Physique pour la Médecine, Paris, INSERM U1273, CNRS FRE2031, ESPCI Paris, Paris, France.

© 2020 The Obesity Society. **Received:** 30 July 2020; **Accepted:** 14 September 2020; **Published online 10 November 2020. doi:10.1002/oby.23051**

To study neurovascular mechanisms allowing local adaptation of hemodynamics to neuronal activity, sensory cortices in rodents were used as a system model. Odor-evoked neurovascular mechanisms in the main olfactory bulb (OB), the first cerebral structure coding for odors (16), have been studied for a couple of decades. Hemodynamic changes in the OB have been recorded using several imaging techniques with complementary spatiotemporal resolution (17-18), which made it possible to characterize functional hyperemia (a local increase of CBF triggered by neural activation) and neurovascular coupling mechanisms at different vasculature scales, from pial arteries to single capillaries. In addition, the role of the different cellular entities (19-22) has been determined in odor-evoked functional hyperemia. In the present study, to map vascular activity at the OB surface, we used a full-field optical imaging technique: multiexposure speckle imaging (MESI) (23-25). We recorded CBF at rest and in response to odor presentation in anesthetized obese mice fed a HFD for 3 or 8 months and their age-matched lean controls. We also characterized the metabolic phenotype, vascular density, cardiac function, and olfactory behavior of these obese mice. Our results indicate a specific functional feature of OB vasculature in obese mice, compared with control mice, that is characterized by impaired odor-evoked CBF and a specific deleterious effect of aging on resting CBF.

Methods

Animals

All procedures were approved by the animal care and use committee of the University of Paris (CEEA40, ethical project 7582) in accordance with the European directive 2010/63/UE. Male C57BL/6 mice (received at 5 weeks of age; Janvier Labs) were housed in cages with ad libitum regular food (A04 diet, 2,791 kcal/kg; Safe) and tap water and maintained on a 12-hour light/12-hour dark cycle. Cages were enriched with tunnels. To trigger obesity, mice were given an ad libitum HFD (HF230 diet, 5,317 kcal/kg; Safe) together with regular food starting at 6 weeks of age (after 1 week of acclimatization). Control mice were kept on regular food. According to the HFD duration, mice were divided into two groups, each of them including obese and control mice: 4.5-month-old control mice fed regular food versus 4.5-month-old obese mice fed a HFD for a duration of 3 months (3M group; adult mice) and 9.5-month-old control mice fed regular food versus 9.5-month-old obese mice fed a HFD for a duration of 8 months (8M group; middle-aged mice). Comparing the 8M group with the 3M group enabled us to study aging in control and obese mice. A total of 112 mice were used for the six independent experiments. Subgroup composition is indicated in the figure captions (Figures 1-5; also see Supporting Information Table S1).

Metabolic phenotyping

Body weight and body mass composition. Body weight was measured weekly. Body mass composition was determined by an EchoMRI-900 (Echo Medical Systems).

Oral glucose tolerance test. To evaluate the impact of a HFD on glycemia, oral glucose tolerance tests (OGTT) were performed in 5-hour-fasted mice. A glucose solution (1 g/kg) was administrated by oral gavage. Blood glucose was quantified from the tip of the tail vein

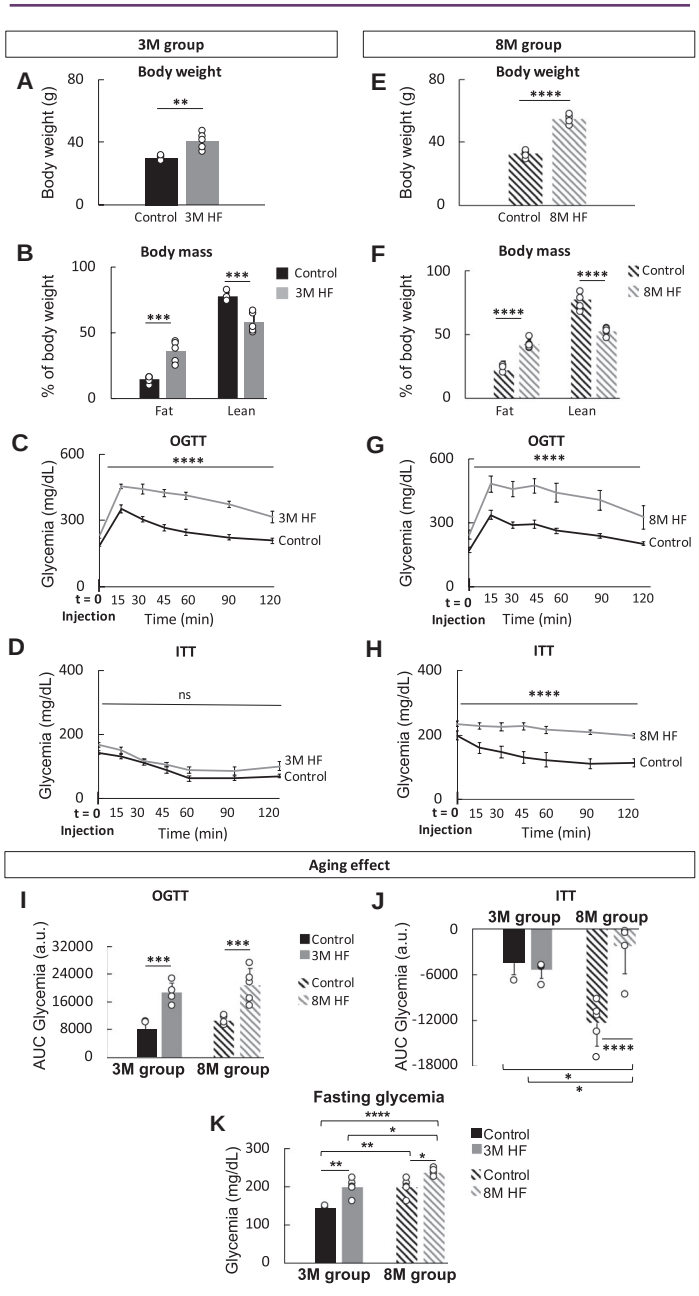

Figure 1 (**A**-**D**) Metabolic phenotyping of 4.5-month-old control mice fed regular food and 4.5-month-old obese mice fed a high-fat diet (HF) for a duration of 3 months (3M group; young-adult mice) (left column). (**A**) Body weight, (**B**) fat and lean mass, and (**C**) time course of glycemia during oral glucose tolerance tests (OGTT). Time 0 corresponds to glucose gavage (1 g/kg). (**D**) Time course of glycemia during insulin tolerance tests (ITT). Time 0 corresponds to intraperitoneal administration of insulin (0.75 U/kg). (**E**-**H**) Metabolic phenotyping of 9.5-month-old control mice fed regular food and 9.5-month-old obese mice fed a HF for a duration of 8 months (8M group; middle-aged mice) (right column). The right column depicts the same diagram types as the left column. Effects of physiological aging in control mice and HF duration (aging superimposed on obesity) in obese mice were tested and compared. The mean area under the curve (AUC) was obtained by calculating the integral of glycemia values from the plots in panels C and G for (**I**) OGTT; for (**J**) ITT, plots in panels D and H were used. (**K**) Fasting glycemia. Values are mean ± SD; $n = 5$ per group (total of 20 mice). Unpaired Student t tests in panels A, B, E, and F and two-way ANOVA in panels C, D, G, and H followed by post hoc Bonferroni tests in panels I, J, and K. $^{*}P < 0.05$, $^{**}P < 0.01$, $^{***}P < 0.001$, and $^{****}P < 0.0001$. a.u., arbitrary units; ns, not significant.

with a glucose meter (Glucofix Lector, Menarini Diagnostics). Blood samples were collected from the tail vein to assay plasma insulin with a wide-range Ultra Sensitive Mouse Insulin ELISA Kit (catalog no. 90080; Crystal Chem, Inc.).

Insulin tolerance test. To assess insulin sensitivity, insulin tolerance tests (0.75 U/kg) were performed in 5-hour-fasted mice. Mice were given an intraperitoneal injection of insulin (0.75 U/kg of body weight; Novo Nordisk), and glycemia was monitored following the same protocol as was used for OGTT.

Multiple-exposure speckle imaging

Mice were anesthetized intraperitoneally with a cocktail of ketamine (100 mg/kg) and medetomidine (0.5 mg/kg). The anesthesia level was adjusted if necessary throughout the experiment, and the temperature was kept at 37 ± 0.5 °C using a heating pad. After a craniotomy of 1.5 mm^2 centered on the anterior–posterior and medial–lateral stereotaxic coordinates of +4 to 5 mm from bregma and 1 mm from midline (26), respectively, imaging was carried out.

CBF at rest and CBF in response to olfactory stimulations were determined using an in house–designed MESI imager. The MESI protocol was fully described previously (23) and is illustrated in Supporting Information Figure S1. It relies on the determination of the correlation time τ_c of scatterers (i.e., red blood cells) using multiple exposure acquisitions. The inverse correlation times derived from MESI have been shown to be robust metrics of blood flow changes (27). For simplicity, it will be referred in this article as the "CBF index." Optimized procedures to derive CBF-index maps from MESI have been described in detail previously (23). Briefly, at rest, CBF-index values were obtained for each pixel as the absolute inverse correlation time and averaged during 12 seconds of the baseline recordings for each mouse. Olfactory stimulations were obtained by presentation of a pure odor diluted in mineral oil and placed in one vial of a custom-designed olfactometer. A simulation trial consists of 12 seconds of the baseline state (air flow) and 12 seconds of odorant stimulation, followed by 24 seconds of air flow to clean up the system. One experiment consisted of the recording of five trials with hexanal 5% or isoamyl acetate 5% as odors. Stimulations with two odorants were interleaved randomly to prevent habituation. Following stimulation, the relative changes in the CBF index were calculated pixelwise as the percentage change relative to the baseline CBF index. The average values obtained during the baseline state were subtracted from the average value achieved during stimulation, revealing the locations where CBF had changed during the stimulation. This difference was then divided by baseline values to obtain a variation in the percentage. Values of five trials were averaged.

Immunolabeling-enabled imaging of solvent-cleared organs

Mice were perfused transcardially with PBS one time for a duration of 5 minutes and then with 4% paraformaldehyde for a duration of 5 more minutes. Brains were postfixed in 4% paraformaldehyde overnight at 4 °C and were then then submerged in sucrose. For the analysis of laminin-stained mouse OB (illustrated in Supporting Information Figure S2), we used the immunolabeling-enabled imaging of solvent-cleared organs (iDISCO) protocol from Renier et al. (2014) (28), with minor adjustments. The primary antibody used was rabbit anti-laminin antibody (1:1,000, catalog no. ab11575; Abcam). The secondary antibody used was donkey anti-rabbit AlexaFluor 568 (1:500; Thermo Fisher Scientific).

Light-sheet imaging. Imaging was performed on the Ultramicroscope (LaVision Biotec) light-sheet microscope available at the BioImaging Center of Lille. The field and depth were set to cover the two bulbs, and the z-step was set to 2 µm.

Data extraction and analysis. Data from light-sheet imaging were first converted to the Imaris file format. The Surfaces tool of Imaris 9.3 (Bitplane) was used to create surfaces on the basis of the laminin signal, with a fixed threshold for detection, in a region of interest (ROI) set to cover a 500 µm–thick volume in the center of the second part of the OB (+4.28 mm anterior to bregma (26)). The resulting surface was used as a mask to create a new channel of fixed intensity, which was then extracted as a sequence of 2-µm slices and further processed in Fiji. A macro relying on the particle-analysis tool was used on the stacks to detect, classify, and segment the vessels on the basis of their cross-sectional area (5-10 pixels squared [px^2], 10-20 px^2, 20-50 px^2, and >50 px^2). The relative frequency of each class was calculated for the different groups as follows: frequency = number of particles in the class / total number of particles > 5 px^2 (Supporting Information Figure S2).

Echocardiography

Left ventricular (LV) function was assessed by transthoracic echocardiography with a VEVO2100 Biomicroscope (VisualSonics). Mice were anesthetized with isoflurane (1.5% in air) and monitored for respiratory frequency and temperature. Parasternal long-axis views of the left ventricle were obtained with a 40-MHz ultrasound probe (MS550D) at a frame rate between 180 and 240 frames per second. Measurements of LV end-diastolic volume (LVEDV) and LV end-systolic volume (LVESV) were performed offline (Cardio Package/VEVO2100 software; VisualSonics). The ejection fraction (EF) percentage was calculated by using the following formula: EF percentage = ([LVEDV − LVESV] / LVEDV) × 100.

Real-time quantitative polymerase chain reaction

Total RNA was isolated using RNeasy Lipid Tissue mini kit (Qiagen). Real-time quantitative polymerase chain reaction (PCR) was carried out in a LightCycler 480 detection system (Roche) using the LightCycler FastStart DNA Master plus SYBR Green I kit (Roche). The primers were derived from mouse sequences. We targeted the glial fibrillary acidic protein (GFAP) mRNA expressed in astrocytes (GFAP_mAS agccgtccagagggaacta/GFAP_mS agccgtccagagggaacta) normalized against the mean of two reference house-keeping genes (TBP_m_S ggggagctgtgatgtgaagt/TBP_m_AS ccaggaaataattctggctca; rpL19_m_S gggcaggcatatgggcata/rpL19_m_AS ggcggtcaatcttcttggatt). TATA-binding protein and ribosomal protein L19 were previously used as reference genes in the mouse OB (29) and the human neocortex (30).

Buried-food test

Because rodents naturally use olfactory cues for food foraging, we used the buried-food test as a general and reliable estimation of olfactory sensitivity (29,31).

Individual mice underwent two consecutive days (day 1 and day 2) of odorized-food familiarization to prevent neophobia during the test. One gram of chocolate-flavored cookie was placed in the home

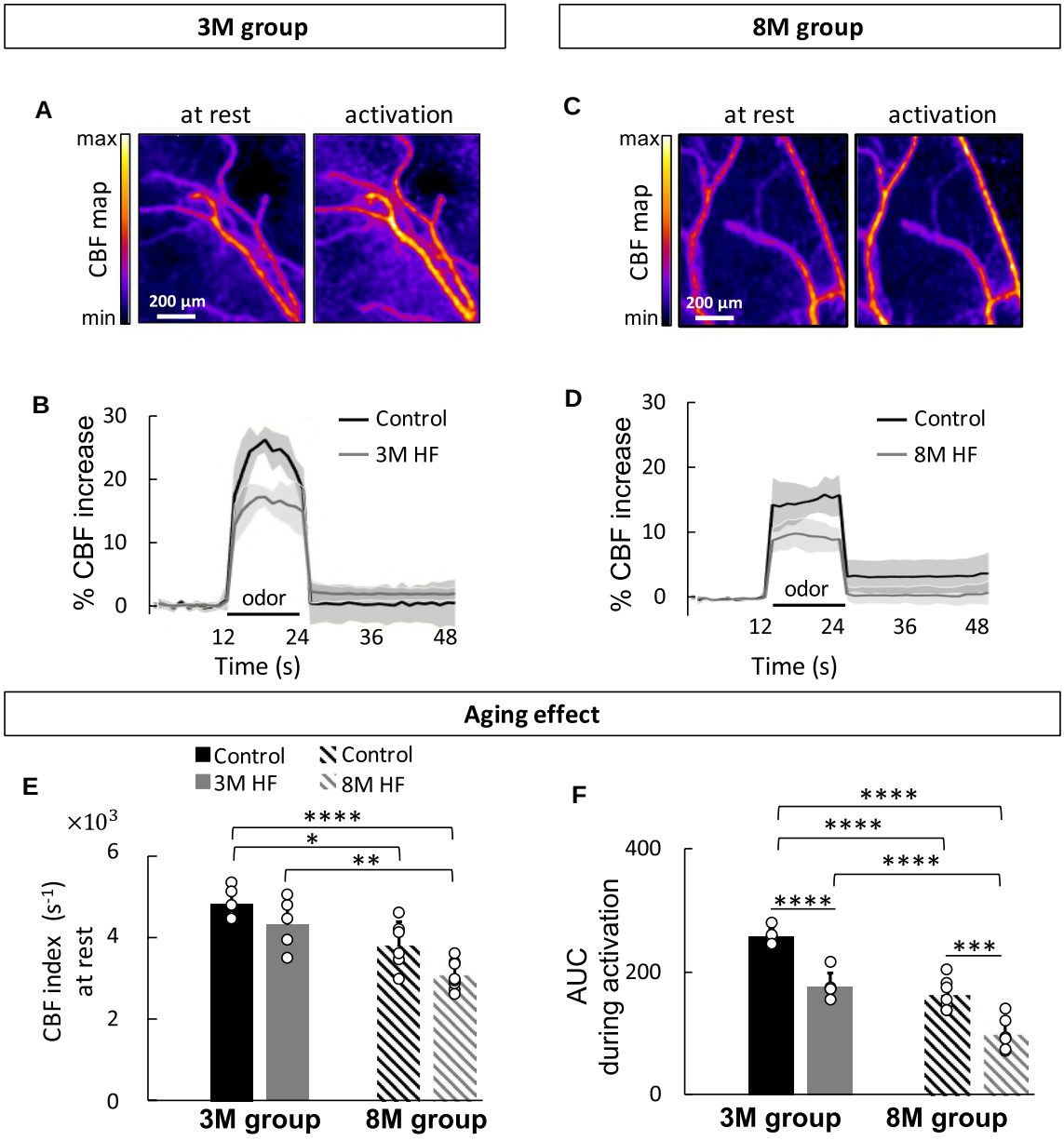

Figure 2 *In vivo* multiexposure speckle imaging (MESI) data at rest and under sensory activation in the olfactory bulb (OB) of 4.5-month-old control mice fed regular food and 4.5-month-old obese mice fed a high-fat diet (HF) for a duration of 3 months (3M group; young-adult mice) (left column). (**A**) Representative cerebral blood flow (CBF) maps at rest and under odor stimulation with 5% hexanal recorded on the dorsal OB of HF-fed mice. (**B**) Mean relative changes in CBF during olfactory stimulation with hexanal 5% for control and HF-fed mice (curves in transparency define the SD; $n=5$ per group, total of 10 mice). (**C**-**D**) *In vivo* MESI data at rest and under sensory activation in the OB of 9.5-month-old control mice fed regular food and 9.5-month-old obese mice fed a HF for a duration of 8 months (8M group; middle-aged mice) (right column). Represented data are of the same types depicted in the left column, with $n=6$ for control mice and $n=8$ for HF-fed mice (total of 14 mice). Effects of physiological aging in control mice and HF duration (aging superimposed on obesity) in obese mice were tested and compared. (**E**) CBF index at rest in the same control and HF-fed mice described in panels B and D (two-way ANOVA followed by post hoc Bonferroni test). (**F**) The area under the curve (AUC) was derived from the plots in panels B and D for the 3M and 8M groups to further probe the aging effect. Values are mean ± SD ($n=5$ per 3M group and $n=6$-8 per 8M group; two-way ANOVA followed by post hoc Bonferroni test). *$P<0.05$, **$P<0.01$, ***$P<0.001$, and ****$P<0.0001$. max, maximum; min, minimum.

cage in a location visible to the animal before the night shift and left overnight. The next morning, total food consumption was inspected. The day before the test day (day 3), mice were deprived of food overnight.

The test was performed on day 4 in a test cage containing 5 cm of fresh mouse bedding and equipped with a video camera. A piece of chocolate-flavored cookie was buried 2 cm beneath the surface of the bedding in a random corner of the cage. Latency time was defined as the amount

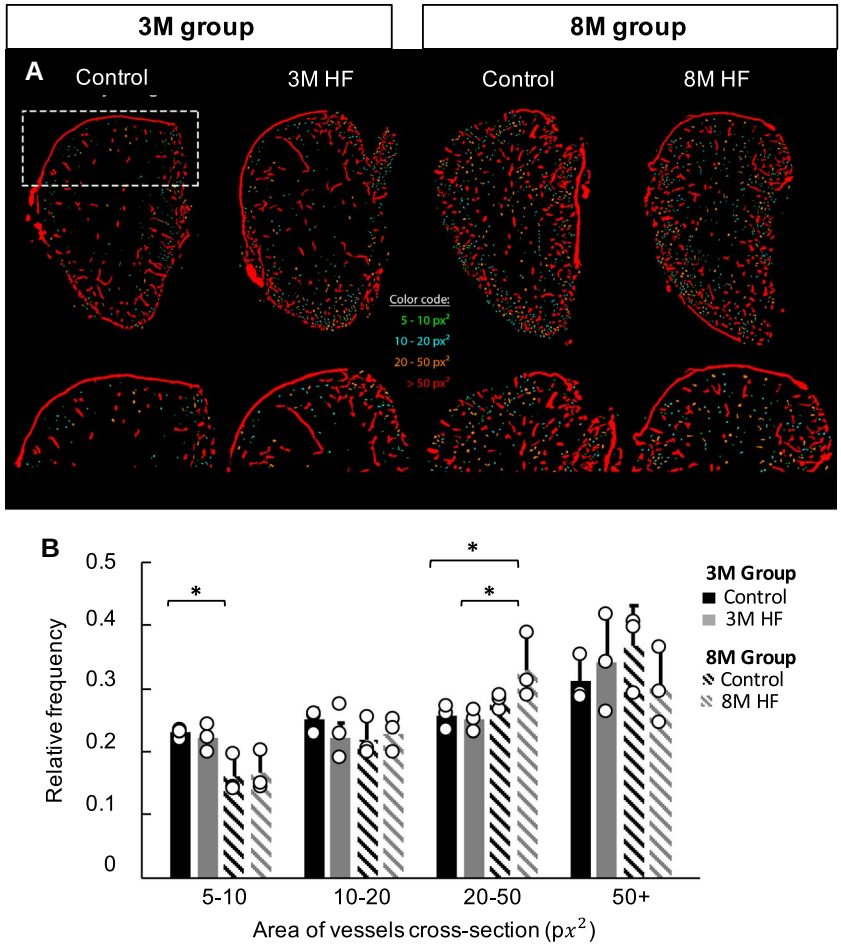

Figure 3 Detection, classification, and analysis of the olfactory bulb (OB) vessels. (**A**) Vessels detected by the particle analysis in a 500-µm–thick subvolume of the OB were classified according to their cross-sectional area. The first row shows representative pseudocolored reslices of the processed stacks. The white box highlights the dorsal layer of the OB, which is magnified in the second raw layer for each reslice, and represents the depth reachable by the laser speckle contrast imaging analysis. Green and blue particles correspond to the classes of vessels expected to be capillaries and arterioles/venules,respectively, whereas orange and red particles depict larger vessels consisting of veins and arteries. (**B**) The segmentation of the vessels revealed the distribution of the vessels in the different groups and conditions. Statistical analysis of the frequencies for each class notably points to a reduction in capillaries with age in control animals and an increase in arteries and veins with age in high-fat diet (HF)-fed animals (mean ± SD, $n = 3$ per group, total of 12 mice, two-way ANOVA test followed by post hoc Fisher least significant difference test). *$P < 0.05$. px^2, pixels squared.

of time between the introduction of the mouse in the cage and retrieval of the cookie after foraging. Each mouse was tested twice (60-minute interval) and had to find the cookie in both trials to be included in statistics (mean latency of Two trials). Latency was manually counted using Kinovea.

Statistical analysis

Results were expressed as the mean ± SD. Statistical analysis was performed in XLSTAT or GraphPad Prism. The Shapiro-Milk test was used to assess data normality. Then, as indicated in each figure caption (Figures 1-5), intergroup comparison was performed using parametric statistics, either through an unpaired Student *t* test or through two-way ANOVA followed by an appropriate post hoc test for two-by-two comparisons. Values were considered statistically different if the *P* value was <0.05, except for in multiple comparisons in which *P* was adjusted as required. Levels of significance are indicated by *$P < 0.05$, **$P < 0.01$, ***$P < 0.001$, and ****$P < 0.0001$.

Results

The obesity phenotype is worsened in HFD-fed mice as they age

Three months of HFD feeding caused body weight gain in HFD-fed mice (+40%) compared with age-matched young-adult control mice (3M group, Figure 1A; $P = 0.0002$). Overweight was accompanied by a

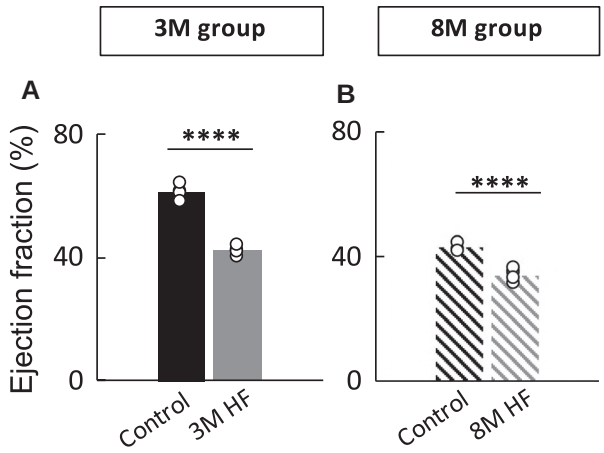

Figure 4 Cardiac ejection fraction in high-fat diet (HF)-fed mice compared with age-matched control mice. (**A**) Young-adult (4.5-month-old) mice fed for a duration of 3 months (3M group): control (black column) versus HF-fed mice (gray column); $n=4$ mice per group. (**B**) Middle-aged (9.5-month-old) mice fed for a duration of 8 months (8M group): control (column with black dashed lines) versus HF-fed mice (column with gray dashed lines); $n=5$ mice per group. Values are mean ± SD; unpaired Student *t* tests. $^{****}P<0.0001$.

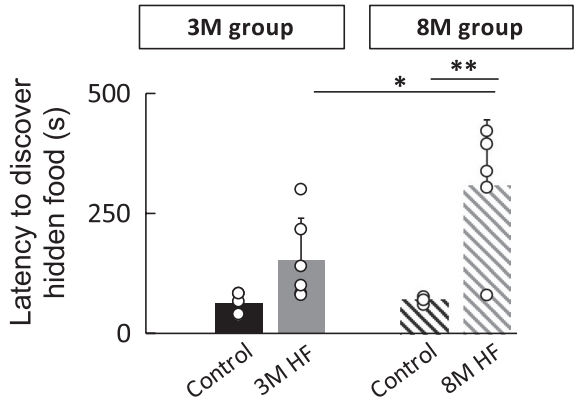

Figure 5 Latency in olfactory foraging to uncover an aromatized food pellet. Food discovery time was measured during a buried-food test after an overnight fast in each group. Values are mean ± SD (control and high-fat diet [HF]-fed mice: $n=5$ and $n=6$, respectively, for the 4.5-month-old mice fed over 3 months [3M group]; $n=4$ and $n=5$ respectively for 9.5-month-old mice fed over 8 months [8M group]). Two-way ANOVA followed by post hoc Bonferroni test. $^{*}P<0.05$ and $^{**}P<0.01$.

significant increase in fat mass (+147%) to the detriment of lean mass (−25%) in 3M HFD-fed mice compared with control mice (Figure 1B; $P=0.0006$ and 0.0007, respectively). OGTT results showed glucose intolerance in HFD-fed mice compared with control mice (Figure 1C; $P<0.0001$). This intolerance was associated with increased insulinemia during the test and with the loss of the glucose-dependent insulin secretion response (Supporting Information Figure S3). 3M HFD-fed mice were sensitive to insulin (Figure 1J), although they had already displayed fasted hyperglycemia compared with 3M controls (+40%, Figure 1K; $P=0.003$).

Eight months of HFD feeding further increased body weight gain in HFD-fed mice (+61%) compared with age-matched middle-aged control mice (8M group, Figure 1E; $P<0.0001$). Fat mass was severely increased (+165%), and lean mass (−33%) was decreased (Figure 1F; $P<0.0001$). OGTT revealed that 8M HFD-fed mice were glucose intolerant compared with control mice (Figure 1G; $P<0.0001$). This intolerance was associated with sustained increased insulinemia during the test and with the loss of the glucose-dependent insulin secretion response (Supporting Information Figure S3). Importantly, 8M HFD-fed mice were insensitive to insulin (Figure 1J; $P<0.0001$) and displayed hyperglycemia (+20%, Figure 1K; $P=0.048$).

We further probed aging effects on metabolic parameters by representing the area under the curve (AUC) of metabolic data from the 3M and 8M groups. There was no effect of physiological aging (8M vs. 3M control mice) or HFD duration (aging superimposed on obesity, 8M vs. 3M HFD-fed mice) on glucose tolerance (Figure 1I). We found a significant effect of HFD duration (Figure 1J; $P=0.0001$) and a slight effect of combined age and diet (8M HFD-fed mice vs. 3M control mice, Figure 1J; $P=0.036$) but found no effect of aging on insulin sensitivity. In addition, aging, HFD duration, and combined age and diet had a significant effect on fasted hyperglycemia (Figure 1K; $P=0.0027$, 0.048, and 0.0001, respectively).

Odor-evoked CBF is decreased in obese mice at both ages compared with control mice, and resting CBF is impaired with aging in control and obese mice

The CBF index was derived from MESI data to evaluate blood flow changes in HFD-fed mice versus control mice at rest and under odor-evoked activation. Figure 2A and 2C present CBF-index maps at rest and during olfactory stimulation in the OB of HFD-fed mice from the 3M group and 8M group, respectively. MESI enabled the visualization of the complex vascular architecture at the surface of the OB with a network of microvessels (mean diameter of 25 ± 8 μm) (23). The size (<20 μm) and the blood speed (3-15 mm/s) within these vessels match the arteriolar compartment. In both groups, there was a significant shift toward higher CBF indexes during olfactory stimulation compared with rest. Further comparison of the CBF index between control and HFD-fed mice during odor stimulation (Figure 2B and 2D) was performed in ROIs defined over regions in the blood vessels (Supporting Information Figure S1C). For all groups, a clear and transient increase in CBF was observed in response to a short puff of odorant. In the 3M group, the odor-evoked increase in CBF in HFD-fed mice was lower than that of control mice (Figure 2B, +17% vs. +26% respectively; $P<0.0001$). In the 8M group, the odor-evoked increase in CBF in the HFD-fed mice was also lower than that of control mice (Figure 2D, +9% vs. +15% respectively; $P<0.001$). These data showed a significant decrease in odor-evoked CBF in the OB of HFD-fed mice compared with age-matched control mice.

To quantify resting CBF, the CBF index at rest was calculated in vascular ROIs. Age and diet significantly impacted resting CBF (Figure 2E; $P<0.001$): resting CBF decreased with age in control mice ($P=0.02$) and with HFD duration in obese mice ($P=0.001$). In the 3M and 8M groups, the average resting CBF of HFD-fed mice was not different from that of control mice (3M group: $P=0.7$; 8M group: $P=0.06$). Thus, there was a specific deleterious effect of aging, in control as well as obese mice, on resting CBF.

To further quantify hemodynamic responses to sensory stimulation and their changes with aging, the AUC (Figure 2F) was derived from odor-evoked CBF values in Figure 2B and 2D. The AUC decreased with age in control mice ($P<0.0001$), with HFD duration in obese mice ($P<0.0001$), and with age and diet combined (3M control mice vs. 8M HFD-fed mice; $P<0.0001$). Very interestingly, we also observed that the AUC of 3M HFD-fed mice was not different from that of 8M control mice ($P>0.05$; i.e., odor-evoked CBF in young-adult HFD-fed mice was equal to that of middle-aged controls); this could indicate that functional hyperemia in HFD-fed mice is impaired by premature aging mechanisms.

HFD and aging modulate vascular network architecture

In order to investigate potential changes in the vasculature of the OB in the 3M and 8M groups, we performed whole-mount immunohistochemistry using the iDISCO tissue-clearing method coupled with light-sheet microscopy imaging (methods illustrated in Supporting Information Figure S2). Vasculature was immunostained using an antibody against laminin, which allows efficient labeling of both large and small vessels. The detected vessels were then ordered in classes depending on their size and expected nature: 5 to 10 px^2 (capillaries), 10 to 20 px^2 (arterioles, venules), 20 to 50 px^2 (arterioles, pial arteries, veins), and >50 px^2 (pial arteries and veins). The frequency of each class was determined for the four groups (Figure 3A).

Our analysis (Figure 3B) showed a significant reduction with age in the frequency of the first (smallest) class of vessels (5-10 px^2) for control mice (3M vs. 8M mice; $P=0.04$) but did not show a significant reduction for HFD-fed mice. The third class of vessels (20-50 px^2) notably revealed an increased frequency with HFD duration (3M vs. 8M mice; $P=0.02$), but this was not present in control mice. Overall, we did not detect any changes in the frequencies of the four classes between HFD and control mice of the same age (Figure 3B). These results indicate that impaired CBF in obese mice is independent of changes in vascular density.

Cardiac function is impaired in HFD-fed mice compared with age-matched control mice

The processes involved in the regulation of resting CBF are multifaceted and include a constant blood supply from the heart. Because we observed a decreased resting CBF in our groups, we monitored cardiac function (Figure 4). The EF was reduced in HFD-fed mice compared with control mice in the 3M group ($P<0.0001$) and was also reduced in older HFD-fed mice (8M group; $P<0.0001$).

Prolonged HFD triggers a decrease in olfactory sensitivity

We performed a buried-food test to evaluate the effect of the HFD on olfactory behavior (Figure 5). HFD-fed mice spent more time to find the hidden cookie than control mice in the 8M group ($P=0.004$), but this difference was not significant in the 3M group ($P=0.56$). Although the latency to uncover the cookie for control mice was the same for the 3M and 8M control groups, the latency for HFD-fed mice increased with HFD duration ($P=0.049$). These data show that HFD duration, but not physiological aging, triggered a decrease in olfactory sensitivity.

Discussion

In this study, we analyzed the hemodynamic profiles of 3M and 8M HFD-fed mice and compared them with their age-matched lean controls. We also analyzed aging effects by comparing middle-aged mice with young-adult mice. A summary of all results is presented in Supporting Information Table S1.

We found that a HFD (60% kcal from fat) triggered obesity, with a significant gain in weight due to an increase in fat mass at both ages. Young-adult obese mice had already presented metabolic defects such as fasted hyperglycemia and glucose intolerance. These abnormalities were largely amplified in middle-aged mice, which had a shift from insulin sensitivity to insulin resistance (IR). Previous studies have reported similar metabolic defects with a comparable HFD (8-9). Our results clearly showed a deleterious impact of obesity on odor-evoked CBF (impairment for young-adult and middle-aged obese mice compared with their age-matched lean controls). Physiological aging as well as HFD duration also induced a decrease in odor-evoked CBF. These results revealing neurovascular uncoupling are in line with previous observations showing (i) a decrease in visually evoked functional hyperemia recorded by functional magnetic resonance imaging in people with obesity and type 2 diabetes (32) and in lean, older individuals (33) in clinics and (ii) a decrease in sensory-evoked CBF in the somatosensory cortex of young-adult and older obese rodents (10,14-15).

To our knowledge, this is the first time that decreased levels of resting CBF with aging in a defined brain structure in control and obese mice have been evidenced. In addition, we observed a very significant decrease in the cardiac EF, a common sign of cardiomyopathy in human and rodent obesity (34), in our obese mice. We postulate that there could be a significant impact of cardiac dysfunction on resting CBF, resulting from the failure of the regulatory systems of neurovascular tone in the OB of obese mice. Indeed, it has been shown in the rat OB that stimulation of sympathetic adrenergic nerves induces a decrease in resting CBF (35). Interestingly, resting CBF changes induced by noradrenalin were larger in the OB of older rats than in the OB of young-adult rats (35), showing a loss of neuromodulatory control of resting CBF in the OB with aging. Whether this noradrenergic dysregulation in the OB is present in obese mice is currently unknown. In this context, future studies will be focused on the description of molecular mechanisms involved in CBF impairment; molecular pathways implicated in endothelial dysfunction, mitochondrial oxidative stress, and neuroinflammation have been shown to be causal in age-related neurovascular uncoupling in mice (36) and will have to be studied in our HFD model. Of note, it has recently been shown that deficiency in transcription nuclear factor erythroid-2-related factor 2, a prosurvival transcription factor with antioxidant properties, is implicated in neurovascular dysfunction in both aging and obesity (37).

One explanation of compromised functional hyperemia in HFD-fed mice could be anatomical changes in the vasculature. In order to get inside the vascular anatomy in the OB, we estimated the vascular network density using iDISCO for the three-dimensional analysis of laminin-labeled endothelial cells (28). Our results did not reveal any significant changes in the vascular density in obese mice compared with control mice. On the contrary, middle-aged obese mice showed increased density of the pial and parenchymal arteriolar compartment compared with young-adult obese mice, which could potentially compensate for the decrease of capillaries with aging that we observed in middle-aged versus young-adult control mice. This counterintuitive protective effect has to be discussed in light of controversial data published about the density of capillaries under a HFD: on one hand, a HFD (15) and aging (38) have been shown to have a detrimental effect

on capillary density, but on the other hand, the endothelial network has been shown to remain stable in the hippocampus of long-term HFD-fed rats (39) or mice (13). The use of different vascular quantitation techniques as well as the quality and duration of HFD can be causal in these discrepancies. Changes in vessel densities that we detected in aging and obesity in our HFD model could be due to modifications in endothelial-cell proliferation. In the context of obesity and diabetes, data about angiogenesis are mainly centered on the adipose tissue and the heart and are sparse concerning the brain. It has been shown in the heart of patients with obesity and diabetes that capillaries and pericytes are destabilized and the ratio of pro- to antiangiotic factors is decreased, causing a loss in the renewal capacity of peripheral blood vessels (40). Additionally, in diabetic patients, cardiac micro- and macrovessels present similarly deficient regeneration (41). Some of these mechanisms involved in the loss of endothelial proliferation in response to angiogenic stimuli have also been described in the brain during aging and obesity (42), showing a possible convergence of pathological pathways in these conditions. We can conclude that functional hyperemia was impaired in the OB of young-adult and middle-aged obese mice, whereas the density of the vascular network was globally intact.

The global metabolic state of young-adult obese mice deteriorated, but insulin sensitivity, a major metabolic factor for proper brain function, was preserved. By contrast, middle-aged obese mice presented IR, increased levels of GFAP transcripts in the OB (Supporting Information Figure S4), and deficits in olfactory foraging. Thus, the mechanistic link between a deteriorated metabolic state and impaired neurovascular coupling and behavior in middle-aged obese mice could be the emergence of IR. Indeed, obesity and aging are the two major risk factors for IR occurrence in humans (43). IR negatively impacts cardiovascular activity and brain perfusion in middle-aged human adults (44). Deficiency of insulin-like growth factor-1 (IGF-1), an insulin-like peptide, has been shown to impair neurovascular coupling in lean mice, a mechanism involving changes in astrocytic signaling (45). Insulin has been shown to regulate OB activity (46) and promote olfactory perception in humans (47). Consequently, regarding our findings and the literature, the next experimental step would be to further describe the role of insulin in neurovascular coupling in obese mice.

Because aging was shown to further compromise vascular activity in obese mice (13,15), we asked whether it could trigger hemodynamic impairment per se or in combination with obesity. We first observed that resting CBF and odor-evoked CBF were significantly decreased in middle-aged control mice compared with young-adult control mice, as previously reported in the barrel cortex (15,38). Vascular density in the OB was also decreased with aging, conforming with previous results (48). Such an age-related compromised anatomical–functional feature of the microvasculature in the OB has been repetitively demonstrated in other brain regions previously (38,49-50). However, middle-aged control mice with decreased capillary density in the OB did not show impairment in olfactory foraging. Thus, impaired functional hyperemia with apparent healthy aging in mice can be considered as an early sign of future deleterious effects on brain function, as has been suggested in humans (51-52). Very interestingly, we did not find any functional test through which we could distinguish middle-aged control mice from young-adult obese mice (Supporting Information Table S1). These results could indicate a premature age-related neurovascular defect in young-adult obese mice. Indeed, the brains of middle-aged human adults may age prematurely if the individuals have obesity (51). Protection of the cerebral microvasculature could be a biomedical strategy to prevent brain dysfunction in people with obesity as they age.

One limitation of our study is the animals' age. In middle-aged lean mice (at 25% of the potential lifespan for laboratory mice), we showed that CBF was already jeopardized, whereas metabolism and behavior were intact, leading to a misleadingly healthy phenotype. Characterizing the anatomical–functional features of the brain vasculature in older mice will be the subject of experiments in the near future, which will provide insight for geroscience (53).

In conclusion, obesity-related vascular dysfunction in the OB of our HFD model concerns both resting and sensory-evoked CBF regulation and it is independent of blood-vessel density. We also provided new evidence in support of the deleterious effect of (i) aging on resting CBF and (ii) aging in obese mice, with prolonged HFD feeding, on brain hemodynamics. We propose that IR could be responsible for compromised functional hyperemia and impaired behavioral outcomes in obese mice as they age.O

Acknowledgments

We thank Aurélie Djemat, Magguy Boa, Ludovic Maingault, Angélique Dauvin, Florianne Michel, Daniel Quintas, and Isabelle Le Parco for animals' care at the animal core facility "Buffon" of the University of Paris/Jacques Monod Institute. We also thank Flore Torsy for assistance with real-time quantitative PCR.

Funding agencies: This work was funded by a grant ANR-16-CE14-0026 (fat4brain) to HG and CM. HS and MM are funded by a PhD fellowship from the French Ministry of Research.

Disclosure: The authors declared no conflict of interest.

Author contributions: HS, MM, GT, ML, and NK carried out experiments and analyzed data. HS, J-SS, PG, CM, FP, and HG conceived the experiments and analyzed data. All authors were involved in writing the paper and had final approval of the submitted version.

Supporting information: Additional Supporting Information may be found in the online version of this article.

References

1. World Health Organization. Overweight and obesity. Updated April 1, 2020. Accessed July 17, 2020. https://www.who.int/news-room/fact-sheets/detail/obesity-and-overweight
2. Goossens GH. The metabolic phenotype in obesity: fat mass, body fat distribution, and adipose tissue function. *Obes Facts* 2017;10:207-215.
3. Sorop O, Olver TD, van de Wouw J, et al. The microcirculation: a key player in obesity-associated cardiovascular disease. *Cardiovasc Res* 2017;113:1035-1045.
4. Kopelman PG. Obesity as a medical problem. *Nature* 2000;404:635-643.
5. Iadecola C. The neurovascular unit coming of age: a journey through neurovascular coupling in health and disease. *Neuron* 2017;96:17-42.
6. Roger VL, Go AS, Lloyd-Jones DM, et al. Heart disease and stroke statistics–2011 update: a report from the American Heart Association. *Circulation* 2011;123:e18-e209.
7. Rhea EM, Salameh TS, Logsdon AF, Hanson AJ, Erickson MA, Banks WA. Blood–brain barriers in obesity. *AAPS J* 2017;19:921-930.
8. Haley MJ, Krishnan S, Burrows D, et al. Acute high-fat feeding leads to disruptions in glucose homeostasis and worsens stroke outcome. *J Cereb Blood Flow Metab* 2019;39:1026-1037.
9. Maysami S, Haley MJ, Gorenkova N, Krishnan S, McColl BW, Lawrence CB. Prolonged diet-induced obesity in mice modifies the inflammatory response and leads to worse outcome after stroke. *J Neuroinflammation* 2015;12:140. doi:10.1186/s12974-015-0359-8
10. Li W, Prakash R, Chawla D, et al. Early effects of high-fat diet on neurovascular function and focal ischemic brain injury. *Am J Physiol Regul Integr Comp Physiol* 2013;304:R1001-R1008.
11. Gustafson DR, Bäckman K, Joas E, et al. 37 years of body mass index and dementia: observations from the prospective population study of women in Gothenburg, Sweden. *J Alzheimers Dis* 2012;28:163-171.
12. Beydoun MA, Beydoun HA, Wang Y. Obesity and central obesity as risk factors for incident dementia and its subtypes: a systematic review and meta-analysis. *Obes Rev* 2008;9:204-218.
13. Pétrault O, Pétrault M, Ouk T, Bordet R, Bérézowski V, Bastide M. Visceral adiposity links cerebrovascular dysfunction to cognitive impairment in middle-aged mice. *Neurobiol Dis* 2019;130:104536. doi:10.1016/j.nbd.2019.104536

14. Coucha M, Abdelsaid M, Ward R, Abdul Y, Ergul A. Impact of metabolic diseases on cerebral circulation: structural and functional consequences. *Compr Physiol* 2018;8:773-799.
15. Tucsek Z, Toth P, Tarantini S, et al. Aging exacerbates obesity-induced cerebromicrovascular rarefaction, neurovascular uncoupling, and cognitive decline in mice. *J Gerontol A Biol Sci Med Sci* 2014;69:1339-1352.
16. Schaefer AT, Margrie TW. Spatiotemporal representations in the olfactory system. *Trends Neurosci* 2007;30:92-100.
17. Osmanski BF, Martin C, Montaldo G, et al. Functional ultrasound imaging reveals different odor-evoked patterns of vascular activity in the main olfactory bulb and the anterior piriform cortex. *NeuroImage* 2014;95:176-184.
18. Pain F, L'Heureux B, Gurden H. Visualizing odor representation in the brain: a review of imaging techniques for the mapping of sensory activity in the olfactory glomeruli. *Cell Mol Life Sci* 2011;68:2689-2709.
19. Otsu Y, Couchman K, Lyons DG, et al. Calcium dynamics in astrocyte processes during neurovascular coupling. *Nat Neurosci* 2015;18:210-218.
20. Petzold GC, Albeanu DF, Sato TF, Murthy VN. Coupling of neural activity to blood flow in olfactory glomeruli is mediated by astrocytic pathways. *Neuron* 2008;58:897-910.
21. Gurden H, Uchida N, Mainen ZF. Sensory-evoked intrinsic optical signals in the olfactory bulb are coupled to glutamate release and uptake. *Neuron* 2006;52:335-345.
22. Rungta RL, Chaigneau E, Osmanski B-F, Charpak S. Vascular compartmentalization of functional hyperemia from the synapse to the pia. *Neuron* 2018;99:362-375.e4.
23. Soleimanzad H, Smekens F, Peyronnet J, et al. Multiple speckle exposure imaging for the study of blood flow changes induced by functional activation of barrel cortex and olfactory bulb in mice. *Neurophotonics* 2019;6:015008. doi:10.1117/1.NPh.6.1.015008
24. Kazmi SMS, Faraji E, Davis MA, Huang Y-Y, Zhang XJ, Dunn AK. Flux or speed? Examining speckle contrast imaging of vascular flows. *Biomed Opt Express* 2015;6:2588-2608.
25. Schrandt CJ, Kazmi SMS, Jones TA, Dunn AK. Chronic monitoring of vascular progression after ischemic stroke using multiexposure speckle imaging and two-photon fluorescence microscopy. *J Cereb Blood Flow Metab* 2015;35:933-942.
26. Paxinos G, Franklin KBJ. *Paxinos and Franklin's the Mouse Brain in Stereotaxic Coordinates*. Academic Press; 2019.
27. Parthasarathy AB, Tom WJ, Gopal A, Zhang X, Dunn AK. Robust flow measurement with multi-exposure speckle imaging. *Opt Express* 2008;16:1975-1989.
28. Renier N, Wu Z, Simon DJ, Yang J, Ariel P, Tessier-Lavigne M. iDISCO: a simple, rapid method to immunolabel large tissue samples for volume imaging. *Cell* 2014;159:896-910.
29. Mortreux M, Foppen E, Denis RG, et al. New roles for prokineticin 2 in feeding behavior, insulin resistance and type 2 diabetes: studies in mice and humans. *Mol Metab* 2019;29:182-196.
30. Wierschke S, Gigout S, Horn P, et al. Evaluating reference genes to normalize gene expression in human epileptogenic brain tissues. *Biochem Biophys Res Commun* 2010;403:385-390.
31. Yang M, Crawley JN. Simple behavioral assessment of mouse olfaction. *Curr Protoc Neurosci* 2009;48:8.24.1-8.24.12.
32. Duarte JV, Pereira JMS, Quendera B, et al. Early disrupted neurovascular coupling and changed event level hemodynamic response function in type 2 diabetes: an fMRI study. *J Cereb Blood Flow* 2015;35:1671-1680.
33. Panczel G, Daffertshofer M, Ries S, Spiegel D, Hennerici M. Age and stimulus dependency of visually evoked cerebral blood flow responses. *Stroke* 1999;30:619-623.
34. Karason K, Wallentin I, Larsson B, Sjöström L. Effects of obesity and weight loss on cardiac function and valvular performance. *Obes Res* 1998;6:422-429.
35. Shiba K, Machida T, Uchida S, Hotta H. Sympathetic neural regulation of olfactory bulb blood flow in adult and aged rats. *Auton Neurosci* 2009;147:75-79.
36. Toth P, Tarantini S, Csiszar A, Ungvari Z. Functional vascular contributions to cognitive impairment and dementia: mechanisms and consequences of cerebral autoregulatory dysfunction, endothelial impairment, and neurovascular uncoupling in aging. *Am J Physiol Heart Circ Physiol* 2017;312:H1-H20.
37. Tarantini S, Valcarcel-Ares MN, Yabluchanskiy A, et al. Nrf2 deficiency exacerbates obesity-induced oxidative stress, neurovascular dysfunction, blood-brain barrier disruption, neuroinflammation, amyloidogenic gene expression, and cognitive decline in mice, mimicking the aging phenotype. *J Gerontol A Biol Sci Med Sci* 2018;73:853-863.
38. Li Y, Choi WJ, Wei W, et al. Aging-associated changes in cerebral vasculature and blood flow as determined by quantitative optical coherence tomography angiography. *Neurobiol Aging* 2018;70:148-159.
39. Fu Z, Wu J, Nesil T, Li MD, Aylor KW, Liu Z. Long-term high-fat diet induces hippocampal microvascular insulin resistance and cognitive dysfunction. *Am J Physiol Endocrinol Metab* 2017;312:E89-E97.
40. Hinkel R, Howe A, Renner S, et al. Diabetes Mellitus-Induced Microvascular Destabilization in the Myocardium. *J Am Coll Cardiol* 2017;69:131-143.
41. Spinetti G, Kraenkel N, Emanueli C, Madeddu P. Diabetes and vessel wall remodelling: from mechanistic insights to regenerative therapies. *Cardiovasc Res* 2008;78:265-273.
42. Ungvari Z, Tarantini S, Donato AJ, Galvan V, Csiszar A. Mechanisms of vascular aging. *Circ Res* 2018;123:849-867.
43. Ye J. Mechanisms of insulin resistance in obesity. *Front Med* 2013;7:14-24.
44. Hoscheidt SM, Kellawan JM, Berman SE, et al. Insulin resistance is associated with lower arterial blood flow and reduced cortical perfusion in cognitively asymptomatic middle-aged adults. *J Cereb Blood Flow Metab* 2017;37:2249-2261.
45. Toth P, Tarantini S, Ashpole NM, et al. IGF-1 deficiency impairs neurovascular coupling in mice: implications for cerebromicrovascular aging. *Aging Cell* 2015;14:1034-1044.
46. Aimé P, Hegoburu C, Jaillard T, et al. A physiological increase of insulin in the olfactory bulb decreases detection of a learned aversive odor and abolishes food odor-induced sniffing behavior in rats. *PLoS One* 2012;7:e51227. doi:10.1371/journal.pone.0051227
47. Edwin Thanarajah S, Hoffstall V, Rigoux L, Hanssen R, Brüning JC, Tittgemeyer M. The role of insulin sensitivity and intranasally applied insulin on olfactory perception. *Sci Rep* 2019;9:7222. doi:10.1038/s41598-019-43693-7
48. Hinds JW, McNelly NA. Capillaries in aging rat olfactory bulb: a quantitative light and electron microscopic analysis. *Neurobiol Aging* 1982;3:197-207.
49. Villena A, Vidal L, Díaz F, Pérez De Vargas I. Stereological changes in the capillary network of the aging dorsal lateral geniculate nucleus. *Anat Rec A Discov Mol Cell Evol Biol* 2003;274:857-861.
50. Burns EM, Kruckeberg TW, Gaetano PK. Changes with age in cerebral capillary morphology. *Neurobiol Aging* 1981;2:283-291.
51. Ronan L, Alexander-Bloch AF, Wagstyl K, et al. Obesity associated with increased brain age from midlife. *Neurobiol Aging* 2016;47:63-70.
52. Aanerud J, Borghammer P, Chakravarty MM, et al. Brain energy metabolism and blood flow differences in healthy aging. *J Cereb Blood Flow Metab* 2012;32:1177-1187.
53. Dutta S, Sengupta P. Men and mice: relating their ages. *Life Sci* 2016;152:244-248.

Bibliography

Abbott, N.J., Ronnback, L., and Hansson, E. (2006). Astrocyte-endothelial interactions at the bloodbrain barrier. Nat Rev Neurosci 7, 41-53

Abizaid, A., Liu, Z. W., Andrews, Z. B., Shanabrough, M., Borok, E., Elsworth, J. D., ... & Horvath, T. L. (2006). Ghrelin modulates the activity and synaptic input organization of midbrain dopamine neurons while promoting appetite. The Journal of clinical investigation, 116(12), 3229-3239.

Adriaenssens, A.E., Biggs, E.K., Darwish, T., Tadross, J., Sukthankar, T., Girish, M., Polex-Wolf, J., Lam, B.Y., Zvetkova, I., Pan, W., et al. (2019). Glucose-dependent insulinotropic polypeptide receptor-expressing cells in the hypothalamus regulate food intake. Cell Metab. 30, 987–996.e6.

Adrian, T.E., Savage, A.P., Sagor, G.R., Allen, J.M., Bacarese-Hamilton, A.J., Tatemoto, K., Polak, J.M., and Bloom, S.R. (1985). Effect of peptide YY on gastric, pancreatic, and biliary function in humans. Gastroenterology 89, 494-499.

Agrawal R, Reno CM, Sharma S, Christensen C, Huang Y, Fisher SJ. Insulin action in the brain regulates both central and peripheral functions. Am J Physiol Endocrinol Metab. 2021 Jul 1;321(1):E156-E163. doi: 10.1152/ajpendo.00642.2020. Epub 2021 May 31. PMID: 34056920; PMCID: PMC8321819.

Ahima, R.S. (2000). Leptin and the neuroendocrinology of fasting. Front Horm Res 26, 42-56.

Ahmadian M, Duncan RE, Sul HS. The skinny on fat: lipolysis and fatty acid utilization in adipocytes. Trends Endocrinol Metab. 2009 Nov;20(9):424-8. doi: 10.1016/j.tem.2009.06.002. Epub 2009 Sep 30. PMID: 19796963; PMCID: PMC2764815.

Ahn, S., Choi, M., Kim, H., Yang, E. J., Mahmood, U., Kang, S. I., ... & Kim, H. S. (2018). Transient anosmia induces depressive-like and anxiolytic-like behavior and reduces amygdalar corticotropin-releasing hormone in a ZnSO4-induced mouse model. Chemical senses, 43(4), 213-221.

Ahrén B (2000) Autonomic regulation of islet hormone secretion –- implications for health and disease. Diabetologia 43(4):393–410. https://doi.org/10.1007/s001250051322

Ahrén B. Glucagon--Early breakthroughs and recent discoveries. Peptides. 2015 May;67:74-81. doi: 10.1016/j.peptides.2015.03.011. Epub 2015 Mar 23. PMID: 25814364.

Ahrén, B., & Holst, J. J. (2001). The cephalic insulin response to meal ingestion in humans is dependent on both cholinergic and noncholinergic mechanisms and is important for postprandial glycemia. Diabetes, 50(5), 1030–1038.

Aimé P, Palouzier-Paulignan B, Salem R, Al Koborssy D, Garcia S, Duchamp C, Romestaing C, Julliard a. K (2014) Modulation of olfactory sensitivity and glucose-sensing by the feeding state in obese Zucker rats. Front Behav Neurosci 8:1–17 Available at: http://journal.frontiersin.org/journal/10.3389/fnbeh.2014.00326/full.

Aimé, P., Duchamp-Viret, P., Chaput, M. A., Savigner, A., Mahfouz, M., & Julliard, A. K. (2007). Fasting increases and satiation decreases olfactory detection for a neutral odor in rats. Behavioural brain research, 179(2), 258-264.

Aimé, P., Hegoburu, C., Jaillard, T., Degletagne, C., Garcia, S., Messaoudi, B., ... & Julliard, A. K. (2012). A physiological increase of insulin in the olfactory bulb decreases detection of a learned aversive odor and abolishes food odor-induced sniffing behavior in rats. PLoS One, 7(12), e51227.

Air EL, Benoit SC, Blake Smith KA, Clegg DJ, Woods SC. Acute third ventricular administration of insulin decreases food intake in two paradigms. Pharmacol Biochem Behav. 2002 May;72(1-2):423-9. doi: 10.1016/s0091-3057(01)00780-8. PMID: 11900815.

Al Koborssy D, Palouzier-Paulignan B, Salem R, Thevenet M, Romestaing C, Julliard a. K (2014) Cellular and molecular cues of glucose sensing in the rat olfactory bulb. Front Neurosci 8:1–14 Available at: http://journal.frontiersin.org/article/10.3389/fnins.2014.00333/abstract.

Alberts, J. R., & Galef Jr, B. G. (1971). Acute anosmia in the rat: a behavioral test of a peripherally-induced olfactory deficit. Physiology & behavior, 6(5), 619-621.

Allen, Y.S., Adrian, T.E., Allen, J.M., Tatemoto, K., Crow, T.J., Bloom, S.R., and Polak, J.M. (1983). Neuropeptide Y distribution in the rat brain. Science 221, 877-879.

Alvarez, E., Roncero, I., Chowen, J. A., Thorens, B., & Blázquez, E. (1996). Expression of the glucagon-like peptide-1 receptor gene in rat brain. Journal of neurochemistry, 66(3), 920-927.

Amouyal C, Castel J, Guay C, Lacombe A, Denom J, Migrenne-Li S, Rouault C, Marquet F, Georgiadou E, Stylianides T, Luquet S, Le Stunff H, Scharfmann R, Clément K, Rutter GA, Taboureau O, Magnan C, Regazzi R, Andreelli F. A surrogate of Roux-en-Y gastric bypass (the enterogastro anastomosis surgery) regulates multiple beta-cell pathways during resolution of diabetes in ob/ob mice. EBioMedicine. 2020 Aug;58:102895. doi: 10.1016/j.ebiom.2020.102895. Epub 2020 Jul 30. PMID: 32739864; PMCID: PMC7393530.

Amouyal, C, and F Andreelli. “What is the evidence for metabolic surgery for type 2 diabetes? A critical perspective.” Diabetes & metabolism vol. 43,1 (2017): 9-17. doi:10.1016/j.diabet.2016.06.005.

Anand BK, Brobeck JR (1951) Localization of a “feeding center” in the hypothalamus of the rat. Proc Soc Exp Biol Med. 77: 323-4.

Anand, B.K., Chhina, G.S., Sharma, K.N., Dua, S., and Singh, B. (1964). Activity of single neurons in the hypothalamic feeding centers: effect of glucose. Am J Physiol 207, 1146-1154.

Andreelli F, Ziegler O. Comment prendre en charge le syndrome métabolique? [How to manage the metabolic syndrome?]. Ann Endocrinol (Paris). 2005 Apr;66(2 Pt 3):2S36-45. French. PMID: 15959395.

Apelbaum AF, Perrut A, Chaput M. Orexin A effects on the olfactory bulb spontaneous activity and odor responsiveness in freely breathing rats. Regul Pept. 2005 Jul 15;129(1-3):49-61. doi: 10.1016/j.regpep.2005.01.003. PMID: 15927698.

Ariyasu, H., Takaya, K., Tagami, T., Ogawa, Y., Hosoda, K., Akamizu, T., Suda, M., Koh, T., Natsui, K., Toyooka, S., et al. (2001). Stomach is a major source of circulating ghrelin, and feeding state determines plasma ghrelin-like immunoreactivity levels in humans. J Clin Endocrinol Metab 86, 4753- 4758.

Astic L, Saucier D, Coulon P, Lafay F, Flamand A (1993) The CVS strain of rabies virus as transneuronal tracer in the olfactory system of mice. Brain Res 619:146-156.

Ast J, Arvaniti A, Fine NHF, Nasteska D, Ashford FB, Stamataki Z, Koszegi Z, Bacon A, Jones BJ, Lucey MA, Sasaki S, Brierley DI, Hastoy B, Tomas A, D'Agostino G, Reimann F, Lynn FC, Reissaus CA, Linnemann AK, D'Este E, Calebiro D, Trapp S, Johnsson K, Podewin T, Broichhagen J, Hodson DJ. Super-resolution microscopy compatible fluorescent probes reveal endogenous glucagon-like peptide-1 receptor distribution and dynamics. Nat Commun. 2020 Jan 24;11(1):467. doi: 10.1038/s41467-020-14309-w. Erratum in: Nat Commun. 2020 Oct 9;11(1):5160. PMID: 31980626; PMCID: PMC6981144.

Avruch J. MAP kinase pathways: the first twenty years. Biochim Biophys Acta 1773:1150-1160, 2007

Azegami, T., Yuki, Y., Sawada, S., Mejima, M., Ishige, K., Akiyoshi, K., ... & Kiyono, H. (2017). Nanogel-based nasal ghrelin vaccine prevents obesity. Mucosal immunology, 10(5), 1351-1360.

Baggio LL, Drucker DJ. Glucagon-like peptide-1 receptor co-agonists for treating metabolic disease. Mol Metab. 2021 Apr;46:101090. doi: 10.1016/j.molmet.2020.101090. Epub 2020 Sep 25. PMID: 32987188; PMCID: PMC8085566.

Baggio, L.L., Huang, Q., Brown, T.J., Drucker, D.J., 2004. Oxyntomodulin and glucagon-like peptide-1 differentially regulate murine food intake and energy expenditure. Gastroenterology 127:546e558.

Bakos J, Zatkova M, Bacova Z, Ostatnikova D. The Role of Hypothalamic Neuropeptides in Neurogenesis and Neuritogenesis. Neural Plast. 2016;2016:3276383. doi: 10.1155/2016/3276383. Epub 2016 Jan 13. PMID: 26881105; PMCID: PMC4737468.

Baly C, Aioun J, Badonnel K, Lacroix M-C, Durieux D, Schlegel C, Salesse R, Caillol M (2007) Leptin and its receptors are present in the rat olfactory mucosa and modulated by the nutritional status. Brain Res 1129:130–141.

Banks WA, Kastin AJ, Pan W (1999) Uptake and degradation of blood-borne insulin by the olfactory bulb. Peptides 20:373–378.

Baroncini, M., Jissendi, P., Balland, E., Besson, P., Pruvo, J.P., Francke, J.P., Dewailly, D., Blond, S., and Prevot, V. (2012). MRI atlas of the human hypothalamus. Neuroimage 59, 168-180.

Barone FC, Wayner MJ, Scharoun SL, Guevara-Aguilar R, Aguilar-Baturoni HU (1981) Afferent connections to the lateral hypothalamus: a horseradish peroxidase study in the rat. Brain Res Bull 7:75-88.

Barrera, J. G., Jones, K. R., Herman, J. P., D'Alessio, D. A., Woods, S. C., & Seeley, R. J. (2011). Hyperphagia and increased fat accumulation in two models of chronic CNS glucagon-like peptide-1 loss of function. The Journal of neuroscience : the official journal of the Society for Neuroscience, 31(10), 3904–3913.

Bastías-Pérez, M., Serra, D., & Herrero, L. (2020). Dietary options for rodents in the study of obesity. Nutrients, 12(11), 3234.

Bataille, D., Tatemoto, K., Gespach, C., Jornvall, H., Rosselin, G., Mutt, V., 1982. Isolation of glucagon-37 (bioactive enteroglucagon/oxyntomodulin) from porcine jejuno-ileum. Characterization of the peptide. FEBS Letters 146:79e86.

Batterham, R. L., D. H. ffytche, J. M. Rosenthal, F. O. Zelaya, G. J. Barker, D. J. Withers & S. C. Williams: PYY modulation of cortical and hypothalamic brain areas predicts feeding behaviour in humans. Nature, 450, 106-9 (2007).

Baumgartner, I., Pacheco-Lopez, G., Ruttimann, E.B., Arnold, M., Asarian, L., Langhans, W., et al., 2010. Hepatic-portal vein infusions of glucagon-like peptide-1 reduce meal size and increase c-Fos expression in the nucleus tractus solitarii, area postrema and central nucleus of the amygdala in rats. Journal of Neuroendocrinology 22:557e563.

Beiroa D, Imbernon M, Gallego R, Senra A, Herranz D, Villarroya F, Serrano M, Fernø J, Salvador J, Escalada J, Dieguez C, Lopez M, Frühbeck G, Nogueiras R. GLP-1 agonism stimulates brown adipose tissue thermogenesis and browning through hypothalamic AMPK. Diabetes. 2014 Oct;63(10):3346-58. doi: 10.2337/db14-0302. Epub 2014 Jun 10. PMID: 24917578.

Belfort-DeAguiar, R., & Seo, D. (2018). Food cues and obesity: overpowering hormones and energy balance regulation. Current obesity reports, 7(2), 122-129.

Bell, G.I., Santerre, R.F., Mullenbach, G.T., 1983. Hamster preproglucagon contains the sequence of glucagon and two related peptides. Nature 302: 716e718.

Benedict C, Brede S, Schiöth HB, Lehnert H, Schultes B, Born J, Hallschmid M. Intranasal insulin enhances postprandial thermogenesis and lowers postprandial serum insulin levels in healthy men. Diabetes. 2011 Jan;60(1):114-8. doi: 10.2337/db10-0329. Epub 2010 Sep 28. PMID: 20876713; PMCID: PMC3012162.

Benoit, S.C., Air, E.L., Coolen, L.M., Strauss, R., Jackman, A., Clegg, D.J., Seeley, R.J., and Woods, S.C. (2002). The catabolic action of insulin in the brain is mediated by melanocortins. J Neurosci 22, 9048-9052.

Berger S, Pho H, Fleury-Curado T, Bevans-Fonti S, Younas H, Shin MK, Jun JC, Anokye-Danso F, Ahima RS, Enquist LW, Mendelowitz D, Schwartz AR, Polotsky VY. Intranasal Leptin Relieves Sleep-disordered Breathing in Mice with Diet-induced Obesity. Am J Respir Crit Care Med. 2019 Mar 15;199(6):773-783. doi: 10.1164/rccm.201805-0879OC. PMID: 30309268; PMCID: PMC6423095.

Bernstein IL, Woods SC. Ontogeny of cephalic insulin release by the rat. Physiol Behav. 1980 Mar;24(3):529-32. doi: 10.1016/0031-9384(80)90247-4. PMID: 6990431.

Berthoud, H. R., & Jeanrenaud, B. (1982). Sham feeding-induced cephalic phase insulin release in the rat. American Journal of Physiology-Endocrinology And Metabolism, 242(4), E280-E285.

Berthoud, H. R., Albaugh, V. L., & Neuhuber, W. L. (2021). Gut-brain communication and obesity: Understanding functions of the vagus nerve. The Journal of Clinical Investigation, 131(10), e143770. https://doi.org/ 10.1172/JCI143770

Berthoud, H. R., Trimble, E. R., Siegel, E. G., Bereiter, D. A., & Jeanrenaud, B. (1980). Cephalic-phase insulin secretion in normal and pancreatic islet-transplanted rats. American Journal of Physiology, 238(4), E336–340.

Berthoud, H.R. (2006). Homeostatic and non-homeostatic pathways involved in the control of food intake and energy balance. Obesity (Silver Spring) 14 Suppl 5, 197S-200S.

Beverly, J.L., Gietzen, D.W., and Rogers, Q.R. (1990). Effect of dietary limiting amino acid in prepyriform cortex on food intake. Am J Physiol 259, R709-715.

Birsoy K, Festuccia WT, Laplante M. A comparative perspective on lipid storage in animals. J Cell Sci. 2013;126(Pt 7):1541-1552. doi:10.1242/jcs.104992

Blouet, C., Jo, Y.H., Li, X., and Schwartz, G.J. (2009). Mediobasal hypothalamic leucine sensing regulates food intake through activation of a hypothalamus-brainstem circuit. J Neurosci 29, 8302- 8311.

Blum ID, Patterson Z, Khazall R, Lamont EW, Sleeman MW, Horvath TL, Abizaid A (2009) Reduced anticipatory locomotor responses to scheduled meals in ghrelin receptor deficient mice. Neuroscience 164:351–359.

Boesveldt, S., & de Graaf, K. (2017). The differential role of smell and taste for eating behavior. Perception, 46(3-4), 307-319.

Boesveldt, S., & Lundström, J. N. (2014). Detecting fat content of food from a distance: olfactory-based fat discrimination in humans. PLoS One, 9(1), e85977.

Born J, Lange T, Kern W, McGregor GP, Bickel U, Fehm HL. Sniffing neuropeptides: a transnasal approach to the human brain. Nat Neurosci 2002;5:514–516

Bouna, S., Gysling, K., Calas, A., & Araneda, S. (1994). Some noradrenergic neurons of locus ceruleus-olfactory pathways contain neuropeptide-Y. Brain research bulletin, 34(4), 413-417.

Brady, S., Lalli, P., Midha, N., Chan, A., Garven, A., Chan, C., & Toth, C. (2013). Presence of neuropathic pain may explain poor performances on olfactory testing in diabetes mellitus patients. Chemical senses, 38(6), 497-507.

Brandt SJ, Müller TD, DiMarchi RD, Tschöp MH, Stemmer K. Peptide-based multi-agonists: a new paradigm in metabolic pharmacology. J Intern Med. 2018 Dec;284(6):581-602. doi: 10.1111/joim.12837. Epub 2018 Oct 23. PMID: 30230640.

Braun, J.-J., Renaud, M., Moliere, S., Noblet, V., Kremer, S., Dolfus, H., Riehm, S., 2019. Diagnostic findings in 60 cases of isolated and syndromic congenital olfactory dysfunction. Int. Arch Transl. Med. 5, 008.

Bray GA, Flatt JP, Volaufova J, Delany JP, Champagne CM. Corrective responses in human food intake identified from an analysis of 7-d food-intake records. Am J Clin Nutr. 2008;88(6):1504-1510. doi:10.3945/ajcn.2008.26289

Brierley, D. I., Holt, M. K., Singh, A., de Araujo, A., McDougle, M., Vergara, M., ... & Trapp, S. (2021). Central and peripheral GLP-1 systems independently suppress eating. Nature metabolism, 3(2), 258-273.

Brubaker, P.L., Anini, Y., 2003. Direct and indirect mechanisms regulating secretion of glucagon-like peptide-1 and glucagon-like peptide-2. Canadian Journal of Physiology and Pharmacology 81:1005e1012.

Bruce CR, Hamley S, Ang T, Howlett KF, Shaw CS, Kowalski GM. Translating glucose tolerance data from mice to humans: Insights from stable isotope labelled glucose tolerance tests. Mol Metab. 2021 Nov;53:101281. doi: 10.1016/j.molmet.2021.101281. Epub 2021 Jun 24. PMID: 34175474; PMCID: PMC8313600.

Brüning JC, Gautam D, Burks DJ, Gillette J, Schubert M, Orban PC, Klein R, Krone W, Müller-Wieland D, Kahn CR. Role of brain insulin receptor in control of body weight and reproduction. Science. 2000 Sep 22;289(5487):2122-5. doi: 10.1126/science.289.5487.2122. PMID: 11000114.

Buck L, Axel R (1991) A novel multigene family may encode odorant receptors: a molecular basis for odor recognition. Cell 65:175–187.

Buffa, R., Capella, C., Fontana, P., Usellini, L., Solcia, E., 1978. Types of endocrine cells in the human colon and rectum. Cell and Tissue Research 192:227e240.

Buijs RM, Chun SJ, Niijima A, Romijn HJ, Nagai K (2001) Parasympathetic and sympathetic control of the pancreas: a role for the suprachiasmatic nucleus and other hypothalamic centers that are involved in the regulation of food intake. J Comp Neurol 431(4):405–423. https://doi.org/10.1002/1096-9861(20010319) 431:43.0.CO;2-D

Bullock BP, Heller RS, Habener JF: Tissue distribution of messenger ribonucleic acid encoding the rat glucagon-like peptide-1 receptor. Endocrinology 137:2968-2978, 1996

Buonviso, N., and Gurden, H. (2013). Codage dans le bulbe olfactif principal des Mammifères. Odorat et goût: De la neurobiologie des sens chimiques aux applications, 171. Eds : Roland Salesse et Rémi Gervais.

Burmeister, M. A., Ayala, J. E., Smouse, H., Landivar-Rocha, A., Brown, J. D., Drucker, D. J., ... & Ayala, J. E. (2017). The hypothalamic glucagon-like peptide 1 receptor is sufficient but not necessary for the regulation of energy balance and glucose homeostasis in mice. Diabetes, 66(2), 372-384.

Cabanac M, Duclaux R (1973) Olfactory-gustatory alliesthesia and food intake in humans. J Physiol (Paris) 66:113–135.

Cabanac, M., & Fantino, M. (1977). Origin of olfacto-gustatory alliesthesia: intestinal sensitivity to carbohydrate concentration?. Physiology & Behavior, 18(6), 1039-1045.

Cabou C, Vachoux C, Campistron G, Drucker DJ, Burcelin R. Brain GLP-1 signaling regulates femoral artery blood flow and insulin sensitivity through hypothalamic PKC-δ. Diabetes. 2011 Sep;60(9):2245-56. doi: 10.2337/db11-0464. Epub 2011 Aug 1. PMID: 21810595; PMCID: PMC3161335.

Cahill GF Jr. The Banting Memorial Lecture 1971. Physiology of insulin in man. Diabetes. 1971 Dec;20(12):785-99. doi: 10.2337/diab.20.12.785. PMID: 4941092

Caillol, M., Aïoun, J., Baly, C., Persuy, M. A., & Salesse, R. (2003). Localization of orexins and their receptors in the rat olfactory system: possible modulation of olfactory perception by a neuropeptide synthetized centrally or locally. Brain research, 960(1-2), 48-61.

Calanna, S., Christensen, M., Holst, J.J., Laferrere, B., Gluud, L.L., Vilsboll, T., et al., 2013. Secretion of glucagon-like peptide-1 in patients with type 2 diabetes mellitus: systematic review and meta-analyses of clinical studies. Diabetologia 56:965e972.

Campfield, L. A., & Blocker, D. C. (1979). Simulation of the autonomic neural control of insulin secretion. Computers in biology and medicine, 9(3), 191-203.

Campfield LA, Smith FJ, Eskinazi RE. Glucose responsiveness and acetylcholine sensitivity of pancreatic -cells after vagotomy. Am J Physiol Regul Integr Comp Physiol 246: R985–R993, 1984.

Campfield LA, Smith FJ, Settle JE, Sohaey R. Effect of the order of application of neural inputs on insulin secretion. Adv Exp Med Biol 211: 343–349, 1986.

Cantley LC. The phosphoinositide 3-kinase pathway. Science 296:1655-1657, 2002

Catamo, E., Tornese, G., Concas, M. P., Gasparini, P., & Robino, A. (2021). Differences in taste and smell perception between type 2 diabetes mellitus patients and healthy controls. Nutrition, Metabolism and Cardiovascular Diseases, 31(1), 193-200.

Chaudhury, A., Duvoor, C., Reddy Dendi, V. S., Kraleti, S., Chada, A., Ravilla, R., ... & Mirza, W. (2017). Clinical review of antidiabetic drugs: implications for type 2 diabetes mellitus management. Frontiers in endocrinology, 8, 6.

Chelette BM, Loeven AM, Gatlin DN, Landi Conde DR, Huffstetler CM, Qi M, Fadool DA. Consumption of dietary fat causes loss of olfactory sensory neurons and associated circuitry that is not mitigated by voluntary exercise in mice. J Physiol. 2022 Mar;600(6):1473-1495. doi: 10.1113/JP282112. Epub 2021 Dec 7. PMID: 34807463.

Chelminski Y, Magnan C, Luquet SH, Everard A, Meunier N, Gurden H, Martin C. Odor-Induced Neuronal Rhythms in the Olfactory Bulb Are Profoundly Modified in ob/ob Obese Mice. Front Physiol. 2017 Jan 19;8:2. doi: 10.3389/fphys.2017.00002. PMID: 28154537; PMCID: PMC5244437.

Chen, Y., Lin, Y. C., Kuo, T. W., & Knight, Z. A. (2015). Sensory detection of food rapidly modulates arcuate feeding circuits. Cell, 160(5), 829-841.

Chess A, Simon I, Cedar H, Axel R (1994) Allelic inactivation regulates olfactory receptor gene expression. Cell 78:823–834.

Chien HJ, Chiang TC, Peng SJ et al (2019) Human pancreatic afferent and efferent nerves: mapping and 3-D illustration of exocrine, endocrine, and adipose innervation. Am J Physiol Gastrointest Liver Physiol 317(5):G694–G706. https://doi.org/10. 1152/ajpgi.00116.2019

Christensen DH, Rungby J, Thomsen RW. Nationwide trends in glucose-lowering drug use, Denmark, 1999-2014. Clin Epidemiol. 2016 Oct 14;8:381-387. doi: 10.2147/CLEP.S113211. PMID: 27789974; PMCID: PMC5072551.

Christensen, M., Vedtofte, L., Holst, J.J., Vilsbøll, T., and Knop, F.K. (2011). Glucose-dependent insulinotropic polypeptide: a bifunctional glucose-dependent regulator of glucagon and insulin secretion in humans. Diabetes 60, 3103–3109.

Clark, J.T., Kalra, P.S., Crowley, W.R., and Kalra, S.P. (1984). Neuropeptide Y and human pancreatic polypeptide stimulate feeding behavior in rats. Endocrinology 115, 427-429.

Clement, L., C. Cruciani-Guglielmacci, C. Magnan, M. Vincent, L. Douared, M. Orosco, F. AssimacopoulosJeannet, L. Penicaud & A. Ktorza: Intracerebroventricular infusion of a triglyceride emulsion leads to both altered insulin secretion and hepatic glucose production in rats. Pflugers Arch, 445, 375-80 (2002).

Cohen, A. O., Matese, N. G., Filimontseva, A., Shen, X., Shi, T. C., Livne, E., & Hartley, C. A. (2019). Aversive learning strengthens episodic memory in both adolescents and adults. Learning & Memory, 26(7), 272-279.

Collin, M., Backberg, M., Ovesjo, M.L., Fisone, G., Edwards, R.H., Fujiyama, F., and Meister, B. (2003). Plasma membrane and vesicular glutamate transporter mRNAs/proteins in hypothalamic neurons that regulate body weight. Eur J Neurosci 18, 1265-1278.

Collins, S., Martin, T. L., Surwit, R. S., & Robidoux, J. (2004). Genetic vulnerability to diet-induced obesity in the C57BL/6J mouse: physiological and molecular characteristics. Physiology & behavior, 81(2), 243-248.

Coluzzi, I., Raparelli, L., Guarnacci, L., Paone, E., Del Genio, G., le Roux, C.W., Silecchia, G., 2016. Food intake and changes in eating behavior after laparoscopic sleeve gastrectomy. Obes. Surg. 26, 2059–2067.

Cowley, M.A., Smith, R.G., Diano, S., Tschöp, M., Pronchuk, N., Grove, K.L., Strasburger, C.J., Bidlingmaier, M., Esterman, M., Heiman, M.L., et al. (2003). The distribution and mechanism of action of ghrelin in the CNS demonstrates a novel hypothalamic circuit regulating energy homeostasis. Neuron 37, 649-661.

Creutzfeldt W: The [pre-] history of the incretin concept. Regul Pept 128:87-91, 2005.

Cruciani-Guglielmacci C, Magnan C. Brain lipoprotein lipase as a regulator of energy balance. Biochimie. 2017 Dec;143:51-55. doi: 10.1016/j.biochi.2017.07.012. Epub 2017 Jul 24. PMID: 28751218.

Cruciani-Guglielmacci, C., A. Hervalet, L. Douared, N. M. Sanders, B. E. Levin, A. Ktorza & C. Magnan: Beta oxidation in the brain is required for the effects of nonesterified fatty acids on glucose-induced insulin secretion in rats. Diabetologia, 47, 2032-8 (2004).

Cruciani-Guglielmacci, C., Vincent-Lamon, M., Rouch, C., Orosco, M., Ktorza, A., & Magnan, C. (2005). Early changes in insulin secretion and action induced by high-fat diet are related to a decreased sympathetic tone. American Journal of Physiology-Endocrinology and Metabolism, 288(1), E148-E154.

Cummings, D.E., and Overduin, J. (2007). Gastrointestinal regulation of food intake. J Clin Invest 117, 13-23.

Cummings, D.E., Purnell, J.Q., Frayo, R.S., Schmidova, K., Wisse, B.E., and Weigle, D.S. (2001). A preprandial rise in plasma ghrelin levels suggests a role in meal initiation in humans. Diabetes 50, 1714-1719.

Czernichow S, Renuy A, Rives-Lange C, Carette C, Airagnes G, Wiernik E, Ozguler A, Kab S, Goldberg M, Zins M, Matta J. Evolution of the prevalence of obesity in the adult population in France, 2013-2016: the Constances study. Sci Rep. 2021 Jul 8;11(1):14152. doi: 10.1038/s41598-021-93432-0. PMID: 34238998; PMCID: PMC8266816.

Date, Y., Kojima, M., Hosoda, H., Sawaguchi, A., Mondal, M.S., Suganuma, T., Matsukura, S., Kangawa, K., and Nakazato, M. (2000). Ghrelin, a novel growth hormone-releasing acylated peptide, is synthesized in a distinct endocrine cell type in the gastrointestinal tracts of rats and humans. Endocrinology 141, 4255-4261.

Daumas-Meyer V, Champeil-Potokar G, Chaumontet C, Dahirel P, Papillon C, Congar P, Denis I. Fasting induces astroglial plasticity in the olfactory bulb glomeruli of rats. Glia. 2018 Apr;66(4):762-776. doi: 10.1002/glia.23280. Epub 2017 Dec 11. PMID: 29226549.

Davidson, T.L., Chan, K., Jarrard, L.E., Kanoski, S.E., Clegg, D.J., and Benoit, S.C. (2009). Contributions of the hippocampus and medial prefrontal cortex to energy and body weight regulation. Hippocampus 19, 235-252.

De Olmos J, Hardy H, Heimer L (1978) The afferent connections of the main and the accessory olfactory bulb formations in the rat: an experimental HRP-study. J Comp Neurol 181:213-244.

De Silva, A., Salem, V., Long, C.J., Makwana, A., Newbould, R.D., Rabiner, E.A., et al., 2011. The gut hormones PYY 3-36 and GLP-1 7-36 amide reduce food intake and modulate brain activity in appetite centers in humans. Cell Metabolism 14:700e706.

Deacon CF, Johnsen AH, Holst JJ: Degradation of glucagon-like peptide-1 by human plasma in vitro yields an N-terminally truncated peptide that is a major endogenous metabolite in vivo. J Clin Endocrinol Metab 80:952-957, 1995.

Deacon CF, Plamboeck A, Moller S, Holst JJ: GLP-1-(9-36) amide reduces blood glucose in anesthetized pigs by a mechanism that does not involve insulin secretion. Am J Physiol Endocrinol Metab 282:E873-879, 2002.

Deacon CF, Pridal L, Klarskov L, Olesen M, Holst JJ: Glucagon-like peptide 1 undergoes differential tissue-specific metabolism in the anesthetized pig. Am J Physiol 271:E458-464, 1996.

DeFronzo, R. A. (2009). From the triumvirate to the ominous octet: a new paradigm for the treatment of type 2 diabetes mellitus. Diabetes, 58(4), 773-795.

Derewenda, U., Derewenda, Z., Dodson, E. et al. Phenol stabilizes more helix in a new symmetrical zinc insulin hexamer. Nature 338, 594–596 (1989). https://doi.org/10.1038/338594a0.

Diamond P, LeBlanc J. A role for insulin in cephalic phase of postprandial thermogenesis in dogs. Am J Physiol. 1988 May;254(5 Pt 1):E625-32. doi: 10.1152/ajpendo.1988.254.5.E625. PMID: 3284384.

Dinarello CA, Donath MY, Mandrup-Poulsen T. Role of IL-1beta in type 2 diabetes. Curr Opin Endocrinol Diabetes Obes. 2010 Aug;17(4):314-21. doi: 10.1097/MED.0b013e32833bf6dc. PMID: 20588114.

Ding L, Gao R, Xiong XQ, Gao XY, Chen Q, Li YH, Kang YM, Zhu GQ. GABA in Paraventricular Nucleus Regulates Adipose Afferent Reflex in Rats. PLoS One. 2015 Aug 28;10(8):e0136983. doi: 10.1371/journal.pone.0136983. PMID: 26317425; PMCID: PMC4552845.

Doty, R. L. (1986). Odor-guided behavior in mammals. Experientia, 42(3), 257-271.

Doyle, K. L., Karl, T., Hort, Y., Duffy, L., Shine, J., & Herzog, H. (2008). Y1 receptors are critical for the proliferation of adult mouse precursor cells in the olfactory neuroepithelium. Journal of neurochemistry, 105(3), 641-652.

Drewnowski, A., Krahn, D.D., Demitrack, M.A., Nairn, K., Gosnell, B.A., 1995. Naloxone, an opiate blocker, reduces the consumption of sweet high-fat foods in obese and lean female binge eaters. Am. J. Clin. Nutr. 61, 1206–1212.

Drewnowski, A., Renderson, S.A., Driscoll, A., Rolls, B.J., 1997. The dietary variety score: assessing diet quality in healthy young and older adults. J. Am. Diet Assoc. 97, 266–271.

Drucker, D.J., 2006. The biology of incretin hormones. Cell Metabolism 3:153e165.

Drucker, D. J., Philippe, J., Mojsov, S., Chick, W. L., & Habener, J. F. (1987). Glucagon-like peptide I stimulates insulin gene expression and increases cyclic AMP levels in a rat islet cell line. Proceedings of the National Academy of Sciences, 84(10), 3434-3438.

Dupre, J., Ross, S. A., Watson, D., and Brown, J. C. (1973). Stimulation of insulin secretion by gastric inhibitory polypeptide in man. Journal of Clinical Endocrinology and Metabolism, 37, 826-828.

Edwin Thanarajah S, Hoffstall V, Rigoux L, Hanssen R, Brüning JC, Tittgemeyer M. The role of insulin sensitivity and intranasally applied insulin on olfactory perception. Sci Rep. 2019 May 10;9(1):7222. doi: 10.1038/s41598-019-43693-7. PMID: 31076634; PMCID: PMC6510903.

Egawa, M., Yoshimatsu, H., and Bray, G.A. (1989). Lateral hypothalamic injection of 2-deoxy-Dglucose suppresses sympathetic activity. Am J Physiol 257, R1386-1392.

Eissele, R., Goke, R., Willemer, S., Harthus, H.P., Vermeer, H., Arnold, R., et al., 1992. Glucagon-like peptide-1 cells in the gastrointestinal tract and pancreas of rat, pig and man. European Journal of Clinical Investigation 22:283e291.

Elias, C.F., Lee, C., Kelly, J., Aschkenasi, C., Ahima, R.S., Couceyro, P.R., Kuhar, M.J., Saper, C.B., and Elmquist, J.K. (1998). Leptin activates hypothalamic CART neurons projecting to the spinal cord. Neuron 21, 1375-1385.

Elmquist JK, Bjørbaek C, Ahima RS, Flier JS, Saper CB (1998) Distributions of leptin receptor mRNA isoforms in the rat brain. J Comp Neurol 395:535–547.

Elmquist JK, Elias CF, Saper CB. From lesions to leptin: hypothalamic control of food intake and body weight. Neuron. 1999 Feb;22(2):221-32. doi: 10.1016/s0896-6273(00)81084-3. PMID: 10069329.

Elmquist, J. K. & J. N. Marcus: Rethinking the central causes of diabetes. Nat Med, 9, 645-7 (2003).

Emond, M., Schwartz, G.J., and Moran, T.H. (2001). Meal-related stimuli differentially induce c-Fos activation in the nucleus of the solitary tract. Am J Physiol Regul Integr Comp Physiol 280, R1315- 1321.

Erbil D, Eren CY, Demirel C, Küçüker MU, Solaroğlu I, Eser HY. GLP-1's role in neuroprotection: a systematic review. Brain Inj. 2019;33(6):734-819. doi: 10.1080/02699052.2019.1587000. Epub 2019 Apr 2. PMID: 30938196.

Eschwege, Eveline & Charles, M. & Basdevant, A.. (2009). Obepi Enquête épidémiologique nationale sur le surpoids et l'obésité. Une enquête INSERM, TNS Healthcare (Kantarhealth), Roche.

Esteban, O., Birman, D., Schaer, M., Koyejo, O. O., Poldrack, R. A., & Gorgolewski, K. J. (2017). MRIQC: Advancing the automatic prediction of image quality in MRI from unseen sites. PloS one, 12(9), e0184661.

Esteban O, Markiewicz CJ, Blair RW, Moodie CA, Isik AI, Erramuzpe A, Kent JD, Goncalves M, DuPre E, Snyder M, Oya H, Ghosh SS, Wright J, Durnez J, Poldrack RA, Gorgolewski KJ. fMRIPrep: a robust preprocessing pipeline for functional MRI. Nat Methods. 2019 Jan;16(1):111-116. doi: 10.1038/s41592-018-0235-4. Epub 2018 Dec 10. PMID: 30532080; PMCID: PMC6319393.

Eyre MD, Antal M, & Nusser Z (2008). Distinct deep short-axon cell subtypes of the main olfactory bulb provide novel intrabulbar and extrabulbar GABAergic connections. J Neurosci 28, 8217–8229.

Faber CL, Deem JD, Campos CA, Taborsky GJ Jr, Morton GJ. CNS control of the endocrine pancreas. Diabetologia. 2020 Oct;63(10):2086-2094. doi: 10.1007/s00125-020-05204-6. Epub 2020 Sep 7. PMID: 32894319; PMCID: PMC7983553.

Fadool DA, Tucker K, Pedarzani P (2011) Mitral cells of the olfactory bulb perform metabolic sensing and are disrupted by obesity at the level of the Kv1.3 ion channel. PLoS One 6.

Fadool DA, Tucker K, Perkins R, Fasciani G, Thompson RN, Parsons AD, Overton JM, Koni PA, Flavell RA, Kaczmarek LK (2004) Kv1.3 channel gene-targeted deletion produces "Super-Smeller Mice" with altered glomeruli, interacting scaffolding proteins, and biophysics. Neuron 41:389-404.

Fadool DA, Tucker K, Phillips JJ, Simmen JA (2000) Brain insulin receptor causes activity-dependent current suppression in the olfactory bulb through multiple phosphorylation of Kv1.3. J Neurophysiol 83:2332–2348.

Fadool, D. A., & Levitan, I. B. (1998). Modulation of olfactory bulb neuron potassium current by tyrosine phosphorylation. Journal of Neuroscience, 18(16), 6126-6137.

Faerch, K., Torekov, S.S., Vistisen, D., Johansen, N.B., Witte, D.R., Jonsson, A., et al., 2015. GLP-1 response to oral glucose is reduced in prediabetes, screen-detected type 2 diabetes, and obesity and influenced by sex: the ADDITION-PRO study. Diabetes 64:2513e2525.

Faour, M., Magnan, C., Gurden, H., & Martin, C. (2022). Olfaction in the context of obesity and diabetes: insights from animal models to humans. Neuropharmacology, 206, 108923.

Faria, A. V., Joel, S. E., Zhang, Y., Oishi, K., van Zjil, P. C., Miller, M. I., ... & Mori, S. (2012). Atlas-based analysis of resting-state functional connectivity: Evaluation for reproducibility and multi-modal anatomy–function correlation studies. Neuroimage, 61(3), 613-621.

Ferriday, D., & Brunstrom, J. M. (2008). How does food-cue exposure lead to larger meal sizes?. British Journal of Nutrition, 100(6), 1325-1332.

Field BC, Chaudhri OB, Bloom SR. Bowels control brain: gut hormones and obesity. Nat Rev Endocrinol. 2010 Aug;6(8):444-53. doi: 10.1038/nrendo.2010.93. PMID: 20585346.

Figlewicz, D. P., Evans, S. B., Murphy, J., Hoen, M., & Baskin, D. G. (2003). Expression of receptors for insulin and leptin in the ventral tegmental area/substantia nigra (VTA/SN) of the rat. Brain research, 964(1), 107-115.

Figlewicz, D.P., Stein, L.J., West, D., Porte, D., Jr., and Woods, S.C. (1986). Intracisternal insulin alters sensitivity to CCK-induced meal suppression in baboons. Am J Physiol 250, R856-860.

Finan, B., Ma, T., Ottaway, N., Muller, T.D., Habegger, K.M., Heppner, K.M., et al., 2013. Unimolecular dual incretins maximize metabolic benefits in rodents, monkeys, and humans. Science Translational Medicine 5, 209ra151.

Finan, B., Müller, T.D., Clemmensen, C., Perez-Tilve, D., DiMarchi, R.D., and Tschöp, M.H. (2016). Reappraisal of GIP pharmacology for metabolic diseases. Trends Mol. Med. 22, 359–376.

Fioramonti X, Chrétien C, Leloup C, Pénicaud L. Recent Advances in the Cellular and Molecular Mechanisms of Hypothalamic Neuronal Glucose Detection. Front Physiol. 2017 Nov 14;8:875. doi: 10.3389/fphys.2017.00875. PMID: 29184506; PMCID: PMC5694446.

Firestein S (2001) How the olfactory system makes sense of scents. Nature 413:211–218.

Friedman JM (1998) Leptin, leptin receptors, and the control of body weight. Nutr Rev 56:s38–s46; discussion s54–s75.

Frimurer, T. M., & Bywater, R. P. (1999). Structure of the integral membrane domain of the GLP1 receptor. Proteins: Structure, Function, and Bioinformatics, 35(4), 375-386.

Fujita, N., Sakamaki, H., Uotani, S., Takahashi, R., Kuwahara, H., Kita, A., Oshima, K., Yamasaki, H., Yamaguchi, Y., and Eguchi, K. (2003). Intracerebroventricular administration of insulin and glucose inhibits the anorectic action of leptin in rats. Exp Biol Med (Maywood) 228, 1156-1161.

Furman BL. Streptozotocin-Induced Diabetic Models in Mice and Rats. Curr Protoc Pharmacol. 2015 Sep 1;70:5.47.1-5.47.20. doi: 10.1002/0471141755.ph0547s70. PMID: 26331889.

Gallwitz B, Schmidt WE, Conlon JM, Creutzfeldt W: Glucagon-like peptide-1(7- 36)amide: characterization of the domain responsible for binding to its receptor on rat insulinoma RINm5F cells. J Mol Endocrinol 5:33-39, 1990.

García-García I, Jurado MÁ, Garolera M, Marqués-Iturria I, Horstmann A, Segura B, Pueyo R, Sender-Palacios MJ, Vernet-Vernet M, Villringer A, Junqué C, Margulies DS, Neumann J. Functional network centrality in obesity: A resting-state and task fMRI study. Psychiatry Res. 2015 Sep 30;233(3):331-8. doi: 10.1016/j.pscychresns.2015.05.017. Epub 2015 Jun 19. PMID: 26145769.

Gascuel J, Lemoine A, Rigault C, Datiche F, Benani A, Penicaud L, Lopez-Mascaraque L. Hypothalamus-olfactory system crosstalk: orexin a immunostaining in mice. Front Neuroanat. 2012 Nov 8;6:44. doi: 10.3389/fnana.2012.00044. PMID: 23162437; PMCID: PMC3492705.

Gentilella, R., Pechtner, V., Corcos, A., & Consoli, A. (2019). Glucagon-like peptide-1 receptor agonists in type 2 diabetes treatment: are they all the same?. Diabetes/metabolism research and reviews, 35(1), e3070.

Gerozissis K. Brain insulin and feeding: a bi-directional communication. Eur J Pharmacol. 2004 Apr 19;490(1-3):59-70. doi: 10.1016/j.ejphar.2004.02.044. PMID: 15094073.

Gervais R, Pager J (1979) Combined modulating effects of the general arousal and the specific hunger arousal on the olfactory bulb responses in the rat. Electroencephalogr Clin Neurophysiol 46(1): 87–94.

Gervais R, Pager J (1982) Functional changes in waking and sleeping rats after lesions in the olfactory pathways. Physiol Behav 29(1): 7–15.

Getchell T V, Kwong K, Saunders CP, Stromberg AJ, Getchell ML (2006) Leptin regulates olfactory-mediated behavior in ob/ob mice. Physiol Behav 87:848–856.

Ghasemi R, Haeri A, Dargahi L, Mohamed Z, Ahmadiani A. Insulin in the brain: sources, localization and functions. Mol Neurobiol. 2013 Feb;47(1):145-71. doi: 10.1007/s12035-012-8339-9. Epub 2012 Sep 7. PMID: 22956272.

Ghrelin enhances olfactory sensitivity and exploratory sniffing in rodents and humans. Journal of Neuroscience, 31(15), 5841-5846.

Gray SM, Meijer RI, Barrett EJ. Insulin regulates brain function, but how does it get there? Diabetes. 2014 Dec;63(12):3992-7. doi: 10.2337/db14-0340. PMID: 25414013; PMCID: PMC4237995.

Gregg, B., & Thiessen, D. D. (1981). A simple method of olfactory discrimination of urines for the Mongolian gerbil, Meriones unguiculatus. Physiology & behavior, 26(6), 1133-1136.

Gribble, F.M., Williams, L., Simpson, A.K., Reimann, F., 2003. A novel glucose-sensing mechanism contributing to glucagon-like peptide-1 secretion from the GLUTag cell line. Diabetes 52:1147e1154.

Grimelius, L., Capella, C., Buffa, R., Polak, J.M., Pearse, A.G., Solcia, E.,1976. Cytochemical and ultrastructural differentiation of enteroglucagon and pancreatic-type glucagon cells of the gastrointestinal tract. Virchows Archiv B Cell Pathology 20:217e228.

Gorgolewski, K. J., Auer, T., Calhoun, V. D., Craddock, R. C., Das, S., Duff, E. P., ... & Poldrack, R. A. (2016). The brain imaging data structure, a format for organizing and describing outputs of neuroimaging experiments. Scientific data, 3(1), 1-9.

Gudziol, V., Buschhüter, D., Abolmaali, N., Gerber, J., Rombaux, P., Hummel, T., 2009. Increasing olfactory bulb volume due to treatment of chronic rhinosinusitis—a longitudinal study. Brain 132, 3096–3101.

Guevara-Aguilar R, Jimenez-Montufar LL, Garcia-Diaz DE, Wayner MJ, Armstrong DL (1988) Olfactory and visceral projections to the paraventricular nucleus. Brain Res Bull 20:799-801.

Gupta V. Glucagon-like peptide-1 analogues: An overview. Indian J Endocrinol Metab. 2013 May;17(3):413-21. doi: 10.4103/2230-8210.111625. PMID: 23869296; PMCID: PMC3712370.

Gutièrrez-Mecinas M, Crespo C, Blasco-Ibáñez JM, Gracia-Llanes FJ, Marqués-Marí AI, Martínez-Guijarro FJ (2005) Characterization of somatostatin- and cholecystokinin-immunoreactive periglomerular cells in the rat olfactory bulb. J Comp Neurol 489:467–479.

Hajnal, A., Norgren, R., and Kovacs, P. (2009). Parabrachial coding of sapid sucrose: relevance to reward and obesity. Ann N Y Acad Sci 1170, 347-364.

Hansen L, Deacon CF, Orskov C, Holst JJ: Glucagon-like peptide-1-(7-36)amide is transformed to glucagon-like peptide-1-(9-36)amide by dipeptidyl peptidase IV in the capillaries supplying the L cells of the porcine intestine. Endocrinology 140:5356-5363, 1999.

Hansen, L., Hartmann, B., Bisgaard, T., Mineo, H., Jorgensen, P.N., Holst, J.J., 2000. Somatostatin restrains the secretion of glucagon-like peptide-1 and -2 from isolated perfused porcine ileum. American Journal of Physiology Endocrinology and Metabolism 278:E1010eE1018.

Han P, Roitzsch C, Horstmann A, Pössel M, Hummel T. Increased Brain Reward Responsivity to Food-Related Odors in Obesity. Obesity (Silver Spring). 2021 Jul;29(7):1138-1145. doi: 10.1002/oby.23170. Epub 2021 Apr 28. PMID: 33913254.

Hayden S, Bekaert M, Crider TA, Mariani S, Murphy WJ, Teeling EC (2010) Ecological adaptation determines functional mammalian olfactory subgenomes. Genome Res 20:1–9.

Hayes, M.R., Leichner, T.M., Zhao, S., Lee, G.S., Chowansky, A., Zimmer, D., et al., 2011. Intracellular signals mediating the food intake-suppressive effects of hindbrain glucagon-like peptide-1 receptor activation. Cell Metabolism 13:320e330.

Hegarty BD, Furler SM, Ye J, Cooney GJ, Kraegen EW. The role of intramuscular lipid in insulin resistance. Acta Physiol Scand. 2003 Aug;178(4):373-83. doi: 10.1046/j.1365-201X.2003.01162.x. PMID: 12864742.

Heinrich, G., Gros, P., Habener, J.F., 1984. Glucagon gene sequence. Four of six exons encode separate functional domains of rat pre-proglucagon. Journal of Biological Chemistry 259:14082e14087.

Hentges, S.T., Nishiyama, M., Overstreet, L.S., Stenzel-Poore, M., Williams, J.T., and Low, M.J. (2004). GABA release from proopiomelanocortin neurons. J Neurosci 24, 1578-1583.

Herath CB, Reynolds GW, MacKenzie DD, Davis SR, Harris PM. Vagotomy suppresses cephalic phase insulin release in sheep. Exp Physiol 84: 559–569, 1999.

Herman, J. P., Tasker, J. G., Ziegler, D. R., & Cullinan, W. E. (2002). Local circuit regulation of paraventricular nucleus stress integration: glutamate–GABA connections. Pharmacology Biochemistry and Behavior, 71(3), 457-468.

Herrmann C, Göke R, Richter G, Fehmann H, -C, Arnold R, Göke B: Glucagon-Like Peptide-1 and Glucose-Dependent Insulin-Releasing Polypeptide Plasma Levels in Response to Nutrients. Digestion 1995;56:117-126. doi: 10.1159/000201231

Hill JM, Lesniak MA, Pert CB, Roth J (1986) Autoradiographic localization of insulin receptors in rat brain: prominence in olfactory and limbic areas. Neuroscience 17: 1127–1138.

Hill, J.W., Williams, K.W., Ye, C., Luo, J., Balthasar, N., Coppari, R., Cowley, M.A., Cantley, L.C., Lowell, B.B., and Elmquist, J.K. (2008). Acute effects of leptin require PI3K signaling in hypothalamic proopiomelanocortin neurons in mice. J Clin Invest 118, 1796-1805.

Holinski, F., Menenakos, C., Haber, G., Olze, H., Ordemann, J., 2015. Olfactory and gustatory function after bariatric surgery. Obes. Surg. 25, 2314–2320.

Holst JJ, Orskov C, Nielsen OV, Schwartz TW. Truncated glucagon-like peptide I, an insulin-releasing hormone from the distal gut. FEBS Lett. (1987) 211:169–74. doi: 10.1016/0014-5793(87)81430-8.

Holst, J. J. (2007). The physiology of glucagon-like peptide 1. Physiological reviews, 87(4), 1409-1439.

Holst JJ, Vilsbøll T, Deacon CF. The incretin system and its role in type 2 diabetes mellitus. Mol Cell Endocrinol. 2009 Jan 15;297(1-2):127-36. doi: 10.1016/j.mce.2008.08.012. Epub 2008 Aug 20. PMID: 18786605.

Holt, M. K., Cook, D. R., Brierley, D. I., Richards, J. E., Reimann, F., Gourine, A. V., ... & Trapp, S. (2020). PPG neurons in the nucleus of the solitary tract modulate heart rate but do not mediate GLP-1 receptor agonist-induced tachycardia in mice. Molecular metabolism, 39, 101024.

Holt, M. K., Richards, J. E., Cook, D. R., Brierley, D. I., Williams, D. L., Reimann, F., ... & Trapp, S. (2019). Preproglucagon neurons in the nucleus of the solitary tract are the main source of brain GLP-1, mediate stress-induced hypophagia, and limit unusually large intakes of food. Diabetes, 68(1), 21-33.

Hommel JD, Trinko R, Sears RM, Georgescu D, Liu ZW, Gao XB, Thurmon JJ, Marinelli M, DiLeone RJ. Leptin receptor signaling in midbrain dopamine neurons regulates feeding. Neuron. 2006 Sep 21;51(6):801-10. doi: 10.1016/j.neuron.2006.08.023. PMID: 16982424.

Honda T, Wada E, Battey JF, Wank SA (1993) Differential Gene Expression of CCK(A) and CCK(B) Receptors in the Rat Brain. Mol Cell Neurosci 4:143–154.

https://diabetesatlas.org/ *Tenth edition.* IDF Diabetes Atlas. (n.d.). Retrieved June 23, 2022, from https://diabetesatlas.org/

https://web.conn-toolbox.org/fmri-methods/connectivity-measures/roi-to-roi *Conn Toolbox - roi-to-roi*. to. (n.d.). Retrieved June 23, 2022, from https://web.conn-toolbox.org/fmri-methods/connectivity-measures/roi-to-roi

https://www.worldobesity.org/ *Homepage.* World Obesity Federation. (2021, November 5). Retrieved June 23, 2022, from https://www.worldobesity.org/

Hurtado-Chong, A., Yusta-Boyo, M. J., Vergaño-Vera, E., Bulfone, A., De Pablo, F., & Vicario-Abejón, C. (2009). IGF-I promotes neuronal migration and positioning in the olfactory bulb and the exit of neuroblasts from the subventricular zone. European Journal of Neuroscience, 30(5), 742-755.

Husted, A.S., Trauelsen, M., Rudenko, O., Hjorth, S.A., Schwartz, T.W., 2017. GPCR-mediated signaling of metabolites. Cell Metabolism 25:777e796.

Imbernon M, Saponaro C, Helms HCC, Duquenne M, Fernandois D, Deligia E, Denis RGP, Chao DHM, Rasika S, Staels B, Pattou F, Pfrieger FW, Brodin B, Luquet S, Bonner C, Prevot V. Tanycytes control hypothalamic liraglutide uptake and its anti-obesity actions. Cell Metab. 2022 Jun 14:S1550-4131(22)00222-4. doi: 10.1016/j.cmet.2022.06.002. Epub ahead of print. PMID: 35716660.

Isaacson JS (2010) Odor representations in mammalian cortical circuits. Curr Opin Neurobiol 20:328–331.

Islam, M. A., Fagundo, A. B., Arcelus, J., Agüera, Z., Jiménez-Murcia, S., Fernández-Real, J. M., ... & Fernandez-Aranda, F. (2015). Olfaction in eating disorders and abnormal eating behavior: a systematic review. Frontiers in psychology, 6, 1431.

Jamain, S., Radyushkin, K., Hammerschmidt, K., Granon, S., Boretius, S., Varoqueaux, F., ... & Brose, N. (2008). Reduced social interaction and ultrasonic communication in a mouse model of monogenic heritable autism. Proceedings of the National Academy of Sciences, 105(5), 1710-1715.

Jastreboff AM, Sinha R, Arora J, Giannini C, Kubat J, Malik S, Van Name MA, Santoro N, Savoye M, Duran EJ, Pierpont B, Cline G, Constable RT, Sherwin RS, Caprio S. Altered Brain Response to Drinking Glucose and Fructose in Obese Adolescents. Diabetes. 2016 Jul;65(7):1929-39. doi: 10.2337/db15-1216. Epub 2016 Apr 5. PMID: 27207544; PMCID: PMC5384636.

Jensen, C. B., Pyke, C., Rasch, M. G., Dahl, A. B., Knudsen, L. B., & Secher, A. (2018). Characterization of the glucagonlike peptide-1 receptor in male mouse brain using a novel antibody and in situ hybridization. Endocrinology, 159(2), 665-675.

Jia, C., & Hegg, C. C. (2010). NPY mediates ATP-induced neuroproliferation in adult mouse olfactory epithelium. Neurobiology of disease, 38(3), 405-413.

Jiang T, Soussignan R, Rigaud D, Martin S, Royet JP, Brondel L, Schaal B (2008) Alliesthesia to food cues: heterogeneity across stimuli and sensory modalities. Physiol Behav 95:464-470.

Joussain, P., Bessy, M., Faure, F., Bellil, D., Landis, B. N., Hugentobler, M., ... & Bensafi, M. (2016). Application of the European Test of Olfactory Capabilities in patients with olfactory impairment. European Archives of Oto-Rhino-Laryngology, 273(2), 381-390.

Julliard A-K, Al Koborssy D, Fadool DA and Palouzier-Paulignan B (2017) Nutrient Sensing: Another Chemosensitivity of the Olfactory System. Front. Physiol. 8:468. doi: 10.3389/fphys.2017.00468.

Jørgensen, M. B., & Buch, N. H. (1961). Studies on the sense of smell and taste in diabetics. Acta oto-laryngologica, 53(2-3), 539-545.

Kahn BB, Flier JS. Obesity and insulin resistance. J Clin Invest. 2000 Aug;106(4):473-81. doi: 10.1172/JCI10842. PMID: 10953022; PMCID: PMC380258.

Kalsbeek A, Buijs RM. Output pathways of the mammalian suprachiasmatic nucleus: coding circadian time by transmitter selection and specific targeting. Cell Tissue Res. 2002 Jul;309(1):109-18. doi: 10.1007/s00441-002-0577-0. Epub 2002 May 29. PMID: 12111541.

Kalsbeek, A., Foppen, E., Schalij, I., Van Heijningen, C., van der Vliet, J., Fliers, E., & Buijs, R. M. (2008). Circadian control of the daily plasma glucose rhythm: an interplay of GABA and glutamate. PLOS one, 3(9), e3194.

Kalsbeek A, La Fleur SE, Van Heijningen C, Buijs RM (2004) Suprachiasmatic GABAergic inputs to the paraventricular nucleus control plasma glucose concentrations in the rat via sympathetic innervation of the liver. J Neurosci 24:7604–7613.

Kalsbeek A, Ruiter M, La Fleur SE, Cailotto C, Kreier F, et al. (2006) The hypothalamic clock and its control of glucose homeostasis. Prog Brain Res 153:283–307.

Karpińska M, Czauderna M. Pancreas-Its Functions, Disorders, and Physiological Impact on the Mammals' Organism. Front Physiol. 2022 Mar 30;13:807632. doi: 10.3389/fphys.2022.807632. PMID: 35431983; PMCID: PMC9005876.

Kavaliers, M., Choleris, E., & Pfaff, D. W. (2005). Genes, odours and the recognition of parasitized individuals by rodents. Trends in parasitology, 21(9), 423-429.

Keller AD, Noble WM. Further observations on enhanced appetite with resultant adiposity following removal of the posterior lobe of the hypophysis. Am J Physiol 1936;116:90– 1.

Kennedy, G. The role of depot fat in the hypothalamic control of food intake in the rat. Proc. R. Soc. Lond. B 140, 578–592 (1953).

Kern, W., Born, J., Schreiber, H., & Fehm, H. L. (1999). Central nervous system effects of intranasally administered insulin during euglycemia in men. Diabetes, 48(3), 557-563.

Kim B, Feldman EL. Insulin resistance as a key link for the increased risk of cognitive impairment in the metabolic syndrome. Exp Mol Med. 2015 Mar 13;47(3):e149. doi: 10.1038/emm.2015.3. PMID: 25766618; PMCID: PMC4351418.

Kissileff, H.R., Carretta, J.C., Geliebter, A., and Pi-Sunyer, F.X. (2003). Cholecystokinin and stomach distension combine to reduce food intake in humans. Am J Physiol Regul Integr Comp Physiol 285, R992-998.

Kiyokage E, Pan Y-Z, Shao Z, Kobayashi K, Szabo G, Yanagawa Y, Obata K, Okano H, Toida K, Puche AC, Shipley MT (2010) Molecular identity of periglomerular and short axon cells. J Neurosci 30:1185–1196.

Knudsen, L.B., Pridal, L., 1996. Glucagon-like peptide-1-(9-36) amide is a major metabolite of glucagon-like peptide-1-(7-36) amide after in vivo administration to dogs, and it acts as an antagonist on the pancreatic receptor. European Journal of Pharmacology 318:429e435.

Kolling, L. J., Tatti, R., Lowry, T., Loeven, A. M., Fadool, J. M., & Fadool, D. A. (2022). Modulating the excitability of olfactory output neurons affects whole-body metabolism. Journal of Neuroscience, 42(30), 5966-5990.

Konturek, S.J., Pepera, J., Zabielski, K., Konturek, P.C., Pawlik, T., Szlachcic, A., and Hahn, E.G. (2003). Brain-gut axis in pancreatic secretion and appetite control. J Physiol Pharmacol 54, 293-317.

Kuhre, R.E., Wewer Albrechtsen, N.J., Hartmann, B., Deacon, C.F., Holst, J.J., 2015. Measurement of the incretin hormones: glucagon-like peptide-1 and glucose-dependent insulinotropic peptide. Journal of Diabetic Complications 29:445e450.

Kullmann S, Heni M, Veit R, Ketterer C, Schick F, Häring HU, Fritsche A, Preissl H. The obese brain: association of body mass index and insulin sensitivity with resting state network functional connectivity. Hum Brain Mapp. 2012 May;33(5):1052-61. doi: 10.1002/hbm.21268. Epub 2011 Apr 21. PMID: 21520345; PMCID: PMC6870244.

La Barre J, Still EU. Studies on the physiology of secretin. III. Further studies on the effects of secretin on the blood sugar. Am J Physiol. (1930) 91:649–53. doi: 10.1152/ajplegacy.1930.91.2.649 23.

La Barre J. Sur les possibilités d'un traitement du diabète par l'incrétine. Bull Acad Royal Med Belg. (1932) 12:620–34.

Lacroix M-C, Badonnel K, Meunier N, Tan F, Schlegel-Le Poupon C, Durieux D, Monnerie R, Baly C, Congar P, Salesse R, Caillol M (2008) Expression of insulin system in the olfactory epithelium: first approaches to its role and regulation. J Neuroendocrinol 20:1176–1190.

Lang CH (1995) Inhibition of central GABAA receptors enhances hepatic glucose production and peripheral glucose uptake. Brain Res Bull 37: 611–616.

Lankat-Buttgereit, B., Goke, R., Fehmann, H.C., Richter, G., Goke, B., 1994. Molecular cloning of a cDNA encoding for the GLP-1 receptor expressed in rat lung. Experimental and Clinical Endocrinology 102:341e347.

Larraufie, P., Roberts, G.P., McGavigan, A.K., Kay, R.G., Li, J., Leiter, A., et al., 2019. Important role of the GLP-1 Axis for glucose homeostasis after bariatric surgery. Cell Reports 26:1399e1408 e1396.

Larsen, J. K., Hermans, R. C., & Engels, R. C. (2012). Food intake in response to food-cue exposure. Examining the influence of duration of the cue exposure and trait impulsivity. Appetite, 58(3), 907-913.

Larsen, P.J., Tang-Christensen, M., Jessop, D.S., 1997. Central administration of glucagon-like peptide-1 activates hypothalamic neuroendocrine neurons in the rat. Endocrinology 138:4445e4455.

Lasschuijt MP, Mars M, de Graaf C, Smeets PAM. Endocrine Cephalic Phase Responses to Food Cues: A Systematic Review. Adv Nutr. 2020 Sep 1;11(5):1364-1383.

Layer, P., Holst, J.J., Grandt, D., Goebell, H., 1995. Ileal release of glucagonlike peptide-1 (GLP-1). Association with inhibition of gastric acid secretion in humans. Digestive Diseases and Sciences 40:1074e1082.

Le Feuvre, R.A., Woods, A.J., Stock, M.J., and Rothwell, N.J. (1991). Effects of central injection of glucose on thermogenesis in normal, VMH-lesioned and genetically obese rats. Brain Res 547, 110- 114.

Le Magnen J (1999a) Influence of hunger on the expression of discriminative appetite by the rat (first published in French in 1960). Appetite 33:52–54.

Le Magnen J (1999b) Increased food intake induced in rats by changes in the satiating sensory input from food (first published in French in 1956). Appetite 33:33–35.

Le Magnen J (1999c) A role for caloric density of the diet in the mechanism of acquisition of appetites (first published in French in 1957). Appetite 33:17–20.

Le Magnen J (2001) My scientific life: 40 years at the College de France. Neurosci Biobehav Rev 25:375–394.

Le Magnen, J. (1955). Satiety induced by sugars as stimuli in the white rat. Compte rendu des seances de la Societe de biologie, 149, 1339-1342.

Le Magnen J, Julien N (1999) Effects of postprandial administration of insulin on food intake by the white rat and the mechanism of appetite for energy (first published in French in 1956). Appetite 33:8–13.

Leloup, C., Orosco, M., Serradas, P., Nicolaidis, S., and Penicaud, L. (1998). Specific inhibition of GLUT2 in arcuate nucleus by antisense oligonucleotides suppresses nervous control of insulin secretion. Brain Res Mol Brain Res 57, 275-280.

Lemaire, J.J., Frew, A.J., McArthur, D., Gorgulho, A.A., Alger, J.R., Salomon, N., Chen, C., Behnke, E.J., and De Salles, A.A. (2011). White matter connectivity of human hypothalamus. Brain Res 1371, 43-64.

Jessen, L., Aulinger, B. A., Hassel, J. L., Roy, K. J., Smith, E. P., Greer, T. M., ... & D'Alessio, D. A. (2012). Suppression of food intake by glucagon-like peptide-1 receptor agonists: relative potencies and role of dipeptidyl peptidase-4. Endocrinology, 153(12), 5735-5745.

Lietzau G, Davidsson W, Östenson C-G, Chiazza F, Nathanson D, Pintana H, Skogsberg J, Klein T, Nyström T, Darsalia V, Patrone C (2018) Type 2 diabetes impairs odour detection, olfactory memory and olfactory neuroplasticity; effects partly reversed by the DPP-4 inhibitor Linagliptin. acta neuropathol commun 6:14.

Lietzau G, Nyström T, Östenson C-G, Darsalia V, Patrone C (2016) Type 2 diabetes-induced neuronal pathology in the piriform cortex of the rat is reversed by the GLP-1 receptor agonist exendin4. Oncotarget 7:5865–5876.

Lietzau G, Nyström T, Wang Z, Darsalia V, Patrone C (2020) Western Diet Accelerates the Impairment of Odor-Related Learning and Olfactory Memory in the Mouse. ACS Chem Neurosci 11:3590– 3602.

Liman ER, Corey DP. Electrophysiological characterization of chemosensory neurons from the mouse vomeronasal organ. J Neurosci. 1996 Aug 1;16(15):4625-37. doi: 10.1523/JNEUROSCI.16-15-04625.1996. PMID: 8764651; PMCID: PMC6579035.

Lin HV, Accili D. Hormonal regulation of hepatic glucose production in health and disease. Cell Metab. 2011 Jul 6;14(1):9-19. doi: 10.1016/j.cmet.2011.06.003. PMID: 21723500; PMCID: PMC3131084.

Linster C, Johnson BA, Yue E, Morse A, Xu Z, Hingco EE, Choi Y, Choi M, Messiha A, Leon M (2001) Perceptual correlates of neural representations evoked by odorant enantiomers. J Neurosci 21:9837.

Liu, X., Zhou, Y., Li, S., Yang, D., Jiao, M., Liu, X., & Wang, Z. (2020). Type 3 adenylyl cyclase in the main olfactory epithelium participates in depression-like and anxiety-like behaviours. Journal of Affective Disorders, 268, 28-38.

Liu Y., Wang, X., Li, W., Zhang, Q., Li, Y., Zhang, Z., ... & He, Z. (2017). A sensitized IGF1 treatment restores corticospinal axon-dependent functions. Neuron, 95(4), 817-833.

Liu Z, Chen Z, Shang C, Yan F, Shi Y, Zhang J, Qu B, Han H, Wang Y, Li D, Südhof TC, Cao P. IGF1-Dependent Synaptic Plasticity of Mitral Cells in Olfactory Memory during Social Learning. Neuron. 2017 Jul 5;95(1):106-122.e5. doi: 10.1016/j.neuron.2017.06.015. PMID: 28683263; PMCID: PMC5559288.

Llewellyn-Smith, I. J., Marina, N., Manton, R. N., Reimann, F., Gribble, F. M., & Trapp, S. (2015). Spinally projecting preproglucagon axons preferentially innervate sympathetic preganglionic neurons. Neuroscience, 284, 872-887.

Lorentzen, M., Madsbad, S., Kehlet, H., & Tronier, B. (1987). Effect of sham-feeding on glucose tolerance and insulin secretion. Acta Endocrinologica, 115, 0-2.

Louis-Sylvestre J, Le Magnen J. Fall in blood glucose level precedes meal onset in free-feeding rats. Neurosci Biobehav Rev. 1980;4 Suppl 1:13-5. doi: 10.1016/0149-7634(80)90041-x. PMID: 6765504.

Louis-Sylvestre, J. E. A. N. I. N. E. (1978). Relationship between two stages of prandial insulin release in rats. American Journal of Physiology-Endocrinology And Metabolism, 235(2), E103.

Louis-Sylvestre J., Le Magnen J., 1980a. Palatability and preabsorptive insulin release. Neurosci. Biobehav. Rev. 4 (suppl. 11, 43-46.

Louis-Sylvestre J., Le Magnen J., 1980b. A fall in blood glucose level precedes meal onset in free-feeding rats. Neurosci. Biobehav. Rev., 4 (suppl. 1), 13-16.

Luppino FS, de Wit LM, Bouvy PF, Stijnen T, Cuijpers P, Penninx BW, Zitman FG. Overweight, obesity, and depression: a systematic review and meta-analysis of longitudinal studies. Arch Gen Psychiatry. 2010 Mar;67(3):220-9. doi: 10.1001/archgenpsychiatry.2010.2. PMID: 20194822.

Luquet S, Magnan C. The central nervous system at the core of the regulation of energy homeostasis. Front Biosci (Schol Ed). 2009 Jun 1;1(2):448-65. doi: 10.2741/s37. PMID: 19482713.

Luquet, S., Joly, A., Denis, R., Palmiter, R., Magnan, C., 2010. Arcuate NPY/AgRP neurons and the control of energy balance. Eur. Neuropsychopharmacol 20, S195–S196.

Luskin MB (1993) Restricted proliferation and migration of postnatally generated neurons derived from the forebrain subventricular zone. Neuron 11:173–189.

Ma J, Dankulich-Nagrudny L, Lowe G (2013) Cholecystokinin: An Excitatory Modulator of Mitral/Tufted Cells in the Mouse Olfactory Bulb. PLoS One 8.

Madhu, S V. (2017). RSSDI Diabetes Update 2016. 10.5005/jp/books/13026.

Malnic B, Hirono J, Sato T, Buck LB (1999) Combinatorial receptor codes for odors. Cell 96:713–723.

Maniscalco JW, Kreisler AD, Rinaman L. Satiation and stress-induced hypophagia: examining the role of hindbrain neurons expressing prolactin-releasing Peptide or glucagon-like Peptide 1. Front Neurosci. 2013 Jan 21;6:199. doi: 10.3389/fnins.2012.00199. PMID: 23346044; PMCID: PMC3549516.

Marks DR, Tucker K, Cavallin MA, Mast TG, Fadool DA (2009) Awake intranasal insulin delivery modifies protein complexes and alters memory, anxiety, and olfactory behaviors. J Neurosci 29:6734–6751.

Marqués-Iturria I, Scholtens LH, Garolera M, Pueyo R, García-García I, González-Tartiere P, Segura B, Junqué C, Sender-Palacios MJ, Vernet-Vernet M, Sánchez-Garre C, de Reus MA, Jurado MA, van den Heuvel MP. Affected connectivity organization of the reward system structure in obesity. Neuroimage. 2015 May 1;111:100-6. doi: 10.1016/j.neuroimage.2015.02.012. Epub 2015 Feb 14. PMID: 25687594.

Martin C, Ravel N. Beta and gamma oscillatory activities associated with olfactory memory tasks: different rhythms for different functional networks? Front Behav Neurosci. 2014 Jun 23;8:218. doi: 10.3389/fnbeh.2014.00218. PMID: 25002840; PMCID: PMC4066841.

Matsui A, Go Y, Niimura Y (2010) Degeneration of olfactory receptor gene repertories in primates: No direct link to full trichromatic vision. Mol Biol Evol 27:1192–1200.

Matsutani, S., & Yamamoto, N. (2008). Centrifugal innervation of the mammalian olfactory bulb. Anatomical science international, 83(4), 218-227.

Mattes RD (1997) Physiologic responses to sensory stimulation by food: nutritional implications. J Am Diet Assoc 97:406–413.

Mayer EA, Tillisch K, Gupta A. Gut/brain axis and the microbiota. J Clin Invest. 2015 Mar 2;125(3):926-38. doi: 10.1172/JCI76304. Epub 2015 Feb 17. PMID: 25689247; PMCID: PMC4362231.

Mayer, J. (1996). Glucostatic mechanism of regulation of food intake. 1953. Obes Res 4, 493-496.

Mayo, K. E., Miller, L. J., Bataille, D., Dalle, S., Göke, B., Thorens, B., & Drucker, D. J. (2003). International Union of Pharmacology. XXXV. The glucagon receptor family. Pharmacological reviews, 55(1), 167-194.

McCance, D.R., Pettitt, D.J., Hanson, R.L., Jacobsson, L.T., Knowler, W.C., and Bennett, P.H. (1994). Birth weight and non-insulin dependent diabetes: thrifty genotype, thrifty phenotype, or surviving small baby genotype? BMJ 308, 942-945.

McNay EC, Ong CT, McCrimmon RJ, Cresswell J, Bogan JS, Sherwin RS. Hippocampal memory processes are modulated by insulin and high-fat-induced insulin resistance. Neurobiol Learn Mem. 2010 May;93(4):546-53. doi: 10.1016/j.nlm.2010.02.002. Epub 2010 Feb 20. PMID: 20176121; PMCID: PMC2878207.

Meister, B. (2007). Neurotransmitters in key neurons of the hypothalamus that regulate feeding behavior and body weight. Physiol Behav 92, 263-271.

Meister, B., Gomuc, B., Suarez, E., Ishii, Y., Durr, K., and Gillberg, L. (2006). Hypothalamic proopiomelanocortin (POMC) neurons have a cholinergic phenotype. Eur J Neurosci 24, 2731-2740.

Mellinkoff, S.M., Frankland, M., Boyle, D., and Greipel, M. (1997). Relationship between serum amino acid concentration and fluctuations in appetite. 1956. Obes Res 5, 381-384.

Mentlein, R., Gallwitz, B., & Schmidt, W. E. (1993). Dipeptidyl-peptidase IV hydrolyses gastric inhibitory polypeptide, glucagon-like peptide-1 (7–36) amide, peptide histidine methionine and is responsible for their degradation in human serum. European journal of biochemistry, 214(3), 829-835.

Merchenthaler, I., Lane, M., & Shughrue, P. (1999). Distribution of pre-pro-glucagon and glucagon-like peptide-1 receptor messenger RNAs in the rat central nervous system. Journal of Comparative Neurology, 403(2), 261-280.

Meyer-Gerspach, A. C., Ly, H. G., Borgwardt, S., Dupont, P., Beglinger, C., Van Oudenhove, L., & Wölnerhanssen, B. K. (2018). Endogenous GLP-1 alters postprandial functional connectivity between homeostatic and reward-related brain regions involved in regulation of appetite in healthy lean males: a pilotstudy. Diabetes, Obesity and Metabolism, 20(10), 2330-2338.

Midroit, M., Chalençon, L., Renier, N., Milton, A., Thevenet, M., Sacquet, J., Breton, M., Forest, J., Noury, N., Richard, M., Raineteau, O., Ferdenzi, C., Fournel, A., Wesson, D.W., Bensafi, M., Didier, A., Mandairon, N., 2021. Neural processing of the reward value of pleasant odorants. Curr. Biol.

Miki, T., Liss, B., Minami, K., Shiuchi, T., Saraya, A., Kashima, Y., Horiuchi, M., Ashcroft, F., Minokoshi, Y., Roeper, J., et al. (2001). ATP-sensitive K+ channels in the hypothalamus are essential for the maintenance of glucose homeostasis. Nat Neurosci 4, 507-512.

Mithieux, G., Misery, P., Magnan, C., Pillot, B., Gautier-Stein, A., Bernard, C., Rajas, F., & Zitoun, C. (2005). Portal sensing of intestinal gluconeogenesis is a mechanistic link in the diminution of food intake induced by diet protein. Cell metabolism, 2(5), 321–329. https://doi-org.insb.bib.cnrs.fr/10.1016/j.cmet.2005.09.010.

Moffett, R.C., Docherty, N.G., le Roux, C.W., 2021. The altered enteroendocrine reportoire following roux-en-Y-gastric bypass as an effector of weight loss and improved glycaemic control. Appetite 156, 104807.

Mojsov S, Heinrich G, Wilson IB, Ravazzola M, Orci L,Habener JF.Preproglucagon gene expression in pancreas andintestine diversifies at the level of post-translational processing.J Biol Chem261: 11880 –11889, 1986.

Mojsov S, Kopczynski MG, Habener JF: Both amidated and nonamidated forms of glucagon-like peptide I are synthesized in the rat intestine and the pancreas. J Biol Chem 265:8001-8008, 1990.

Mojsov S, Weir GC, Habener JF. Insulinotropin: glucagon-like peptide I (7–37) co-encoded in the glucagon gene is a potent stimulator of insulin release in the perfused rat pancreas. J Clin Invest. (1987) 79:616–9. doi: 10.1172/JCI112855.

Mombaerts P (1999) Seven-Transmembrane Proteins as Odorant and Chemosensory Receptors. Science (80-) 286:707–711.

Mombaerts P (2004) Genes and ligands for odorant, vomeronasal and taste receptors. Nat Rev Neurosci 5:263–278.

Mombaerts P, Wang F, Dulac C, Chao SK, Nemes A, Mendelsohn M, Edmondson J, Axel R. Visualizing an olfactory sensory map. Cell. 1996 Nov 15;87(4):675-86. doi: 10.1016/s0092-8674(00)81387-2. PMID: 8929536.

Monda, M., Sullo, A., De Luca, V., Pellicano, M.P., and Viggiano, A. (1997). L-threonine injection into PPC modifies food intake, lateral hypothalamic activity, and sympathetic discharge. Am J Physiol 273, R554-559.

Moody, A.J., Holst, J.J., Thim, L., Jensen, S.L., 1981. Relationship of glicentin to proglucagon and glucagon in the porcine pancreas. Nature 289: 514e516.

Moore B, Edie ES, Abram JS. On the treatment of diabetes mellitus by acid extract of duodenal mucous membrane. Biochem J. (1906) 1:28–38. doi: 10.1042/bj0010028.

Morales I, Berridge KC. 'Liking' and 'wanting' in eating and food reward: Brain mechanisms and clinical implications. Physiol Behav. 2020 Dec 1;227:113152. doi: 10.1016/j.physbeh.2020.113152. Epub 2020 Aug 23. PMID: 32846152; PMCID: PMC7655589.

Morales, I., & Berridge, K. C. (2020). 'Liking' and 'wanting' in eating and food reward: Brain mechanisms and clinical implications. Physiology & behavior, 227, 113152.

Moran, T.H. (2004). Gut peptides in the control of food intake: 30 years of ideas. Physiol Behav 82, 175-180.

Morash B, Li A, Murphy PR, Wilkinson M, Ur E (1999) Leptin gene expression in the brain and pituitary gland. Endocrinology 140:5995–5998.

Mori K, Nagao H, Yoshihara Y. The olfactory bulb: coding and processing of odor molecule information. Science. 1999 Oct 22;286(5440):711-5. doi: 10.1126/science.286.5440.711. PMID: 10531048.

Morquecho-Campos, P., Bikker, F. J., Nazmi, K., de Graaf, K., Laine, M. L., & Boesveldt, S. (2019). Impact of food odors signaling specific taste qualities and macronutrient content on saliva secretion and composition. Appetite, 143, 104399.

Morton GJ, Meek TH, Schwartz MW. Neurobiology of food intake in health and disease. Nat Rev Neurosci. 2014;15(6):367-378. doi:10.1038/nrn3745.

Morton, G. J., Cummings, D. E., Baskin, D. G., Barsh, G. S. & Schwartz, M. W. Central nervous system control of food intake and body weight. Nature 443, 289–295 (2006).

Mortreux, M., Foppen, E., Denis, R. G., Montaner, M., Kassis, N., Denom, J., ... & Migrenne-Li, S. (2019). New roles for prokineticin 2 in feeding behavior, insulin resistance and type 2 diabetes: Studies in mice and humans. Molecular metabolism, 29, 182-196.

Müller, T. D., Finan, B., Bloom, S. R., D'Alessio, D., Drucker, D. J., Flatt, P. R., ... & Tschöp, M. H. (2019). Glucagon-like peptide 1 (GLP-1). Molecular metabolism, 30, 72-130.

Mulligan, C., Moreau, K., Brandolini, M., Livingstone, B., Beaufrère, B., & Boirie, Y. (2002). Alterations of sensory perceptions in healthy elderly subjects during fasting and refeeding. Gerontology, 48(1), 39-43.

Murphy KG, Bloom SR. Gut hormones and the regulation of energy homeostasis. Nature. 2006 Dec 14;444(7121):854-9. doi: 10.1038/nature05484. PMID: 17167473.

Mas M, Brindisi MC, Chabanet C, Nicklaus S, Chambaron S. Weight Status and Attentional Biases Toward Foods: Impact of Implicit Olfactory Priming. Front Psychol. 2019 Aug 9;10:1789. doi: 10.3389/fpsyg.2019.01789. PMID: 31447733; PMCID: PMC6696981.

Myers KP. Sensory-specific satiety is intact in rats made obese on a high-fat high-sugar choice diet. Appetite. 2017 May 1;112:196-200. doi: 10.1016/j.appet.2017.01.013. Epub 2017 Jan 12. PMID: 28089926.

Myers, M.G., Jr., and Simerly, R.B. (2010). The neuroendocrinology and neuroscience of energy balance. Front Neuroendocrinol 31, 1-3.

Nagayama S, Homma R, Imamura F (2014) Neuronal organization of olfactory bulb circuits. Front Neural Circuits 8:1–19 Available at: http://journal.frontiersin.org/journal/10.3389/fncir.2014.00098/full.

Naka, A., Riedl, M., Luger, A., Hummel, T., & Mueller, C. A. (2010). Clinical significance of smell and taste disorders in patients with diabetes mellitus. European archives of oto-rhino-laryngology, 267(4), 547-550.

Nakagawa A, Satake H, Nakabayashi H, Nishizawa M, Furuya K, Nakano S, Kigoshi T, Nakayama K, Uchida K: Receptor gene expression of glucagon-like peptide-1, but not glucose-dependent insulinotropic polypeptide, in rat nodose ganglion cells. Auton Neurosci 110:36-43, 2004.

Nambu T, Sakurai T, Mizukami K, Hosoya Y, Yanagisawa M, Goto K (1999) Distribution of orexin neurons in the adult rat brain. Brain Res 827:243-260.

Nauck MA, Heimesaat MM, Behle K, Holst JJ, Nauck MS, Ritzel R, Hüfner M, Schmiegel WH. Effects of glucagon-like peptide 1 on counterregulatory hormone responses, cognitive functions, and insulin secretion during hyperinsulinemic, stepped hypoglycemic clamp experiments in healthy volunteers. J Clin Endocrinol Metab. 2002 Mar;87(3):1239-46. doi: 10.1210/jcem.87.3.8355. PMID: 11889194.

Nauck MA, Homberger E, Siegel EG, Allen RC, Eaton RP, Ebert R, Creutzfeldt W. Incretin effects of increasing glucose loads in man calculated from venous insulin and C-peptide responses. J Clin Endocrinol Metab. 1986 Aug;63(2):492-8. doi: 10.1210/jcem-63-2-492. PMID: 3522621.

Nauck MA: Unraveling the science of incretin biology. Eur J Intern Med 20 Suppl 2:S303-308, 2009.

Navarro, M., De Fonseca, F. R., Alvarez, E., Chowen, J. A., Zueco, J. A., Gomez, R., ... & Blázquez, E. (1996). Colocalization of glucagon-like peptide-1 (GLP-1) receptors, glucose transporter GLUT-2, and glucokinase mRNAs in rat hypothalamic cells: evidence for a role of GLP-1 receptor agonists as an inhibitory signal for food and water intake. Journal of neurochemistry, 67(5), 1982-1991.

Negoias, S., Visschers, R., Boelrijk, A., & Hummel, T. (2008). New ways to understand aroma perception. Food chemistry, 108(4), 1247-1254.

Negroni J, Meunier N, Monnerie R, Salesse R, Baly C, et al. (2012) Neuropeptide Y Enhances Olfactory Mucosa Responses to Odorant in Hungry Rats. PLoS ONE 7(9): e45266. doi:10.1371/journal.pone.0045266

Newman R, Winans SS (1980) An experimental study of the ventral striatum of the golden hamster. II. Neuronal connections of the olfactory tubercle. J Comp Neurol 191:193-212.

Nieto-Castanon, A. (2020). Handbook of functional connectivity Magnetic Resonance Imaging methods in CONN. Hilbert Press.

Niimura Y (2012) Olfactory Receptor Multigene Family in Vertebrates: From the Viewpoint of Evolutionary Genomics. Curr Genomics 13:103–114.

Niimura Y, Matsui a., Touhara K (2014) Extreme expansion of the olfactory receptor gene repertoire in African elephants and evolutionary dynamics of orthologous gene groups in 13 placental mammals. Genome Res:1485–1496 Available at: http://genome.cshlp.org/cgi/doi/10.1101/gr.169532.113.

Niimura Y, Nei M (2003) Evolution of olfactory receptor genes in the human genome. Proc Natl Acad Sci USA100:12235–12240.

Nishizumi H, Sakano H (2015) Developmental regulation of neural map formation in the mouse olfactory system. Dev Neurobiol:n/a – n/a Available at: http://doi.wiley.com/10.1002/dneu.22268.

Niswender, K.D., Baskin, D.G., and Schwartz, M.W. (2004). Insulin and its evolving partnership with leptin in the hypothalamic control of energy homeostasis. Trends Endocrinol Metab 15, 362-369.

Novak U, Wilks A, Buell G, McEwen S.Identical mRNA forpreproglucagon in pancreas and gut.Eur J Biochem164: 553–558,1987.

Nunn, N., Womack, M., Dart, C. and Barrett-Jolley, R., 2011. Function and Pharmacology of Spinally-Projecting Sympathetic Pre- Autonomic Neurones in the Paraventricular Nucleus of the Hypothalamus. Current Neuropharmacology, 999(999), pp.1-16.

Nyberg J, Jacobsson C, Anderson MF, et al. Immunohistochemical distribution of glucose-dependent insulinotropic polypeptide in the adult rat brain. J Neurosci Res 2007; 85: 2099–2119.

O'doherty, J., Rolls, E. T., Francis, S., Bowtell, R., McGlone, F., Kobal, G., ... & Ahne, G. (2000). Sensory-specific satiety-related olfactory activation of the human orbitofrontal cortex. Neuroreport, 11(2), 399-403.

Obici, S., Feng, Z., Morgan, K., Stein, D., Karkanias, G., and Rossetti, L. (2002). Central administration of oleic acid inhibits glucose production and food intake. Diabetes 51, 271-275.

Obrebowski, A., Obrebowska-Karsznia, Z., Gawli´nski, M., 2000. Smell and taste in children with simple obesity. Int. J. Pediatr. Otorhinolaryngol. 55, 191–196.

Oomura, Y., Ono, T., Ooyama, H., and Wayner, M.J. (1969). Glucose and osmosensitive neurones of the rat hypothalamus. Nature 222, 282-284.

Orskov, C., Poulsen, S. S., Moller, M., & Holst, J. J. (1996). Glucagon-like peptide I receptors in the subfornical organ and the area postrema are accessible to circulating glucagon-like peptide I. Diabetes, 45, 832–835. https://doi.org/10.2337/diab.45.6.832.

Orskov, C., Wettergren, A., Holst, J.J., 1993. Biological effects and metabolic rates of glucagonlike peptide-1 7-36 amide and glucagonlike peptide-1 7-37 in healthy subjects are indistinguishable. Diabetes 42:658e661.

Orskov, C., Wettergren, A., Holst, J.J., 1996. Secretion of the incretin hormones glucagon-like peptide-1 and gastric inhibitory polypeptide correlates with insulin secretion in normal man throughout the day. Scandinavian Journal of Gastroenterology 31:665e670.

Ossum A, van Deurs U, Engstrom T, Jensen JS, Treiman M: The cardioprotective and inotropic components of the postconditioning effects of GLP-1 and GLP-1(9-36)a in an isolated rat heart. Pharmacol Res 60:411-417, 2009.

Ozcan L, Wong CC, Li G, et al. Calcium signaling through CaMKII regulates hepatic glucose production in fasting and obesity. Cell Metab. 2012;15(5):739-751. doi:10.1016/j.cmet.2012.03.002.

O'Rahilly S (2009) Human genetics illuminates the paths to metabolic disease. Nature 462:307–314.

Padmanabhan, K., Osakada, F., Tarabrina, A., Kizer, E., Callaway, E.M., Gage, F.H., Sejnowski, T.J., 2019. Centrifugal inputs to the main olfactory bulb revealed through whole brain circuit-mapping. Front. Neuroanat. 12.

Pager J, Giachetti I, Holley A, Le Magnen J (1972) A selective control of olfactory bulb electrical activity in relation to food deprivation and satiety in rats. Physiol Behav 9:573–579.

Page KA, Chan O, Arora J, Belfort-Deaguiar R, Dzuira J, Roehmholdt B, Cline GW, Naik S, Sinha R, Constable RT, Sherwin RS. Effects of fructose vs glucose on regional cerebral blood flow in brain regions involved with appetite and reward pathways. JAMA. 2013 Jan 2;309(1):63-70. doi: 10.1001/jama.2012.116975. Erratum in: JAMA. 2013 May 1;309(17):1773. PMID: 23280226; PMCID: PMC4076145.

Palouzier-Paulignan, B., Lacroix, M. C., Aimé, P., Baly, C., Caillol, M., Congar, P., ... & Fadool, D. A. (2012). Olfaction under metabolic influences. Chemical senses, 37(9), 769-797.

Parra-Covarrubias, A., Rivera-Rodriguez, I., & Almaraz-Ugalde, A. (1971). Cephalic phase of insulin secretion in obese adolescents. Diabetes, 20, 800–802.

Patzelt, C., Tager, H.S., Carroll, R.J., Steiner, D.F., 1979. Identification and processing of proglucagon in pancreatic islets. Nature 282:260e266.

Paulina Morquecho-Campos, Kees de Graaf, Sanne Boesveldt, Smelling our appetite? The influence of food odors on congruent appetite, food preferences and intake, Food Quality and Preference, Volume 85, 2020, 103959, ISSN 0950-3293, https://doi.org/10.1016/j.foodqual.2020.103959.

Penicaud, L., Leloup, C., Lorsignol, A., Alquier, T., and Guillod, E. (2002). Brain glucose sensing mechanism and glucose homeostasis. Curr Opin Clin Nutr Metab Care 5, 539-543.

Perley MJ, Kipnis DM. Plasma insulin responses to oral and intravenous glucose: studies in normal and diabetic sujbjects. J Clin Invest. 1967 Dec;46(12):1954-62. doi: 10.1172/JCI105685. PMID: 6074000; PMCID: PMC292948.

Peterhoff M, Sieg A, Brede M, Chao CM, Hein L, Ullrich S. Inhibition of insulin secretion via distinct signaling pathways in alpha2-adrenoceptor knockout mice. Eur J Endocrinol 2003;149:343–50.

Petersen MC,Shulman GI.Mechanisms of Insulin Action and Insulin Resistance.PhysiolRev98: 2133–2223, 2018. Published August 1, 2018; doi:10.1152/physrev.00063.2017.

Peters MDJ, Marnie C, Tricco AC, Pollock D, Munn Z, Alexander L, McInerney P, Godfrey CM, Khalil H. Updated methodological guidance for the conduct of scoping reviews. JBI Evid Synth. 2020 Oct;18(10):2119-2126. doi: 10.11124/JBIES-20-00167. PMID: 33038124.

Peyron C, Tighe DK, van den Pol AN, de Lecea L, Heller HC, Sutcliffe JG, Kilduff TS (1998) Neurons containing hypocretin (orexin) project to multiple neuronal systems. J Neurosci 18:9996-10015.

Phan, Andreelli F. Doubles-agonistes, tri-agonistes et multi-agonistes incrétines/glucagon, Médecine des Maladies Métaboliques, Volume 15, Issue 8, 2021, Pages 744-752, ISSN 1957-2557, https://doi.org/10.1016/j.mmm.2021.10.010.

Pinching AJ, Powell TP (1971) The neuropil of the glomeruli of the olfactory bulb. J Cell Sci 9:347–377.

Poessel, M., Breuer, N., Joshi, A., Pampel, A., Villringer, A., Hummel, T., & Horstmann, A. (2020a). Reduced olfactory bulb volume in obesity and its relation to metabolic health status. Frontiers in human neuroscience, 14, 586998.

Poessel, M., Freiherr, J., Wiencke, K., Villringer, A., & Horstmann, A. (2020b). Insulin resistance is associated with reduced food odor sensitivity across a wide range of body weights. Nutrients, 12(8), 2201.

Porrini, M., Santangelo, A., Crovetti, R., Riso, P., Testolin, G., and Blundell, J.E. (1997). Weight, protein, fat, and timing of preloads affect food intake. Physiol Behav 62, 563-570.

Porte D Jr, Williams RH. Inhibition of insulin release by norepinephrine in man. Science 152: 1248 –1250, 1966.

Powley TL, Berthoud HR. Diet and cephalic phase insulin responses. Am J Clin Nutr. 1985 Nov;42(5 Suppl):991-1002. doi: 10.1093/ajcn/42.5.991. PMID: 3933326.

Price, J. L., & Drevets, W. C. (2012). Neural circuits underlying the pathophysiology of mood disorders. Trends in cognitive sciences, 16(1), 61-71.

Price JL, Powell TP. The mitral and short axon cells of the olfactory bulb. J Cell Sci. 1970 Nov;7(3):631-51. doi: 10.1242/jcs.7.3.631. PMID: 5492279.

Price JL, Slotnick BM, Revial MF (1991) Olfactory projections to the hypothalamus. J Comp Neurol 306:447-461.

Price, J. L. (1985). Beyond the primary olfactory cortex: olfactory-related areas in the neocortex, thalamus and hypothalamus. Chemical Senses, 10(2), 239-258.

Proserpio, C., Invitti, C., Boesveldt, S., Pasqualinotto, L., Laureati, M., Cattaneo, C., & Pagliarini, E. (2019). Ambient odor exposure affects food intake and sensory specific appetite in obese women. Frontiers in Psychology, 10, 7.

Prud'homme MJ, Lacroix MC, Badonnel K, Gougis S, Baly C, Salesse R, Caillol M (2009) Nutritional status modulates behavioural and olfactory bulb Fos responses to isoamyl acetate or food odour in rats: roles of orexins and leptin. Neuroscience 162:1287–1298.

Punjabi, M., Arnold, M., Ruttimann, E., Graber, M., Geary, N., Pacheco-Lopez, G., & Langhans, W. (2014). Circulating glucagon-like peptide-1 (GLP-1) inhibits eating in male rats by acting in the hindbrain and without inducing avoidance. Endocrinology, 155, 1690–1699. https://doi. org/10.1210/en.2013-1447.

Puttaert D, Coquelet N, Wens V, Peigneux P, Fery P, Rovai A, Trotta N, Sadeghi N, Coolen T, Bier JC, Goldman S, De Tiège X. Alterations in resting-state network dynamics along the Alzheimer's disease continuum. Sci Rep. 2020 Dec 15;10(1):21990. doi: 10.1038/s41598-020-76201-3. PMID: 33319785; PMCID: PMC7738511.

Qiu Q, Wu Y, Ma L, Xu W, Hills M Jr, Ramalingam V, Yu CR. Acquisition of innate odor preference depends on spontaneous and experiential activities during critical period. Elife. 2021 Mar 26;10:e60546. doi: 10.7554/eLife.60546. PMID: 33769278; PMCID: PMC8032394.

Rahman, M.S.; Hossain, K.S.; Das, S.; Kundu, S.; Adegoke, E.O.; Rahman, M..A.; Hannan, M..A.; Uddin, M.J.; Pang, M.-G. Role of Insulin in Health and Disease: An Update. Int. J. Mol. Sci. 2021, 22, 6403. https://doi.org/10.3390/ijms22126403.

Rapoport, S. I., M. C. Chang & A. A. Spector: Delivery and turnover of plasma-derived essential PUFAs in mammalian brain. J Lipid Res, 42, 678-85 (2001).

Reichelt AC, Morris MJ, Westbrook RF. Cafeteria diet impairs expression of sensory-specific satiety and stimulus-outcome learning. Front Psychol. 2014 Aug 27;5:852. doi: 10.3389/fpsyg.2014.00852. PMID: 25221530; PMCID: PMC4146395.

Reimann F, Gribble FM. Glucose-sensing in glucagon-like peptide-1-secreting cells. Diabetes. 2002 Sep;51(9):2757-63. doi: 10.2337/diabetes.51.9.2757. PMID: 12196469.

Reimann F, Habib AM, Tolhurst G, Parker HE, Rogers GJ, Gribble FM. Glucose sensing in L cells: a primary cell study. Cell Metab. 2008 Dec;8(6):532-9. doi: 10.1016/j.cmet.2008.11.002. PMID: 19041768; PMCID: PMC2697331.

Ribeiro-Parenti, L., Jarry, A. C., Cavin, J. B., Willemetz, A., Le Beyec, J., Sannier, A., Benadda, S., Pelletier, A. L., Hourseau, M., Léger, T., Morlet, B., Couvelard, A., Anini, Y., Msika, S., Marmuse, J. P., Ledoux, S., Le Gall, M., & Bado, A. (2021). Bariatric surgery induces a new gastric mucosa phenotype with increased functional glucagon-like peptide-1 expressing cells. Nature communications, 12(1), 110. https://doi.org/10.1038/s41467-020-20301-1

Riera, C. E., Tsaousidou, E., Halloran, J., Follett, P., Hahn, O., Pereira, M. M., ... & Dillin, A. (2017). The sense of smell impacts metabolic health and obesity. Cell metabolism, 26(1), 198-211.

Rinaman L. Interoceptive stress activates glucagon-like peptide-1 neurons that project to the hypothalamus. Am J Physiol. 1999 Aug;277(2):R582-90. doi: 10.1152/ajpregu.1999.277.2.R582. PMID: 10444567.

Rodriguez-Diaz R, Abdulreda MH, Formoso AL et al (2011) Innervation patterns of autonomic axons in the human endocrine pancreas. Cell Metab 14(1):45–54. https://doi.org/10.1016/j.cmet. 2011.05.008.

Rogers PJ, Blundell JE. Meal patterns and food selection during the development of obesity in rats fed a cafeteria diet. Neurosci Biobehav Rev. 1984 Winter;8(4):441-53. doi: 10.1016/0149-7634(84)90003-4. PMID: 6542632.

Rolls, B. J., Rolls, E. T., Rowe, E. A., & Sweeney, K. (1981). Sensory specific satiety in man. Physiology & behavior, 27(1), 137-142.

Rosenstock J, Wysham C, Frías JP, Kaneko S, Lee CJ, Fernández Landó L, Mao H, Cui X, Karanikas CA, Thieu VT. Efficacy and safety of a novel dual GIP and GLP-1 receptor agonist tirzepatide in patients with type 2 diabetes (SURPASS-1): a double-blind, randomised, phase 3 trial. Lancet. 2021 Jul 10;398(10295):143-155. doi: 10.1016/S0140-6736(21)01324-6. Epub 2021 Jun 27. Erratum in: Lancet. 2021 Jul 17;398(10296):212. PMID: 34186022.

Rouille Y, Westermark G, Martin SK, Steiner DF.Proglucagonis processed to glucagon by prohormone convertase PC2 in alphaTC1– 6 cells.Proc Natl Acad Sci USA91: 3242–3246, 1994.

Routh, V.H. (2010). Glucose Sensing Neurons in the Ventromedial Hypothalamus. Sensors (Basel) 10, 9002-9025.

Rowlands, J., Heng, J., Newsholme, P., & Carlessi, R. (2018). Pleiotropic effects of GLP-1 and analogs on cell signaling, metabolism, and function. Frontiers in endocrinology, 9, 672.

Rowzee, A. M., Cawley, N. X., Chiorini, J. A., & Di Pasquale, G. (2011). Glucagon-like peptide-1 gene therapy. Experimental diabetes research, 2011.

Russo, C., Russo, A., Pellitteri, R., Stanzani, S., 2018. Ghrelin-containing neurons in the olfactory bulb send collateralized projections into medial amygdaloid and arcuate hypothalamic nuclei: neuroanatomical study. Exp. Brain Res. 236, 2223–2229.

Saive, A. L., Royet, J. P., Ravel, N., Thévenet, M., Garcia, S., & Plailly, J. (2014). A unique memory process modulated by emotion underpins successful odor recognition and episodic retrieval in humans. Frontiers in Behavioral Neuroscience, 8, 203.

Savigner A, Duchamp-Viret P, Grosmaitre X, Chaput M, Garcia S, Ma M, Palouzier-Paulignan B (2009) Modulation of spontaneous and odorant-evoked activity of rat olfactory sensory neurons by two anorectic peptides, insulin and leptin. J Neurophysiol 101:2898–2906.

Schaal, B. (1988). Olfaction in infants and children: developmental and functional perspectives. Chemical Senses, 13(2), 145-190.

Schaal, B., Saxton, T. K., Loos, H., Soussignan, R., & Durand, K. (2020). Olfaction scaffolds the developing human from neonate to adolescent and beyond. Philosophical Transactions of the Royal Society B, 375(1800), 20190261.

Schellinck, H. M., Smyth, C., Brown, R., & Wilkinson, M. (1993). Odor-induced sexual maturation and expression of c-fos in the olfactory system of juvenile female mice. Developmental brain research, 74(1), 138-141.

Schulz, C., Paulus, K., Jöhren, O., & Lehnert, H. (2012). Intranasal leptin reduces appetite and induces weight loss in rats with diet-induced obesity (DIO). Endocrinology, 153(1), 143-153.

Schwartz, M.W., Seeley, R.J., Campfield, L.A., Burn, P., and Baskin, D.G. (1996). Identification of targets of leptin action in rat hypothalamus. J Clin Invest 98, 1101-1106.

Schwartz, M.W., Seeley, R.J., Woods, S.C., Weigle, D.S., Campfield, L.A., Burn, P., and Baskin, D.G. (1997). Leptin increases hypothalamic pro-opiomelanocortin mRNA expression in the rostral arcuate nucleus. Diabetes 46, 2119-2123.

Schwartz, M.W., Woods, S.C., Porte, D., Jr., Seeley, R.J., and Baskin, D.G. (2000). Central nervous system control of food intake. Nature 404, 661-671.

Scott, L. J. (2013). Lixisenatide: a review of its use in patients with type 2 diabetes mellitus. BioDrugs, 27(5), 509-523.

Secher A, Jelsing J, Baquero AF, Hecksher-Sørensen J, Cowley MA, Dalbøge LS, Hansen G, Grove KL, Pyke C, Raun K, Schäffer L, Tang-Christensen M, Verma S, Witgen BM, Vrang N, Bjerre Knudsen L. The arcuate nucleus mediates GLP-1 receptor agonist liraglutide-dependent weight loss. J Clin Invest. 2014 Oct;124(10):4473-88. doi: 10.1172/JCI75276. Epub 2014 Sep 9. PMID: 25202980; PMCID: PMC4215190.

Seino, Y., Fukushima, M., & Yabe, D. (2010). GIP and GLP-1, the two incretin hormones: similarities and differences. Journal of diabetes investigation, 1(1-2), 8-23.

Sharabi K, Tavares CD, Rines AK, Puigserver P. Molecular pathophysiology of hepatic glucose production. Mol Aspects Med. 2015 Dec;46:21-33. doi: 10.1016/j.mam.2015.09.003. Epub 2015 Nov 5. PMID: 26549348; PMCID: PMC4674831.

Shepherd, The synaptic organization of the brain, 2004, Ed. 5, Oxford University Press. (Book)

Shipley MT, Adamek GD (1984) The connections of the mouse olfactory bulb: a study using orthograde and retrograde transport of wheat germ agglutinin conjugated to horseradish peroxidase. Brain Res Bull 12:669-688.

Shughrue, P. J., Lane, M. V., & Merchenthaler, I. S. T. V. A. N. (1996). Glucagon-like peptide-1 receptor (GLP1-R) mRNA in the rat hypothalamus. Endocrinology, 137(11), 5159-5162.

Siegel EG, Trimble ER, Renold AE, Berthoud HR. Importance of preabsorptive insulin release on oral glucose tolerance: studies in pancreatic islet transplanted rats. Gut 21: 1002–1009, 1980.

Silver IA, Erecińska M. Extracellular glucose concentration in mammalian brain: continuous monitoring of changes during increased neuronal activity and upon limitation in oxygen supply in normo-, hypo-, and hyperglycemic animals. J Neurosci. 1994 Aug;14(8):5068-76. doi: 10.1523/JNEUROSCI.14-08-05068.1994. PMID: 8046468; PMCID: PMC6577171.

Simpson KA, Martin NM, Bloom SR. Hypothalamic regulation of food intake and clinical therapeutic applications. Arq Bras Endocrinol Metabol. 2009 Mar;53(2):120-8. doi: 10.1590/s0004-27302009000200002. PMID: 19466203.

Sims JS, Lorden JF. Effect of paraventricular nucleus lesions on body weight, food intake and insulin levels. Behav Brain Res. 1986 Dec;22(3):265-81. doi: 10.1016/0166-4328(86)90071-9. PMID: 3098259.

Smith, G.P., and Epstein, A.N. (1969). Increased feeding in response to decreased glucose utilization in the rat and monkey. Am J Physiol 217, 1083-1087.

Soleimanzad, H., Montaner, M., Ternier, G., Lemitre, M., Silvestre, J. S., Kassis, N., ... & Gurden, H. (2021). Obesity in Midlife Hampers Resting and Sensory-Evoked Cerebral Blood Flow in Mice. Obesity, 29(1), 150-158.

Soria-Gómez, E., Bellocchio, L., Reguero, L., Lepousez, G., Martin, C., Bendahmane, M., ... & Marsicano, G. (2014). The endocannabinoid system controls food intake via olfactory processes. Nature neuroscience, 17(3), 407-415.

Sorokowski, P., Karwowski, M., Misiak, M., Marczak, M. K., Dziekan, M., Hummel, T., & Sorokowska, A. (2019). Sex differences in human olfaction: a meta-analysis. Frontiers in psychology, 10, 242.

Sosulski, D. L., Bloom, M. L., Cutforth, T., Axel, R., & Datta, S. R. (2011). Distinct representations of olfactory information in different cortical centres. Nature, 472(7342), 213-216.

Speakman, J. R. (2019). Use of high-fat diets to study rodent obesity as a model of human obesity. International journal of obesity, 43(8), 1491-1492.

Stafford, L. D., & Whittle, A. (2015). Obese individuals have higher preference and sensitivity to odor of chocolate. Chemical senses, 40(4), 279-284.

Starling EH. The croonian lectures on the chemical correlation of the function of the body. Lecture 1. The Lancet (1905) 2:339–41.

Steinbusch L, Labouèbe G, Thorens B. Brain glucose sensing in homeostatic and hedonic regulation. Trends Endocrinol Metab. 2015 Sep;26(9):455-66. doi: 10.1016/j.tem.2015.06.005. Epub 2015 Jul 8. PMID: 26163755.

Stevenson, R. J., & Boakes, R. A. (2004). 5 Sweet and Sour Smells: Learned. The handbook of multisensory processes, 69.

Stockhorst U, de Fries D, Steingrueber HJ, Scherbaum WA. Insulin and the CNS: effects on food intake, memory, and endocrine parameters and the role of intranasal insulin administration in humans. Physiol Behav. 2004 Oct 30;83(1):47-54. doi: 10.1016/j.physbeh.2004.07.022. PMID: 15501490.

Suk, S. H., Sacco, R. L., Boden-Albala, B., Cheun, J. F., Pittman, J. G., Elkind, M. S., & Paik, M. C. (2003). Abdominal obesity and risk of ischemic stroke: the Northern Manhattan Stroke Study. Stroke, 34(7), 1586-1592.

Sun C, Tang K, Wu J, Xu H, Zhang W, Cao T, Zhou Y, Yu T, Li A. Leptin modulates olfactory discrimination and neural activity in the olfactory bulb. Acta Physiol (Oxf). 2019 Oct;227(2):e13319. doi: 10.1111/apha.13319. Epub 2019 Jun 18. PMID: 31144469.

Sun, X., Liu, X., Starr, E. R., & Liu, S. (2020). CCKergic tufted cells differentially drive two anatomically segregated inhibitory circuits in the mouse olfactory bulb. Journal of Neuroscience, 40(32), 6189-6206.

Sutherland EW, De Duve C: Origin and distribution of the hyperglycemicglycogenolytic factor of the pancreas. J Biol Chem 175:663-674, 1948

Sutton, G.M., Patterson, L.M., and Berthoud, H.R. (2004). Extracellular signal-regulated kinase 1/2 signaling pathway in solitary nucleus mediates cholecystokinin-induced suppression of food intake in rats. J Neurosci 24, 10240-10247.

Suzuki K, Simpson K a, Minnion JS, Shillito JC, Bloom SR (2010) The role of gut hormones and the hypothalamus in appetite regulation. Endocr J 57:359–372.

Swanson LW, Sawchenko PE. Hypothalamic integration: organization of the paraventricular and supraoptic nuclei. Annu Rev Neurosci. 1983;6:269-324. doi: 10.1146/annurev.ne.06.030183.001413. PMID: 6132586.

Szentirmai, E., Kapas, L., and Krueger, J.M. (2007). Ghrelin microinjection into forebrain sites induces wakefulness and feeding in rats. Am J Physiol Regul Integr Comp Physiol 292, R575-585.

Tang-Christensen, M., Larsen, P.J., Goke, R., Fink-Jensen, A., Jessop, D.S., Moller, M., et al., 1996. Central administration of GLP-1-(7-36) amide inhibits food and water intake in rats. American Journal of Physiology 271:R848eR856.

Tang-Christensen M, Vrang N, Larsen PJ. Glucagon-like peptide containing pathways in the regulation of feeding behaviour. Int J Obes Relat Metab Disord. 2001 Dec;25 Suppl 5:S42-7. doi: 10.1038/sj.ijo.0801912. PMID: 11840214.

Tavakoli, A., Schmaltz, A., Schwarz, D., Margrie, T. W., Schaefer, A. T., & Kollo, M. (2018). Quantitative association of anatomical and functional classes of olfactory bulb neurons. Journal of Neuroscience, 38(33), 7204-7220.

Teff KL, Devine J, Engelman K. Sweet taste: effect on cephalic phase insulin release in men. Physiol Behav. 1995 Jun;57(6):1089-95. doi: 10.1016/0031-9384(94)00373-d. PMID: 7652029.

Teff KL, Mattes RD, Engelman K. Cephalic phase insulin release in normal weight males: verification and reliability. Am J Physiol. 1991 Oct;261(4 Pt 1):E430-6. doi: 10.1152/ajpendo.1991.261.4.E430. PMID: 1928335.

Teff KL. Cephalic phase pancreatic polypeptide responses to liquid and solid stimuli in humans. Physiol Behav. 2010 Mar 3;99(3):317-23. doi: 10.1016/j.physbeh.2009.11.009. Epub 2009 Nov 26. PMID: 19944113; PMCID: PMC2834473.

Thiebaud N, Johnson MC, Butler JL, Bell G a, Ferguson KL, Fadool AR, Fadool JC, Gale AM, Gale DS, Fadool D a (2014) Hyperlipidemic diet causes loss of olfactory sensory neurons, reduces olfactory discrimination, and disrupts odorreversal learning. J Neurosci 34:6970–6984 Available at: http://www.ncbi.nlm.nih.gov/pubmed/24828650.

Thiebaud, N., Gribble, F., Reimann, F., Trapp, S., & Fadool, D. A. (2019). A unique olfactory bulb microcircuit driven by neurons expressing the precursor to glucagon-like peptide 1. Scientific Reports, 9, 15542. https://doi.org/10.1038/s41598-019-51880-9

Thiebaud, N., Llewellyn-Smith, I. J., Gribble, F., Reimann, F., Trapp, S., & Fadool, D. A. (2016). The incretin hormone glucagon-like peptide 1 increases mitral cell excitability by decreasing conductance of a voltage-dependent potassium channel. The Journal of Physiology, 594, 2607–2628. https://doi.org/10.1113/JP272322

Thomas-Danguin T, Sinding C, Romagny S, El Mountassir F, Atanasova B, Le Berre E, Le Bon A-M, Coureaud G (2014) The perception of odor objects in everyday life: a review on the processing of odor mixtures. Front Psychol 5:504 Available at:http://www.pubmedcentral.nih.gov/articlerender.fcgi?artid=4040494&tool=pmcentrez&rendertype=abstract.

Thompson, D.A., and Campbell, R.G. (1977). Hunger in humans induced by 2-deoxy-D-glucose: glucoprivic control of taste preference and food intake. Science 198, 1065-1068.

Thorens B, Porret A, Buhler L, Deng SP, Morel P, Widmann C.Cloning and functional expression of the human islet GLP-1 recep-tor. Demonstration that exendin-4 is an agonist and exendin- (9 –39) an antagonist of the receptor.Diabetes42: 1678 –1682, 1993.

Thorens, B. (1992). Expression cloning of the pancreatic beta cell receptor for the gluco-incretin hormone glucagon-like peptide 1. Proceedings of the National Academy of Sciences, 89(18), 8641-8645.

Tichansky, D.S., Boughter, J.D., Madan, A.K., 2006. Taste change after laparoscopic Roux-en-Y gastric bypass and laparoscopic adjustable gastric banding. Surg. Obes. Relat. Dis. 2, 440–444.

Timper K, Del Río-Martín A, Cremer AL, Bremser S, Alber J, Giavalisco P, Varela L, Heilinger C, Nolte H, Trifunovic A, Horvath TL, Kloppenburg P, Backes H, Brüning JC. GLP-1 Receptor Signaling in Astrocytes Regulates Fatty Acid Oxidation, Mitochondrial Integrity, and Function. Cell Metab. 2020 Jun 2;31(6):1189-1205.e13. doi: 10.1016/j.cmet.2020.05.001. Epub 2020 May 19. PMID: 32433922; PMCID: PMC7272126.

Toft-Nielson, M., Madsbad, S., Holst, J.J., 1996. The effect of glucagon-like peptide I (GLP-I) on glucose elimination in healthy subjects depends on the pancreatic glucoregulatory hormones. Diabetes 45:552e556.

Tolhurst, G., Reimann, F., Gribble, F.M., 2009. Nutritional regulation of glucagon-like peptide-1 secretion. Journal of Physiology 587:27e32.

Tong, J., Mannea, E., Aimé, P., Pfluger, P. T., Yi, C. X., Castaneda, T. R., ... & Tschöp, M. H. (2011).

Trapp, S., & Brierley, D. I. (2022). Brain GLP-1 and the regulation of food intake: GLP-1 action in the brain and its implications for GLP-1 receptor agonists in obesity treatment. British Journal of Pharmacology, 179(4), 557-570.

Troy S, Soty M, Ribeiro L, Laval L, Migrenne S, Fioramonti X, Pillot B, Fauveau V, Aubert R, Viollet B, Foretz M, Leclerc J, Duchampt A, Zitoun C, Thorens B, Magnan C, Mithieux G, Andreelli F. Intestinal gluconeogenesis is a key factor for early metabolic changes after gastric bypass but not after gastric lap-band in mice. Cell Metab. 2008 Sep;8(3):201-11. doi: 10.1016/j.cmet.2008.08.008. PMID: 18762021.

Truong, B.G., Magrum, L.J., and Gietzen, D.W. (2002). GABA(A) and GABA(B) receptors in the anterior piriform cortex modulate feeding in rats. Brain Res 924, 1-9.

Tschöp, M., Smiley, D.L., and Heiman, M.L. (2000). Ghrelin induces adiposity in rodents. Nature 407, 908-913.

Tschritter O, Machicao F, Stefan N, Schäfer S, Weigert C, Staiger H, Spieth C, Häring H-U, Fritsche A (2006) A new variant in the human Kv1.3 gene is associated with low insulin sensitivity and impaired glucose tolerance. J Clin Endocrinol Metab 91:654–658.

Tucker K, Cavallin MA, Jean-Baptiste P, Biju KC, Overton JM, Pedarzani P, Fadool DA. The Olfactory Bulb: A Metabolic Sensor of Brain Insulin and Glucose Concentrations via a Voltage-Gated Potassium Channel. Results Probl Cell Differ. 2010;52:147-57. doi: 10.1007/978-3-642-14426-4_12. PMID: 20865378; PMCID: PMC3068916.

Tucker, K., Cho, S., Thiebaud, N., Henderson, M. X., & Fadool, D. A. (2013). Glucose sensitivity of mouse olfactory bulb neurons is conveyed by a voltage-gated potassium channel. The Journal of physiology, 591(10), 2541-2561.

Tucker, K., Overton, J.M., Fadool, D.A., 2012. Diet-induced obesity resistance of Kv1.3 -/- mice is olfactory bulb dependent. J. Neuroendocrinol. 24, 1087–1095.

Turton, M. D., O'shea, D., Gunn, I., Beak, S. A., Edwards, C. M. B., Meeran, K., ... & Bloom, S. R. (1996). A role for glucagon-like peptide-1 in the central regulation of feeding. Nature, 379(6560), 69-72.

Ueno, H., Mizuta, M., Shiiya, T., Tsuchimochi, W., Noma, K., Nakashima, N., ... & Nakazato, M. (2014). Exploratory trial of intranasal administration of glucagon-like peptide-1 in Japanese patients with type 2 diabetes. Diabetes care, 37(7), 2024-2027.

Ueno, M., Akiguchi, I., Naiki, H., Fujibayashi, Y., Fukuyama, H., Kimura, J., ... & Takeda, T. (1991). The persistence of high uptake of serum albumin in the olfactory bulbs of mice throughout their adult lives. Archives of gerontology and geriatrics, 13(2), 201-209.

Unger J, McNeill TH, Moxley RT, White M, Moss A, Livingston JN (1989) Distribution of insulin receptor-like immunoreactivity in the rat forebrain. Neuroscience 31:143–157.

Unger JW, Livingston JN, Moss AM. Insulin receptors in the central nervous system: localization, signalling mechanisms and functional aspects. Prog Neurobiol. 1991;36(5):343-62. doi: 10.1016/0301-0082(91)90015-s. PMID: 1887067.

Unger, R.H., Ketterer, H., Eisentraut, A.M., 1966. Distribution of immunoassayable glucagon in gastrointestinal tissues. Metabolism 15:865e867.

Unger, Roger H. "Lipotoxicity in the pathogenesis of obesity-dependent NIDDM: genetic and clinical implications." Diabetes 44.8 (1995): 863-870.

Vahl, T. P., Drazen, D. L., Seeley, R. J., D'Alessio, D. A., & Woods, S. C. (2010). Meal-anticipatory glucagon-like peptide-1 secretion in rats. Endocrinology, 151(2), 569-575.

Vahl, T.P., Paty, B.W., Fuller, B.D., Prigeon, R.L., D'Alessio, D.A., 2003. Effects of GLP-1-(7-36)NH2, GLP-1-(7-37), and GLP-1- (9-36)NH2 on intravenous glucose tolerance and glucose-induced insulin secretion in healthy humans. The Journal of Cinical Endocrinology and Metabolism 88:1772e1779.

Van den Top, M., Lee, K., Whyment, A.D., Blanks, A.M., and Spanswick, D. (2004). Orexigensensitive NPY/AgRP pacemaker neurons in the hypothalamic arcuate nucleus. Nat Neurosci 7, 493- 494.

van Opstal AM, Hafkemeijer A, van den Berg-Huysmans AA, Hoeksma M, Blonk C, Pijl H, Rombouts SARB, van der Grond J. Brain activity and connectivity changes in response to glucose ingestion. Nutr Neurosci. 2020 Feb;23(2):110-117. doi: 10.1080/1028415X.2018.1477538. Epub 2018 May 27. PMID: 29806553.

Van Oudenhove L, McKie S, Lassman D, Uddin B, Paine P, Coen S, Gregory L, Tack J, Aziz Q. Fatty acid-induced gut-brain signaling attenuates neural and behavioral effects of sad emotion in humans. J Clin Invest. 2011 Aug;121(8):3094-9. doi: 10.1172/JCI46380. Epub 2011 Jul 25. PMID: 21785220; PMCID: PMC3148741.

Vecchio I, Tornali C, Bragazzi NL, Martini M. The Discovery of Insulin: An Important Milestone in the History of Medicine. Front Endocrinol (Lausanne). 2018 Oct 23;9:613. doi: 10.3389/fendo.2018.00613. PMID: 30405529; PMCID: PMC6205949.

Veedfald, S., Plamboeck, A., Deacon, C. F., Hartmann, B., Knop, F. K., Vilsbøll, T., & Holst, J. J. (2016). Cephalic phase secretion of insulin and other enteropancreatic hormones in humans. American Journal of Physiology-Gastrointestinal and Liver Physiology, 310(1), G43-G51.

Vendrell, J., El Bekay, R., Peral, B., Garcia-Fuentes, E., Megia, A., Macias-Gonzalez, M., et al., 2011. Study of the potential association of adipose tissue GLP-1 receptor with obesity and insulin resistance. Endocrinology 152:4072e4079.

Ventura, A. K., & Worobey, J. (2013). Early influences on the development of food preferences. Current biology, 23(9), R401-R408.

Verhagen LAW, Egecioglu E, Luijendijk MCM, Hillebrand JJG, Adan RAH, Dickson SL (2011) Acute and chronic suppression of the central ghrelin signaling system reveals a role in food anticipatory activity. Eur Neuropsychopharmacol 21:384–392.

Vilsboll, T., Krarup, T., Sonne, J., Madsbad, S., Volund, A., Juul, A.G., et al., 2003. Incretin secretion in relation to meal size and body weight in healthy subjects and people with type 1 and type 2 diabetes mellitus. The Journal of Cinical Endocrinology and Metabolism 88:2706e2713.

Wang, D., Wu, J., Liu, P., Li, X., Li, J., He, M., & Li, A. (2022). VIP interneurons regulate olfactory bulb output and contribute to odor detection and discrimination. Cell Reports, 38(7), 110383.

Weinstock, R. S., Wright, H. N., & Smith, D. U. (1993). Olfactory dysfunction in diabetes mellitus. Physiology & behavior, 53(1), 17-21.

Wersinger, S. R., Caldwell, H. K., Martinez, L., Gold, P., Hu, S. B., & Young 3rd, W. S. (2007). Vasopressin 1a receptor knockout mice have a subtle olfactory deficit but normal aggression. Genes, Brain and Behavior, 6(6), 540-551.

Wettergren A, Wojdemann M, Holst JJ: The inhibitory effect of glucagon-like peptide-1 (7-36)amide on antral motility is antagonized by its N-terminally truncated primary metabolite GLP-1 (9-36)amide. Peptides 19:877-882, 1998.

Wiedemann, S. J., Trimigliozzi, K., Dror, E., Meier, D. T., Molina-Tijeras, J. A., Rachid, L., ... & Donath, M. Y. (2022). The cephalic phase of insulin release is modulated by IL-1β. Cell Metabolism, 34(7), 991-1003.

Wiedemann SJ, Rachid L, Illigens B, Böni-Schnetzler M, Donath MY. Evidence for cephalic phase insulin release in humans: A systematic review and meta-analysis. Appetite. 2020 Dec 1;155:104792. doi: 10.1016/j.appet.2020.104792. Epub 2020 Jul 21. PMID: 32707265.

Wilcox G. Insulin and insulin resistance. Clin Biochem Rev. 2005 May;26(2):19-39. PMID: 16278749; PMCID: PMC1204764.

Will, M.J., Franzblau, E.B., and Kelley, A.E. (2003). Nucleus accumbens mu-opioids regulate intake of a high-fat diet via activation of a distributed brain network. J Neurosci 23, 2882-2888.

Willander, J.; Larsson, M. Olfaction and emotion: The case of autobiographical memory. Mem. Cognit. 2007, 35, 1659–1663.

Williams, G., Bing, C., Cai, X.J., Harrold, J.A., King, P.J., and Liu, X.H. (2001). The hypothalamus and the control of energy homeostasis: different circuits, different purposes. Physiol Behav 74, 683- 701.

Woods SC, Bernstein IL. Cephalic insulin response as a test for completeness of vagotomy to the pancreas. Physiol Behav 24: 485–488, 1980.

Woods SC, D'Alessio D a (2008) Central control of body weight and appetite. J Clin Endocrinol Metab 93:S37–S50.

Woods, S. C., Lotter, E. C., McKay, L. D. & Porte, D. Jr. Chronic intracerebroventricular infusion of insulin reduces food intake and body weight of baboons. Nature 282, 503–505 (1979).

World Health Organization. (n.d.). Home. World Health Organization. Retrieved June 29, 2022, from https://www.who.int/

Wu Y, Pan Q, Yan H, Zhang K, Guo X, Xu Z, Yang W, Qi Y, Guo CA, Hornsby C, Zhang L, Zhou A, Li L, Chen Y, Zhang W, Sun Y, Zheng H, Wondisford F, He L, Guo S. Novel Mechanism of Foxo1 Phosphorylation in Glucagon Signaling in Control of Glucose Homeostasis. Diabetes. 2018 Nov;67(11):2167-2182. doi: 10.2337/db18-0674. Epub 2018 Sep 10. PMID: 30201683; PMCID: PMC6198346.

Wu, Z., Kim, E. R., Sun, H., Xu, Y., Mangieri, L. R., Li, D. P., ... & Tong, Q. (2015). GABAergic projections from lateral hypothalamus to paraventricular hypothalamic nucleus promote feeding. Journal of Neuroscience, 35(8), 3312-3318.

Wu, J., Liu, P., Chen, F., Ge, L., Lu, Y., & Li, A. (2020). Excitability of neural activity is enhanced, but neural discrimination of odors is slightly decreased, in the olfactory bulb of fasted mice. Genes, 11(4), 433.

Wynne, K., Stanley, S., and Bloom, S. (2004). The gut and regulation of body weight. J Clin Endocrinol Metab 89, 2576-2582.

Yang, X.J., Kow, L.M., Funabashi, T., and Mobbs, C.V. (1999). Hypothalamic glucose sensor: similarities to and differences from pancreatic beta-cell mechanisms. Diabetes 48, 1763-1772.

Yan, X., Joshi, A., Zang, Y., Assunção, F., Fernandes, H. M., & Hummel, T. (2022). The Shape of the Olfactory Bulb Predicts Olfactory Function. Brain Sciences, 12(2), 128.

Ye, J., Hao, Z., Mumphrey, M.B., Townsend, R.L., Patterson, L.M., Stylopoulos, N., et al., 2014. GLP-1 receptor signaling is not required for reduced body weight after RYGB in rodents. American Journal of Physiology Regulatory Integrative and Comparative Physiology 306:R352eR362.

Yeomans, M. R. (2006). Olfactory influences on appetite and satiety in humans. Physiology & behavior, 87(4), 800-804.

Zaghloul, H., Pallayova, M., Al-Nuaimi, O., Hovis, K. R., & Taheri, S. (2018). Association between diabetes mellitus and olfactory dysfunction: current perspectives and future directions. Diabetic Medicine, 35(1), 41-52.

Zander M, Madsbad S, Deacon CF, Holst JJ: The metabolite generated by dipeptidylpeptidase 4 metabolism of glucagon-like peptide-1 has no influence on plasma glucose levels in patients with type 2 diabetes. Diabetologia 49:369-374, 2006.

Zhang, Q., Delessa, C. T., Augustin, R., Bakhti, M., Colldén, G., Drucker, D. J., Feuchtinger, A., Caceres, C. G., Grandl, G., Harger, A., Herzig, S., Hofmann, S., Holleman, C. L., Jastroch, M., Keipert, S., Kleinert, M., Knerr, P. J., Kulaj, K., Legutko, B., Lickert, H., … Müller, T. D. (2021). The glucose-dependent insulinotropic polypeptide (GIP) regulates body weight and food intake via CNS-GIPR signaling. Cell metabolism, 33(4), 833–844.e5.

Zhang, X., Pan, W. J., & Keilholz, S. (2019). The relationship between local field potentials and the blood-oxygenation-level dependent MRI signal can be non-linear. Frontiers in neuroscience, 13, 1126.

Zhang Y, Proenca R, Maffei M, Barone M, Leopold L, Friedman JM (1994) Positional cloning of the mouse obese gene and its human homologue. Nature 372:425–432.

Zhang, Z., Zhang, B., Wang, X., Zhang, X., Yang, Q. X., Qing, Z., ... & Bi, Y. (2019). Olfactory dysfunction mediates adiposity in cognitive impairment of type 2 diabetes: insights from clinical and functional neuroimaging studies. Diabetes care, 42(7), 1274-1283.

Zheng, H., Cai, L., & Rinaman, L. (2015). Distribution of glucagon-like peptide 1-immunopositive neurons in human caudal medulla. Brain structure & function, 220(2), 1213–1219. https://doi.org/10.1007/s00429-014-0714-z

Zhou G, Lane G, Cooper SL, Kahnt T, Zelano C. Characterizing functional pathways of the human olfactory system. Elife. 2019 Jul 24;8:e47177. doi: 10.7554/eLife.47177. PMID: 31339489; PMCID: PMC6656430.

Zhou G, Olofsson JK, Koubeissi MZ, Menelaou G, Rosenow J, Schuele SU, Xu P, Voss JL, Lane G, Zelano C. Human hippocampal connectivity is stronger in olfaction than other sensory systems. Prog Neurobiol. 2021 Jun;201:102027. doi: 10.1016/j.pneurobio.2021.102027. Epub 2021 Feb 25. PMID: 33640412; PMCID: PMC8096712.

Zhu X, Zhou A, Dey A, Norrbom C, Carroll R, Zhang C, Lau-rent V, Lindberg I, Ugleholdt R, Holst JJ, Steiner DF.Disrup-tion of PC1/3 expression in mice causes dwarfism and multipleneuroendocrine peptide processing defects.Proc Natl Acad SciUSA99: 10293–10298, 2002.

Zierath JR, Ryder JW, Doebber T, Woods J, Wu M, Ventre J, Li Z, McCrary C, Berger J, Zhang B, Moller DE. Role of skeletal muscle in thiazolidinedione insulin sensitizer (PPARgamma agonist) action. Endocrinology. 1998 Dec;139(12):5034-41. doi: 10.1210/endo.139.12.6364. PMID: 9832442.

Zoon, H. F., De Graaf, C., & Boesveldt, S. (2016). Food odours direct specific appetite. Foods, 5(1), 12.

Zunz, E., La Barre, J., 1929. Contributiona a l'etude des variations physiologiques de la secretion interne du pancreas: relations entre les secretions externe et interne du pancreas. Archives Internationales de Physiologie et de Biochimie 31:20e44.

List of figures

Section I – Introduction

Chapter I

- **Figure I.1.** The metabolic wheel, a dynamic equilibrium between energy intake and expenditure.
- **Figure I.2.** Schematic illustration of the PI3K/AKT insulin signaling pathway.
- **Figure I.3.** Insulin-regulating factors.
- **Figure I.4.** Localization and connectivity of the hypothalamus.
- **Figure I.5**. Symmetric overview of the major hypothalamic nuclei.
- **Figure I.6.** Overview of the gut-brain axis and the regulation of food intake.
- **Figure I.7.** Brain integration of peripheral signals for the regulation of energy homeostasis.
- **Figure I.8.** Brain neurocircuits involved in the efferent outflow to the pancreatic islet.
- **Figure I.9.** Sensory and autonomic innervation of the endocrine pancreas.
- **Figure I.10.** Evolution of the prevalence of obesity in France.
- **Figure I.11.** Natural history of T2D.
- **Figure I.12.** Chemical structure of GLP-1 and GLP-1R agonists.
- **Table I.1.** List of central and peripheral signals involved in feeding behavior and energy balance.

Chapter II

- **Figure II.1.** Tissue-selective processing of proglucagon.
- **Figure II.2.** Direct (late) and indirect (early) nutrient-induction intestinal GLP-1 secretion.
- **Figure II.3.** Brain-derived, gut-derived and exogenous GLP-1 action pathways.
- **Figure II.4.** Illustration of the metabolic effects of GLP-1.
- **Figure II.5.** GLP-1 mediated insulin secretion in the β-cell.
- **Figure II.6.** Nutrient-induced stimulation of L-cell GLP-1 secretion and main GLP-1 biological activities

Chapter III

- **Figure III.1.** Structures of the olfactory system.
- **Figure III.2.** Vanilla flavoring molecules from natural or artificial sources.
- **Figure III.3.** View of the olfactory mucosa and the medial aspect of the OB in mice and olfactory maps at the dorsal surface of the OB in rats.

- **Figure III.4.** Synaptic organization within the OB.
- **Figure III.5.** The pathways of olfactory information processing.
- **Figure III.6.** Representation of the different receptors found in the olfactory bulb in the context of energy balance regulation.
- **Figure III.7.** Different hypothesis for the roles of GLP-1 in the OB.
- **Figure III.8.** Schematic representation of the interactions between the olfactory system, glucose homeostasis and food intake, and obesity and T2D.
- **Table III.1.** Fasting glucose and insulin levels of lean and DIO mice vs. healthy and prediabetic humans.

Section II – Thesis statement

No figures

Section III – Materials and methods

No figures

Section IV – Results

- **Figure IV.1.** The GLP-1 signaling pathway is present in the OB and can be a regulator of neuronal activity.
- **Figure IV.2.** Odor-induced cephalic phase of insulin secretion is reversed by Ex9 in the OB and offers an optimal olfactory foraging in RD mice.
- **Figure IV.3.** Up and down chemogenetic modulation of GLP-1R+ neurons in the OB oppositely regulates food intake and glucose homeostasis.
- **Figure IV.4.** Pharmacological modulation of GLP-1R in the OB regulates glucose homeostasis.
- **Figure IV.5.** The activation of GLP-1R in the OB leads to an inhibition of the SNS through the pancreas.
- **Figure IV.6.** A GABAergic inhibitory relay to the PVN, driven by GLP-1R^{OB} neurons, decreases the sympathetic nerve activity leading to an increase of insulin release from the pancreas in WD mice.
- **Figure IV.7.** Human brain connectivity under glucose and exendin9+glucose conditions.

Section V – Discussion

- **Figure V.1.** Schematic illustration of the hypothetical circuits involving CPIR in foraging activity.
- **Figure V.2.** Olfactory bulb-to-β cell circuit modulates insulin secretion: graphical abstract.

Meetings and publications

Meetings :

Montaner M., Denom J., Magnan C., Migrenne-Li S., Gurden H., The olfactory bulb GLP-1 system mediates regulation of pre- and post-prandial energy metabolism in health and obesity. **BFA Young Researcher's Meeting –** Paris, June 2022. Oral communication.

Montaner M., Denom J., Rouch C., Foppen E., Magnan C., Migrenne-Li S., Gurden H. Le récepteur central du GLP-1 dans le buble olfactif stimule la sécrétion d'insuline chez la souris obèse via l'inhibition sympathique. **Congrès de la Société Francophone du Diabète,** Nice, March 2022. Oral communication.

Montaner M., Denom J., Emery-Fillon N., Magnan C., Gurden H., Migrenne-Li S. Acute injection of the GLP-1 analog Exendin-4 in the olfactory bulb improves glucose tolerance in diet-induced obese mice. **Annual Meeting of the European Association for the Study of Diabetes,** Barcelone, September 2019. Discussed poster. *Awarded with a travel grant.*

Montaner M., Denom J., Emery-Fillon N., Magnan C., Gurden H., Migrenne-Li S. Acute injection of the GLP-1 analog Exendin-4 in the olfactory bulb improves glucose tolerance in diet-induced obese mice. **BFA Young Researcher's Meeting – Physiology: from basic to applied research**, Paris, June 2019. Oral communication.

Montaner M., Denom J., Emery-Fillon N., Magnan C., Migrenne-Li S., Gurden H. L'injection aiguë de l'analogue du GLP-1 Exendin-4 dans le bulbe olfactif améliore la tolérance au glucose chez la souris obèse. **Congrès de la Société Francophone du Diabète,** Marseille, March 2019. Poster. *Awarded with a travel grant.*

Montaner M., Denom J., Emery-Fillon N., Magnan C., Gurden H., Migrenne-Li S. Acute injection of the GLP-1 analog Exendin-4 in the olfactory bulb improves glucose tolerance in diet-induced obese mice. **Third EASD Incretin Study Group Meeting,** Bochum, January 2019. Discussed poster.

The results presented during these international congresses allowed very enriching discussions with leaders of large international laboratories and to initiate collaborations with them.

Publications :

Soleimanzad, H.*, **Montaner, M.***, Ternier, G., Lemitre, M., Silvestre, J., Kassis, N., Giacobini, P., Magnan, C., Pain, F. and Gurden, H. Obesity in Midlife Hampers Resting and Sensory-Evoked Cerebral Blood Flow in Mice. Obesity, 29(1), pp.150-158, 2020. ***co-first authors.**

Mortreux, M., Foppen, E., Denis, R., **Montaner, M.**, Kassis, N., Denom, J., Vincent, M., Fumeron, F., Kujawski-Lafourcade, M., Andréelli, F., Balkau, B., Marre, M., Roussel, R., Magnan, C., Gurden, H. and Migrenne-Li, S. New roles for prokineticin 2 in feeding behavior, insulin resistance and type 2 diabetes: Studies in mice and humans. *Molecular Metabolism*, 29, pp.182-196, 2019.

- In progress:

Montaner, M., Denom, J., Holt, M., Wanqing, J., Brierley, D., Simon, V., James, S., Rouch, C., Jarriault, D., Gault, V., Foppen, E., Kassis, N., Meyer-Gerspach, A., Van Oudenhove, L., Fioramonti, X., Cota, D., Reimann, F., Gribble, F., Trapp, S., Magnan, C., Migrenne-Li, S., Gurden, H. The Glucagon-like peptide 1 in the olfactory bulb modulates insulin secretion via the sympathetic nervous system in the context of metabolic disorders. We are considering a submission in *Cell Metabolism.*

Soleimanzad, H.*, Morisset, C.*, **Montaner, M.**, Deffieux, T., Pain, F., Magnan, C., Tanter, M., Gurden, H. Long-lasting impairment of sensory-evoked cerebrovascular activity probed with functional ultrasound imaging in adolescent mice fed with high-fat diet: protection by polyunsaturated fatty acid supplementation. We are considering a submission in *Nature Neuroscience (Brief Communications)*. *co-first authors.

- Others:

Translation in Spanish of the olfactory training protocol elaborated by the association Anosmie.org, directed by Jean-Michel Maillard. Translation by Montaner, M., Roman, V., Luna, JM., October 2020. More than 140,000 downloads. The protocol was developed by Dr. Hirac Gurden and is based on the international publications and work of Dr. Thomas Hummel in Dresden (Germany). It aims to help people suffering from anosmia to regain their sense of smell (especially patients with Covid-19).